YAEC-1331

SUPPLEMENTAL SEISMIC PROBABILISTIC STUDY

YANKEE ATOMIC ELECTRIC COMPANY

ROWE, MASSACHUSETTS

Yankee Atomic Electric Company
Nuclear Services Division
1671 Worcester Road
Framingham, Massachusetts 01701
December 2, 1982

DISCLAIMER OF RESPONSIBILITY

This document was prepared by Yankee Atomic Electric Company and its consultants and is believed to be completely true and accurate to the best of our knowledge and information. It is authorized for use specifically by Yankee Atomic Electric Company and the appropriate subdivisions within the Nuclear Regulatory Commission.

With regard to any unauthorized use whatsoever, Yankee Atomic Electric Company and their officers, directors, agents, and employees assume no liability nor make any warranty or representation with respect to the content, accuracy, or completeness of this document.

ACKNOWLEDGEMENTS

This report was prepared by the Yankee Atomic Electric Company's Environmental Science Group (ESG). The work was performed by a task force that included Russel B. MacPherson, Thomas F. O'Hara and John P. Jacobson of Yankee and Dr. Daniele Veneziano of MIT. This report was prepared under the technical guidance of Dr. C. Allin Cornell. Appendix D1 was prepared by Mr. George Klimkiewicz of Weston Geophysical Corporation.

TABLE OF CONTENTS

		Page
	DISCLAIMER OF RESPONSIBILITY	ii
	ACKNOWLEDGEMENTS	iii
	LIST OF FIGURES	v
	LIST OF TABLES	vii
	EXECUTIVE SUMMARY	1
1.0	INTRODUCTION AND SUMMARY	6
2.0	ZONATION METHOD	13
3.0	HISTORIC METHOD	23
4.0	COMPARISON AND SYNTHESIS OF RESULTS	27
5.0	REFERENCES	32
APPENDIX A:	Intensity - Magnitude Conversion of Historical Data and Attenuation Functions	A-1
APPENDIX B:	Sensitivity Zonation of New England	B-1
APPENDIX C:	Historical Earthquake Catalogs for the Eastern United States	C-1
APPENDIX D:	Estimation of Seismicity Parameters and Completeness of Earthquake Catalogs in New England	D-1
APPENDIX E:	Attenuation Models for New England	E-1
APPENDIX F:	Sensitivity of Hazard to Input Parameters	F-1
APPENDIX G:	Historic Methods of Seismic Hazard Analysis	G-1
APPENDIX H:	Seismic Probabilistic Risk Assessment Results	H-1
APPENDIX I:	Results of Velocity Hazard Analysis	I-1
APPENDIX J:	Comments Concerning Recent Earthquakes in New Brunswick and New Hampshire	J-1
APPENDIX K:	Integration of the Results of Soil Amplification and Probabilistic Seismic Analysis	K-1

LIST OF FIGURES

Number	Title	Page
1	Integrated Seismic Results	34
2	Full Historic Method Seismic Hazard Results	35
3	Comparison of Seismic Probabilistic Results	36
4	Comparison of Present Seismic Hazard Estimates at Rowe With Those in NUREG/CR-1582	37
5	Comparison of Present Seismic Hazard Estimates With Those in YAEC-1263	38
6	Comparison of Historic Results Using Weston Catalog	39
7	Comparison of Historic Results Using Chiburis Catalog	40
8	Comparison of Historic Results Using TERA CATALOG	41
9	Illustration of Fractile Hazard Curve	42
10	Generation of Hypotheses for Zonation Method and Calculation of Their Probabilities	43
11	Distribution of Site Acceleration for Selected Values of the Annual Exceedance Probability - Construction of Fractile Hazard Functions	44
12	0.16, 0.50, and 0.84 Fractile Hazard Function From the Zonation Method	45
13	"Cloud Plot" of Curves From the Zonation Method in Terms of A_{10}^{-4} and A_{10}^{-3}.	46
14	Steps of the Parametric "Full Historic " Method	47
15	Uncertainty on Hazard Function and its Discretized Representation	48
16	Distribution of Site Acceleration for Selected Volume of the Annual Exceedance Probability - Construction of Fractile Hazard Function	49
17	0.16, 0.5, and 0.84 - Fractile Hazard Function Using Historic Method	50
18	Earthquake Epicenters During the Period October, 1975 - March, 1981 With 10^{-2} Isoseismals Overlaid	51

LIST OF FIGURES
(Continued)

Number	Title	Page
19	Earthquake Epicenters During the Period October, 1975 - March, 1981 With 10^{-3} Isoseismals Overlaid	52
20	Earthquake Epicenters During the Period October 1975 - March, 1981 With 10^{-4} Isoseismals Overlaid	53

LIST OF TABLES

Number	Title	Page
1	Accelerations (Fractions of g) That are Exceeded With Annual Probability 10^{-2}, 10^{-3}, and 10^{-4}. Comparison of This Study With Earlier Results	54
2	Examples of Intensity Re-Evaluations from Chiburis	55
3	Different Procedures of Estimating Seismic Hazard at the Rowe Site	56
4	Comparison of Acceleration Values (g's) That are Exceeded at Rowe With Annual Probability 10^{-2}. The Values From the Zonation Method Corrrespond to the WGC Source Map, b, and m_1 Values. In All Cases, the Attenuation Error has Truncated Normal Distribution With $\sigma_E = 0.7$ and Truncation at $\pm 3\sigma_E$	57
5	Comparison of Acceleration Values (g's) That are Exceeded at Rowe With Annual Probability 10^{-3}. The Values From the Zonation Method Correspond to the WGC Source Map, b, and m_1 Values. In All Cases, the Attenuation Error has Truncated Normai Distribution With $\sigma_E = 0.7$ and Truncation at $\pm 3\sigma_E$	58
6	Comparison of Acceleration Values (g's) That are Exceeded at Rowe With Annual Probability 10^{-4}. The Values From the Zonation Method Correspond to the WGC Source Map, b, and m_1 Values. In All Cases, the Attenuation Error has Truncated Normal Distribution with $\sigma_E = 0.7$ and Truncation at $\pm 3\sigma_E$	59

EXECUTIVE SUMMARY

A supplemental seismic probabilistic study of the Yankee Atomic Electric Company site, Rowe, Massachusetts, was initiated in September 1981 by Dr. C. A. Cornell, Dr. D. Veneziano, and Yankee Atomic Electric Company. The study had four principal objectives:

1. To develop input for the Yankee Seismic Probabilistic Risk Assessment (SPRA), including a quantitative statement of uncertainty;

2. To explain the differences between previous seismic probabilistic estimates by TERA Corporation and Lawrence Livermore Labs (Report NUREG/CR-1582), NRC, and Yankee (Report YAEC-1263);

3. To expand the seismic probabilistic assessment in the previous Yankee report (YAEC-1263) with the following:

   (a) independent (historically based) seismic probabilistic analysis,

   (b) improved attenuation models, and

   (c) additional sensitivity analyses;

4. To incorporate potential soil amplification effects into the probabilistic seismic spectra for the Yankee site.

This report confirms and supplements Yankee's previous report, YAEC-1263. Furthermore, it represents a more comprehensive and up-to-date analysis of eastern United States seismicity than previously studied by TERA Corporation (TERA) and Lawrence Livermore National Labs (LLNL). This study incorporates a far more complete and rigorous treatment of uncertainty than in the two previous studies. Furthermore, it also presents a new seismic probabilistic calculation procedure based on expansion and improvement of the pseudo-historical method of NUREG/CR-1582. This new historically based procedure is called the "Full Historic" method.

This study considers many alternative hypotheses as to earthquake source zonations, magnitude distributions, attenuation models, and catalogs. They are used, first, to display sensitivity of the results to such differences. Then the alternative hypotheses are grouped into 1350 distinct sets and the current methods of seismic probabilistic assessment are applied to each set resulting in 1350 seismic probabilistic estimates. Augmented by 396 historically based alternative hypotheses sets, the total of 1746 hypotheses sets is subjected to a "fully Bayesian" analysis in order to formally quantify and display the uncertainty in the seismic estimates. These are referred to as the "Integrated Seismic Results". They are displayed in Figure 1.

Many of the alternative hypotheses used in the "Integrated Seismic Results" are, however, demonstrably conservative leading to upwardly biased seismic probabilistic estimates. Therefore, we have also produced a "Best-Estimate" by combining only the best-estimate seismic hypotheses recommended by Weston Geophysical Research, Inc.

This report introduces a new seismic probabilistic analysis method based more directly on historical data than the formal analytic hazard analysis program commonly used. The results, including the quantitative uncertainty bounds produced by the new historic method, are shown in Figure 2.

The more straightforward historic method avoids many of the debated hypotheses contained in the formal analytic ("zonation") probabilistic seismic assessment. But, if the input hypotheses in the latter are reasonable, then the results they produce should agree relatively well with the historic results, at least in the (higher) probability levels where the historical data are most dependable. Therefore, the historic results provide a strong check on the analytic hypotheses. Figure 3 compares the median "Full Historic" results to Yankee's "Best-Estimate" analytic results. The agreement is excellent in the 10^{-2} range, confirming the applicability of these analytic results at higher probability levels.

As anticipated above, the "Integrated Seismic Results" give somewhat more conservative values, as is indicated by the median curve, also shown in Figure 3.

In addition, Figure 3 shows several seismic probabilistic curves from NUREG/CR-1582 including (1) a curve based on the "Pseudo-Historic" method prepared by TERA from Appendix C of NUREG/CR-1582, (2) the TERA synthesis results from Appendix C of NUREG/CR-1582, and (3) the curve associated with the NRC proposed 10^{-3} spectra.

As shown on Figure 3, the TERA "Pseudo-Historic" curve lies above our historic estimates. This difference can be traced to TERA's use of a now-obsolete earthquake catalog and an inconsistent procedure for conversion of epicentral intensities to magnitudes. For these and other reasons, the TERA synthesis curves are still higher.

Note that the seismic probabilistic curve resulting from the NRC's 4 August 1980 proposed spectra disagrees markedly with all the other curves shown. This disagreement results from the following deficiencies:

- Incorrect, out-of-date earthquake catalog.
- Out-of-date source zonation and anchoring bias.
- Improper attenuation regression analysis.
- Partial, occasionally incorrect and incomplete treatment of uncertainty (e.g., background sources).
- Use of mean values, which are not good central measures of highly skewed probability distributions.
- Catalog completeness factors inappropriate to New England.
- Incomplete treatment of alternative hypotheses.

In contrast, the Yankee historic and analytic results are much more reliable because our analyses included the following:

- Complete and rigorous treatment of uncertainty.

- o Incorporation of many alternative hypotheses.
- o Up-to-date earthquake catalogs.
- o Source zonation based on site-specific studies without bias.
- o Up-to-date attenuation modeling for ground motion prediction.
- o Confirmation of results by two independent methods.
- o Agreement of results with actual historical record.

This study (Appendix K) also describes a methodology for incorporating potential soil amplification effects into the determination of the probabilistic seismic spectra for the Yankee site. The results of this study show that even in the amplified region, the Yankee Composite Spectrum is substantially higher (by about 35%) than the explicitly soil amplified 10^{-3} spectrum.

Based on this study, we concluded the following:

1. The 0.1g Yankee Composite Spectrum (YAEC-1263) is a conservative estimate of the 10^{-3} annual seismic probability for the Yankee site.

2. The median best-estimate of the annual 10^{-3} peak ground acceleration is 0.07g. The median best-estimate of the annual 10^{-4} peak ground acceleration is 0.15g.

3. The median estimates of the annual 10^{-3} and 10^{-4} (1 hertz, 5% damped) spectral velocity are 4 in/sec and 10 in/sec, respectively.

4. The median integrated estimate of the annual 10^{-3} peak ground acceleration is 0.08g. The 16th and 84th percentile confidence limits on this acceleration are 0.05g to 0.13g, respectively.

5. As stated, the composite spectrum adequately incorporates the effect of local soil amplification.

Finally, specific consideration of recent (January 1982) events in New Brunswick and New Hampshire has shown that they have little or no influence upon these results and conclusions.

1.0 INTRODUCTION AND SUMMARY

Objective:

A study of the seismic probability at the Rowe site was initiated by Yankee Atomic in September, 1981, with three main objectives:

1. To develop input for the plant's seismic probabilistic risk assessment (SPRA), including a quantitative statement of uncertainty;

2. To explain the differences between previous seismic probabilistic estimates by TERA Corporation and Lawrence Livermore National Labs, (NUREG/CR-1582) [1], NRC, and Yankee (YAEC-1263) [2];

3. To improve and supplement the previous Yankee report [2] with:

   (a) independent (historically based) seismic probabilistic analysis method,

   (b) improved attenuation models, and

   (c) additional sensitivity analyses.

To accomplish these three objectives we have analyzed a more exhaustive set of hypothesis about eastern United States seismicity than was done in the previous studies [1 and 2]. We have also applied quantitative uncertainty statements to these hypotheses and processed these uncertainties in a far more complete and rigorous manner than in either previous study. Furthermore, we have developed a new probabilistic estimation procedure, the "Full Historic" method, based on that used in NUREG/CR-1582, Appendix 5, but expanded to include quantitative uncertainty analysis.

Summary of Numerical Results

The quantitative results of this and previous studies are summarized for convenience in Figures 4 through 8 and in Table 1. The net "Integrated"

results of this study are shown in Figure 4 as the median seismic probabilistic curve (denoted M) together with an "uncertainty band" defined by the 0.16 and 0.84 fractile hazard curves. The "Integrated" results are obtained from weighting and pooling the results of two independent analyses methods: the now-conventional "zonation" method (used in [1] and [2]) and the "Full Historic" method (used supplementally in [1] and further developed here). The median curves from each of these two analyses methods are denoted MZ (for median-zonation method) and MH (median-historic method) in Figure 4. In fact, the zonation method results shown are conservative because they include zonation and magnitude recurrence-law hypotheses which we believe to be demonstrably conservative (Appendices B, C, and D). These hypotheses introduce a conservative upward bias in the zonation method results (e.g., curve MZ) and hence, the "Integrated" results (curve M).

By removing these conservative hypotheses, we developed unbiased seismic probabilistic curves. These are developed by using only what we believe to be the unbiased best values of the zonation and recurrence hypotheses. Using these parameter values, we obtain results from simple applications of the zonation method that are close to results from the independent "Full Historic" method. Details are shown in Figures 6 through 8 and Tables 4 through 6. The results of these "unbiased" zonation analyses are displayed as curve UZ in Figure 1 and as shown, they compare well with curve MH.

This study's results are also compared with those of previous studies on Figures 4 through 8. The TERA synthesis results from NUREG/CR-1582 are shown as curve TS in Figure 4. The NUREG/CR-1582 "psuedo-historic" method results are the curve labeled TH in Figure 4. The reasons for differences between these curves are discussed below. On Figure 4, the curve labeled NS reflects the NRC position of June 1981 [3]. A comparison between results of this study and the previous Yankee study [2] is displayed in Figure 5. The NUREG/CR-1582 "pseudo-historic" method (TH) curve is compared with historic method results from 36 possible combinations of historical seismicity catalogs and attenuation laws in Figures 6 through 8. Finally, Table 1 summarizes all the numerical results from Figures 4 through 8 for selected values of the annual frequency of exceedance.

Seismic PRA

The input required for a modern seismic probabilistic risk assessment (SPRA) is a "full Bayesian" seismic probabilistic analysis. Such an analysis includes a full quantitative statement of the uncertainty in the annual frequency of exceeding ground acceleration level, A, as a function of A. The curve M together with the [0.16, 0.84] uncertainty band shown in Figure 1 are one example of a form of presentation of the results of such an analysis. Such a study requires explicit consideration of a set of contending hypotheses about each critical input parameter or assumption in a seismic hazard analysis (be it by the zonation or the historic method). Weights on the hypotheses produce weights (probabilities) on the results which are pooled statistically for presentation as in Figure 4 or for use in SPRA analyses*. Such full Bayesian studies have been completed for recent published SPRA's (e.g., Oyster Creek [4] and Zion [5]). The analysis here is similar in concept, but far more detailed and thorough in its execution.

For clarity, it should be explained that neither of the previous seismic analyses [1,2] of the Yankee site has been of this "full Bayesian" kind. For most purposes it is sufficient simply to show the effects of variation of the seismic input parameters by conventional sensitivity analyses. The reader/reviewer can then make his own implicit or explicit evaluation of the influence of input uncertainty on the conclusions. This strategy was used for the Yankee site in YAEC-1263 [2], and it has been used in virtually all past seismic hazard analyses for the NRC. The major exception has been NUREG/CR-1582 in which a second method, "mean Bayesian", was also employed. This method considers various hypotheses, assigns them weights, and averages the results, producing a single, mean hazard curve. Compared to the full Bayesian method of this report, which is more comprehensive and costly, the mean method fails to express quantitatively the uncertainty bands about the mean. Therefore, it is not only less informative, it is insufficient for modern SPRA's. In fact, the mean method was only partially employed in NUREG/CR-1582, e.g., it was used for (within expert) uncertainty in particular seismicity parameters, but not for example, for

---

* Actually SPRA computations require an alternate presentation of the results, Appendix H.

uncertainty in the attenuation model. The latter was treated only by sensitivity analysis.

Zonation Versus Historic Analysis Methods

As mentioned above, this study employs both the zonation and the historic methods of seismic hazard analysis. The former, more common method (that associated with R. K. McGuire's program [6]) requires that the input be in terms of hypothesized homogeneous zones of potential future seismic activity and in terms of analytical models of earthquake recurrence laws. These "smooth" hypotheses permit the user to include professional information (such as tectonic structure and universally applicable functional forms of recurrence laws) in order to avoid the potential problems associated with estimating rare events from small historical, statistical data sets. In contrast, the historic method uses simply the regional earthquake catalog of dates, locations, and sizes of past events. (Note that both methods require the use of attenuation models.) A non-parametric model similar to that used in NUREG/CR-1582, and a parametric model similar to that developed by Milne and Davenport [7] are used in the historic method.

Summary of Explanations of Differences Among Various Current and Past Analyses

The differences between the results of this study and the results of the various analyses in NUREG/CR-1582 can be explained as follows:

A. Historic Method Results:

The TH (TERA-Historic) curve of NUREG/CR-1582 is much higher than the curves obtained here using the same historic method (Figures 6, 7, 8) for two primary reasons:

(1) In NUREG/CR-1582, all the results are based on a single catalog, referred to here as the TERA catalog. For the northeast United States, the source of TERA catalog is an unpublished preliminary catalog compiled by E. F. Chiburis, referred to here as Chiburis' old catalog. That catalog has been significantly revised prior to recent publication as a

NUREG document [8]; the published version we shall refer to as Chiburis' new catalog. One reason the TERA-Historic hazard results are too high is because higher epicentral intensities were assigned to a few historical events in Chiburis' old catalog, most critically to the 1732 Montreal event. Several recently published studies [8,9], including Chiburis' new catalog, have concluded that the actual epicentral intensity of the 1732 Montreal event and other events was less than reported in the Chiburis' old catalog. Examples of other revisions to the Chiburis' old catalog are given in Table 2. The effect of using two more accurate catalogs can be inferred by comparing the 12 historic curves in Figures 6 and 7 with the analogous curves in Figure 8. (The accurate catalogs are referred to here as "Weston Geophysical" and as simply "Chiburis", the latter reflecting the Chiburis' new published catalog.) Catalogs are discussed in detail in Appendix C.

(2) A second more important source of overestimation of risk in the TERA-Historic (TH) curve is the procedure used in NUREG/CR-1582 to convert epicentral intensity I_o and local magnitude M_L to body-wave magnitude m_b. See Appendices A and C for details. The effect is demonstrated by comparing in Figure 8 the curve TH and the heavy solid curve, which is our result for the same catalog and attenuation law used in NUREG/CR-1582, but with proper intensity-magnitude conversion.

B. Zonation Method Results:

Several elements jointly explain why in Figure 4 the TS (TERA-Synthesis) and NS (NRC-Synthesis) curves are much higher than our MZ (Median-Zonation) curve. These elements are:

(1) Zonation. The Yankee site hazard results are very sensitive to this parameter. Important differences can be described as:

(a) the relatively large credibility given in NUREG/CR-1582 to the Piedmont zone; and to a lesser degree to the Boston-Ottawa zone; and

(b) the improper procedure for inclusion of a Background zone. (See Appendix B).

(2) Recurrence Relationships. Differences in these relationships are due to mainly the catalogs. As discussed above, this study uses updated and more reliable estimates of historical intensities, and therefore, of the a, b, and m_1 parameters, see Appendix C and D. It is also due to the catalog completeness periods. More careful analysis of the earthquake data and of the demography of New England supports completeness periods longer than the all-eastern United States values given in NUREG/CR-1582, see Appendix D.

(3) Attenuation. The NS curve in NUREG/CR-1582 is based upon an attenuation model ("Ossipee") that produces very high site effects both in the near-field and at intermediate distances. Several objections to the validity of this model have been raised by Yankee (see Appendix E). Furthermore, the "Ossipee" model has been superceded by a more recent model by its author (letter to LLNL, dated May 29, 1980). This new "Ossipee" model results in significantly lower ground motion [10].

C. Zonation vs. Historic Results in This Study:

Differences between the zonation and the two sets of historic results obtained in this study (curves MZ and MH in Figure 4) can also be reconciled. They are due primarily to inclusion in the zonation method of sets of conservative hypotheses used by others. These hypotheses are about source configuration, b values, and m_1 values. If this conservatism is removed by using unbiased best-estimates of zonation, a, b and m_1 values as supplied by Weston Geophysical Corporation, then the three methods produce very similar results. This is illustrated in Tables 4, 5, and 6 and in the detailed discussion in the final section. This also means that our "synthesis", curve M, gives conservative estimates of seismic

probability (e.g., it overstates the actual likelihood of experiencing a seismic event).

Summary:

Because the methods used, zonation and historic, are substantially independent and procedurally different, their agreement in terms of numerical results reinforces our confidence in the conclusions of this study. These methods include consideration of:

(1) A wide variety of representations of regional seismicity. This includes five very different source geometries in the zonation method, as well as zonation-free models in the historic procedures;

(2) Uncertainty in the recurrence parameters a, b and m_1 in the zonation method and three distribution shape parameters in the historic method are treated as random variables;

(3) Different procedures of statistical estimation including non-parametric and parametric in the historical analysis;

(4) A wide range of attenuation models including empirical and theoretical, intensity-based and magnitude-based;

(5) Three different catalogs of historical earthquakes.

Furthermore, all of these items are treated by explicit uncertainty quantification to generate the confidence bands.

We summarize our numerical conclusions as follows:

1. The median unbiased best-estimate of the 10^{-3} annual probability of exceedance peak ground acceleration is 0.06g.

2. The median unbiased best-estimate of the 10^{-4} annual probability of exceedance peak ground acceleration is 0.13g.

3. Inclusion of hypotheses that reflect others opinions about certain key parameters increases the median values of conclusions 1 and 2 by about 15%.

4. The median unbiased best-estimates of the annual 10^{-3} and 10^{-4} (1 hertz, 5% damped) spectral velocity are 4 in/sec and 10 in/sec, respectively.

5. Lastly, specific consideration of recent (January 1982) events in New Brunswick and New Hampshire (Appendix J) has shown that they have little or no influence upon the results and conclusions of this study.

2.0 ZONATION METHOD

The McGuire computer program [6] used in this study to calculate seismic hazard is based on the conventional probabilistic model of seismicity. This program relies upon the following assumptions:

- Homogeneous earthquake sources zones are assumed to exist in the region. Each source generates earthquakes at random times, at random geographical locations, and with random magnitudes.

- The effect at the site of an earthquake of given magnitude m_b and epicentral distance R is a random function of m_b and R. Such a function is often called the "attenuation model".

- Seismic hazard at the site, e.g., the mean annual rate at which a peak acceleration value A is exceeded, is obtained by adding the mean exceedance-rate contributions from all the sources. The probability of exceeding A during a given time interval is then calculated under the assumption of Poisson events in time.

Input to the program includes:

1. The configuration of the homogeneous sources ("zonation").

2. A magnitude-recurrence relationship for each source, usually in the form of a truncated exponential function. Parameters of this function are: the mean rate of earthquake occurrence, a, the logarithmic slope, b, and the magnitude upperbound, m_1.

3. An attenuation model, typically of the form

$$\ln A = b_1 + b_2 m_b + b_3 R + b_4 \ln R + E \qquad (1)$$

in which the b's are coefficients of the mean attenuation function, R is distance in kilometers, and E is a zero-mean "error term" with a truncated normal distribution defined by dispersion parameter $\sigma_{\ln A}$.

Because of uncertainty in many of the input variables, such as zonation, recurrence and attenuation parameters, a single use of McGuire's program cannot fully characterize the uncertainty in the seismic hazard at a site. Several strategies are available to determine the impact of input parameter uncertainty on the seismic hazard results of the McGuire program. By far, the most popular strategy has been the sensitivity study. This involves assigning incremental values for certain input parameters and rerunning the program to determine the change in the hazard results. It is not necessarily implied that the value of this increment reflects the degree of uncertainty in the parameter. The experienced reader can usually judge that for himself. The sensitivity study only shows the influence on the results per given parameter increment. The reader must then make his own judgment as to how to use all these results. This procedure has been used in virtually all past seismic hazard studies.

Another approach to quantifying uncertainty is to assign weights ("degrees of belief" or "subjective probabilities") to various possible values of the parameters. The McGuire program is then run for all possible combinations of parameter values. The results of each run are weighted by the product of the individual, independent parameter value weights. This produces a weighted average of the hazard at each acceleration value. This can be called the full Bayesian method. More formally, it produces what can be called the "predictive distribution of A", the annual maximum acceleration. This method was used in part in NUREG/CR-1582 for some input parameters but not all.

The full Bayesian method has advantages, especially in cases involving economically-based decisions. It does not yield more than a single hazard curve, and that curve is the mean curve. It is currently recognized [11] that median curves are preferred in the case of the strongly skewed distributions (on hazard values) that we face.

Quantitative statements of uncertainty are commonly required by decision makers and regulators who have begun to ask analysts for more explicit representations of their confidence in the low probability estimates. Also, seismic PRA studies require that the results of the seismic hazard analysis be integrated with plant "fragility" curves which are

themselves subject to uncertainty. Thus, the PRA analysts require that the net uncertainty in their result be evaluated and this requires full, explicit presentation of the uncertainty in the hazard curves.

All these demands require a "full Bayesian" analysis of the uncertainty. In this procedure, each hypothesis (i.e., each possible combination of parameter values) has its own weight and each has an associated seismic hazard curve. Each curve is "correct" with that probability or weight.

In this study of the Yankee site, 1350 different hypotheses were considered. Because of the difficulty of displaying such a large number of hazard curves, the results have been statistically analyzed to produce "fractile hazard curves". The concept is illustrated in Figure 9 in terms of the 0.16, 0.50, and 0.84 fractiles. Notice (in Figure 9) that identical fractile hazard curves are obtained by using either the distribution of H (hazard) given A (acceleration) or the distribution of A given H. For example, if one reads a typical curve with 84% probability ("confidence"), the frequency of occurrence of this event (e.g., $A \leq 0.1g$) is less than or equal to 1×10^{-3} per year, or with 84% probability the acceleration which is exceeded with frequency 1×10^{-3} per year is less than or equal to 0.1g.

For some purposes, such as for sensitivity studies or for seismic PRA studies, it is desirable to group the many hazard curves or to display them in alternative ways to be described below.

The 1350 hypotheses have been generated from all possible combinations of several alternative zonations, recurrence law parameters, attenuation model coefficients, and attenuation error-term distributions. Graphically, one may visualize the various hypotheses as the end branches of a combination tree, as shown in Figure 10. The figure also explains how the probability of each hypothesis is calculated. First, probabilities adding to one are assigned to each parameter of the tree. That is, the probabilities of the different zonations add to one, those of the different attenuation models add to one, etc. These probabilities are assessed on the basis of information in the literature and expert opinion as discussed in Appendices B, C, D, and E. Second, the probability of each hypothesis is obtained as the product of the probabilities of the various components that define that hypothesis. This

procedure guarantees that the sum of the probabilities of the hypotheses add to one.

Description of Alternative Hypotheses

1. Zonation

Five different configurations of the earthquake source zones for the Yankee site have been considered. These configurations and their probabilities are:

(1) Boston-Ottawa/Piedmont as described in NUREG/CR-1582 for Expert 3. Probability, $P_1 = 0.22$;

(2) Weston Geophysical Corporation (WGC) zones as described in Reference 2. Probability, $P_2 = 0.31$;

(3) A combination of the Piedmont zone at the site and south of the site with WGC zones to the north. Probability, $P_3 = 0.31$;

(4) A combination of WGC zones at the site and south of the site with the Boston-Ottawa zone to the north. Probability, $P_4 = 0.08$;

(5) Same as (3) except the WGC source that includes the site extends further to the south. Probability, $P_5 = 0.08$.

The basic zonation alternatives are (1) and (2). Alternatives (3), (4) and (5) are obtained through various combinations of zones in (1) and (2). Appendix B contains maps of the five zonations and a detailed review of the relevant literature. Appendix B provides more information on the zonation and probabilities.

2. Seismicity Parameters, a, b and m_1

Uncertainty on the upperbound magnitude m_1 and on the Gutenberg-Richter slope parameter b, and activity rate a, is included in this study. It would be unrealistic and unconservative to treat the m_1 or b

values as independent variables from source to source. Whereas it is conservative to assume perfect spatial dependence (e.g., that is if m_1 is high for one source, then m_1 is necessarily high for all the other sources). To reduce computational effort we have based our analysis on the latter conservative assumption by considering the following cases:

For m_1,

(1) Historical maximum in each source zone plus 0.5 m_b unit. Probability, $P_1 = 0.8$;

(2) Historical maximum in each source zone plus 1.0 m_b unit. Probability, $P_2 = 0.15$;

(3) Historical maximum in each source zone plus 1.25 m_b unit. Probability, $P_3 = 0.05$. If this value exceeds $m_b = 7.30$, it is taken equal to $m_b = 7.30$.

For a,

(1) As calculated by WGC for each source zone. Probability, $P_1 = 0.60$;

(2) WGC calculated "a" times 1.5 for each source zone. Probability, $P_2 = 0.30$;

(3) WGC calculated "a" times 2.0 for each source zone. Probability, $P_3 = 0.10$.

For b,

(1) As calculated by WGC for each source zone. Probability, $P_1 = 2/3$;

(2) 0.9 for all source zones. Probability, $P_2 = 1/3$.

In short, for each parameter we have added what we believe to be conservative alternatives to the WGC estimates. In particular, the hypothesis that b = 0.9 for all sources without modification of the activity rates produces significantly larger hazard values at the site. Appendices A and D support the WGC estimates of the seismicity parameters a and b. The probabilities assigned to these alternatives are also discussed in Appendix D.

Also, the lower bound magnitude, m_o, is 3.5 m_b for all zones in all cases. A minor variation in the McGuire [6] computer code allows for analytical integration over each source area by way of McGuire's subroutine "Risk 1".

3. Attenuation Models

We have considered five alternative sets of attenuation coefficients in Equation 1 and for each set, three different distributions of the attenuation error term, E. The coefficients, which are given in Appendix E, correspond to the following models:

(1) Nuttli and Herrmann [12]

(2) Bollinger 1 [13]

(3) Bollinger 2 [13]

(4) WGC (Modified) [14]

(5) Gupta-Nuttli [1]

The most recently reported of the sequence of "theoretical" models developed by Nuttli and Herrmann has been adopted because its authors favor it over its predecessors. In particular, it therefore replaces the so-called "Nuttli Theoretical" model used in YAEC-1263 (2).

Two versions of Bollinger [13] have been considered. As explained in Appendix A, the original attenuation, which is in terms of epicentral intensity, can be converted to body-wave magnitude m_b by replacing I_o by the inverse of $m_b(I_o)$, the expected value of m_b given I_o. This operation, with

$$m_b(I_o) = 0.5\ I_o + 1.75 \qquad (2)$$

leads to "Bollinger 1". The other model, "Bollinger 2", follows from replacing I_o by the expected value of I_o given m_b (for details, see Appendix E).

The WGC model originally presented in YAEC-1263 has been modified by applying a more realistic magnitude scaling factor value of 1.1 (see Appendix E). This change is considered necessary because, according to the unmodified attenuation, a large fraction of the risk at the Yankee site would be predicted to come from magnitudes in the range from 3.5 to 4.0, which is known to be unrealistic.

Finally, a Gupta-Nuttli model in terms of m_b has been obtained through the conversion of Equation 2.

Appendix E makes a detailed evaluation and comparison of these models and shows plots of the attenuation functions including the unmodified WGC version. Based on this evaluation, the following probabilities have been assigned (see Appendix E):

$$P_1 = 0.35,\ P_2 = 0.06,\ P_3 = 0.11,\ P_4 = 0.35,\ P_5 = 0.13$$

Dispersion about each median attenuation has been included through the random error term E in Equation 1. This term has been assumed to have mean zero and the following truncated or untruncated normal distributions:

(1) $\sigma_E = 0.6$, no truncation ($P_1 = 0.3$)

(2) $\sigma_E = 0.7$, truncation at $\pm 3\sigma_E$ ($P_2 = 0.6$)

(3) $\sigma_E = 0.9$, truncation at $\pm 2\sigma_E$ $\quad (P_3 = 0.1)$

The indicated probability assignments are discussed in Appendix E.

Analysis of the Results

The 1350 hazard curves $H_i(A)$ $(i = 1,\ldots,1350)$, produced by the McGuire program under the conditions of input previously identified, have been statistically analyzed as illustrated in Figure 9. Denote by P_i the probability of the ith hypotheses and by $A_i(H)$ the site acceleration that is exceeded with annual probability H under that hypothesis. The pairs $[A_i(H), P_i]$ $(i = 1,\ldots,1350)$ define the probability distribution of A(H) for given H. For example, the cumulative distribution function of A(H), $F_{A(H)}$, is given by

$$F_{A(H)}(a) = P[A(H) \leq a] = \sum_{\substack{\text{hypotheses i for} \\ \text{which } A_i(H) \leq a}} P_i \qquad (3)$$

Figure 11 shows a few such functions for selected values of the annual exceedance frequency (H = 0.02, 0.01, 0.003, 0.001, 0.0002, 0.0001). One can easily use Figure 11 and the technique demonstrated in Figure 9 to obtain various fractile hazard curves: one obtains from Figure 11 the accelerations that correspond to a given value of $F_{A(H)}$, say 0.84, and plots these accelerations against the annual exceedance frequency. These operations are given in Figures 11 and 12 for the fractiles 0.16, 0.50 and 0.84. The 0.50-fractile (median) curve in Figure 12 is also reproduced in Figure 4, as curve MZ.

Additional analyses have been performed on 450 hazard curves associated with the base case activity rate, to identify parameters to which the results are particularly sensitive, and to explain the difference between the present hazard estimates and those obtained in previous studies. To facilitate these studies we have chosen to represent each curve in terms of just two acceleration values, called $A_{10^{-3}}$ and $A_{10^{-4}}$, the values that are exceeded with annual probability 10^{-3} and 10^{-4}, respectively. It is possible in this way to represent each hazard curve by just one point on the $(A_{10^{-4}}, A_{10^{-3}})$ plane making it easy to compare a large number of different curves. The cloud of all

450 points is shown in Figure 13. The fact that A_{10}-4 and A_{10}-3 appear to be highly "correlated" indicates that the various hazard curves differ in location but not significantly in slope, when plotted on logarithmic paper.

Sensitivity of hazard to different input parameters can be evaluated by making several "cloud plots" of the type in Figure 13, each limited, however, to an exclusive subset of points, for example, by making five plots with points separated according to the five zonation alternatives. Twenty-one such sensitivity plots are presented in Appendix F, each associated with one parameter value: one plot for each zonation (all other parameters varied), one for each median attenuation model, one for each distribution of the attenuation error, and one for each m_1, a and b alternative. From these plots it is concluded that:

1. Zonation is a critical parameter, with alternatives (1), (3) and (4) giving higher hazard than alternatives (2) and (5).

2. Results are much less sensitive to the median attenuation function. The five attenuations are nearly equivalent in terms of A_{10}-4, with attenuation model (3) giving somewhat lower estimates of A_{10}-3.

3. The distribution of the attenuation error has mixed effects on the results: for annual exceedance probabilities between 10^{-2} and 10^{-4} (the range of primary interest here), distributions with higher σ_E values produce larger accelerations. For smaller exceedance probabilities, the tail of the distribution becomes increasingly important and the above trend is reversed due to the truncation effect.

4. When the b values are changed from the WGC estimates to 0.9 for all the sources (without simultaneously changing the occurrence rates), the values of A_{10}-4 and A_{10}-3 increase significantly. Results are also sensitive to the choice of m_1.

In summary, zonation, b, and m_1 values are the most critical components of input. Next comes the distribution of the attenuation error and last the coefficients of the median attenuation model.

3.0 HISTORIC METHODS

"Historic" methods of seismic hazard estimation are an alternative to the traditional zonation methods. The "Historic" methods derive directly from the actual historical record of seismic events without the need to assign zonation or seismic input parameters. The problem with the traditional zonation method is making unassailable definitions of source zones in the eastern United States. This problem is well known and is illustrated by the variety of zonation alternatives as discussed in Section 2 and Appendix B. In addition, there are further questions as to the precise values of parameters such as a, b, and m_1, in the zonation models. All these concerns are reflected in the variety of hypotheses, the spread in the assigned weights and in the subsequent multitude of runs required.

"Historic" methods of seismic hazard estimation have been used by investigators such as Lomnitz [15], Milne and Davenport [7], and others in the past. The "Historic" methods still require attenuation laws, but they have the benefit of avoiding explicit estimation of source zones and a, b, and m_1, parameters. Application of "Historic" methods gives a largely independent assessment of the seismic hazard at a site.

TERA in NUREG/CR-1582, Volume 4, Appendix C, has developed and applied the most advanced of these methods to date. It is referred to as the "Psuedo-Historical" method. Each historical earthquake in a catalog is attenuated to the site and the average rate $\lambda_{(A)}$ at which site acceleration A is exceeded is calculated as:

$$\lambda_{(A)} = \frac{N(A)}{T} \tag{4}$$

N(A) is the (expected) number of events during the past T years that have produced site acceleration in excess of A. Appendix H provides a complete discussion of the historic methodology. The calculation of N(A) can include attenuation errors (uncertainty on the peak acceleration experienced at the site during each historical earthquake) and also catalog incompleteness. The TERA method is still not entirely satisfactory, however.

The main problems with the TERA "Pseudo-Historical" procedure are:

(1) It produces estimates of hazard without quantifying estimation uncertainty; and

(2) Hazard estimates are found to be unduly oversensitive to the maximum historical acceleration at the site in the range of accelerations of engineering interest.

We have used a similar procedure, but we have also developed an alternative historic method of hazard analysis that overcomes the above stated limitations of the TERA methodology. Our "Full Historic" procedure quantifies estimation uncertainty and it provides more stable estimates of seismic hazard. Appendix H provides a complete explanation of each method. These benefits are achieved by fitting a very general but smooth distribution to the upper tail of peak ground acceleration at the site, and by considering the parameters of this distribution as uncertain quantities due to the limited amount of historical data. This version of the historic method also accounts for attenuation law errors and catalog incompleteness. The "Full Historic" method's main steps are illustrated in Figure 14.

One might call the original TERA "Psuedo-Historic" method "non-parametric" and our new "Full Historic" method "parametric". This is to reflect the different non-parametric and parametric statistical procedures used in the estimation of $\lambda(A)$.

Not all the input information needed by the historic method is precisely known. In particular, there are several possible attenuation models and different earthquake catalogs are available. In the numerical calculations, we have used three catalogs: WGC, Chiburis' new catalog, and NUREG/CR-1582 (see Appendix C). We have also used four different attenuation models, each with three alternative combinations of error variance and truncation. The attenuation models and the distributions of the attenuation error are the same as those used with the zonation method (Section 2) except that here the attenuation functions are in terms of epicentral intensity I_o, and therefore, only one Bollinger model needs to be considered.

For each catalog and attenuation model, the parametric "Full Historic" method characterizes hazard through the distribution of acceleration that is exceeded with any given annual probability H (Figure 15.a). For convenience of computation, each such distribution has been discretized, as shown in Figure 15.b. Eleven discretization points have been used so that, for any given catalog and attenuation model, the program generates eleven hazard curves, each with a non-zero probability of being correct.

The total number of curves obtained by the parametric method is, therefore, 396 (36 catalog-attenuation combinations and 11 curves for each combination). Probabilities have been assigned as follows (see Appendices noted):

Catalogs (Appendix C)

(1) WGC $P_1 = 0.60$

(2) Chiburis $P_2 = 0.30$

(3) NUREG/CR-1582 $P_3 = 0.10$

Attenuation Models (Appendix E)

(1) Herrmann $P_1 = 0.35$

(2) Bollinger $P_2 = 0.17$

(3) WGC $P_3 = 0.35$

(4) Gupta-Nuttli $P_4 = 0.13$

Attenuation Error Parameters (Appendix E)

(1) $\sigma_E = 0.6$, no truncation $P_1 = 0.30$

(2) $\sigma_E = 0.7$, truncation at $\pm 3\,\sigma_E$ $P_2 = 0.60$

(3) $\sigma_E = 0.9$, truncation at $\pm 2\,\sigma_E$ $P_3 = 0.10$

As discussed above, the probability of each of the 36 combinations (calculated as the product of the associated P_i's) has been further partitioned into eleven parameter-uncertainty-based probabilities, yielding probability assignments to the individual 396 hazard curves. Finally, these 396 curves have been statistically analyzed as before, in order to generate fractile hazard functions. The distributions of the acceleration values that are exceeded with annual probabilities H = 0.01, 0.003, 0.001, 0.0002 are shown in Figure 16. The 0.16, 0.50 (median), and 0.84 fractile hazard functions are plotted in Figure 17. The median curve is also reproduced in Figure 4, as curve MH.

In addition to the above calculations with the parametric method, we have estimated hazard through the (original) non-parametric historical procedure used in NUREG/CR-1582. Because it produces only a single ("best-estimate") curve, this method yields only 36 curves in total, one for each of the catalog-attenuation combinations. Results are shown in Figures 6, 7, and 8, grouped in 3 sets of 12 curves, according to the earthquake catalog.

4.0 COMPARISON AND SYNTHESIS OF RESULTS

The estimates of hazard at the Yankee site obtained by the parametric and non-parametric historic methods are typically lower than those from the zonation method. The main reason for the difference is the conservatism of the zonation analysis; specifically, the inclusion of conservative zonations which allow far away earthquake sources to "migrate" close to the site, as well as conservative assumptions about the recurrence slope b (e.g., the hypothesis that b = 0.9 for all sources without coupled reduction of the recurrence rate) and m_1 (upper bound magnitudes as large as 7.30). Results from the historical and zonation analysis are in much closer agreement if in the zonation analysis one uses the zonation, a and b values, and upper bound magnitudes as determined by Weston on the basis of detailed mapping of New England seismicity and of careful interpretation and analysis of the data.

A comparison of this type is made in Tables 4, 5, and 6 in terms of the acceleration values A_{10}-2, A_{10}-3, and A_{10}-4, the values that are exceeded at the Yankee site with annual probability 10^{-2}, 10^{-3}, and 10^{-4}, respectively. In all cases, the attenuation error has been assumed to have normal distribution with σ_E=0.7, truncated at $\pm 3\sigma_E$ (most likely case). For each attenuation model, the tables give estimates of A_{10}-2, A_{10}-3, and A_{10}-4 from the zonation method and the two historic methods. Because the parametric historic procedure yields results in the form of probability distributions of A_H for given exceedance probability H, Tables 4, 5 and 6 summarize the distributions through the median and the 0.16 and 0.84 fractile values. Results from the historic methods further depend on the earthquake catalog; the Weston catalog and Chiburis's new catalog are used in the tables. At the 10^{-3} level (Table 5) the three procedures are in excellent agreement, with a "consensus value" of about 0.06. At the 10^{-2} level (Table 4), the zonation method produces values of acceleration that are about 30% lower than those of the historic method. Considering only the higher estimates, one would conclude that A_{10}-2 is about 0.03g. The opposite is true for H = 10^{-4} (Table 6). In this case, the zonation results are higher by about 30%. If one again considers only the higher estimates (zonation method

and historic method with Gupta-Nuttli's attentuation) then one concludes that $A_{10^{-4}}$ is about 0.13g.

The agreement between the historic methods and the zonation method using the WGC parameters for source zones, a's, b's, and m_1's is "end-result" confirmation of the latter values.

Further insight into the historic method, and therefore into the results generally, can be gained by looking at geographical maps of seismic hazard. We have used the non-parametric procedure with Gupta-Nuttli's attenuation, $\sigma_E = 0.6$ and no truncation, to produce such maps over a region of 400 x 400 km, centered at Rowe. Results are displayed in Figures 18, 19, and 20 as contour lines of the acceleration that is exceeded annually with probability $H = 10^{-2}$, 10^{-3}, and 10^{-4}, respectively. One may notice that:

1. At all sites only the historical event with largest (expected) site acceleration is important at the 10^{-4} probability level (Figure 20). (This is a weakness of the non-parametric method, of course.) For most sites, such an event is one of the earthquakes of intensity greater than VI recorded in the region and marked as solid circles in the figures. At the other extreme (10^{-2} probability level, Figure 18), lower-intensity events and their frequencies become most important.

2. There is a change with probability, H, of the relative hazard at different sites which is explained by the fact that historical events in New England do not conform well to an exponential recurrence model with the same b value everywhere. In comparison, the zonation method would produce acceleration maps which vary more smoothly both in space and with H. Spatial smoothing is more pronounced for smaller values of H. Therefore, for any given probability, H, conservatism of one method with respect to the other depends on site location. At Rowe, the historical method is found to give higher accelerations than the zonation method (with

WGC source map, b and m_1 values) for $H \geq 10^{-3}$ and smaller accelerations for $H < 10^{-3}$ (see Tables 4, 5, and 6). However, there are regions within 200 km from Rowe where the opposite is true because for these regions, the zonation method allows physical earthquake sources to migrate away from the site.

3. There is a large region near the Rowe site (with long extensions in the west and northeast directions and a smaller extension in the southeast direction), in which acceleration is consistently low for all H values. This consistency, which is due to the low level of activity with respect to both large and small earthquakes, adds credibility to those zonation models (e.g., the WGC source areas) that do not consider the site either as part of the Piedmont region or as very close to a hypothetical Boston-Ottawa region.

4. All previous historic analyses have considered the epicentral location of historical earthquakes as deterministically known. In order to conservatively bound the hazard effect of epicentral location uncertainty, we have produced maps of the type on Figures 18 to 20 after moving <u>all</u> historical earthquakes 25 km closer to each site, i.e., by calculating epicentral distance as the nominal epicentral distance minus 25 km for each earthquake and for each site. At sites near regions of high seismicity, the effect of epicentral-location uncertainty is small. At sites such as Rowe, accelerations A_H are increased by about 30% for all H values; again, these increases are conservative upper bounds.

In order to produce a single composite, historic and zonation based, estimate of hazard at Rowe, the probabilities of the 396 parametric-historic curves were weighted by 1/3 and the probabilities of the 1350 zonation curves by 2/3. The zonation method has effectively replaced in practice the early versions of the historic method; therefore it is clearly preferred by the many users and developers of hazard analysis. The newly developed parametric historic method should, however, bring renewed interest to historic procedures because it overcomes many of their previously perceived weaknesses. Hence, the 2 to 1 relative weighting of the two sets of results. Because the zonation results include some very conservative input alternatives, we believe

these weights are biased toward higher hazard estimates. The entire set of 1746 curves was then subjected to statistical analysis to obtain 0.16, 0.50, and 0.84 fractile hazard functions (0.16, M, and 0.84 curves in Figures 4 and 5 and first 3 rows of Table 1). Notice the increase-of-variance effect (broadening of the uncertainty band) of pooling together results from the two methods. These three curves summarize as succinctly as is possible the numerical results of the present study.

Several other studies have previously produced hazard estimates at the Rowe site using different assumptions and methods of analysis. Comparisons are made in Figures 4 and 5 and in Table 1. More important than mere numerical comparison is the explanation of the differences among the various results, which are sometimes very pronounced. The very extensive calculations in this study have permitted us to evaluate the effects on calculated hazard of alternative procedures, assumptions, and parameter values, and to explain such differences. (For a detailed comparison see Introduction and the Appendicies cited there.)

In summary, the main qualitative conclusions of this study are:

1. We have found that if the input to the zonation method is obtained by detailed mapping of seismicity and by statistical analysis of the historical data from each source rather than by over-generalized zones and parameter values then zonation based results are in good agreement with those of the historic methods (see Tables 4, 5, 6).

2. The difference between results obtained here and those presented in NUREG/CR-1582 using the same (non-parametric) historic method is due to conservative estimation in the NUREG/CR-1582 catalog of the intensity of a few historical earthquakes and to an inconsistency in the conversion from epicentral intensity and local magnitude to body-wave magnitude (Figures 6, 7, 8).

3. The difference between zonation method results obtained here and in NUREG/CR-1582 is explained primarily by the conservative zonations used in NUREG/CR-1582 and to a lesser degree by differences in catalog and magnitude conversion mentioned in point (2).

4. After removal of inaccuracies, inconsistencies, and obvious sources of conservatism, all methods of analysis (zonation, parametric historic, non-parametric historic) lead to comparable acceleration values for the range of annual probability 10^{-4} to 10^{-3}.

In consideration of all results from the zonation and historical procedures, the numerical conclusions of this study are that, with some degree of conservatism (due to assumptions about zonation, a and b values, and m_1 values),

1. The acceleration that is exceeded with an annual frequency of 10^{-3} has a median value equal to 0.08g and a [16%, 84%] probability (or "confidence") range equal to [0.05g, 0.13g].

2. The median value and a [0.16, 0.84] probability range for annual exceedance probability of 10^{-4} are 0.16g and [0.08g, 0.26g], respectively.

5.0 REFERENCES

[1] Bernreuter, D. L., 1981, Seismic Hazard Analysis, NUREG/CR-1582.

[2] Yankee Atomic Electric Company, 1981, Seismic Response Spectra for the Yankee Nuclear Power Station, Rowe, Massachusetts, YAEC-1263.

[3] Crutchfield, D., 1981, Letter, NRC to Yankee Atomic, June 8, 1981.

[4] Oyster Creek Probabilistic Risk Assessment for New Jersey Central Power and Light, (Draft) 1979.

[5] Zion Probabilistic Safety Study For Commonwealth Edison Company, 1981.

[6] McGuire, R. K., 1976, FORTRAN Computer Program for Seismic Risk Analysis, USGS Open File Report 76-67.

[7] Milne, W. G., A. G. Davenport, 1969, Distribution of Earthquake Risk in Canada, BSSA, Volume 59, No. 2, Pages 729-754.

[8] Chiburis, E. F., 1981, Seismicity, Recurrence Rates, and Regionalization of the Northeastern United States and Adjacent Southeastern Canada, NUREG/CR-2309.

[9] LeBlanc, G., 1981, A Closer Look at the September 16, 1732, Montreal Earthquake, Canadian Journal of Earth Sciences, Vol. 18, Number 3, Pages 539-550.

[10] Wight, L., Letter, TERA Corporation to LLNL, dated May 22, 1980.

[11] Apostolakis, G. E., Data Analysis in Risk Assessment, Accepted for Publication, Nuclear Engineering and Design.

[12] Nuttli, O. W., R. B. Herrmann, 1981, Consequence of Earthquakes in the Mississippi Valley, ASCE, Pre-print 81-519.

[13] Bollinger, G. A., 1976, Reinterpretation of the Intensity Data for the 1886 Charleston, South Carolina Earthquake, USGS Professional Paper 1028-B.

[14] Klimkiewicz, G. A., 1981, Personal Communication, Weston Geophysical Corporation.

[15] Lomnitz, C., 1969, An Earthquake Risk Map of Chile, Proceeding of the Fourth World Conference on Earthquake Engineering, Volume 1, Pages 161-184.

INTEGRATED SEISMIC RESULTS

For each acceleration level, read annual seismic probability associated with three quantitative confidence levels. These results are based on weighted combinations of 1746 alternative seismic parameter value hypotheses.

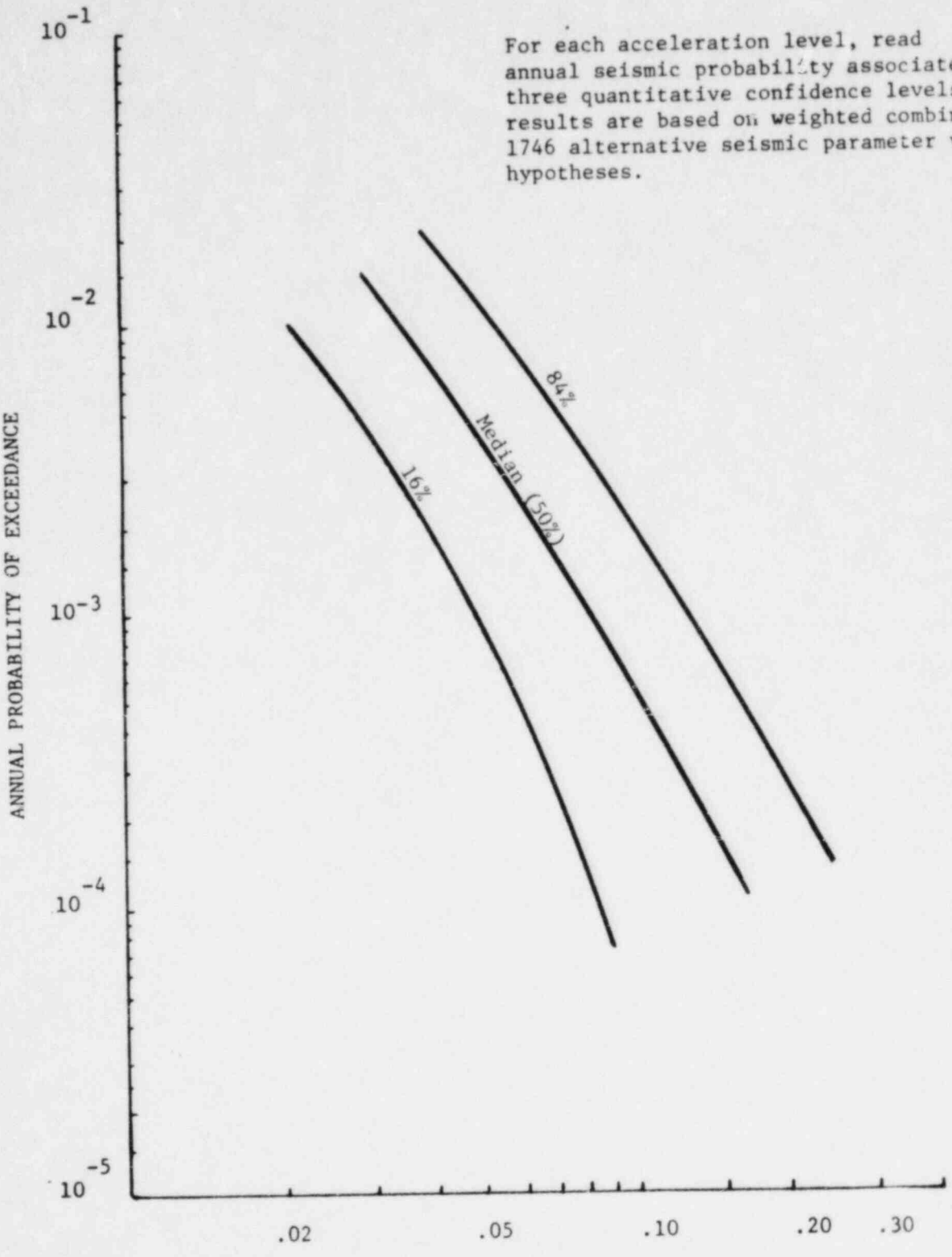

Fig. 1

FULL HISTORIC METHOD SEISMIC HAZARD RESULTS

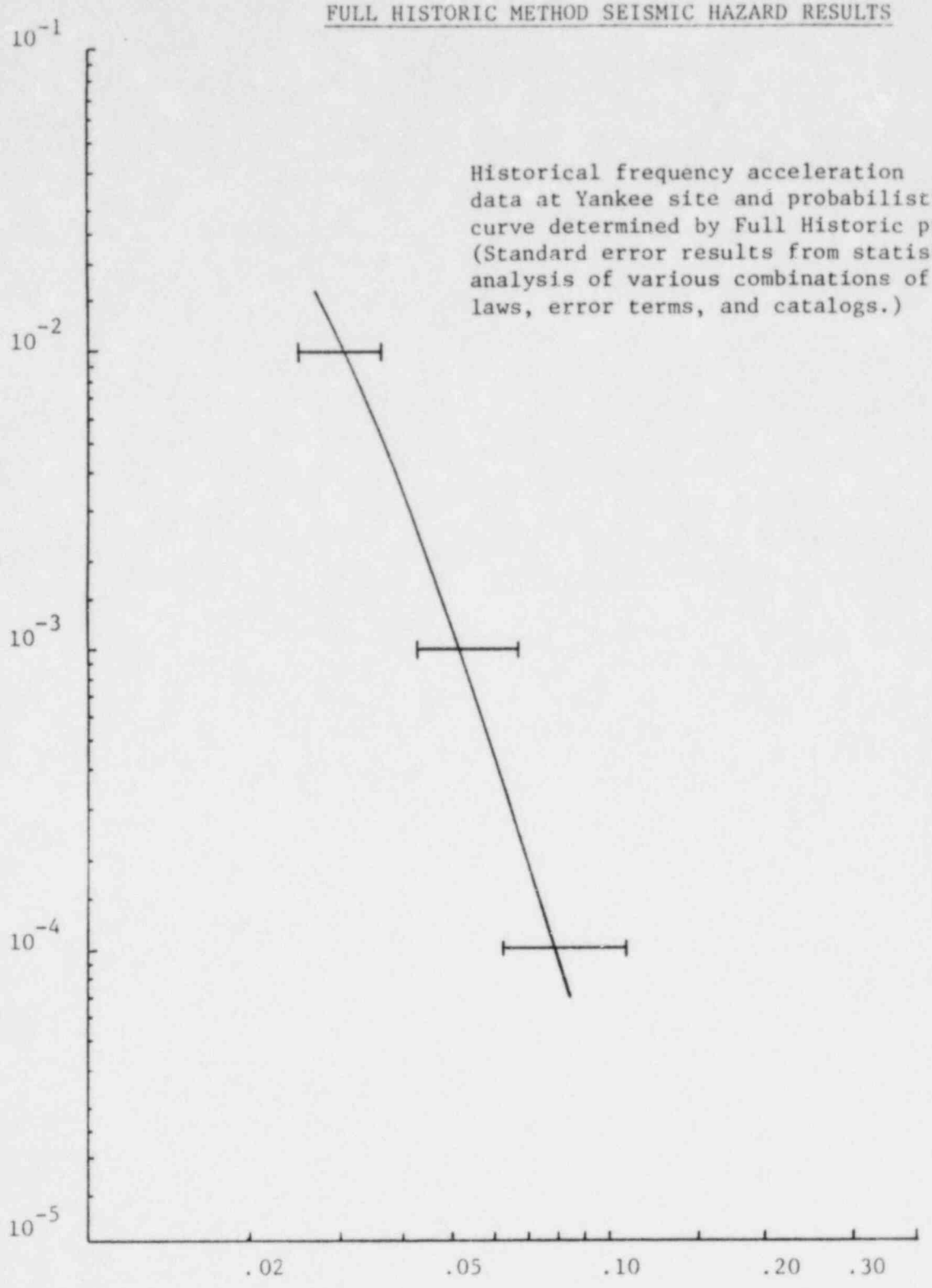

Fig. 2

COMPARISON OF SEISMIC

PROBABILISTIC RESULTS FROM:

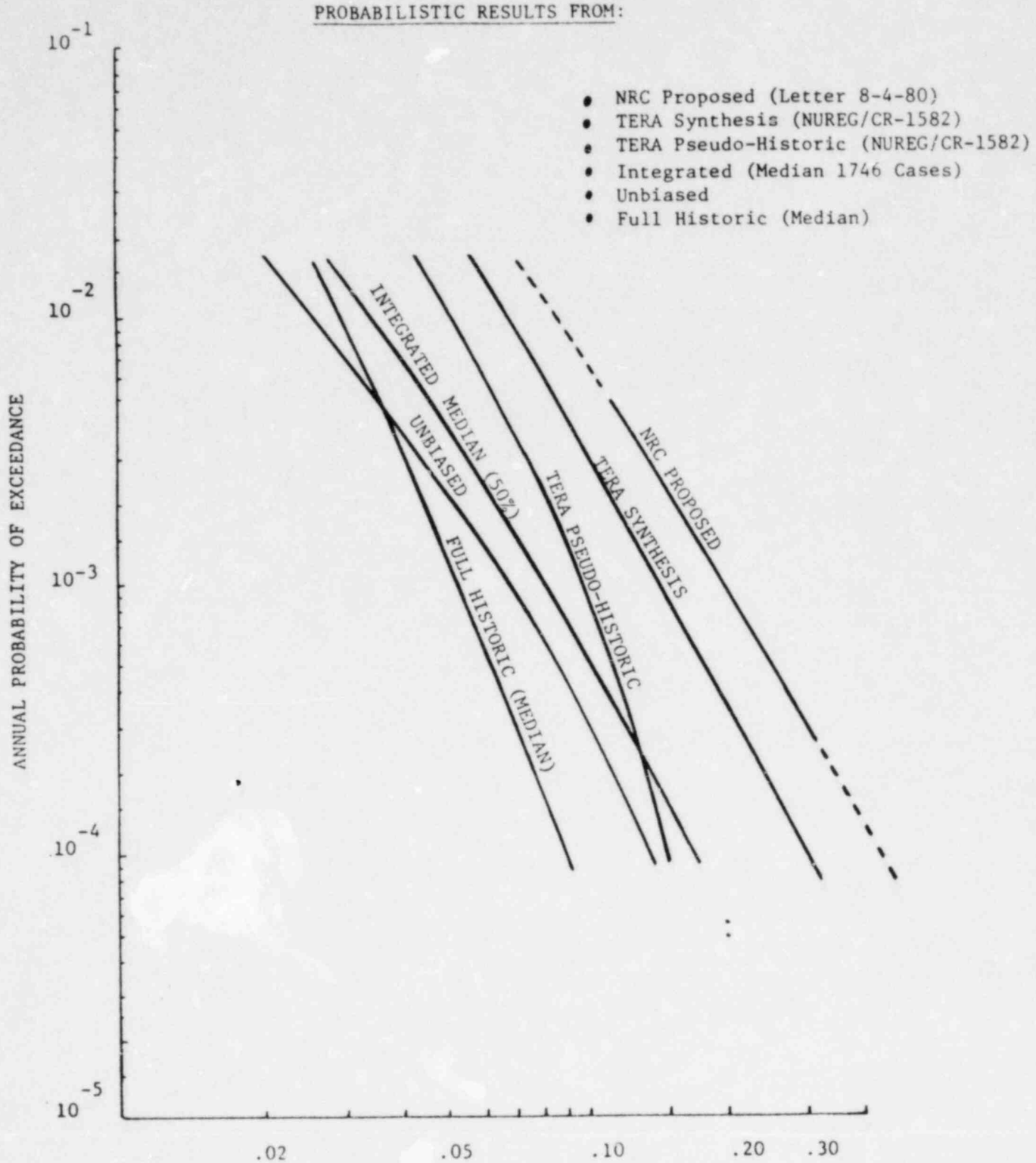

Fig. 3

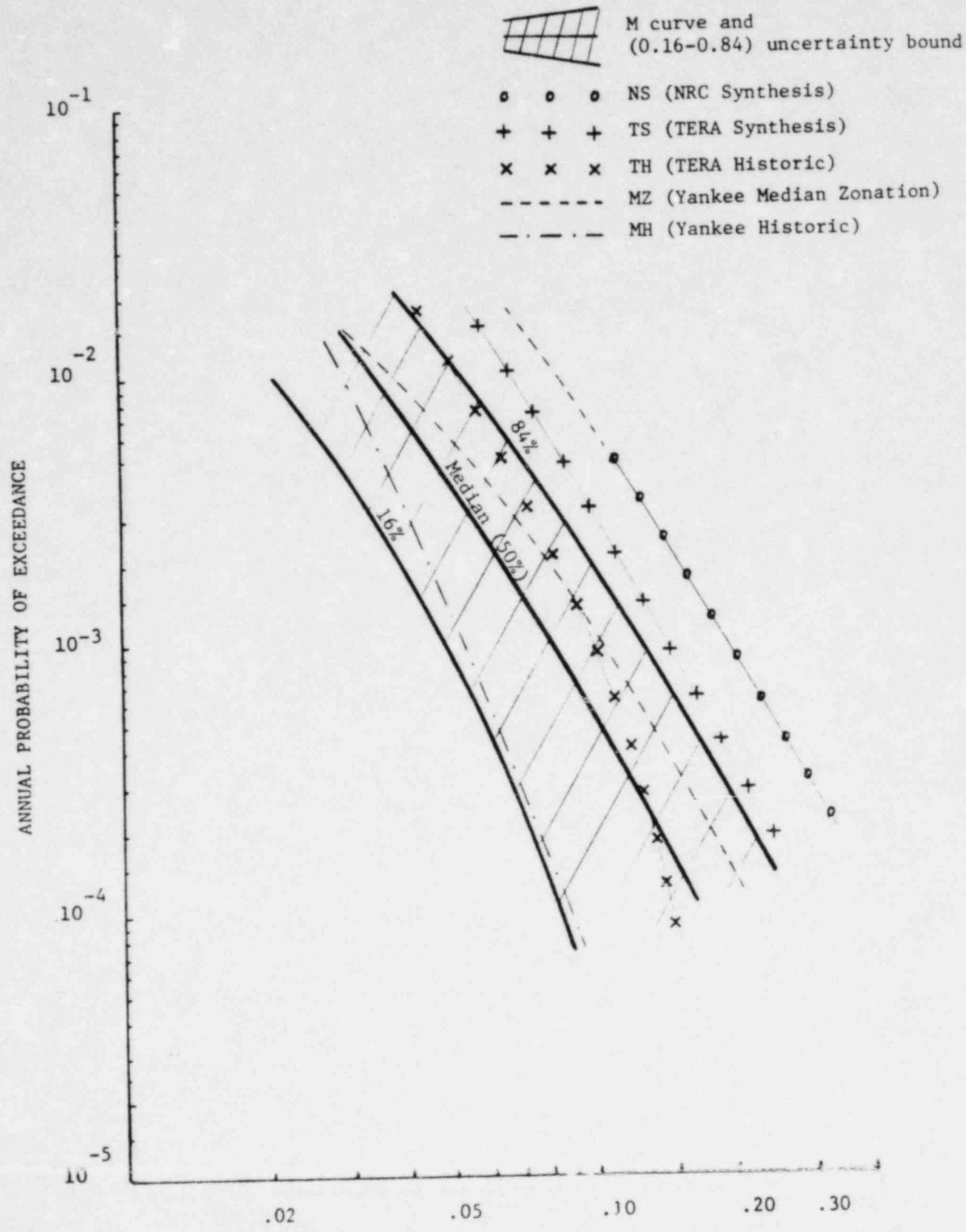

Fig. 4. Comparison of present seismic hazard estimates at Rowe with those in NUREG/CR-1582 (g).

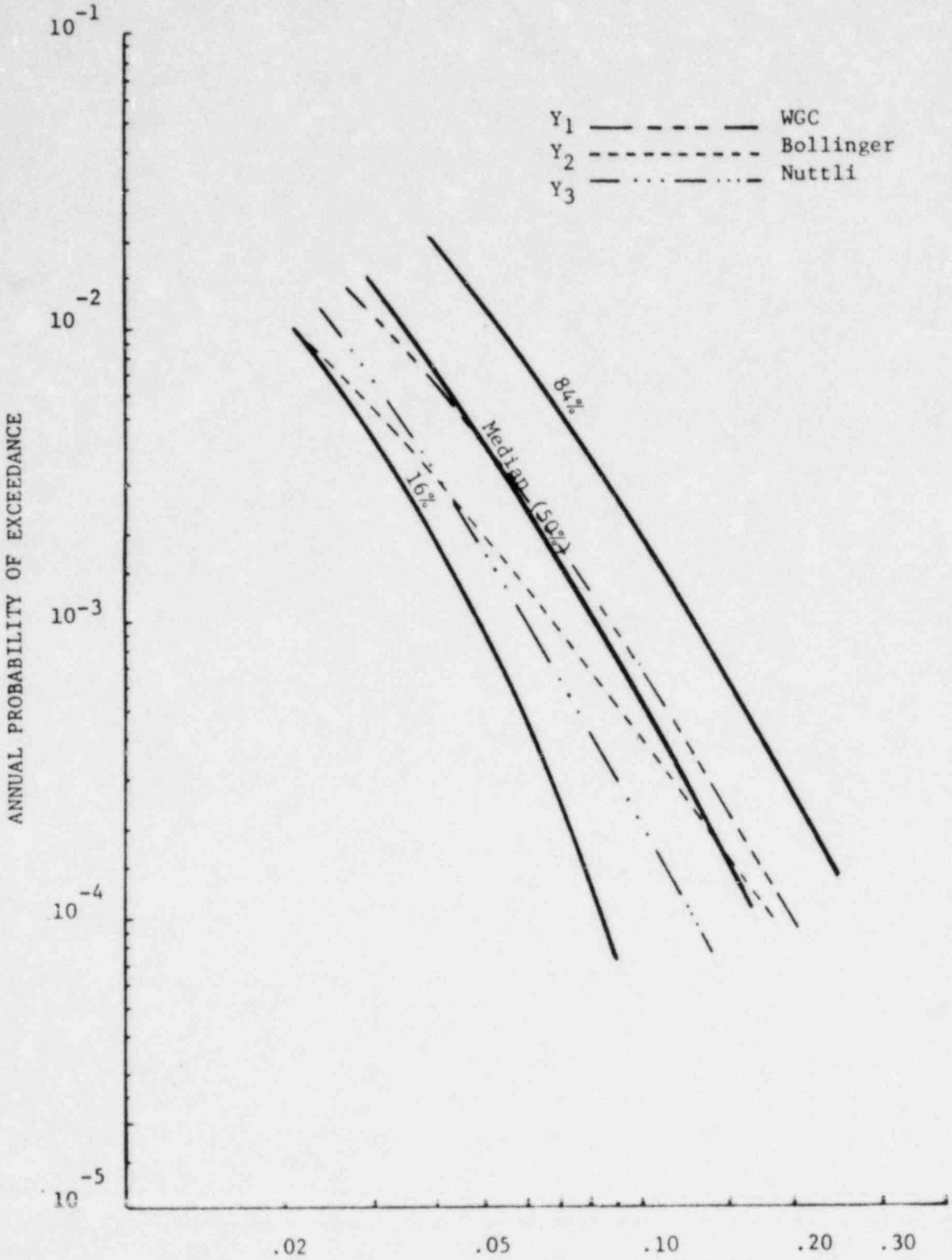

Fig. 5. Comparison of present seismic hazard estimates with those in YAEC-1263 (g)

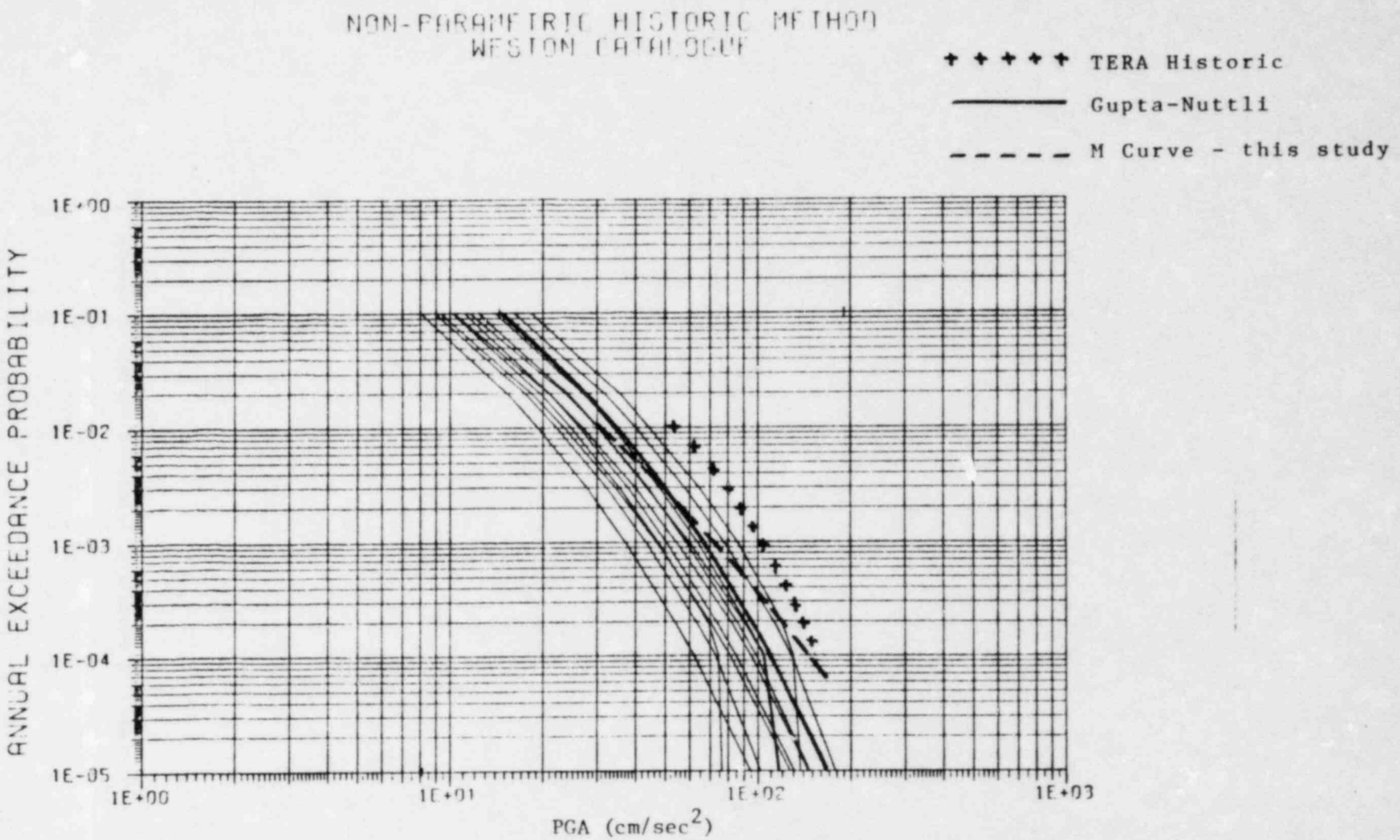

Fig. 6. Comparison of historic results using Weston catalog

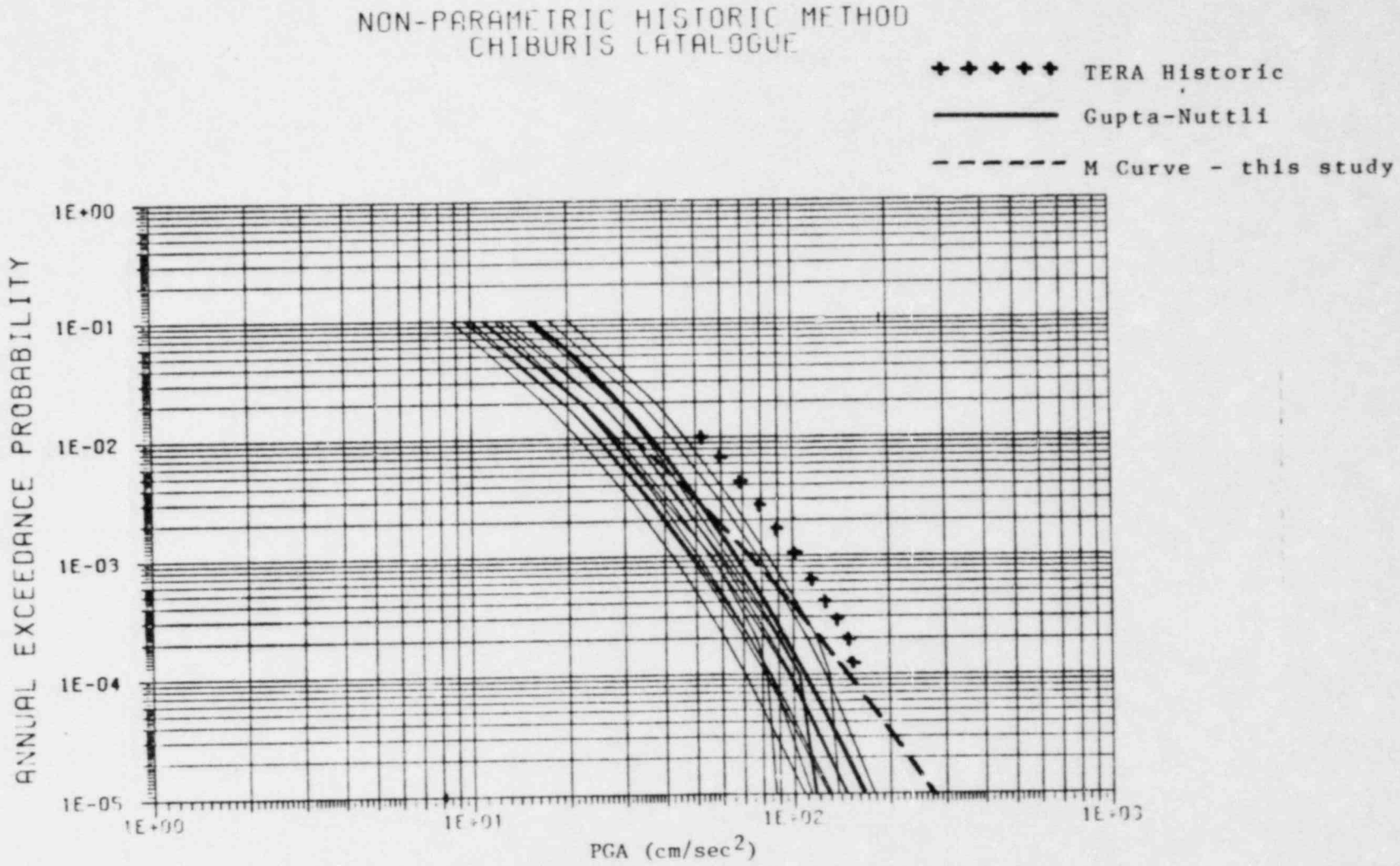

Fig. 7. Comparison of historic results using Chiburis catalog

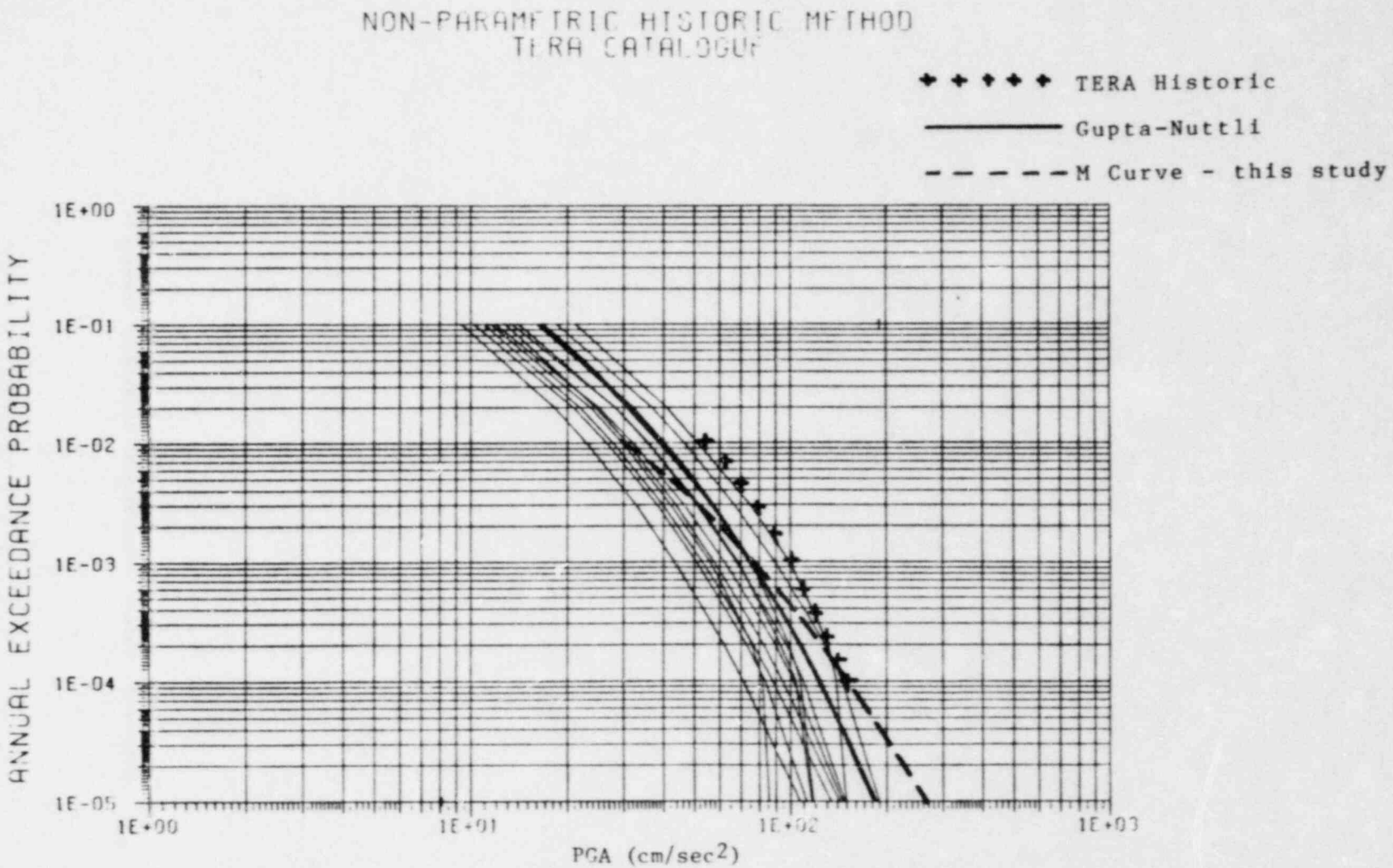

Fig. 8. Comparison of historic results using TERA catalog

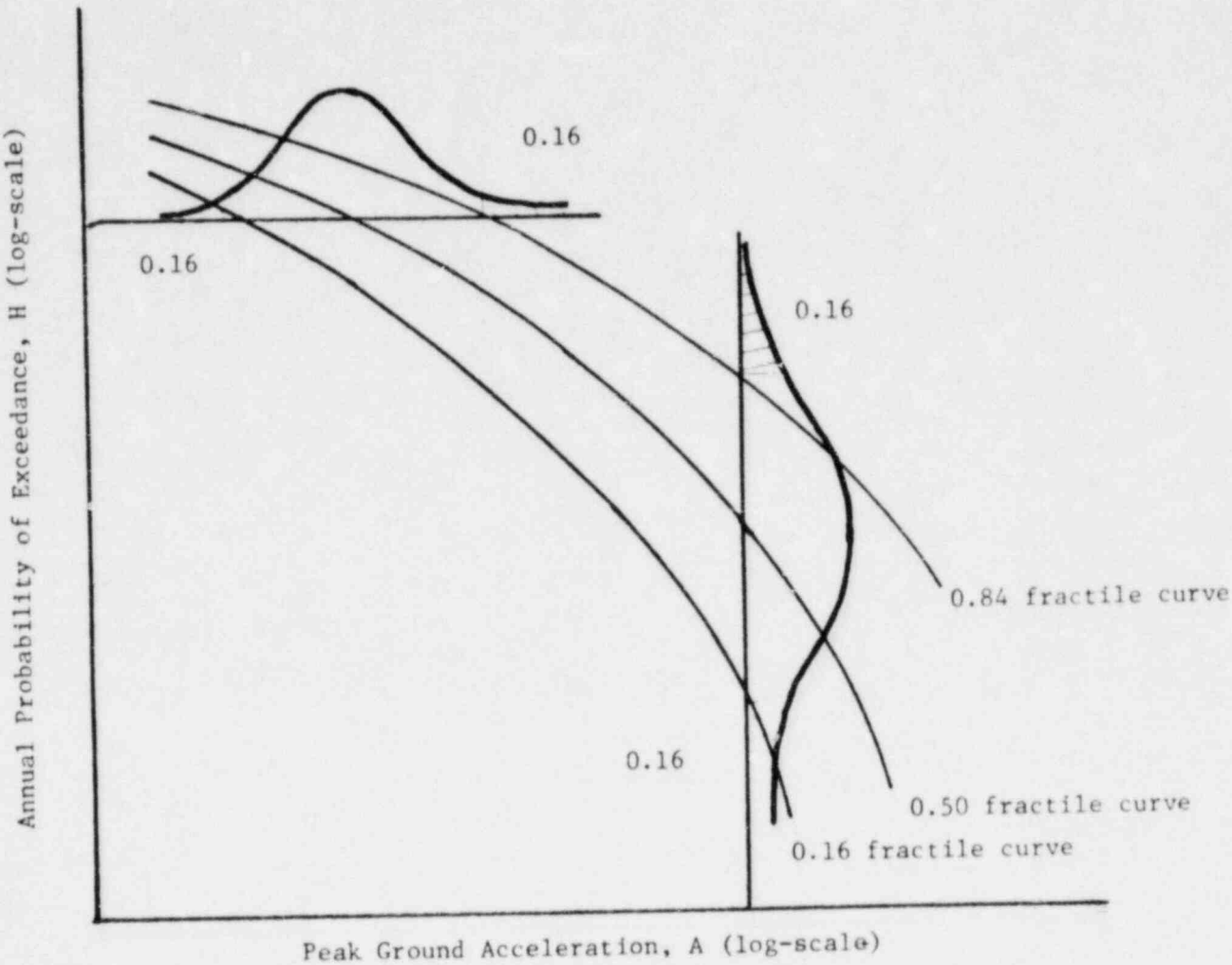

Fig. 9. Illustration of fractile hazard curves

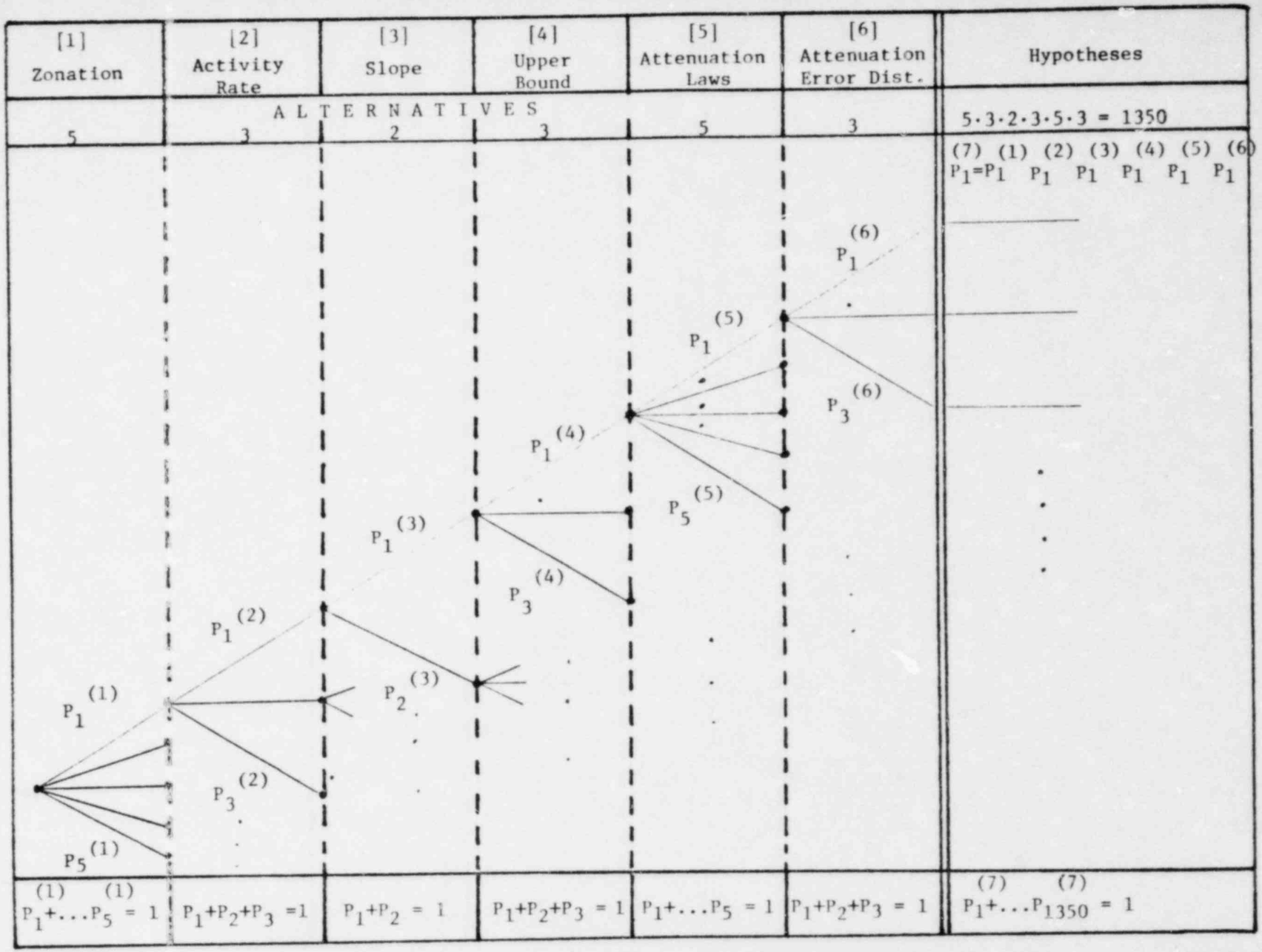

Fig. 19. Generation of hypotheses for zonation method and calculation of their probabilities

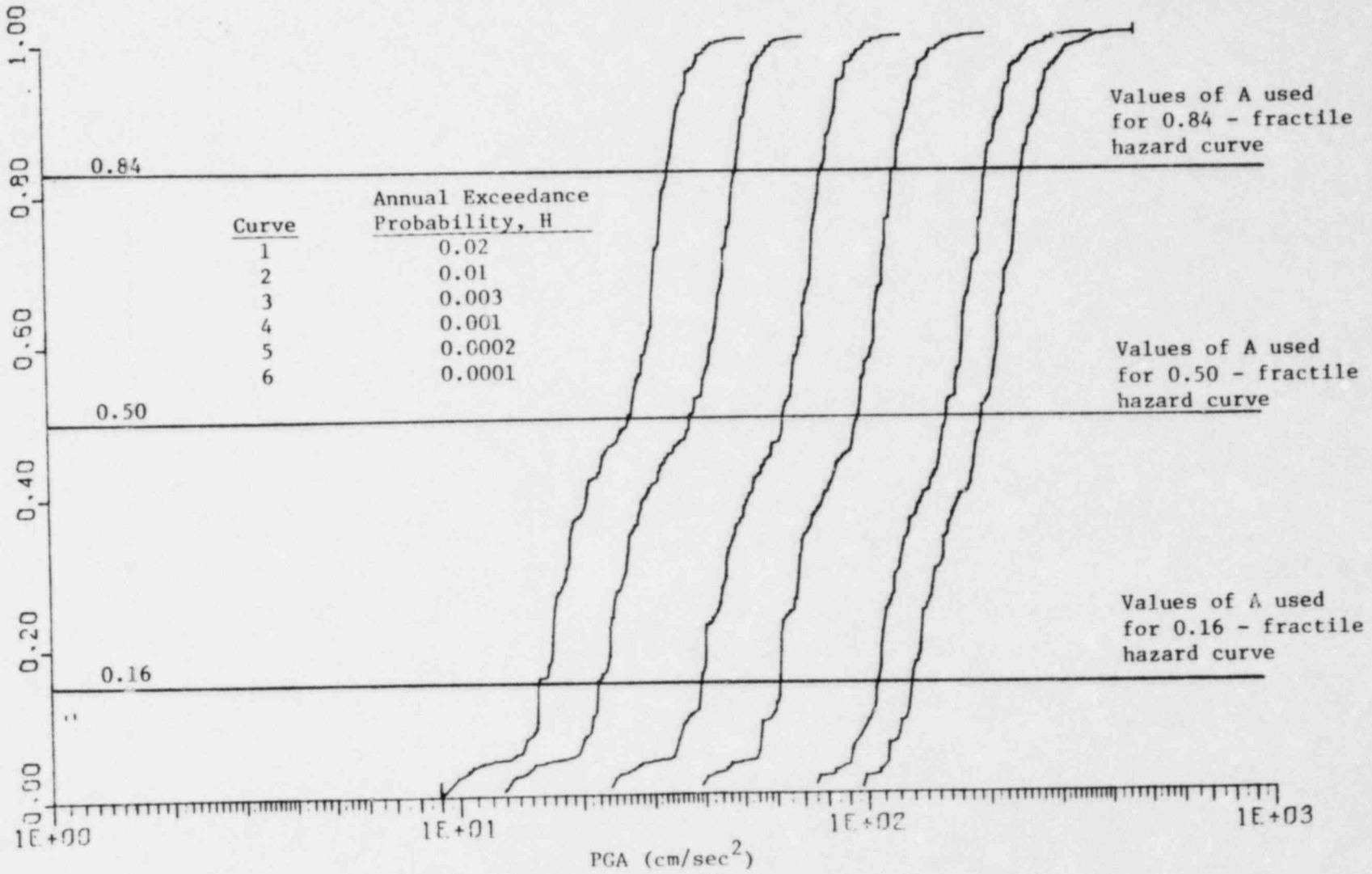

Fig. 11. Distribution of site acceleration for selected values of the annual exceedance probability - construction of fractile hazard functions

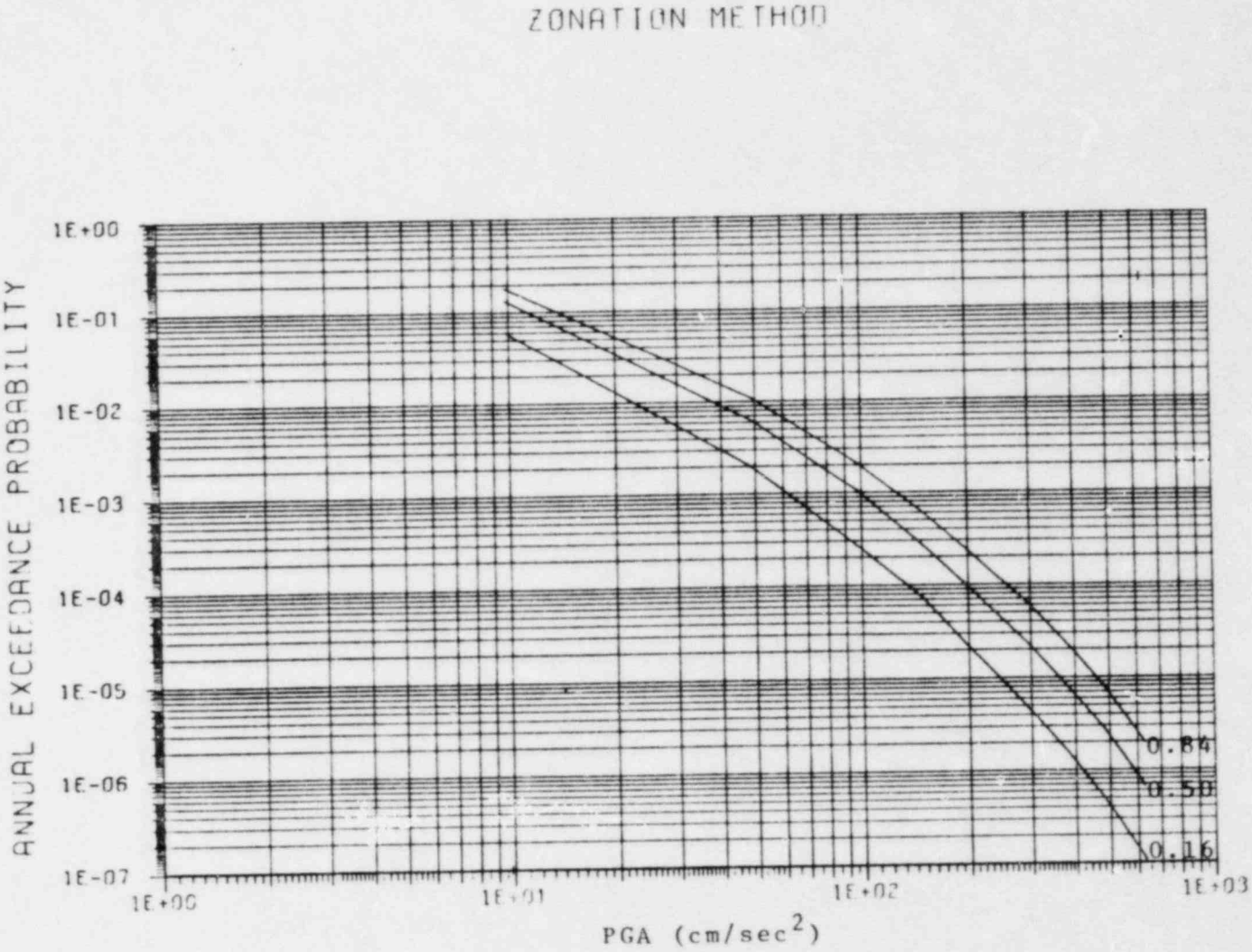

Fig. 12. 0.16, 0.50, and 0.84 fractile hazard function from the zonation method

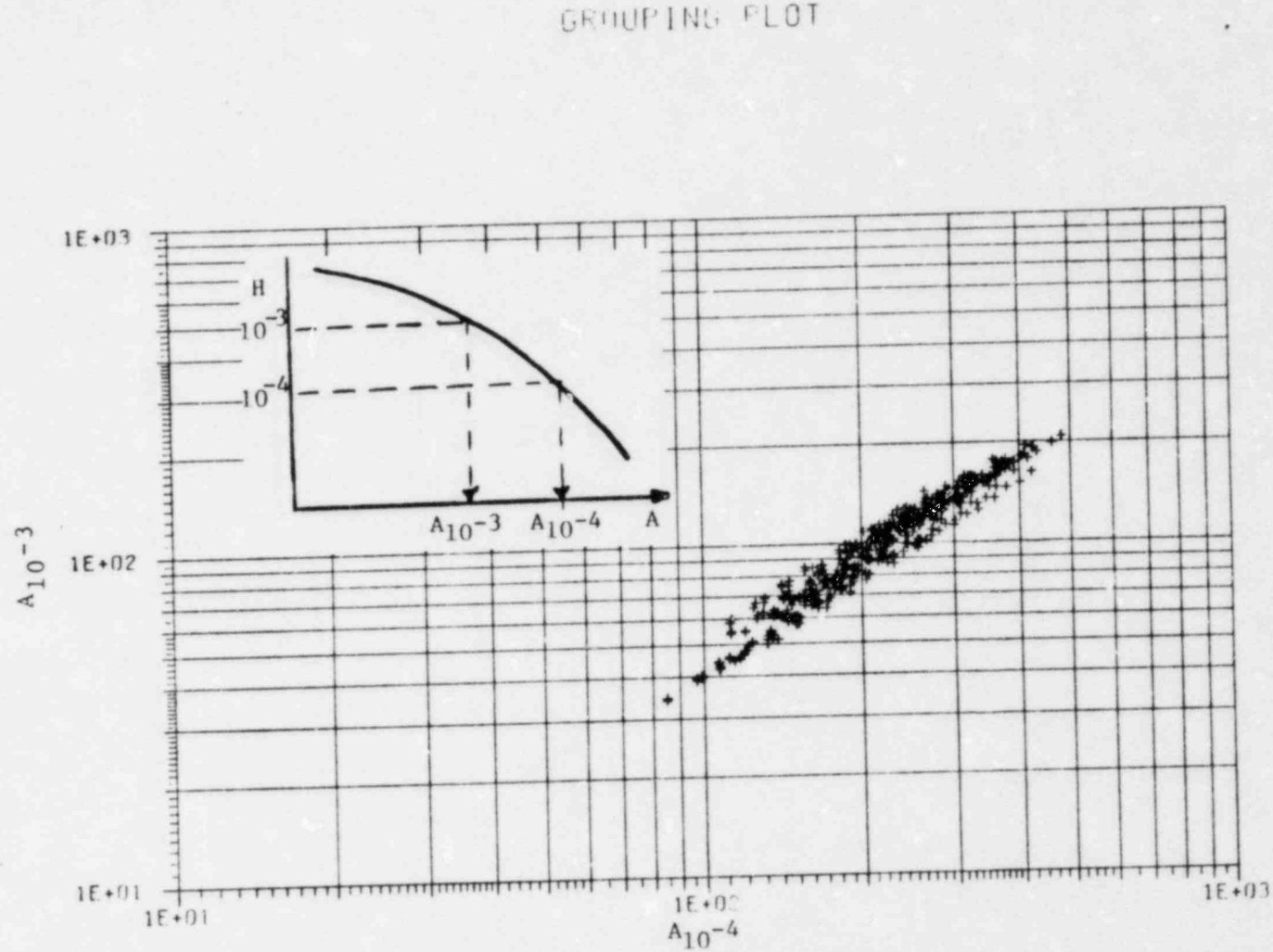

Fig. 13. "Cloud plot" of curves from the zonation method in terms of $A_{10^{-4}}$ and $A_{10^{-3}}$

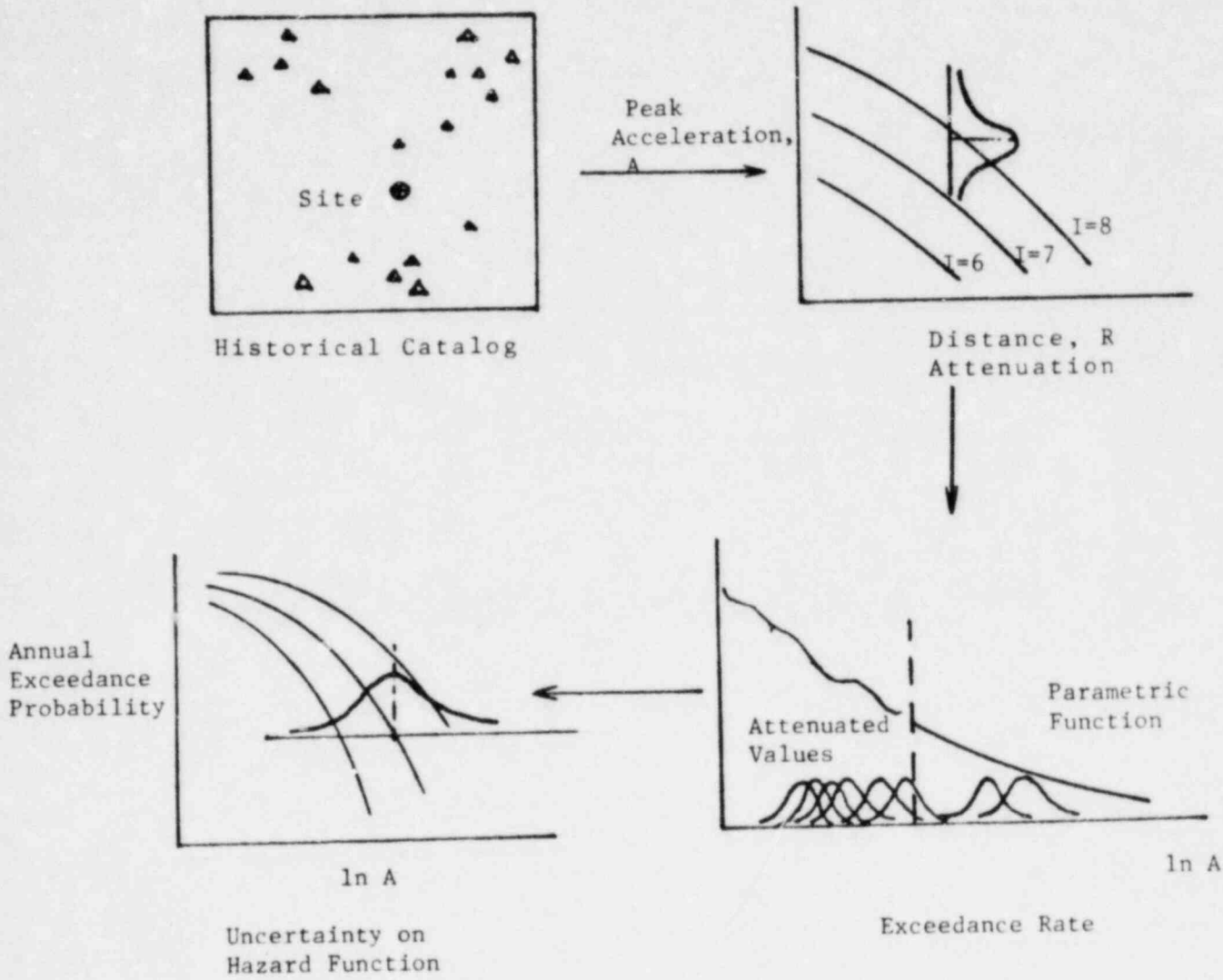

Fig. 14. Steps of the parametric "Full-Historic" method

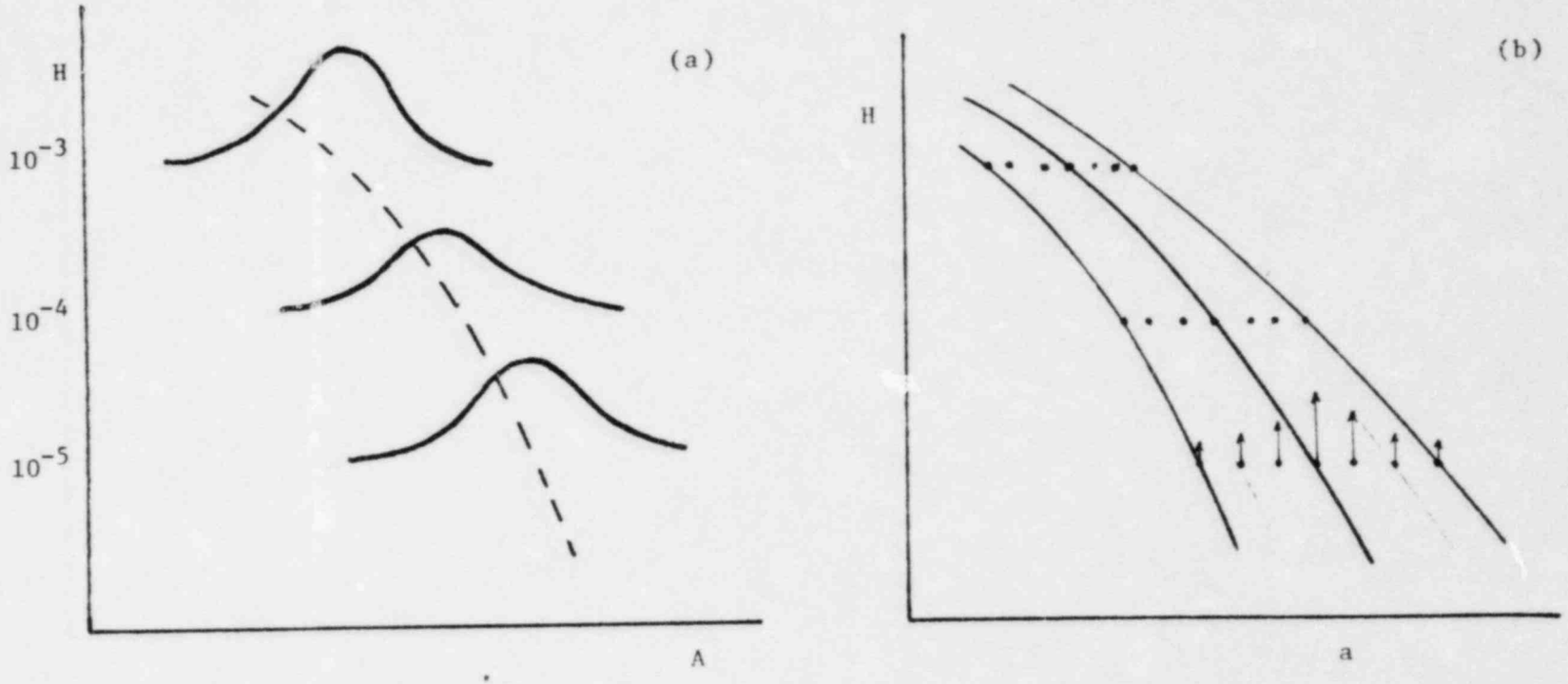

Fig. 15. Uncertainty on hazard function and its discretized representation

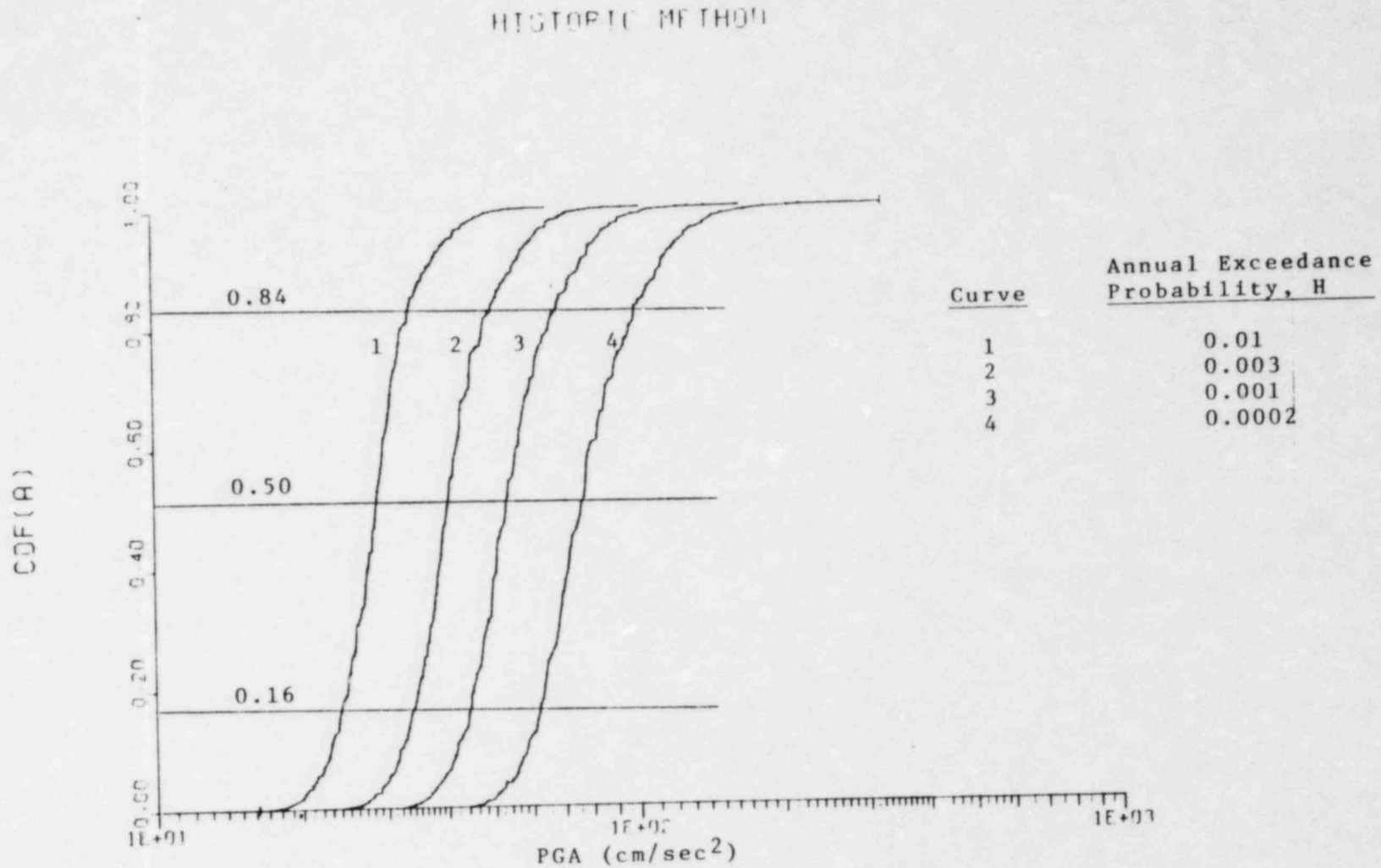

Fig. 16. Distribution of site acceleration for selected values of the annual exceedance probability--construction of fractile hazard function

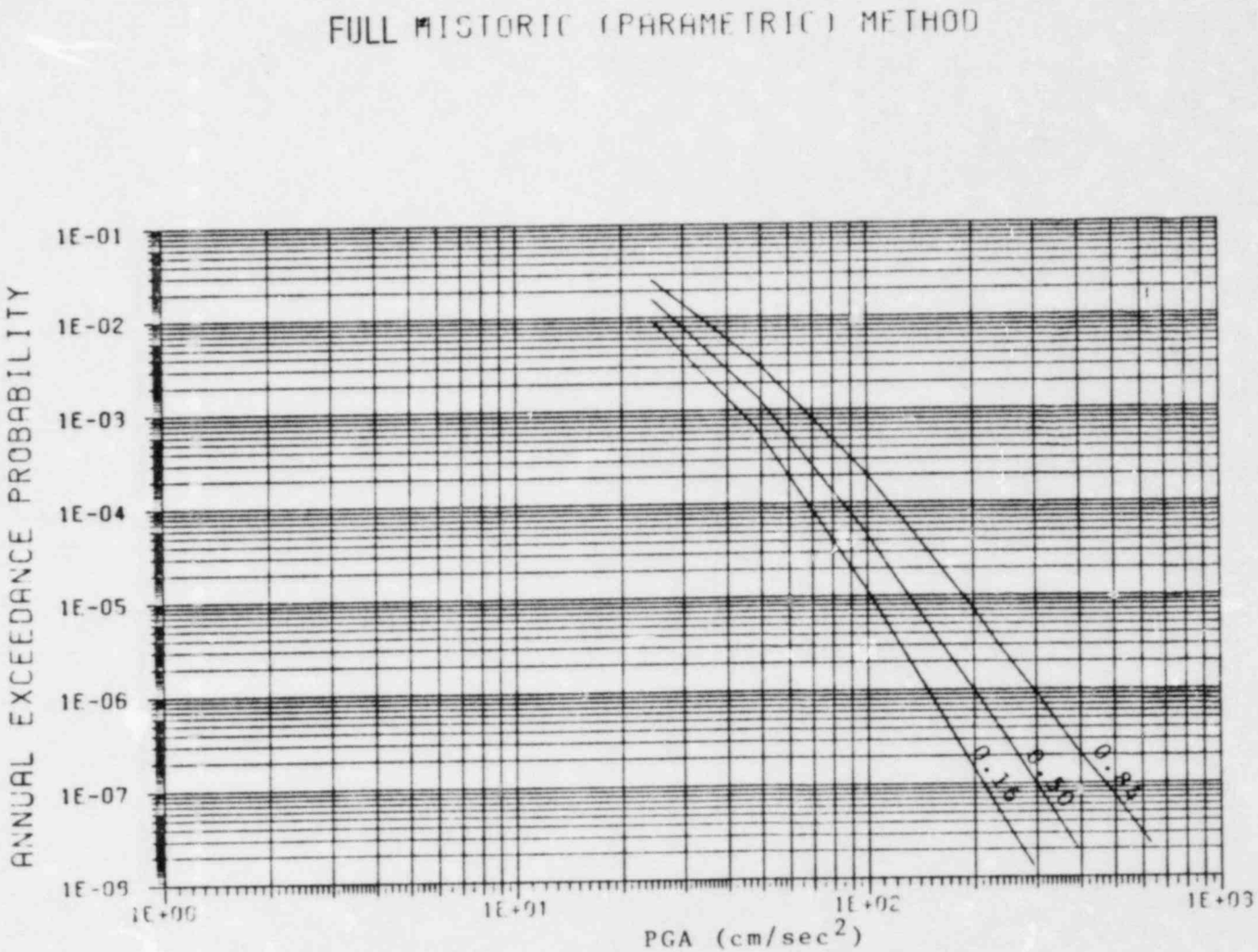

Fig. 17. 0.16, 0.50, and 0.84--Fractile hazard function using historic method

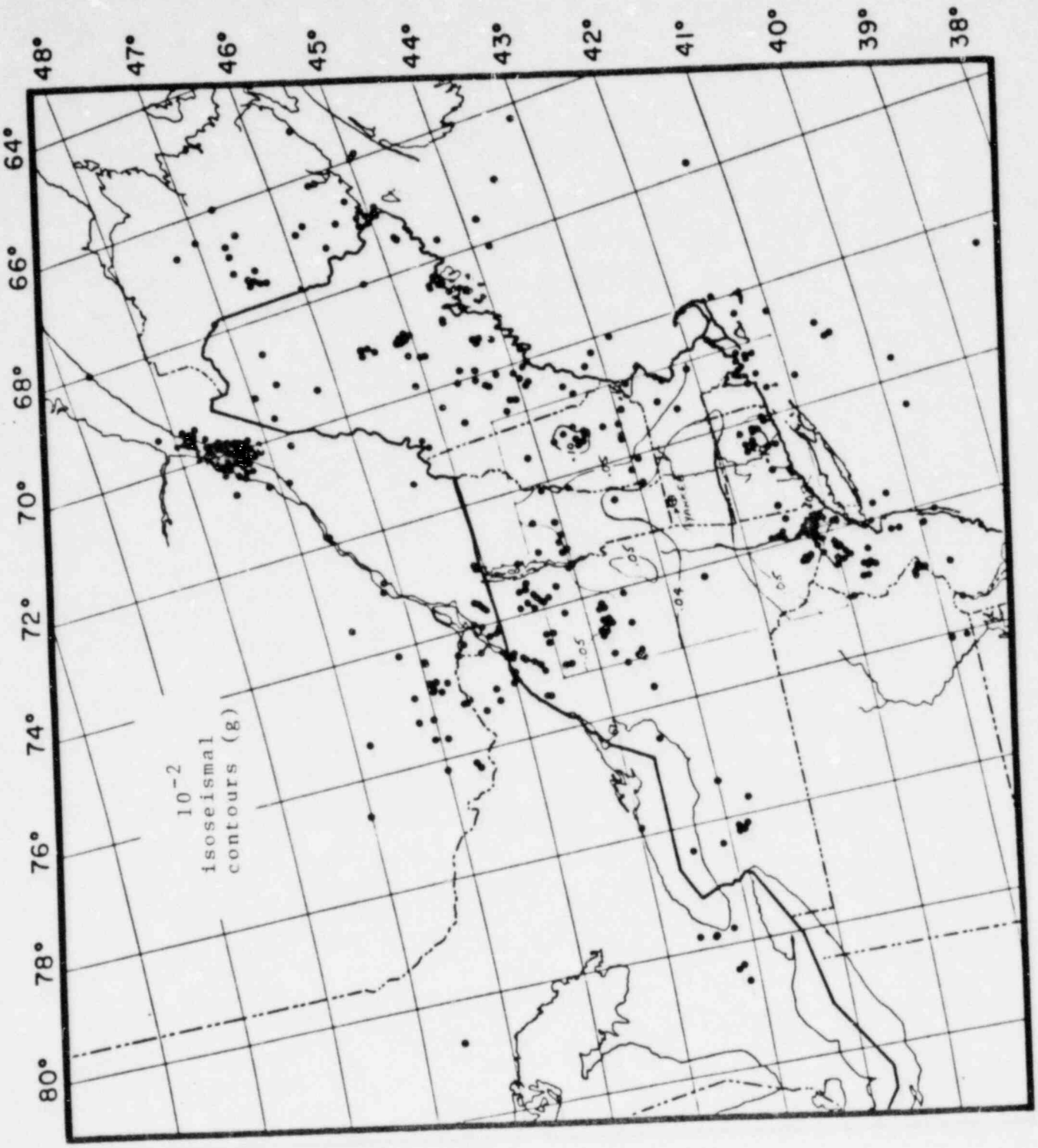

Fig. 18. Earthquake Epicenters during the period October 1975 - March 1981 with 10^{-2} isoseismals overlaid

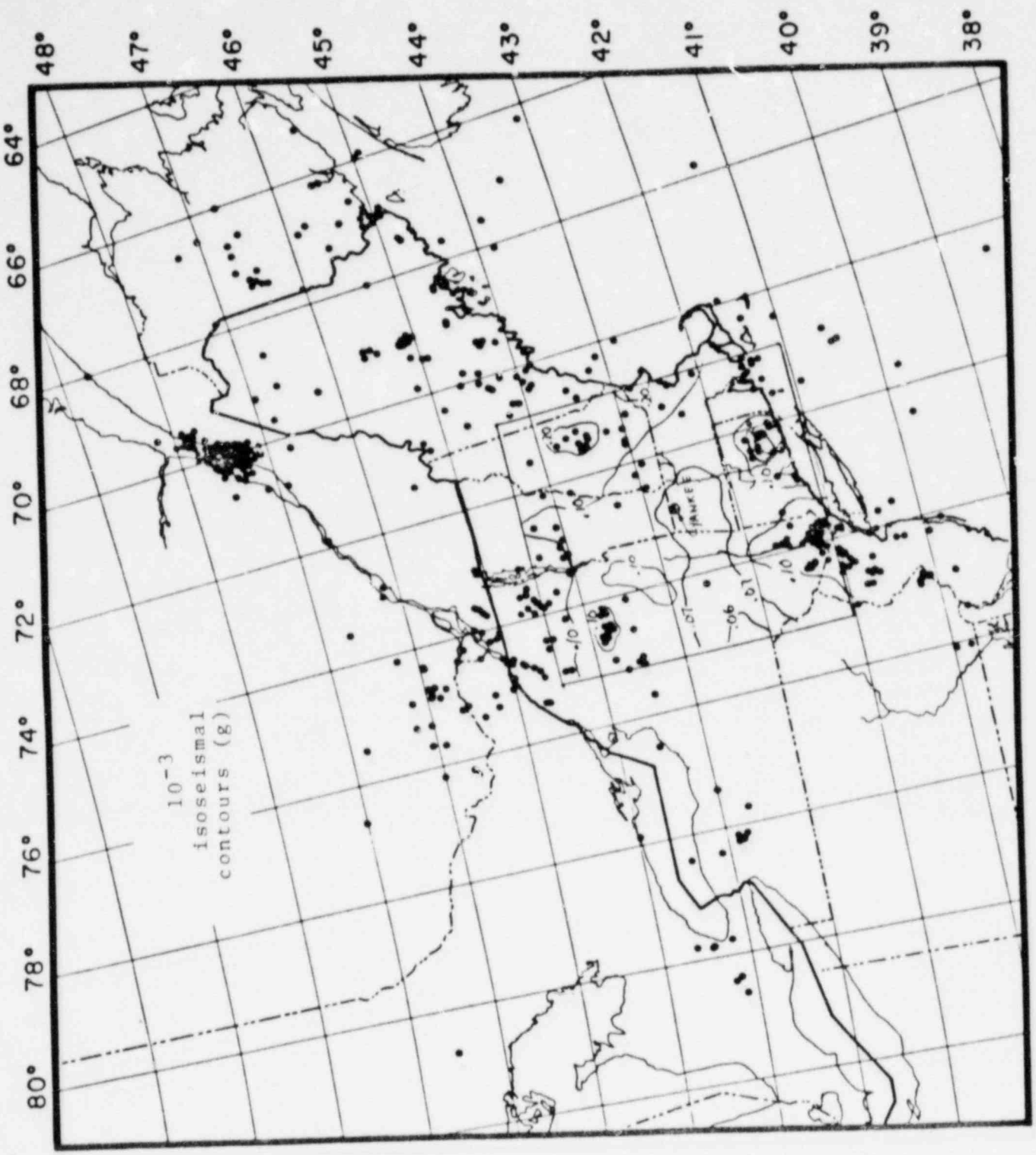

Fig. 19. Earthquake Epicenters during the period October 1975 - March 1981 with 10^{-3} isoseismals overlaid

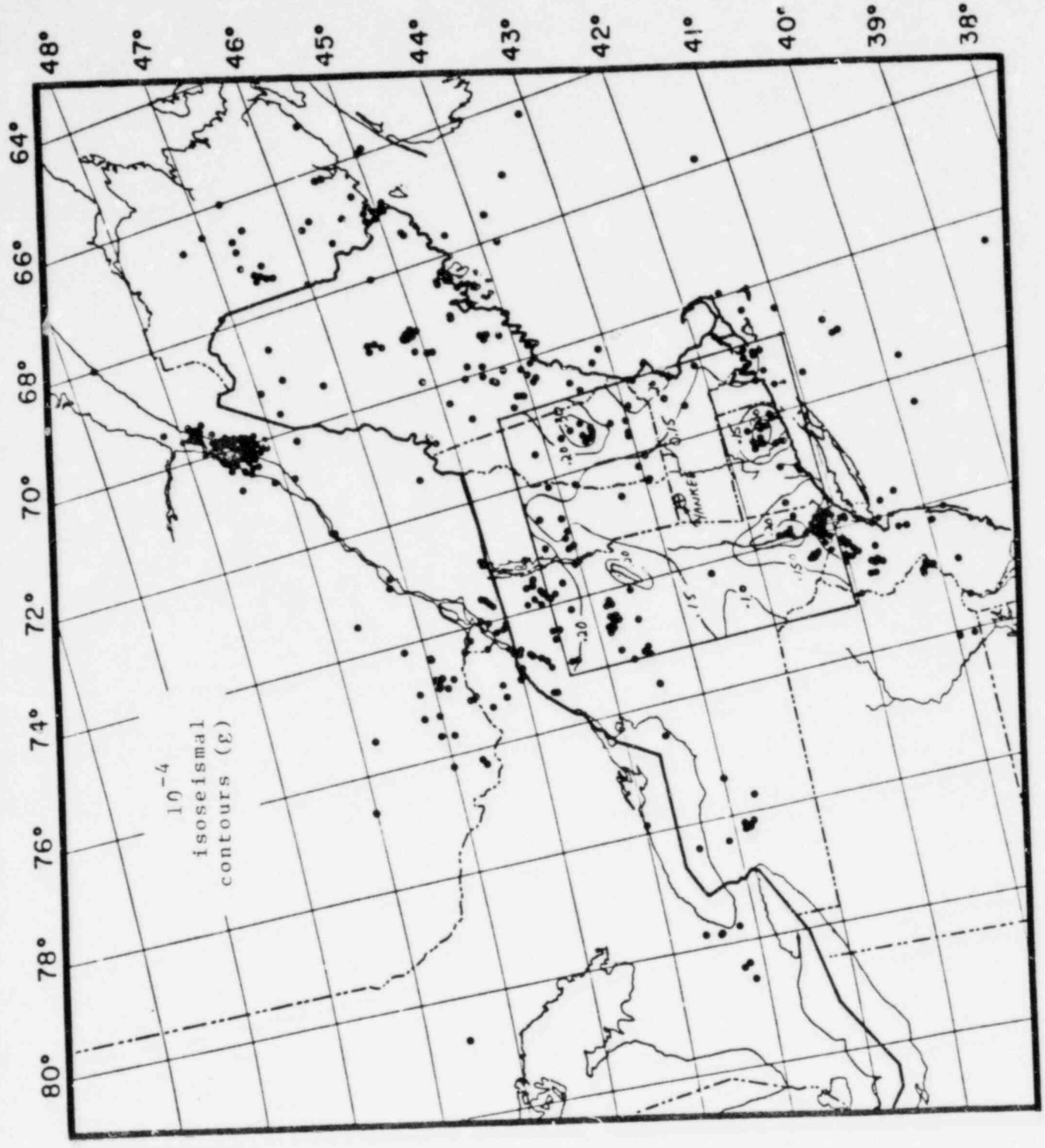

Fig. 20. Earthquake Epicenters during the period October 1975 - March 1981 with 10^{-4} isoseismals overlaid

TABLE 1

Accelerations (Fractions of g) That are Exceeded With Annual Probabilities 10^{-2}, 10^{-3}, and 10^{-4}. Comparison of This Study With Earlier Results

	CURVE	ANALYSIS	ANNUAL EXCEEDANCE PROBABILITY 10^{-2}	10^{-3}	10^{-4}
THIS STUDY	M	Median value from 1746 analyses	0.03	0.08	0.16
	0.16	0.16 fractile from 1746 analyses	0.02	0.05	0.08
	0.84	0.84 fractile from 1746 analyses	0.05	0.13	0.25
	UZ	Unbiased estimate (see Section 4)	0.03	0.06	0.13
	MZ	Median value from 1350 analyses using zonation method	0.04	0.11	0.22
	MH	Median value from 396 analyses using historic method	0.03	0.05	0.08
	NH_{min}	Range of estimates from 36 runs using NUREG/CR-1582 historic method	0.02	0.03	0.06
	NH_{max}			0.05	0.10
TERA	TS	Synthesis from zonation method	0.06	0.14	0.26
	TH	Historic method	0.05	0.10	0.15
NRC (4 Aug., 1980)	NS	Synthesis	(*)	0.199	(**)
PREVIOUS YANKEE	Y_1	Weston zonation Weston attenuation (σ_E = 0.85, no truncation)	0.03	0.08	0.19
	Y_2	Weston zonation Bollinger attenuation (σ_E = 0.95, no truncation)	0.02	0.07	0.18
	Y_3	Weston zonation Nuttli theoretical attenuation (σ_E = 0.57, no truncation)	0.02	0.06	0.12

(*) For an annual exceedance probability of 0.5×10^{-2}, NS = 0.11

(**) For an annual exceedance probability of 2.5×10^{-4}, NS = 0.31

TABLE 2

Examples of Intensity Re-Evaluations From Chiburis*

	Event	From	To
1727	Nov 17 MA Cape Ann	IX	VIII
1732	Sep 16 PQ Montreal	IX	VIII
1755	Nov 18 MA Cape Ann	IX	VIII
1791	May 16 CT Moodus-E. Haddam	VIII	VI
1857	Dec 23 ME Lewiston	VII	VI
1860	Oct 17 PQ Riviere Quelle	IX	VIII
1869	Oct 22 NB Bay of Fundy	VIII	VI

* The above are a few examples of the changes made by Chiburis in his new catalog relative to his old catalog, the latter was used in NUREG/CR-1582.

TABLE 3

Different Procedures of Estimating Seismic Hazard at the Rowe Site

REFERENCE METHOD	NUREG/CR-1582/TERA	ORIGINAL YANKEE	THIS STUDY
Non-Parametric Historic	X		X
Parametric Historic			X
Zonation	X	X	X

TABLE 4

ATTENUATION MODEL	CATALOG (*) (HISTORIC METHODS ONLY)	ZONATION (WGC ZONATION, a, b AND m_1 VALUES)	HISTORIC NON-PARAMETRIC	HISTORIC PARAMETRIC MEDIAN	HISTORIC PARAMETRIC [0.16, 0.84] PROBABILITY INTERVAL
Herrmann	W	0.02	0.03	0.03	[0.025, 0.030]
	C		0.03	0.03	[0.026, 0.031]
Bollinger(**)	W	0.02	0.02	0.02	[0.020, 0.025]
	C		0.03	0.02	[0.021, 0.026]
WGC	W	0.02	0.03	0.03	[0.026, 0.031]
	C		0.03	0.03	[0.028, 0.032]
Gupta/ Nuttli	W	0.03	0.04	0.04	[0.033, 0.041]
	C		0.04	0.04	[0.038, 0.045]
AVERAGE ALL ATTENUATIONS AND CATALOGS		0.02	0.03	0.03	

(*) W = WGC Catalog, C = Chiburis 1981 Catalog.

(**) For zonation method, result shown is average of Bollinger 1 and Bollinger 2.

Comparison of acceleration values (g's) that are exceeded at Rowe with annual probability 10^{-2}. The values from the zonation method correspond to the WGC source map, b, and m_1 values. In all cases, the attenuation error has truncated normal distribution with $\sigma_E = 0.7$ and truncation at $\pm 3\sigma_E$.

TABLE 5

ATTENUATION MODEL	CATALOG (*) (HISTORIC METHODS ONLY)	ZONATION (WGC ZONATION, b AND m_1 VALUES)	HISTORIC NON-PARAMETRIC	HISTORIC PARAMETRIC MEDIAN	HISTORIC PARAMETRIC [0.16, 0.84] PROBABILITY INTERVAL
Herrmann	W	0.06	0.05	0.05	[0.046, 0.056]
	C		0.06	0.05	[0.046, 0.056]
Bollinger(**)	W	0.05	0.04	0.04	[0.037, 0.046]
	C		0.05	0.04	[0.040, 0.050]
WGC	W	0.06	0.06	0.06	[0.051, 0.066]
	C		0.06	0.06	[0.052, 0.063]
Gupta/ Nuttli	W	0.07	0.08	0.08	[0.071, 0.091]
	C		0.08	0.08	[0.073, 0.088]
AVERAGE ALL ATTENUATIONS AND CATALOGS		0.06	0.06	0.06	

(*) W = WGC Catalog, C = Chiburis 1981 Catalog.

(**) For zonation method, result shown is average of Bollinger 1 and Bollinger 2.

Comparison of acceleration values (g's) that are exceeded at Rowe with annual probability 10^{-3}. The values from the zonation method correspond to the WGC source map and b, and m_1 values. In all cases, the attenuation error has truncated normal distribution with $\sigma_E = 0.7$ and truncation at $\pm 3\sigma_E$.

TABLE 6

ATTENUATION MODEL	CATALOG (*) (HISTORIC METHODS ONLY)	ZONATION (WGC ZONATION, b AND m_1 VALUES)	HISTORIC NON-PARAMETRIC	HISTORIC PARAMETRIC MEDIAN	HISTORIC PARAMETRIC [0.16, 0.84] PROBABILITY INTERVAL
Herrmann	W	0.14	0.10	0.08	[0.073, 0.101]
	C		0.10	0.08	[0.072, 0.099]
Bollinger(**)	W	0.12	0.07	0.07	[0.060, 0.081]
	C		0.08	0.07	[0.064, 0.092]
WGC	W	0.13	0.10	0.09	[0.085, 0.118]
	C		0.10	0.09	[0.083, 0.110]
Gupta/ Nuttli	W	0.13	0.13	0.13	[0.120, 0.170]
	C		0.13	0.13	[0.118, 0.155]
AVERAGE ALL ATTENUATIONS AND CATALOGS		0.13	0.10	0.09	

(*) W = WGC Catalog, C = Chiburis 1981 Catalog.

(**) For zonation method, result shown is average of Bollinger 1 and Bollinger 2.

Comparison of acceleration values (g's) that are exceeded at Rowe with annual probability 10^{-4}. The values from the zonation method correspond to WGC zonation, b, and m_1 values. In all cases, the attenuation error has truncated normal distribution with $\sigma_E = 0.7$ and truncation at $\pm 3\sigma_E$.

APPENDIX A

INTENSITY-MAGNITUDE CONVERSION OF HISTORICAL DATA AND ATTENUATION FUNCTIONS

In order to use the zonation method (e.g., the McGuire program), one must specify a recurrence law and an attenuation model. Such a law and model must be stated in terms of the same measure of earthquake "size", typically I_o or m_b.

Suppose that analysis is in terms of body-wave magnitude, m_b. This was the case in the NUREG/CR-1582 study and is the case here for the zonation approach. Because catalogs do not uniformly report the value of m_b and some of the attenuation models (e.g., Gupta-Nuttli and Bollinger) were originally developed in terms of I_o, conversion from I_o to m_b of some of the data and possibly of the attenuation is needed. Questions arise, such as: What conversion formulas should be used? Should conversion be the same for the data and the attenuation? Should uncertainty on the recurrence parameters and on the attenuation be increased because of conversion errors? In answering these questions, we shall first restrict analysis to the ideal case when the catalog reports either I_o or m_b for each earthquake, but later we shall extend considerations to the case when other information is available (e.g., felt area) or other size measures are reported, such as local magnitude m_L which is given for some earthquakes in the NUREG catalog. These questions are also examined in Appendix D1. Four ideal situations are distinguished which are obtained as combinations of:

"Important Data" for Recurrence Law

1. In terms of I_o,

2. In terms of m_b.

Attenuation Function

1. In terms of I_o,

2. In terms of m_b.

By "important data", we mean size information on the earthquakes that more significantly influence hazard at the site, hence primarily on large-sized earthquakes. In the case of New England, such important data is mostly in terms of I_o.

The notation $I_o(m_b)$ and $m_b(I_o)$ is used here for the conditional expectation (regression) of I_o given m_b and of m_b given I_o. Hence,

$$\hat{I}_o(m_b) = E[I_o | m_b]$$
$$\hat{m}_b(I_o) = E[m_b | I_o] \qquad \text{(A1)}$$

The inverse relationships are denoted by $\hat{I}_o^{-1}(m_b)$ and $\hat{m}_b^{-1}(I_o)$, respectively. For example, if $\hat{m}_b(I_o) = 0.5\, I_o + 1.75$, then $\hat{m}_b^{-1}(I_o) = 2\, m_b - 3.5$. Notice that in general, $m_b(I_o) \neq I_o^{-1}(m_b)$ because of differences between the regressions in Equation A1. (The problem is analogous to the magnitude-versus-rupture-length conversion issue.)

1. Important Data in Terms of I_o

1.1 Attenuation in Terms of I_o

In the limiting case when all the data is in terms of I_o, transformation may be avoided. However, identical results are obtained by transforming data and attenuation using the same monotonic function, $f(I_o)$. For example (but not necessarily), $f(I_o) = \hat{m}_b(I_o)$. There is no increase of uncertainty either in the recurrence or in the attenuation law as a result of this transformation.

If only the "unimportant" data is in terms of m_b, then one is close to the limiting case and one can therefore:

- Convert data on I_o by calculating $\hat{m}_b(I_o)$ (e.g., $\hat{m}_b(I_o) = 0.5\ I_o + 1.75$).

- Convert the attenuation function by replacing I_o with $\hat{m}_b^{-1}(I_o)$ $(= 2m_b - 3.5)$.

No increase of uncertainty results from this operation.

1.2 Attenuation in Terms of m_b

In this case, the data in I_o should be converted to m_b using the conditional expectation $\hat{m}_b(I_o)$. The actual body-wave magnitude of the historical events is uncertain, namely due to conversion errors. This uncertainty should be accounted for when fitting the magnitude-recurrence model, resulting in increased uncertainty on the recurrence parameters.

2. Important Data in Terms of m_b

2.1 Attenuation in Terms of I_o

The attenuation model is converted to m_b by replacing I_o with $\hat{I}_o(m_b)$. The attenuation error variance is increased to reflect conversion uncertainty (uncertainty on the error term in $I_o = \hat{I}_o(m_b) + \eta$). The "unimportant" data in I_o can be converted by using the other regression, $\hat{m}_b(I_o)$. Conversion uncertainty may have some effect on uncertainty of the recurrence parameters. However, this effect should be small due to the "small importance" of the data that is being converted.

2.2 Attenuation in Terms of m_b

This case can be treated in the same way as 2.1, except that conversion has a smaller effect on the uncertainty of the recurrence parameters.

The above conditions are clearly ideal, but they provide guidance for devising conversion procedures in more realistic cases, such as those of the NRC/LLL/TERA analysis and of the present analysis. These cases are considered next.

Present Analysis

- Catalog: Completed Weston (see Appendix C). Data in this catalog is in mixed form (I_o and m_b), with the "important data" for Rowe mainly in terms of I_o. On many earthquakes, however additional information is available on isoseismals and felt area to improve (reduce the uncertainty in) the m_b estimate.

- Attenuation. Four models have been used:

  1. Weston, in terms of m_b;

  2. Herrmann, theoretical, in terms of m_b;

  3. Gupta-Nuttli, in terms of I_o;

  4. Bollinger, in terms of I_o.

Ideal cases 1.1 and 1.2 are relevant here. For the first two attenuation models, which are in terms of m_b, catalog data on I_o was converted to m_b using Nuttli-Herrmann's expression for $\hat{m}_b(I_o)$,

$$\hat{m}_b(I_o) = 0.5\ I_o + 1.75 \qquad \text{(A2)}$$

Whenever additional information (felt area, isoseismals) was available, the improved m_b estimate was used.

For the last two attenuations, data on I_o has been converted as before and the attenuations have been converted by replacing I_o with $\hat{m}_b^{-1}(I_o)$, where

$$\hat{m}_b^{-1}(I_o) = 2\, m_b - 3.5 \qquad \text{(A3)}$$

It is important to recall (Case 1-1) that for itensity-based attenuations, hazard results are insensitive to the form of the conversion formula in Equation A2 (and its inverse in Equation A3).

In the case of Bollinger's model, an additional analysis was made, with the attenuation function converted to m_b by replacing I_o with the regression $\hat{I}_o(m_b)$, where $\hat{I}_o(m_b)$ has been calculated from data (see YAEC-1263) to be

$$\hat{I}_o(m_b) = 1.37\, m_b - 0.14 \qquad \text{(A4)}$$

NRC/LLL/TERA Analysis

- NUREG Catalog - This catalog (see Appendix C) is in mixed form, with earthquake intensity measured in terms of I_o, m_b, and M_L. The important data is mainly in I_o.

- Attenuation:

Again, ideal cases 1.1 and 1.2 apply, except that now the catalog uses three different intensity measures. For some major earthquakes, the values of M_L in the catalog were obtained from data originally in I_o by using the relationship

$$m_L(I_o) = E[m_L | I_o] = \frac{2}{3} I_o + 1 \qquad \text{(A5)}$$

In NUREG/CR-1582, all data was converted to m_b by using:

m_b, whenever m_b was available; (a)

$m_b = m_L$, whenever m_L was available (and m_b was not); (b) (A6)

$m_b = 0.5\, I_o + 1.75$, when only I_o was available. (c)

The conversion $m_b = m_L$ was justified on the basis that m_L is a reasonable expected value for $(m_b | m_L)$. However, the three formulas

$$E[m_b | I_o] = 0.5\ I_o + 1.75 \qquad \text{(Equation A6c)}$$

$$E[m_L | I_o] = \frac{2}{3}\ I_o + 1 \qquad \text{(Equation A5)} \qquad \text{(A7)}$$

$$E[m_b | m_L] = m_L \qquad \text{(Equation A6b)}$$

can be proven to be contradictory. The consequence of such mathematical incompatibility would have been small if conversion to m_b had been made wherever possible from I_o (i.e., using Equation A6c) as opposed to m_L (Equation A6b). An example is the 1732 Montreal earthquake. In the NUREG catalog, this event is reported to have had epicentral intensity I_o = IX; hence, the catalog listed $m_L = (\frac{2}{3})(9) + 1 = 7$. It is incorrect in this case to estimate m_b as $m_b = m_L = 7$ as was done in NUREG/CR-1582. Because data is originally in I_o, the appropriate expected value of m_b is

$$E[m_b | I_o = 9] = (0.5)(9) + 1.75 = 6.25 \qquad \text{(A8)}$$

In his revised catalog, Chiburis (1981) concurs with WGC in estimating the epicentral intensity of this earthquake as VIII. In this case, the expected body-wave magnitude is further reduced to 5.75.

Conservatism of the catalog and of the conversion procedure compound in the NUREG analysis to produce high hazard estimates, from both the historic and the zonation methods.

APPENDIX B

SEISMICITY AND ZONATION OF NORTHEASTERN UNITED STATES

In the zonation method of hazard analysis, one must specify zones which are assumed by the program to be internally homogeneous with respect to seismicity. In particular, within each zone it is assumed that the mean activity rate a (per square kilometer, say) is the same everywhere. The value of a, of course, may vary from zone to zone.

Northeastern U.S. Seismicity

Taken as a whole, the northeastern states clearly do not display homogeneous seismicity; Figures B1 and B2, showing historic and recent instrumental activity respectively, display definite spatial variation in the mean activity rate. Furthermore, comparison of the two figures demonstrates the strong stability of those relative activity rates, implying that historic rates will provide the most reliable available estimate of activity over the next twenty years of interest. The data also suggest strongly zones of relatively homogeneous seismicity.

The most recent published detailed scientific study of this region is by Yang and Aggarwal (1). (It appeared after even the second-round questionnaire by TERA.) They have considered both the seismicity (historic and instrumental) and the available geological and tectonic evidence. They state, "Seismic activity in the Northeast is relatively stationary in space: those areas that have had little or no seismicity historically are relatively aseismic today." They also state that there is no evidence supporting the so-called Boston-Ottawa zone. The two authors also explicitly draw attention to the "relatively aseismic" regions of central New York, Vermont and western Massachusetts.

Within this background information, we review next the various hypothesized sets of zones considered in this study.

Zonation

Five different configurations of earthquake zones ("sources") relevant to the Yankee site have been constructed with the aim of covering all the possibilities with significant likelihood of being correct. These configurations are:

A. "Boston-Ottawa/Piedmont", as described by Expert 3 in NUREG/CR-1582; Figure B3;

B. "WGC", as proposed by the project seismological consultants, Weston Geophysical Corporation; Figure B4;

C. "Piedmont/WGC", a combination of the NUREG/CR-1582 proposed Piedmont zone at and south of the site, plus the WGC zones to the north; Figure B5;

D. "Boston-Ottawa/WGC", a combination of the Boston-Ottawa zone to the north and the WGC zones at and to the south of the site; Figure B6;

E. "Modified Piedmont", similar to C except that the WGC zone that includes the site extends below the northern NRC-Piedmont border; Figure B7.

These zones cover cases suggested:

1. By the project's seismological consultants (B);

2. By several NUREG/CR-1582 experts (A and C);

3. By others (D and E).

Several approaches were used to assign relative weights to these configurations. The first is based on published apparent preferences of various knowledgeable persons without significant interpretation by these

writers. For this case, we consider 9 of the 10 NUREG/CR-1582 experts* plus four others not included there: Yang and Aggarwal (Y&A) (1), Algermissen and Perkins (A&P) and, Hadley and Devine (H&D) (Figures B8 and B9 as interpreted by McGuire in Reference (2)), and Hamilton (H) (3). The latter three cases represent USGS experts who were excluded from the NUREG/CR-1582 study for institutional reasons. It can be stated that three of the NUREG experts preferred Configuration A (namely Nos. 3, 7, and 9); two of the NUREG experts preferred Configuration B (Nos. 4 and 8) as do, apparently, Y&A and H; four experts (Nos. 10, 11, 12 and 13) preferred a configuration similar to C; Configuration D coincides with A&P; and Configuration E with H&D. (In some cases, the five configurations do not conicide precisely with those preferred by the individuals cited, but effectively so in terms of the implied Yankee site hazard; that is, in terms primarily of the implied "host zone", the zone which contains the site.) Note, incidentally, that none of the additional references cited (experts "Y&A", "H", "A&P", "H&D") supports the Piedmont as the host zone for Yankee. One possible set of weights is simply proportional to the number of cited preferences or 3/13, 4/13, 4/13, 1/13 and 1/13 to A, B, C, D and E, respectively (or 0.22, 0.31, 0.31, 0.08 and 0.08).

A number of factors do not, however, favor this simple weighting scheme in our opinion and lead to a second weighting approach. First, we believe that, despite its history, there has never been important professional justification for the Boston-Ottawa zone and that thoughtful studies of the region now discredit it. Several NUREG/CR-1582 experts who "self-ranked" themselves highly in the northeast gave very low "credibility" to this zone. Certainly it does not appear to have the uniform activity rate required by the assumptions in the method. We, therefore, believe it does not merit a weight of more than 10% (i.e., the total weight of Configurations A and D should be 0.10).

Second, but most importantly, we believe that a fundamental error in expert opinion assessment was committed in NUREG/CR-1582. In the literature of that field, it is called "anchoring" (4). Rather than give the experts

---

* The tenth, No. 5, prefers a homogeneous zone over the entire Northeast. We did not consider this case to have sufficient weight to deserve an additional set of analyses; it is contained, in terms of results, within the variations of configurations treated.

blank maps, or even maps with historic seismicity and/or with tectonic structure, the NUREG/CR-1582 team gave the experts two "base maps" (Figures B10 and B11) that showed proposed configurations of zones, and were then instructed to "feel free" to change them. The effect, predictable by Tversky [8] and others, is obvious upon inspection of the results. It is not likely that without the influence of these base maps, four experts (Nos. 7, 9, 10 and 12) would develop exact duplicates of the base maps in the Northeast. Nor is it credible that without this biasing effect, all six of the experts who keep a Piedmont-like zone (Nos. 3, 7, 9, 10, 12 and 13) would give it precisely the same northern boundary. The base-map anchoring has clearly introduced a systematic error in the NUREG/CR-1582, rendering the conclusions less dependable than claimed. For this reason, we believe the weight attributed to Configurations A and C should be substantially reduced.

Furthermore, two of the experts who supported these configurations made no changes whatsoever to the base maps in the Northeast, yet they changed substantially the central United States portions of the base maps. We believe this reflects the fact that some experts, although knowledgeable about other areas, simply did not have the time available to study the northeast United States and to draw their own independent opinions from the facts. Note that these experts typically "self-ranked" themselves with low scores in this region. Less obvious are experts who have never before had to draw such maps for seismic hazard analysis purposes, particularly in the Northeast, and who therefore leaned heavily on the base maps. In contrast to others who have studied the area and who have strong opinions (as evidenced, for example, by positive changes to the base maps), we do not believe equal weight should be assigned such experts. Also, it is unlikely that any of the experts have given anywhere near as much attention to the specific region around the site as the project's consultants. Their analysis is, by design, thorough and site-specific.

To summarize the net effects of the issues raised in the last two paragraphs (the anchoring and the relative levels of information about the Northeast in general and the near-site region in particular), we chose simply to ignore expert Nos. 7, 9, 10 and 12 in the counting process. We use this only as a tool to modify the relative weights, not to reflect directly upon these individuals.

As a final element in this second weighting approach, we have received informal information suggesting that the next version of the seismic hazard map by Algermissen and Perkins will reflect more Configuration E than D. Therefore, we shift that weight accordingly.

The net counts are now 1, 4, 2, 0 and 2, for Configurations A, B, C, D and E, respectively, yielding weights 0.11, 0.45, 0.22, 0 and 0.22. These numbers approximately satisfy the 0.10 constraint on the Boston-Ottawa zone (i.e., 0.11 + 0 0.10).

Finally, we consider a third approach to weighting based directly upon our own interpretation of all the evidence. In terms of the effect on the hazard results, the main configuration issue is whether or not one accepts the hypothesis that there is a quieter seismic zone in western Massachusetts (and perhaps beyond). We believe (a) that the historical seismicity strongly supports this hypothesis, especially for short-term (20-year) estimates; (b) that lacking important tectonic evidence to the contrary (e.g., a pattern of active faults), this seismicity pattern is the primary source of homogeneous zone configuration evidence; (c) that the opinion of the seismologists who have studied the specific site region very carefully deserves the major attention (see References 5, 6 and 7); and (d) finally that, today, given recent literature (e.g., Yang and Aggarwal (1)), all available scientific information, and unlimited time to study and decide upon this one issue, virtually all the NUREG/CR-1582 experts (even, perhaps, expert Nos. 3, 13 and 11 who changed base maps but did not show a quieter western Massachusetts zone) would, like the many others cited above, choose in favor of such a quieter zone. In particular, in total, we see no objective supportive evidence and much contrary opinion with respect to the Boston-Ottawa/Piedmont Configuration A, and with respect to extending the Piedmont zone into western Massachusetts with the New Hampshire/Massachusetts line as its border (A and C). Therefore, in our best judgment, we would assign a 0.1 weight to such interpretations. In conclusion, in our best judgment, we assign weights 0.6 and 0.3 to Configurations B and E (this division of the 0.9 total weight is not critical to results), and weights 0.05 to Configurations A and C, with 0 to D.

Looking across the three weight-assigning procedures, we see a total weight assigned to B, D and E (configurations with a quieter western Massachusetts) of 0.47, 0.67 and 0.9. In terms of its effects on the hazard results (see Appendix F for sensitivity studies, Figures F1 to F5), casual inspection reveals that the lower this weight, the higher the hazard at the Yankee site. Therefore, the first set of weights is the most conservative. Although this is not necessarily a benefit, it is also perhaps the most "objectively derived", i.e., with least interpretation by us. The results reported in this study* have been based on the first set of weight, (i.e., 0.22, 0.31, 0.31, 0.08 and 0.08 on Configurations A, B, C, D and E, respectively), but we feel that this assignment is too conservative for the reasons explained above. As mentioned in the main body, this is one reason for the higher-than-historical hazards produced by the median of the zonation results (curve MZ, Figure 1).

Use of "Background Seismicity" in NUREG/CR-1582

Along with our extensive analysis of various source configurations, we feel that it is important to discuss our basis for not using a background as was used in NUREG/CR-1582.

The treatment and, in fact, the notion itself of background in NUREG/CR-1582 is unfounded, adding unnecessary conservatism to the hazard estimates. What we find unsatisfactory about the background zone in that study is:

1. Its physical meaning. Is the background a potential earthquake source? If so, then the experts should have identified it as part of their zonations, described its geometry, and estimated appropriate seismicity parameters, and assigned a probability to it. How can one physical source lie coincident in space with others? If it is an alternate to the expert's preferred configuration, it should be treated, i.e., with an assigned

---

* Sensitivity runs have been made with the others confirming the conservatism of the set reported.

probability. No such analysis has been made by any of the experts. If, on the other hand, the background is not a potential earthquake source, then why was it treated as an additional source with consequent distortion of the experts' opinions?

2. Even assuming that a background source is physically possible, why should its geometry be determined as the union of all experts' zonations? More important, what is the mathematical basis for calculating its probability P_B as $P_B = (1 - C_i)$, where the C_i are the "credibilities" of the various zonation alternatives? What are these credibilities in the first place? How should one operate on them (no mathematical theory of credibility exists)? Are credibilities being interpreted in the same way by different experts?

3. Even if one accepts the notion that a background source may exist and that its probability can be determined as some function of the credibilities of C_i, there is a mathematical inconsistency in the way credibilities are handled in NUREG/CR-1582. Specifically, one cannot call probabilities the ratios $P_i = C_i / \sum_j C_j$ (as was done for the zonations explicitly identified by the experts) and at the same time calculate P_B as $\prod_i (1 - C_i)$. In fact, P_B and the P_i must satisfy $P_B = 1 - \sum_i P_i$ (with the consequence that $P_B = 0$ because $\sum_i P_i = 1$) or at most $P_B = 1 - P_o \sum_i P_i = 1 - P_o$ in which $(1 - P_o)$ is the probability that none of the zonation alternatives explicitly identified by the expert is correct. No expert has been asked about P_o.

In summary, the "background source", as defined and treated in NUREG/CR-1582, is a mathematical concept without physical basis. It is treated inconsistently with the other sources, with parameters (geometry, seismicity, probability) determined by heuristic formulas not related to direct expert opinion. The background problem is one further systematic error in NUREG/CR-1582, reducing the effectiveness of the conclusion that the ten independent experts' results are represented in the study.

Appendix B References

[1] J. P. Yang and Y. P. Aggarwal, 1981, "Seismotectonics of Northeastern United States and Adjacent Canada", Journal of Geophysical Research, Vol. 86, No. B.6, pp. 4981-4998.

[2] R. K. McGuire, 1977, "Effects of Uncertainty in Seismicity of Estimates of Seismic Hazard for the East Coast of the United States", BSSA, Vol. 67, No. 3, pp. 827-848.

[3] R. M. Hamilton, 1981, "Geologic Origin of Eastern United States Seismicity", Proceedings of Earthquakes and Earthquake Engineering: The Eastern United States, Knoxville, Tennessee.

[4] NUREG/CR-1582, 1980, "Seismic Hazard Analysis - Solicitation of Expert Opinion", Vol. 3.

[5] Weston Geophysical Corporation, 1979, "Geology and Seismology, Yankee Rowe Nuclear Power Plant".

[6] Weston Geophysical Corporation, 1979, "Eastern United States Tectonic Structures and Provinces Significant to the Selection of a Safe Shutdown Earthquake".

[7] Weston Geophysical Corporation, 1980, "Site-Dependent Response Spectra, Yankee Rowe".

[8] A. Tversky and D. Kahneman, 1973, Availability: A Heuristic for Judging Frequency and Probability, Cognitive Psychology.

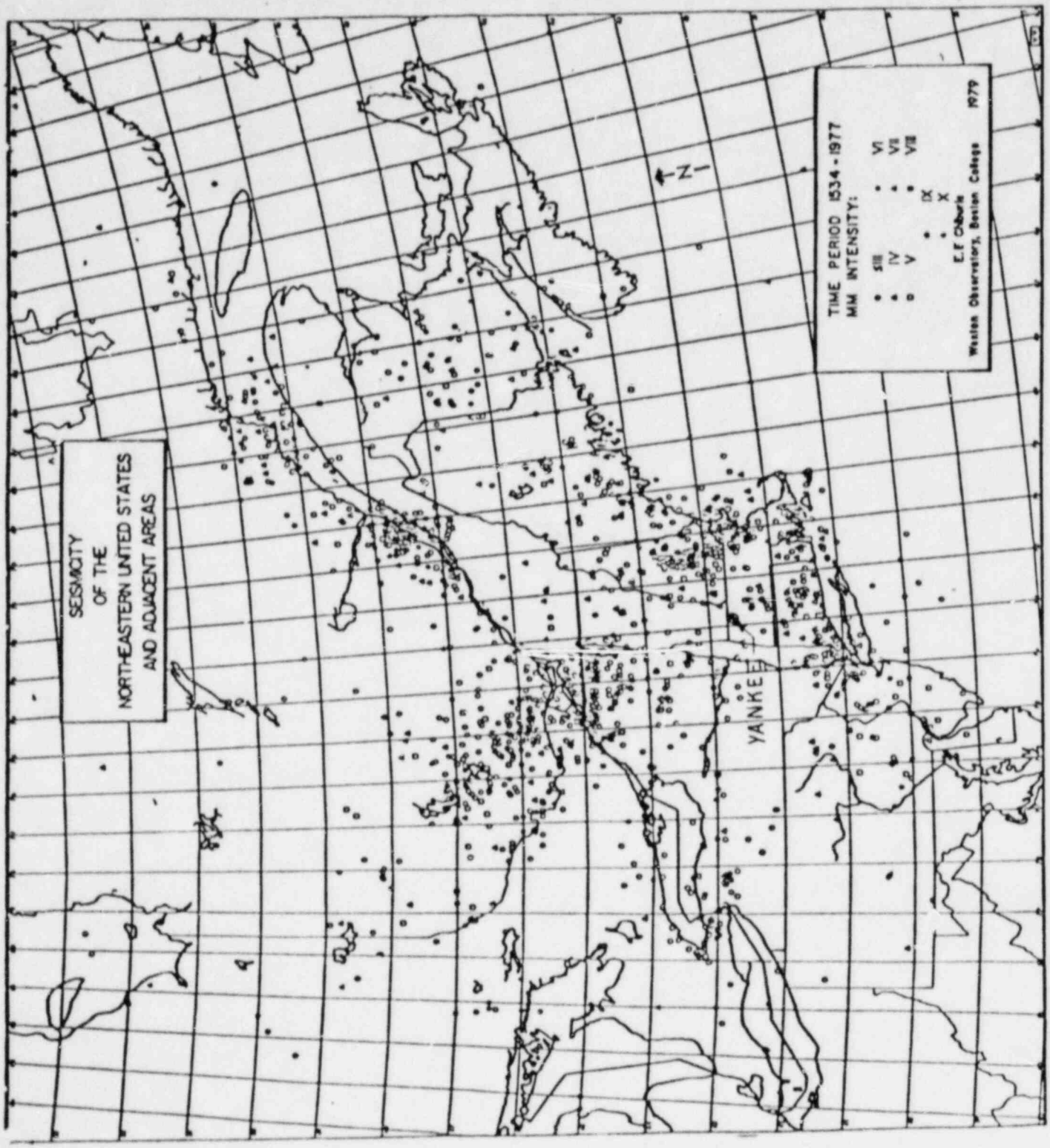

Figure B1. Epicentral map of the northeastern United States and adjacent southeastern Canada for the period 1534-1977 (Chiburis and Ahner, 1979).

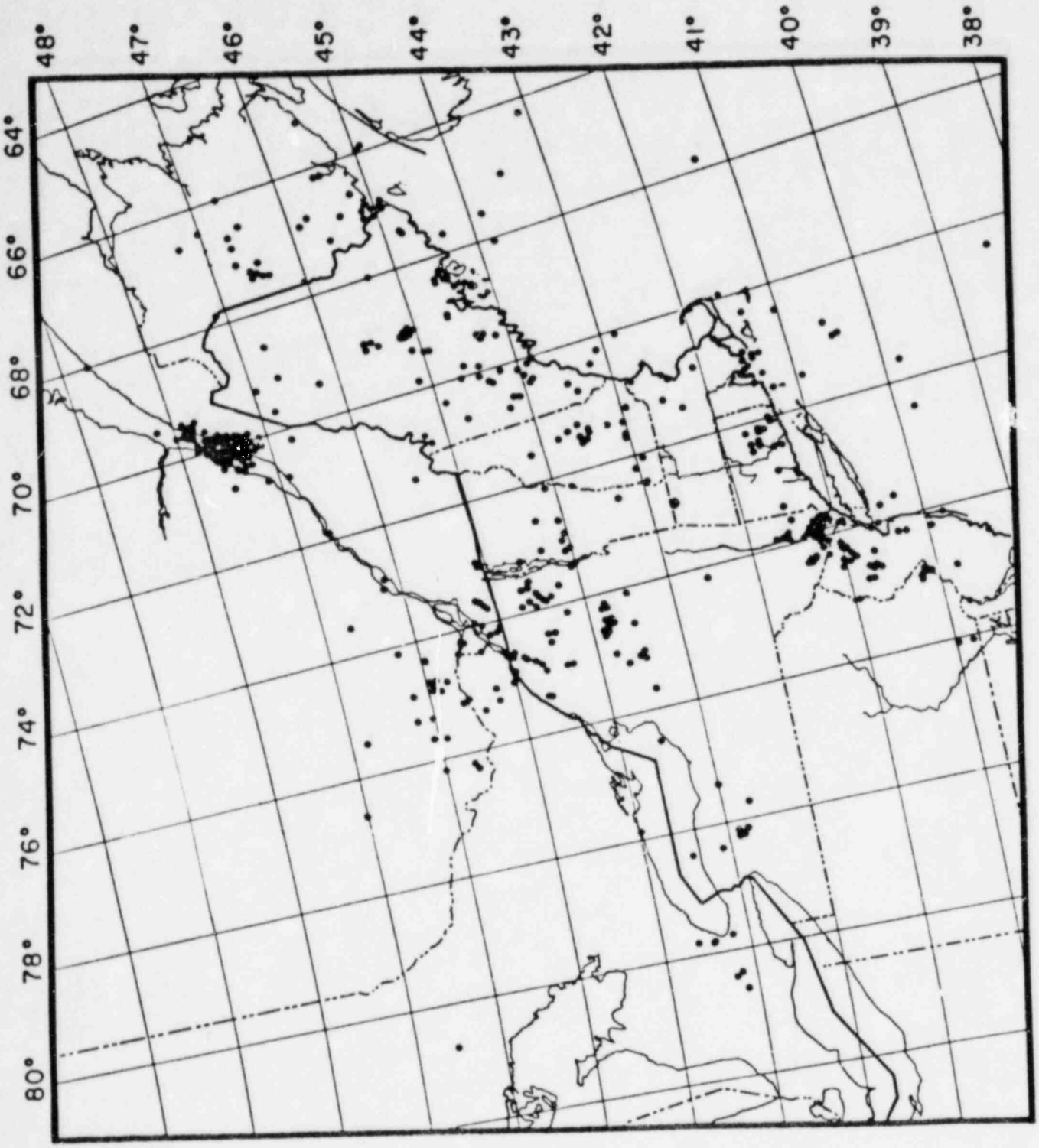

Figure B2. Earthquake Epicenters During the Period
October 1975 - March 1981

Figure B3. Boston-Ottawa/Piedmont Source Areas

Figure B4. Weston Geophysical Corporation Source Areas

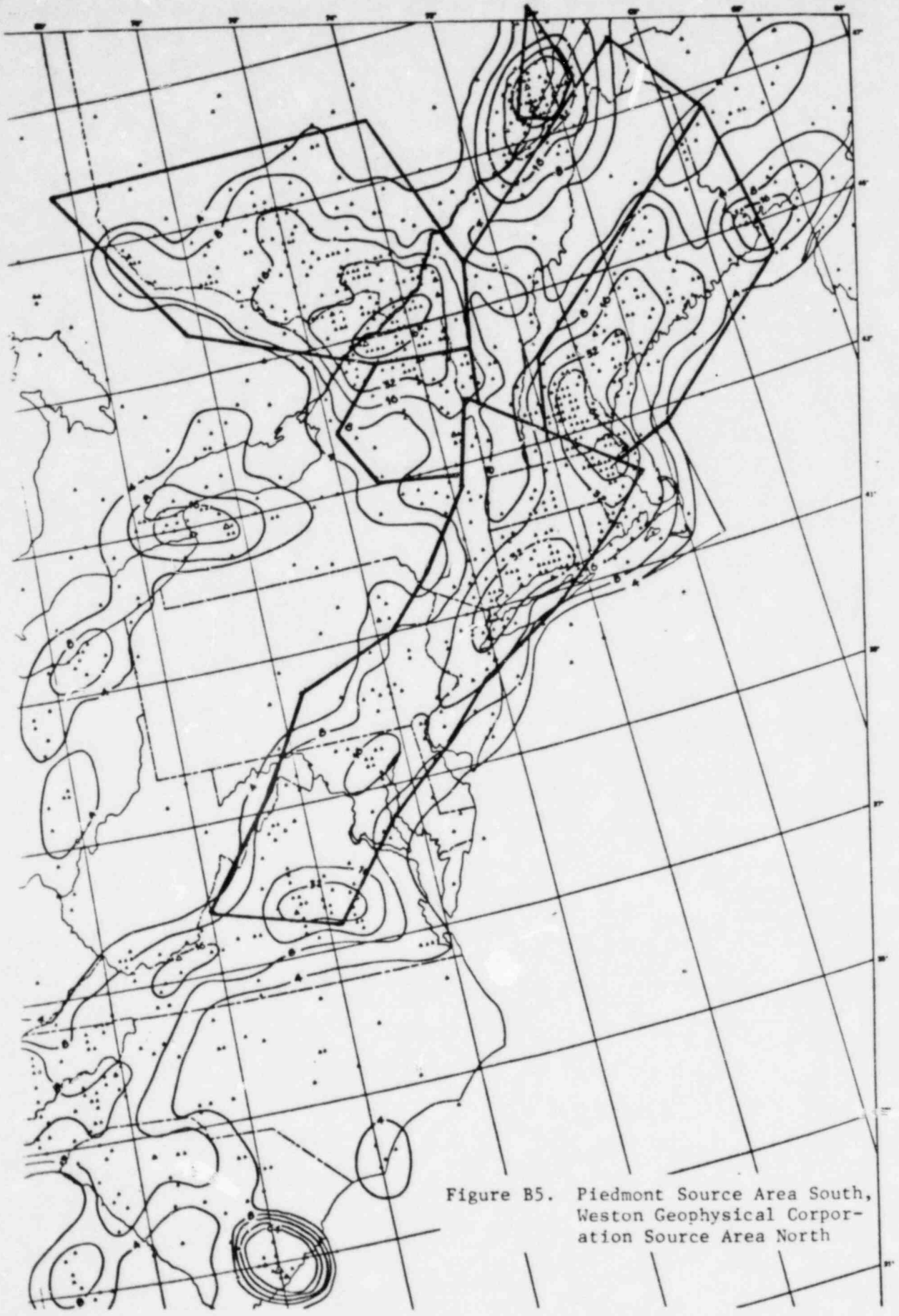

Figure B5. Piedmont Source Area South, Weston Geophysical Corporation Source Area North

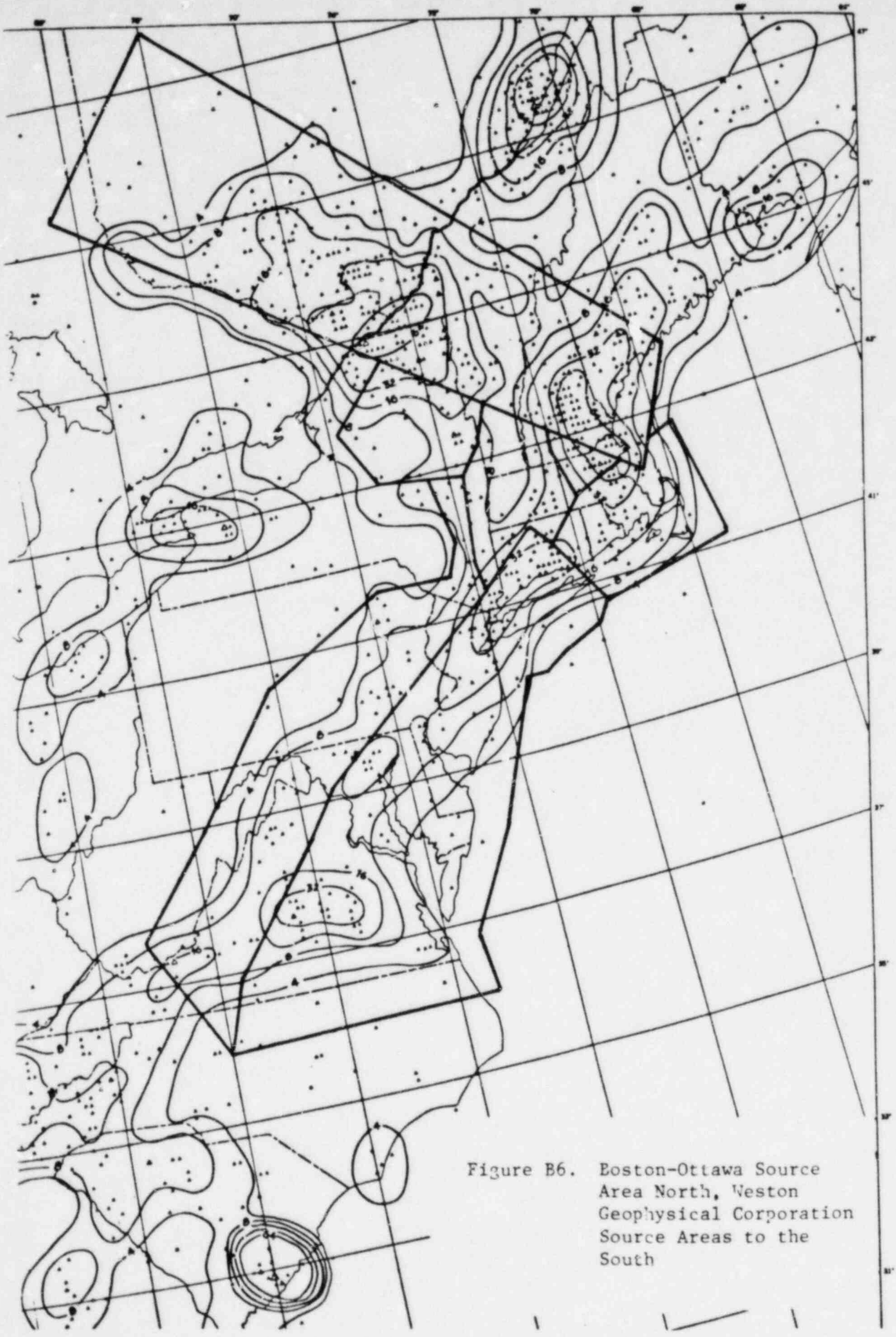

Figure B6. Boston-Ottawa Source Area North, Weston Geophysical Corporation Source Areas to the South

Figure B7. Weston Geophysical Corporation Source Area at Site and to the North

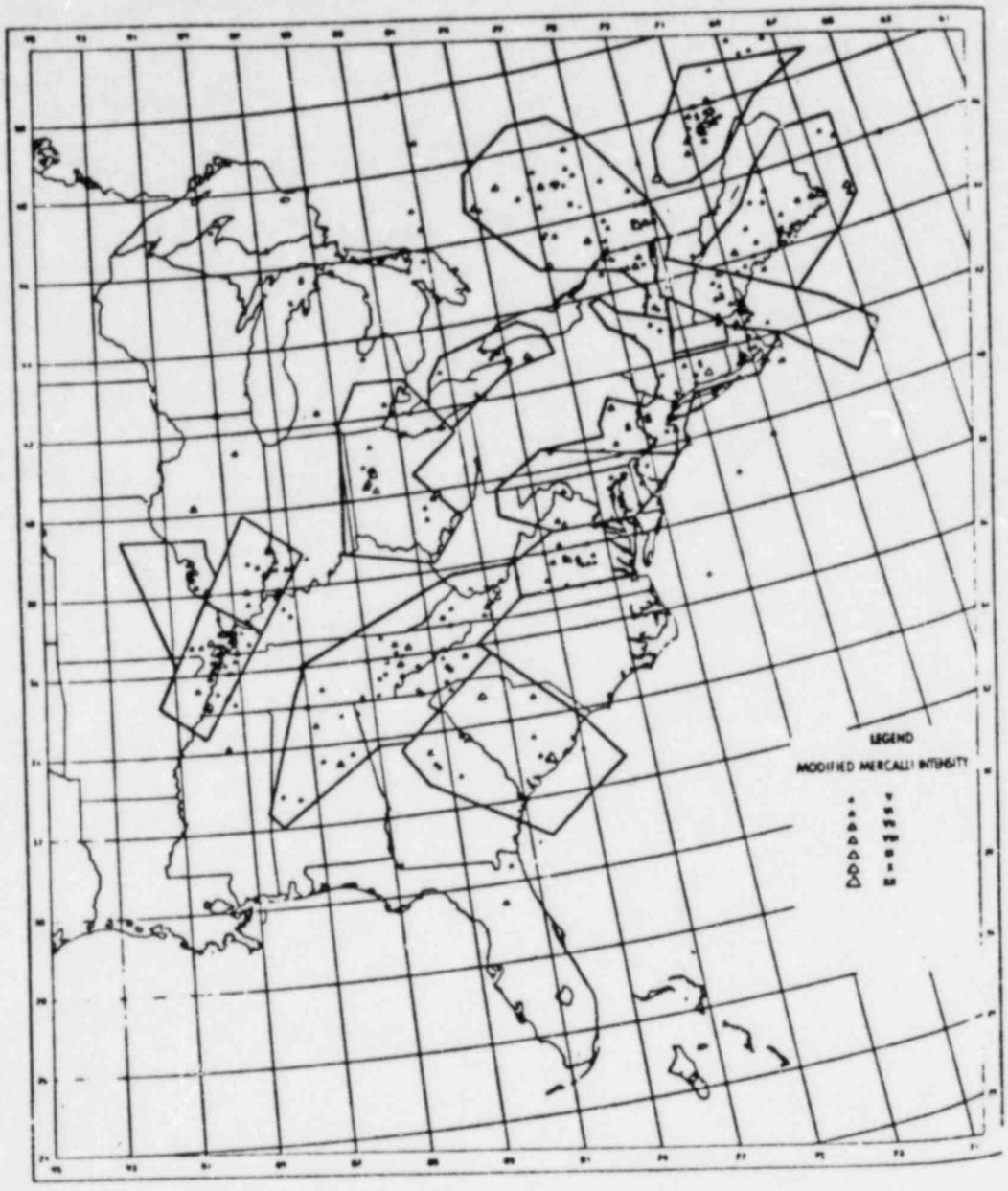

Figure B8. Seismic Sources After Algermissen and Perkins (1976)

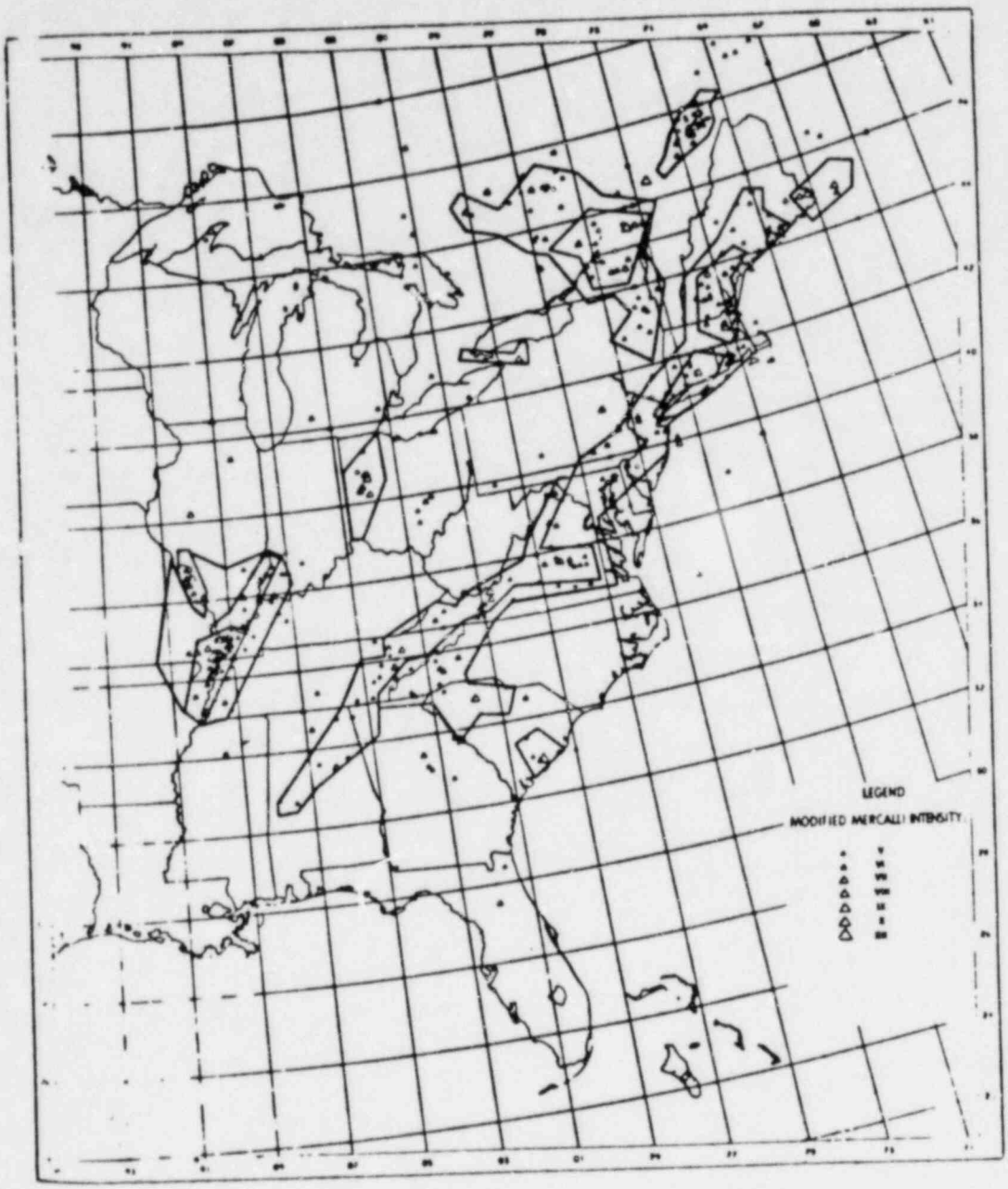

Figure B9. Seismic Source Areas After Hadley and Devine (1974)

QUESTION I-1

BASE MAP 1

Figure B10. Base Map Supplied To Experts

TERA CORPORATION

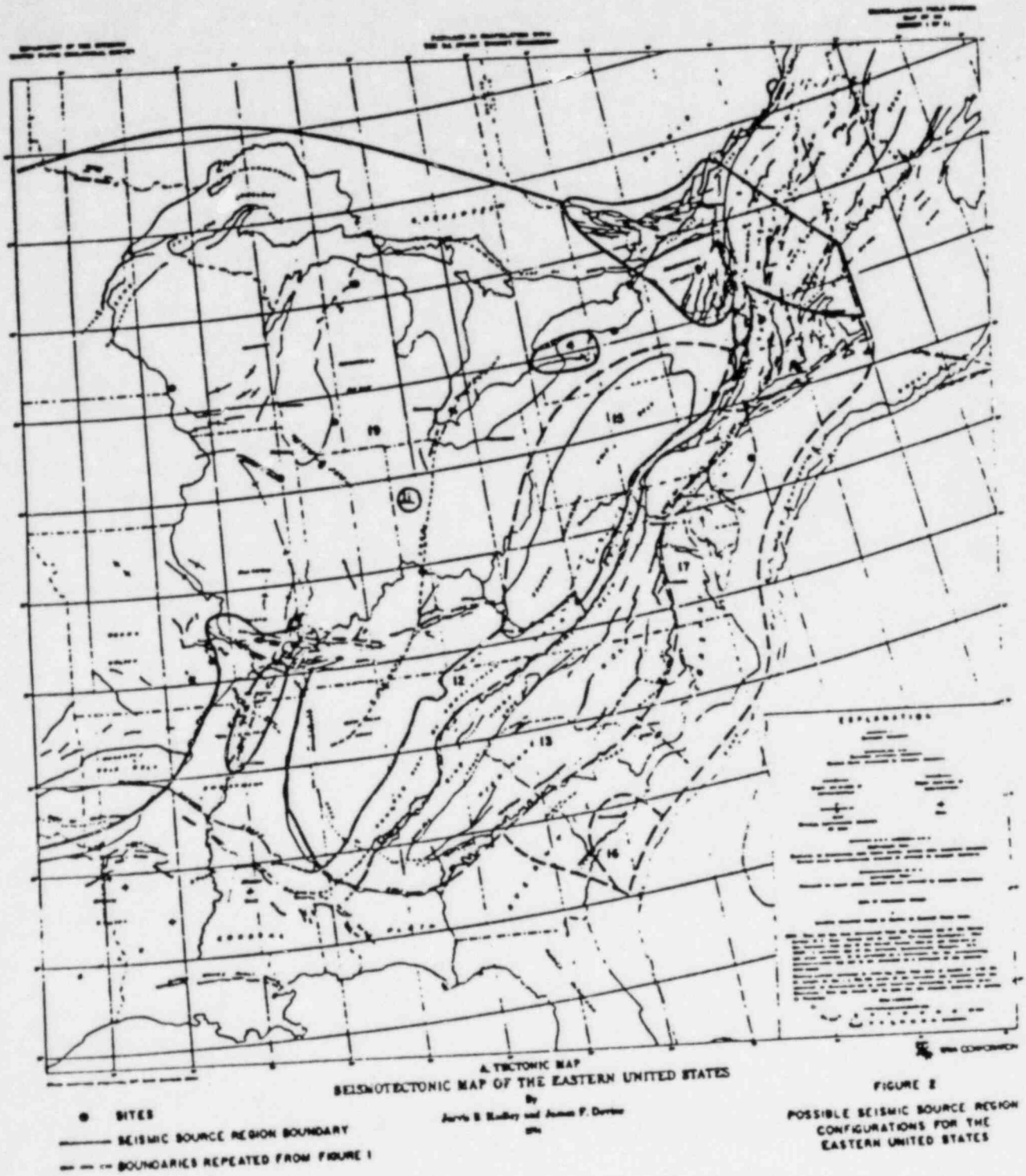

QUESTION 1-1

BASE MAP 2

Figure B11. Base Map Supplied To Experts

APPENDIX C

HISTORICAL EARTHQUAKE CATALOGS FOR THE NORTHEASTERN UNITED STATES

The importance of the choice of catalogs cannot be stated better than was done in NUREG/CR-1582 (Vol. 1, pg. 1-1), "It is essential for any credible seismic hazard analysis to base the study on an accurate and current seismic data base. This is, of course, the case with any seismic hazard analysis, but it is particularly true for probabilistic analysis where earthquakes of all sizes contribute to the hazard." We believe not only that the catalog used to establish the results in NUREG/CR-1582 is in error and out-of-date, but also that its interpretation and use by TERA/LLNL was flawed.

In this study, three catalogs have been evaluated and their impact on the seismic hazard results calculated (as described, for example, in Table C-1). The three catalogs are denoted:

1. Chiburis' Old Catalog (Reference 1)

2. Chiburis' New Catalog (Reference 2)

3. The Weston Geophysical Catalog (Reference 3)

The catalog used has a direct impact on the historic method, of course. In the zonation method, it determines the mean activity rate, a, and the log-slope, b, of the frequency law (the effect of these different catalogs on the a and b values is examined in Appendix D1). In addition, its larger events influence the choice of the upperbound-magnitude m_1.

1. Chiburis' Old Catalog

This single catalog, unpublished and later significantly revised by its author, was the basis of the NUREG/CR-1582. It was sent by TERA to the experts as part of the evidence and it was used by TERA to estimate "a" values and, where unspecified by the expert, the "b" values. Especially for experts less familiar with the details of larger northeastern states' events, it must

have had a major impact, too, on the upper-bound magnitudes they selected. Therefore, contrary to the other factors (such as zonation, upper-bound magnitudes and seismicity parameters, for which several alternatives were considered), the catalog had a systematic biasing effect upon the results of the NUREG/CR-1582 study. Such systematic effects were, of course, precisely what that study intended to avoid (see, e.g., NUREG/CR-1582, Vol. 1, pp. A-3,4).

Preparation of Chiburis' catalogs was supported by the U.S. Nuclear Regulatory Commission as part of the New England Seismotectonic study at Boston College's Weston Observatory. The original version ("Chiburis' Old Catalog"), furnished to TERA for its use, is said now to have been premature; it was reportedly denied publication because of numerous inaccuracies and lack of documentation. These problems have since been resolved in Chiburis' New Catalog; substantial revisions include those cited above in the main body (Table 2).

The version of Chiburis' old catalog supplied to the ten experts includes magnitude values assigned to many older pre-instrumental events; the assignments are clearly the result of applying the Gutenberg-Richter conversion ($m_L = 1 + 2/3\ I_o$), or a conversion developed by Chiburis ($m_L = 1 + 0.6\ I_o$). Curiously, the catalog's author has stated that he did not make these conversions himself. (Indeed, magnitudes are not reported for any pre-instrumental events in his newer catalog.) Although their source is unclear, TERA has stated to Yankee that whenever an intensity and a magnitude appeared in the catalog, they used the latter, assuming it to be "more accurate". (Indeed, pre-instrumental magnitudes estimated by felt-area or intensity fall-off methods are better measures of event size, but the magnitude values in Chiburis' old catalog were not determined this way.)

The joint effect of these two problems (inaccurate intensity assignments and Gutenberg-Richter magnitude conversion) on the NUREG/CR-1582 results can be best illustrated by an example, the 1732 Montreal earthquake. First, in Chiburis' old catalog, the event was assigned an epicentral intensity of IX and a magnitude of 7.0 (from the Gutenberg-Richter conversion). As mentioned, in such a case, TERA used the magnitude value. To predict acceleration at the site given a magnitude they used (e.g., in their

historic analysis), the Gupta-Nuttli (intensity-based) attenuation law modified by substituting for I_o the Nuttli-Herrmann conversion, $m_b = 1.75 + .5\ I_o$. But this is clearly a contradiction; as discussed in Appendix A, the proper analysis in such a case requires use of the same intensity magnitude conversion in both the catalog and the attenuation law. The Nuttli-Herrman conversion applied to the epicentral intensity of IX would have yielded a magnitude 6.25. The use of two different conversions in NUREG/CR-1582 causes an incorrect doubling of the acceleration predicted. Secondly, Chiburis' new catalog (and the Weston Geophysical Catalog) have confirmed that the 1732 Montreal event had an epicentral intensity of VIII rather than IX. This value converts via Nuttli-Herrmann to magnitude 5.75. The combined effect of the too-high I_o and the inconsistent conversion to magnitude is a tripling of the site-predicted peak ground acceleration.

The total effect of Chiburis' old catalog on NUREG/CR-1582 results cannot be isolated easily. In the study reported here (Chapter 3, Table 4, for example), its effect on the historic method is investigated, but it must be emphasized that our historic studies were based on intensities (except when the attenuation law required conversion), thereby avoiding the major problem of inconsistent magnitude conversion found in NUREG/CR-1582. The simplist comparison is between (a) the curve marked TH (TERA-Historic); and (b) the heavy curves (Gupta-Nuttli attenuation) in Figure 8 (Chiburis' new catalog). Clearly, the combined effect on acceleration is very important, e.g., a factor of about 1.6 at 10^{-3}. The effects of the catalog on the zonation results are, of course, even more difficult to isolate.

It can be assumed, however, that both the incorrect I_o assignments and the Gutenberg-Richter converted magnitudes probably increased "a" values, certainly decreased "b" values, probably increased m_1 values, and certainly combined incorrectly with intensity-based attenuation model (such as the Gupta-Nuttli Model and the "Ossipee" Model) important to NUREG/CR-1582 and especially to NRC synthesis results. All these factors lead to the overestimation of hazards.

Chiburis' old catalog had a pervasive, systematic effect on all the experts' results in NUREG/CR-1582 difficult to quantify precisely, but certainly leading to over-conservative hazard estimates, to reduced confidence in the conclusions, and to a major nullifying of the credibility purportedly created by using many "independent experts".

Because of the weak status of this catalog, especially relative to its successor, Chiburis' new catalog, we gave Chiburis' old catalog only nominal weight (P = 0.10) in our own historic method results.

2. Chiburis' New Catalog (2), NUREG/CR-2309

The Chiburis (2) catalog, published as NUREG/CR-2309, is a more complete, accurate and corrected catalog of earthquakes that have occurred in the northeastern United States and in southeastern Canada between the years 1534 and 1977. The primary differences between Chiburis' old and Chiburis' new catalogs are:

1. Many of the historically large events have been re-evaluated (see Table 2 of the text); and

2. No magnitudes are associated with the pre-instrumental events.

The upgrading, clearing and clarification of the Chiburis (2) catalog makes it more suitable at this time for use in seismic hazard analysis. A weight of 0.30 is assumed for this catalog in the historic seismic hazard analysis. Furthermore, the strong agreement between this and the Weston Geophysical catalog implies that if it were used to estimate "a" and "b" values for source zones, the results would not differ significantly (see Appendix D).

3. Weston Geophysical Corporation (WGC) Catalog

The WGC catalog (3) is a current catalog of earthquakes that have occurred in the eastern United States and southeastern Canada. It is the result of integrating all available historical information and recent

instrumental seismicity data. Some of the cross-referenced sources used to compile the catalog are:

1. Earthquake History of the United States [4]
2. United States Earthquakes [5]
3. Smith [6]
4. LaMont-Doherty [7]
5. Nuttli Catalog [8]
6. Weston Observatory [9]
7. Earth Physics Branch in Canada [10]
8. Preliminary Determinations of Epicenters [11]

In addition, WGC has conducted its own direct studies of newspaper and other accounts of historical earthquakes. Many of the large historical events have, in addition, been assigned magnitudes based on felt-area and/or intensity fall-off methods.

Because of the extensive effort by WGC to update and re-evaluate their catalog, a weight of 0.60 is assumed for use in the historic seismic hazard analysis. Indeed, the more recently published catalog by Chiburis (2) does not find major disagreement with the WGC catalog.

Appendix C References

[1] NUREG/CR-1582, 1981, "Seismic Hazard Analysis: Solicitation of Expert Opinion", Vol. 1.

[2] NUREG/CR-2309, 1981, "Seismicity, Recurrence Rates and Regionalization of the Northeastern United States and Adjacent Southeastern Canada".

[3] Weston Geophysical Corporation, 1980, "Site-Dependent Response Spectra, Yankee Rowe".

[4] J. L. Coffman and C. A. VonHake, 1973, "Earthquake History of the United States", U.S. Department of Commerce, NOAA, No. 41-1.

[5] F. Neumann, 1942, "United States Earthquakes, 1940", U.S. Department of Commerce, Coast and Geodetic Survey, Serial No. 647.

[6] W. E. T. Smith, 1962, "Earthquakes of Eastern Canada and Adjacent Areas, 1534-1927", Pub. of the Dominion Observatory Ottawa, Vol. 26, No. J.

[7] LaMont-Doherty Geological Observatory, Palisades, NY.

[8] O. W. Nuttli, Geophysics Department, St. Louis University, St. Louis, MO.

[9] Weston Observatory, Department of Geology and Geophysics, Boston College, Boston, MA.

[10] Earth Physics Branch, Seismological Service of Canada, Ottawa.

[11] Preliminary Determination of Epicenters, National Earthquake Information Service, U.S. Geological Survey.

APPENDIX D

ESTIMATION OF SEISMICITY PARAMETERS AND COMPLETENESS OF EARTHQUAKE CATALOGS IN NEW ENGLAND

This appendix addresses seismicity parameters a, b, and m_1. The subappendix D1 prepared by Weston Geophysical presents a thorough explanation of the methodology used to determine the seismicity parameters used in YAEC-1263. The methodology factors in not only known demographic information as a basis for completeness of large historical events, but also known completeness factors for smaller instrumental events recorded by the New England Seismic Network. It also presents empirical intensity-to-magnitude relationships that are appropriate for the northeast. Seismicity parameters and completeness factors used by Yankee were discussed by D. Bernreuter in his review of YAEC-1263. A detailed response by Weston Geophysical Corporation to his criticism is also found in the attached subappendix D1.

The results of this unusually detailed development of a and b values support the values used by Yankee in YAEC-1263. The thoroughness of this approach, including as it does, comparison of different catalogs, recent historical data, various magnitude-intensity relationships, and review of recurrence estimates by both time period and magnitude has prompted relatively high weights on calculated estimates of a and b. These weights are 0.6 and 0.67, respectively. (Note that the risk analysis results here are, in fact, based on Weston's previously estimated a and b values. This more detailed study became available only very recently but it effectively supports or shows to be conservative the previous values, in particular vis-a-vis the alternative hypothesized values.)

In the light of all this information there seems to be little support for the cruder, undifferentiated b value of 0.9, even though it is supported by several of the NUREG-1582 experts; it may not be as reasonable an assumption in New England as it is considered to be elsewhere in the eastern U.S. Also, the higher a value hypotheses, included here to reflect Dr. Bernreuter's expressed concerns [1] do not appear to be likely values given the differences in thoroughness in the approach to completeness factors adopted by Weston versus that by NUREG/CR-1582.

Selection of upper bound magnitude hypotheses weight is anchored largely on the rather widespread adoption and professional practices of the maximum historical magnitude plus 0.5 units. This is based largely on similarity to other seismotectonic settings (see the NUREG/CR-1582 expert opinion statements). Elementary statistical estimation series suggest, however, a decay likelihood away from the maximum historical values. The element of potential surprise (i.e., events much larger, even one and more magnitude units, than the maximum historical event in the relatively near future) is accounted for by the alternative hypotheses with their not small total weight (0.2).

Appendix D References

[i] D. L. Bernreuter, 1981, Letter to W. Russell, Dated November 4, 1981.

APPENDIX D1

ESTIMATION OF SEISMICITY PARAMETERS

FOR NEW ENGLAND

ESTIMATION OF SEISMICITY PARAMETERS FOR NEW ENGLAND

Prepared for

YANKEE ATOMIC ELECTRIC COMPANY

October 1982

Weston Geophysical
CORPORATION

TABLE OF CONTENTS

		Page
LIST OF TABLES		i
LIST OF FIGURES		iii
1.0	INTRODUCTION	1
2.0	EARTHQUAKE CATALOGS	3
	2.1 Weston Geophysical Corporation Earthquake Catalog	3
	2.2 Chiburis (1981) Earthquake Catalog	4
	2.3 Chiburis (1977) Earthquake Catalog	5
	2.4 Comparison of Earthquake Catalogs	6
3.0	SOURCE REGIONS	7
4.0	CORRELATIONS OF m_b - MAGNITUDE TO EPICENTRAL INTENSITY, I_o, AND TO M_L - MAGNITUDE	8
	4.1 m_b - Magnitude versus I_o	8
	4.2 m_b - Magnitude versus M_L - Magnitude	10
5.0	EVALUATION OF COMPLETENESS OF EARTHQUAKE CATALOGS	12
6.0	MAGNITUDE-FREQUENCY RELATIONSHIPS FOR THE NORTHERN APPALACHIAN FOLDBELT	14
	6.1 Model 1 - WGC Catalog	15
	6.2 Model 2 - CH77 Catalog	17
	6.3 Model 3 - CH81 Catalog	17
	6.4 Comparison of Models	17
	6.5 Sensitivity Analyses	19
	6.5.1 Effect of m_b - I_o, m_b - M_L Conversion Relationships	19
	6.5.2 Effect of Method of Statistical Grouping of Recurrence Data	23
7.0	MAGNITUDE-FREQUENCY MODELS FOR THE WESTERN NEW ENGLAND FOLDBELT	25
	7.1 WGC Catalog	25
	7.1.1 Models Based on WGC Correlations	25
	7.1.2 Models Based on Alternate Correlations	28
	7.2 Chiburis Preliminary Catalog - CH77	30
	7.3 Chiburis Revised Catalog - CH81	31

TABLE OF CONTENTS (Continued)

	Page
8.0 DISCUSSION	32
9.0 CONCLUSIONS	35
10.0 REFERENCES	38
TABLES	
FIGURES	

LIST OF TABLES

Table 1 Discrepancies in Earthquake Catalogs for the Northeast

Table 2 Earthquakes used to Determine Relationship of m_b-Magnitude to Epicentral Intensity in the Northeast

Table 3 Earthquakes used to Determine Relationship of m_b-Magnitude to M_L-Magnitude in the Northeast

Table 4 Recurrence of Earthquakes in the Northern Appalachians - Weston Geophysical Catalog

Table 5 Magnitude-Frequency Relationships for the Northern Appalachians - Weston Geophysical Catalog

Table 6 Recurrence of Earthquakes in the Northern Appalachians - Preliminary Chiburis Catalog - CH77

Table 7 Magnitude-Frequency Relationships for the Northern Appalachians - CH77 Catalog

Table 8 Recurrence of Earthquakes in the Northern Appalachians - Revised Chiburis Catalog - CH81

Table 9 Magnitude-Frequency Relationships for the Northern Appalachians - CH81 Catalog

Table 10 Comparison of Preferred Models for the Northern Appalachian Foldbelt

Table 11 Sensitivity to Choice of Conversion Relationships Weston Geophysical Catalog

Table 12 Magnitude-Frequency Relationships for the Northern Appalachians - Weston Geophysical Catalog

Table 13 Recurrence of Earthquakes in the Northern Appalachians - Weston Geophysical Catalog - (Histogram Centers by Equation 4)

Table 14 Magnitude-Frequency Relationships for the Northern Appalachians - Weston Geophysical Catalog - (Histogram Centers by Equation 4)

Table 15 Recurrence of Earthquakes in the Western New England Foldbelt - Weston Geophysical Catalog

LIST OF TABLES (Continued)

Table 16 Recurrence of Earthquakes in the Western New England Foldbelt - Weston Geophysical Catalog

Table 17 Recurrence of Earthquakes in the Western New England Foldbelt - Weston Geophysical Catalog (m_b - I_o, Equation 2; m_b - M_L, Equation 6)

Table 18 Recurrence of Earthquakes in the Western New England Foldbelt - Weston Geophysical Catalog (m_b - I_o, Equation 2; m_b - M_L, Equation 5)

Table 19 Recurrence of Earthquakes in the Western New England Foldbelt - Weston Geophysical Catalog (m_b - I_o, Equation 2; No m_b - M_L used)

Table 20 Recurrence of Earthquakes in the Western New England Foldbelt - CH77 Catalog

Table 21 Magnitude-Frequency Relationship for the Western New England Foldbelt - CH77 Catalog

Table 22 Recurrence of Earthquakes in the Western New England Foldbelt - CH81 Catalog

Table 23 Magnitude-Frequency Relationship for the Western New England Foldbelt - CH81 Catalog

LIST OF FIGURES

Figure 1	Earthquake Source Zones
Figure 2	m_b versus MMI Data for the NE
Figure 3	m_b versus M_L Data for the NE
Figure 4	Expansion and Settlement in the Colonies and Eastern United States
Figure 5	Settlements in Canada
Figure 6	Northern Appalachians - WGC Catalog
Figure 7	Northern Appalachians - CH77 Catalog
Figure 8	Northern Appalachians - CH81 Catalog
Figure 9	Comparison of Models for the Northern Appalachians
Figure 10	Northern Appalachains: Sensitivity to Magnitude-Intensity Correlations
Figure 11	Comparison of WGC and CH77 - CH81 Models
Figure 12	Sensitivity Analysis - WGC Catalog
Figure 13	Sensitivity to Magnitude Histogram Centers
Figure 14	Comparison of Sensitivity Analysis Results
Figure 15	Western New England Foldbelt - Weston Geophysical Catalog and m_b Correlations ($\geq$ 2.5 m_b)
Figure 16	Western New England Foldbelt - WGC Catalog
Figure 17	Western New England Foldbelt - WGC Catalog; Nuttli and Herrmann (1978) m_b-I_o Correlation ($\geq$ 2.5 m_b)
Figure 18	Western New England Foldbelt Sensitivity Analysis
Figure 19	Western New England Foldbelt - Preliminary Chiburis, CH77 Catalog ($\geq$ 2.5 m_b)
Figure 20	Western New England Foldbelt - CH77 Catalog

LIST OF FIGURES (Continued)

Figure 21 Western New England Foldbelt - Revised Chiburis, CH81 Catalog ($\geq$ 2.5 M)

Figure 22 Western New England Foldbelt - CH81 Catalog

Figure 23 Comparison of Cumulative Recurrence Rates

1.0 INTRODUCTION

The seismicity of several source zones in the northeastern United States and adjacent regions of Canada was described quantitatively using the Gutenberg and Richter (1944) empirical magnitude-frequency relationship, given below in Equation 1. The analyses were performed during mid-1979 using the Weston Geophysical Corporation Earthquake Catalog (WGC Catalog) compiled through mid-1978. Results of these analyses were eventually incorporated by Yankee Atomic Electric Company into their report YAEC-1263 (June, 1981), "Seismic Response Spectra for the Yankee Nuclear Power Station, Rowe, Massachusetts."

$$\text{Log}_{10} N_C = a - b\,M \qquad (1)$$

where N_C = number of earthquake per unit time

M = magnitude

a, b = parameters determined in statistical analyses

The derivations of magnitude-frequency models, reported in YAEC-1263, were based on a best estimate approach, and no rigorous treatment of statistical uncertainty was attempted in these analyses. For example, best estimates of event parameters, as defined by the WGC Catalog, were used although some event parameters differ from those adopted in other listings of earthquakes for the northeast. (It is noted that all revisions included in the WGC Catalog are made on the basis of research conducted on original accounts of historical events.) Similarly, best estimates from two empirical

correlations were used to redefine all events, where necessary, to establish a list wherein all events were scaled to m_b-magnitude. These correlations include relationships of m_b-magnitude to epicentral intensity and of m_b-magnitude to local magnitude, M_L. Finally, best estimates of lengths of completely reported intervals of the earthquake catalog, as inferred from population and seismic network distributions in time, were used in computation of the magnitude-frequency models. Due to the above procedures, magnitude recurrence models were reported as single-valued, best estimates for the various source zones.

Subsequent to the submittal of YAEC-1263, and its critical review by D. L. Bernreuter (LLNL, November 4, 1981), further studies were initiated to establish the level of uncertainty associated with the seismicity parameters of certain tectonic zones, and particularly for the Western New England Foldbelt, the site province of the Rowe, Massachusetts facility. The additional studies examine sensitivity of calculated recurrence models to alternate definitions of event parameters by examining three catalogs compiled for the northeast. These include:

1. the WGC Catalog, currently updated through mid-1980;
2. the Chiburis (1981) Catalog;
3. the preliminary Chiburis Catalog used in the TERA/LLNL Seismic Hazard Analysis prepared for the NRC 's Systematic Evaluation Program.

Also, sensitivities to variation in the empirical relationships used to transform the catalog entries to m_b-magnitude and to variation of the length of time assumed to represent completely reported intervals of the catalogs are demonstrated in this study. These sensitivity analyses are performed within the context of two source zones. The first is a broad region of the northeast approximately coincident with the northern Appalachian mountains extending from northern New Jersey northeastward into New Brunswick. The second source zone is the Western New England Foldbelt, adopted as the site province for the Rowe, Massachusetts facility.

2.0 EARTHQUAKE CATALOGS

Magnitude-frequency relationships are determined using three earthquake catalogs for the northeast. These compilations are described below.

2.1 Weston Geophysical Corporation Earthquake Catalog

The WGC Catalog, which covers much of the central and eastern United States and Canada, has evolved over the past two decades through incorporation of data from numerous published sources as well as from intensive research on important seismic events. Transcription errors, duplications, and discrepancies have been identified by making parallel listings of existing catalogs. In many cases additional research was required to resolve conflicting assessments of earthquakes given in earlier listings. The fundamental sources for the WGC Catalog include

the United States Earthquake Series, the Earthquake History of the United States, the Publications of Dominion Observatory and the Seismological Series of the Earth Physics Branch (both of Canada), bulletins of major seismograph networks such as the Northeast United Stated Seismic Network (NEUSSN), the St. Louis University Network, and former networks operated by the New England Seismological Association (NESA). Important listings such as Brigham (1871), Mather and Godfrey (1927), Brooks (1960), Docekal (1970), Nuttli (1974, 1979), Hopper and Bollinger (1971), Bollinger and Hopper (1972), Bollinger (1969, 1973), and Nuttli and Brill (1980) are also considered. Supplementary information for many historical events has also been collected from newspapers, town histories, private diaries, and related scientific reports. A set of parameters is adopted for each event through a critical examination of the above material.

The time frame covered by the WGC Catalog spans from 1534 to the present for known major activity, including the recent New Brunswick (January 9, 1982, 12:53 UTC, 5.7m_b) and New Hamphshire (January 19, 1982, 00:14 UTC, 4.4 m_b) earthquakes. Smaller activity including instrumental results of network investigations are included through June, 1980.

2.2 Chiburis (1981) Earthquake Catalog

The Chiburis (1981) listing, henceforth referred to as CH81, is published in NUREG/CR-2309. Introductory remarks in this reference detail the source material employed in the

compilation. Included are many references already introduced in Section 2.1. Also, the WGC Catalog was provided to Dr. E. F. Chiburis during the course of his studies and, ultimately, several re-assessments of historical events were incorporated into the CH81 Catalog. The areal extent of CH81 is approximately from 38°-60°N and 48°-81°W. Chronologically, the catalog spans from 1534 through December, 1977.

Although not listed in NUREG/CR-2309, the data tape of CH81, obtained from Dr. John Ebel, Weston Observatory, is updated through December 1980 including the NEUSSN instrumental data. For the sake of comparison in subsequent sections of this report, the CH81 listing was further updated to include the parameters of the Jan., 1982 New Brunswick and New Hampshire main shocks.

2.3 Chiburis (1977) Earthquake Catalog

The Chiburis (1977) Catalog, referred to in remaining sections as CH77, is a preliminary version of CH81 described above. The major difference in catalog format between CH77 and CH81 is that the former listing includes both the smallest and largest epicentral intensity for events that have conflicting values as given by the previously mentioned analysts, without indicating the preferred value. In CH81, however, the preferred parameters are indicated. It is noted that high estimates of intensity given in the CH77 listing were used in

the catalog adopted by TERA/LLNL for their Seismic Hazard Analysis. This catalog also provides the basis for the LLNL review of seismicity parameters given in YAEC-1263.

2.4 Comparison of Earthquake Catalogs

The three earthquake catalogs are indirectly compared in following sections by examination of differences in interpreted recurrence models. The more important events, with magnitude $\geq$ 4.5 or intensities $\geq$ VI, however, are formally compared in this section. These size limitations are enforced to facilitate the comparison by eliminating numerous smaller events. Also, only events contained within the region bounded by 39°-50°N, and 60°-80°W are examined. Table 1 lists the major differences observed in the catalogs. In summary, Table 1 lists eight differences in maximum intensities between the CH77 and CH81 Catalogs. In all cases, the maximum intensity was reduced by a minimum of one intensity level. The most significant revisions include assignments of MMI VIII for the 1732 Montreal earthquake (formerly IX in CH77), and MMI VII for the 1727 Cape Ann event (formerly VIII in CH77). Also, six other events in CH77 are reduced from intensity VII or VII+ to intensity VI in CH81.

With a few exceptions, the WGC and CH81 Catalogs essentially agree. The differences include the February 21, 1954 event listed as a mine collapse event in WGC and as a MMI VII tectonic event in CH81. Also, all magnitudes in CH81 are

listed as local magnitude regardless of the technique used to determine the magnitude. In the WGC Catalog, the magnitude type, i.e. m_b, M_L, m_{bLg}, is differentiated. One example of magnitude discrepancy that results from the non-differentiated magnitude format of the CH81 Catalog is the December 1940 Ossippee earthquake which has both 5.4m_b and 5.8 M_L determinations. The 5.4 m_b is preferred in the WGC listing while 5.8 M_L is adopted in the CH81 Catalog.

3.0 SOURCE REGIONS

Magnitude-frequency relationships are determined for two source regions. The first is a broad region that encompasses much of the northeast, while the second is the site province used in YAEC-1263, namely the Western New England Foldbelt (WNEF). The configurations of these source zones are plotted on Figure 1.

The larger region is defined to encompass the Northern Appalachian Foldbelt extending from northern New Jersey through New England and into New Brunswick. This region, with an area of 3.94×10^5 km^2, is approximately bounded on the west and northwest by Logan's Line and on the south and east by coastal waters.

Included within the area of the Northern Appalachian Foldbelt is the Western New England Foldbelt tectonic province established in YAEC-1263 as the site province. This province, with an area of 1.23×10^5 km^2, lies in the western part of

the Northern Appalachian Foldbelt and is comprised of north and northeast-trending tectonic subdivisions including the Middlebury Synclinorium, Berkshire Green Mountain Anticlinorium, Connecticut Valley Synclynorium, and the Bronson Hill Anticlinorium. Seismic activity rates in these two regions of the northeast are compared in the following sections.

4.0 CORRELATIONS OF THE m_b - MAGNITUDE TO EPICENTRAL INTENSITY, I_o, AND TO M_L - MAGNITUDE

Since recurrence models are to be defined on the basis of m_b - magnitude, it is necessary to convert all non-instrumental events to m_b through empirical correlations with intensity. Also, many older instrumental events, scaled to Local Magnitude, M_L, are assigned m_b - estimates for reasons described in Section 4.2, again through empirical correlations. The several correlations examined in this study are described below.

4.1 m_b - Magnitude versus I_o

Three linear correlations of magnitude to epicentral intensity, I_o, are employed in the analyses to determine recurrence models. Two of these correlations (Nuttli and Herrmann, 1978; and WGC, 1982, this study) are between m_b - magnitude and I_o, while the third (Chiburis, 1981) is between an undifferentiated magnitude type, M and I_o. As described in Chiburis (1981), all magnitudes are considered to be 'local magnitudes' although several methods have historically been used to calculate them, including the Richter (1935) Local

Magnitude, and the more recent Nuttli (1973) m_{bLg} as well as various regional coda-length magnitudes. Therefore, the correlation given in Chiburis (1981) cannot be strictly viewed as m_b versus I_o, but rather as an undifferentiated magnitude type, M, versus I_o. The three correlations are shown in Equations 2, 3 and 4.

$$m_b = 1.75 + 0.50\ I_o \qquad \text{(Nuttli and Herrmann, 1978)} \qquad (2)$$

$$M = 1.00 + 0.60\ I_o \qquad \text{(Chiburis, 1981)} \qquad (3)$$

$$m_b = 0.44 + 0.67\ I_o \qquad \text{(WGC, This Study)} \qquad (4)$$

The WGC correlation (Equation 4) is determined using events taken from the WGC Catalog that have listed both instrumental m_b - magnitudes and I_o evaluations. This analysis uses events located in the northeast region bounded by 40° - 50°N, and 65° - 80°W. Table 2 lists the earthquakes used in the regression analysis to determine the parameters of Equation 4. These data points are plotted on Figure 2 along with the best fit line (Equation 4). Also, compared on Figure 2 are the other correlations (Equations 2 and 3). The comparison illustrates a close agreement of the three correlations at higher intensities. At lower intensities, however, the curves diverge, and the Nuttli and Herrmann (1978) relationship most conservatively assigns m_b - magnitude to these lower I_o values. The effect of choice of m_b - I_o correlation on resultant recurrence models is examined in subsequent sections.

4.2 m_b - magnitude versus M_L - Magnitude

Numerous seismic events listed in earthquake catalogs for the northeast use the Smith (1966) listing as a primary source. Many of these events which occurred from 1928 to 1959, in the U.S. as well as in Canada, were detected by the Canadian Seismograph Network. Local Magnitudes, M_L, were calculated for many events using the procedure described by Smith (1967). This procedure included corrections for instrument response differences between the Canadian short-period seismographs and the standard Wood-Anderson instruments upon which the California Local Magnitude Scale was developed. Differences in attenuation, however, were not considered in the magnitude determinations. Also, the use of the M_L formula was extended beyond the 600 km maximum distance for which Richter (1935) gave constants for the reference amplitude, A_o. Stevens, et al, (1973) suggest that using the M_L scale, extrapolated to beyond 600 km, has resulted in over-estimating magnitudes for events at these distances by as much as 1 1/2 units. Due to this improper use in the northeast of the M_L scale defined for use in California, an empirical study was performed to determine a correlation of m_b - magnitude, calculated using a magnitude scale that properly accounts for northeast attenuation (i.e. Nuttli, 1973) and Local Magnitude, M_L.

As in the previous section, events in the WGC Catalog, located in the northeast (40°-50°N; 65°-80°W) that have both m_b and M_L designations are used to determine a linear correlation between the magnitude types. These events are listed on Table 3. The m_b - magnitudes are taken from Street and Turcotte (1977), who present results of re-analyses of seismograms for 32 earthquakes in the northeast, while M_L - magnitudes are from the Smith (1966) list and also from the Canadian Earthquakes Series, prior to 1968, after which time m_b - magnitudes were routinely reported in these annual publications of the Earth Physics Branch, Department of Energy, Mines and Resources, Ottawa, Canada.

The relationship of m_b to M_L magnitude for the northeast, determined from the events on Table 3, is given in Equation 5.

$$m_b = -0.68 + 1.03\ M_L \qquad (5)$$

This relationship suggests a systematic difference of about 0.5 to 0.6 magnitude units between m_b and overestimated M_L. The effect that this relationship has on calculated recurrence models is examined in following sections.

The data points and Equation 5 are plotted on Figure 3. Also plotted in the figure, as a dashed line, is a correlation of m_b to M_L determined from data collected over a much

larger region, bounded by 30°-50°N and 60°-100°W. This relationship (Equation 6) is shown in comparison to the model determined for northeastern data only, since it was used in the 1979 recurrence model analyses, the results of which are given in YAEC-1263.

$$m_b = 0.63 + 0.75\ M_L \qquad (6)$$

This empirical relationship does not show a systematic reduction of m_b versus M_L, however, it does compare well to Equation 5 in the magnitude range from 3.5 to 5.5 wherein most of the events scaled to M_L occur.

5.0 EVALUATION OF COMPLETENESS OF EARTHQUAKE CATALOGS

The concept of completeness of earthquake catalogs, in general, implies the extent to which the actual seismicity of a region has been recorded either as historical accounts or as instrumental measurements. Secondarily, completeness also implies the extent to which all documentation of seismic events have been found and incorporated into catalogs. For example, intensive research, either of historical accounts or of older seismograms, invariably reveals the existence of a few seismic events previously not cataloged. Several entries in the WGC and the CH81 Catalogs have resulted from such research of historical documents.

As a first approximation, completeness of the catalogs can be bounded at the largest magnitude, greater than 6.0, by the time frame of the early settlement of the U.S. and Canada.

Summarized on Figures 4 and 5, respectively, are the expansion of populations in the U.S. and Canada. It is observed from these figures that coastal areas and the major river valleys were first settled in the early 1600's. Much of the interior was populated during the 1700's. Parts of northern and western Maine, however, remain sparsely populated even at the present time. Although the population was not dense in the earliest years, the widespread distribution of settlements allowed for the detection of large events due to their large perceptible areas (>1,000,000 km^2). In fact, the history of large events in the northeast is contemporaneous with the earliest settlement of the region in the 1600's. Due to variations in level of perception between northern and southern settlements, reasonably accurate locations have been inferred for these oldest events. Therefore, on the basis of population, the catalogs for the northeast are assumed to be complete for large events greater than magnitude 6 for the past 250-300 years.

Conversely, the completeness of catalogs for small events depends on dense populations and suitably configured seismograph networks. The present configuration of the NEUSSN and the Canadian Seismograph Network, which include approximately 50 stations in the New England states and approximately 20 more in adjacent regions of Canada, provides the most complete instrumental coverage achieved to date in the northeast. Hence, the detection capability has been

extended to low magnitude levels. However, these networks have evolved in time, and uniform dense coverage has only been achieved since NEUSSN was instituted during the past 5 to 6 years. During these most recent years, when networks have been expanded, the earthquake catalog is likely complete for events larger than magnitude 2.5 for the study region.

In summary, the completeness of catalogs for large events ($\geq$6.0) is assumed to be 250-300 years on the basis of early settlements and the completeness for small events ($\geq$ 2.5) is about 5 years on the basis of seismograph configuration. Completeness below magnitude 2.5 is likely not yet achieved for the entire study region. Assessment of completeness of the intermediate magnitude ranges is more difficult than bounding the low and high magnitude completeness, since detection of these intermediate magnitudes is influenced by subtle changes in population migration and early seismograph configurations which are difficult to track. Completeness of the intermediate magnitude range is therefore assessed using a technique that assumes completeness for intervals of the earthquake catalog wherein the mean annual rate of occurrence is stable (Stepp, 1972).

6.0 MAGNITUDE-FREQUENCY RELATIONSHIPS FOR THE NORTHERN APPALACHIAN FOLDBELT

Magnitude-frequency models are determined in this section for the northern Appalachian region described in Section 3.0, using the three earthquake catalogs for the northeast.

Sensitivity to choice of conversion relation and to assumptions on length of complete intervals of catalog are also examined.

Three fundamental models are determined, one for each catalog, using criteria that are established by the respective authors of the listings, when such criteria are given. For example, the WGC-derived correlations between m_b and I_o and m_b and M_L are used in conjunction with the WGC Catalog to determine one fundamental model. On the other hand, the Chiburis (1981) M - I_o relation is used with the CH81 Catalog, while the Nuttli and Herrmann (1978) relation is used with the CH77 Catalog, since it was adopted in the TERA/LLNL (1981) Seismic Hazard Analysis. No m_b - M_L relations, however, are used with the CH77 and CH81 Catalogs to determine the fundamental recurrence models for these catalogs. Identical assumptions on catalog completeness are applied to each catalog, so that variation in the fundamental models can be attributed to differences in the catalogs and to differences in the techniques used to estimate magnitudes from catalog entries.

6.1 Model 1 - WGC Catalog

The methodology used throughout this main section (6.0) includes making the adopted correlations to m_b, where necessary, purging all aftershock sequences and then sorting the catalog by magnitude and time to establish a count of events necessary for computing mean annual rates of earthquake occurrence. Magnitude histogram cell widths are specified as 0.5 magnitude units. Sensitivity to variation in this parameter is examined in a later section.

Table 4 summarizes the recurrence rates for the northern Appalachians as inferred from the WGC Catalog. Shown on the table are mean annual rates calculated for several lengths of the catalog. Preferred rates, indicated by parentheses, represent estimates of mean annual rates for assumed complete sections of the catalog. The complete intervals include five to twenty years for magnitudes 2-3, sixty to one hundred forty years for intermediate magnitudes in the range of 4 m_b, one hundred forty to two hundred fifty years for major events above 5.0 m_b, and two hundred fifty to three hundred years for events in the range of 6 m_b or greater.

The interpretation of the values (Table 4) into magnitude-frequency relationships is illustrated on Table 5. Two models are fit to the cumulative recurrence rate data. The first is fit to all of the data, in the magnitude range from 2.0 to 6.0 m_b. The second is fit to the data in the magnitude range of 2.5 to 5.5 only, by eliminating the extreme points from the regression analyses. The preferred model derived using the second method ($2.5 \leq m_b \leq 5.5$), is shown in Equation 7. Discussion of this model is deferred until the remaining two fundamental models from the CH77 and CH81 Catalogs are introduced in the next section.

$$\text{Log}_{10}N_C = 3.267 - .930\ (\pm\ .039)\ m_b \qquad (7)$$

$$\text{S.E.} = 0.147$$

6.2 Model 2 - CH77 Catalog

Assumptions on catalog completeness similar to those used in the previous section, are made to derive recurrence models for the CH77 Catalog. Also, Equation 2 (Section 4.1) is used to relate m_b to I_o, and no m_b-M_L relationship is used. Tables 6 and 7 provide the recurrence statistics and the fundamental model (Equation 8) determined for the CH77 Catalog.

$$\text{Log}_{10}N_C = 3.521 - .952\ (\pm\ .044)\ m_b \qquad (8)$$

S.E. = 0.166

6.3 Model 3 - CH81 Catalog

The third model for the Northern Appalachian Foldbelt, determined for the CH81 Catalog is given below (Equation 9). As in the previous analyses for the CH77 Catalog, no m_b-M_L relation is used, but the Chiburis (1981) M-I_o correlation (Equation 3, Section 4.1) is used to convert the historical intensity data to magnitude. The earthquake recurrence rates and regression models are given on Tables 8 and 9.

$$\text{Log}_{10}N_C = 3.604 - .981\ (\pm\ .034)\ M \qquad (9)$$

S.E. = 0.128

6.4 Comparison of Models

As stated earlier, two models were fit through the earthquake recurrence data. The first is through the data ranging from magnitude 2.0 through 6.0, inclusively, while the

second model is fit through magnitudes 2.5 through 5.5. The second model, which eliminates the extreme points from the regression analyses is preferred, because the completeness of the range of magnitudes 1.8 - 2.2 m_b over the entire region is questionable and the annual rate of magnitude 6.0 and larger is not well established. Only two events close to but likely not above magnitude 6.0 have been observed during historical times. Both models are plotted on Figures 6, 7 and 8, respectively for the WGC, CH77 and CH81 Catalogs, along with the data representing the interpreted cumulative annual rates of earthquake occurrence. The solid line represents the preferred model while the dashed is the model fit through all of the data.

The three preferred models are compared on Figure 9. Also, observed and predicted recurrence rates for the three models are compared on Table 10. With respect to the preferred recurrence models, it is observed from the table and figure that both the CH77 and CH81 models predict higher recurrence rates than does the WGC model at lower magnitudes, while at higher magnitudes the CH77 curve overlies both the CH81 and WGC curves which are approximately equivalent in the magnitude 5-6 range. Differences include predicted recurrence rates of 40% to 50% higher for the CH77 and CH81 Catalogs than for the WGC Catalog at magnitude 3.5, and 45% to 50% higher for the CH77 Catalog relative to the WGC and CH81 Catalogs at magnitude 5.5. The differences at higher magnitudes can be attributed to

revisions of intensities between the CH77 and CH81 Catalogs, shown on Table 1. The similarity of the CH81 and WGC Catalogs, in terms of intensity assignment for the more significant historical earthquakes, is reflected in the similarity of the models at the higher event sizes. The difference in the curves at lower magnitudes likely result from the conversion relationship used to infer magnitudes. For example, the correlations discussed in Section 4.1 predict magnitudes of 3.75, 3.40 and 3.12 (Equations 2, 3 and 4 respectively), for intensity IV events, which predominate the historical earthquake catalog. The effect that choice of correlation relationship has on resulting recurrence models is examined in the following section.

6.5 Sensitivity Analyses

Several sensitivity analyses are performed to examine the effects on computed recurrence models resulting from choices of conversion relationships, and the manner in which the magnitude data are grouped prior to determining recurrence rates.

6.5.1 Effect of m_b - I_o, m_b - M_L Conversion Relationships

Differences between the models at low magnitudes (Figure 9) may be attributed to correlations used to assign magnitudes to the large number of low intensity events that predominate the earthquake catalogs. To evaluate effects that may be attributed to choice of correlations, the WGC Catalog was

interpreted using the procedure adopted for the CH77 Catalog. For example, magnitudes are assigned using Equation 2 (Section 4.1) and no relation between m_b and M_L is assumed. The results of this sensitivity analysis are compared on Table 11 to the original count of earthquake magnitudes derived using the WGC correlations (Equations 4 and 5). Interpreted recurrence rates and regression models are provided on Table 12.

The results of this sensitivity study illustrate the following significant points. First, the differences in recurrence rates derived using the Nuttli and Herrmann (1978) relationship versus the WGC relations are significant in the mid-magnitude range of 3 to 4. This is seen on Figure 10, which is a plot of both sets of points, the circles representing the sensitivity analysis results Little difference is seen at low magnitudes, since these rates are largely based on instrumental measurements over the past 5 to 10 years, and therefore correlations are not required. At higher magnitudes, rates are similar since the correlation gives similar estimates of magnitude for the higher intensities. In the mid-magnitude range, however, the correlations give significantly different estimates, i.e. 3.75 m_b (Equation 2) versus 3.12 m_b (Equation 4) for I_o = IV. This difference is reflected in the data points shown on Figure 10 and in the regression model also shown on the figure as a dashed line.

The sensitivity model is plotted on Figure 11 versus the three fundamental models determined earlier. It is seen from this comparison that the choice of correlations is predominantly responsible for differences observed earlier at low magnitudes. Although no formal event by event check was made at intensities less than VI, the close agreement of the models determined using similar correlations suggests that the catalogs are not significantly different at these lower levels. The approximately 50% difference between CH77, CH81 and the sensitivity analysis versus the WGC model in rates of occurrence of mangitude 3.5 and larger is therefore entirely attributable to the choice of correlations.

The next point observed from the sensitivity analysis involves the parametric form assumed to fit the recurrence data. Although linear models (Equation 1) are used throughout this report, other forms such as bi-linear or quadratic models have also been proposed. Chiburis (1981) uses bi-linear models to fit recurrence curves to his catalog. The parametric form usually is chosen by visual inspection of the data distribution. From Figures 6 and 7, which show the recurrence data for the CH81 and CH77 Catalogs respectively, it is seen that a linear model is not the best possible fit. Rather a bi-linear or polynomial model would provide better fits. The data for the WGC Catalog (Figure 6) suggest a linear model when the WGC correlations are used. The same catalog, however,

defines a set of points that appears similar to the CH77 and CH81 data, when the Nuttli and Herrmann (1978) correlation is used. The bi-linear or quadratic forms of the points for the sensitivity analysis are seen on Figure 10. The conclusion drawn at this point is that the appearance of the magnitude recurrence data, which is strongly influenced by correlations used as is seen on Figure 10, does not necessarily reflect the real distribution of earthquake magnitudes. Emphasis must therefore be placed on the proper assignment of mangitudes to the historical data prior to making any inferences on the parametric form of recurrence models. The simplest form, i.e. the linear model, is therefore used throughout this analysis.

The WGC m_b - I_o correlation (Equation 4) is preferred over the others (Equations 2 and 3) since it is determined on the basis of northeastern United States data. Although the Chiburis (1981) relation is also based on northeastern data, magnitude types are not differentiated and on this basis as discussed earlier, it cannot be viewed as strictly an m_b - I_o relationship.

The performance of the correlations can be evaluated by examination of the annual recurrence rates given on Tables 4, 6 and 8 for the WGC, CH77 and CH81 Catalogs respectively. For example, the WGC Catalog and conversions give relatively stable recurrence rates (Table 4) over the past 100-140 years for the 3.5 m_b category. The most recent 5 to 10 years of data is

instrumental; the remaining data is predominantly historical data which is converted to magnitude. The close agreement of the rates determined from both sets of data suggests proper magnitude assignments. On the other hand, the CH77 and CH81 Catalogs and conversions predict significantly higher rates for the historical data in the 3.5 m_b category, than for the more recent predominantly instrumental data. This discrepancy in rates results from systematically overestimated magnitudes for lower intensities using Equations 2 and 3.

6.5.2 Effect of Method of Statistical Grouping of Recurrence Data

The standard procedure adopted in this study is to group the magnitude recurrence data in histogram cells 0.5 magnitude units wide and centered on even and half-magnitudes, i.e. 3.0, 3.5, 4.0, etc. The effect of alternate statistical grouping is examined in this section, using the WGC Catalog and correlations only.

The following alternate methods of grouping the data are used.

1. histograms with narrow cells of 0.3 magnitude units;
2. histograms with wide cells of 1.0 magnitude units;
3. standard histograms with cells of 0.5 magnitude units but with alternate centers.
4. histograms with centers determined for whole intensities by the m_b - I_o correlation.

Results of the first three of these sensitivity analyses, including recurrence rates and magnitude-frequency models are

shown on Figure 12. Results of the fourth sensitivity analysis are compared to results of the standard procedure on Figure 13. Interpretation of the earthquake catalog using histogram centers defined by the m_b-I_o correlation, equation 4, is given in Tables 13 and 14. Recurrence models for all sensitivity studies are compared to the fundamental model for the WGC Catalog (Equation 7) on Figure 14. The solid curve represents Equation 7, while the four dotted curves are the sensitivity results. Methods 1 and 3 for grouping the recurrence data results in b-values of 1.02 and .95 versus .93 for Equation 7, but the curves predict similar recurrence rates at magnitudes larger than 3.0. The use of wide histogram cells of 1.0 magnitude, however, results in recurrence rates 40% (at 5.5 m_b) to 80% (at 3.5 m_b) larger than those given by Equation 7. These high estimates result directly from the nature of earthquake occurrence data. Within a broad category of one magnitude unit, most events lie in the lowest magnitude end of this range, and the average magnitude would be smaller than the midpoint of the histogram cell which is normally chosen to represent the category. For this reason, assigning the data to the midpoint translates the resulting model to larger magnitudes and higher recurrence rates. This effect of using too-wide of a magnitude histogram cell is also observed in results of the fourth sensitivity analysis which uses a cell width of 0.67 m_b units.

The error introduced by using wide magnitude histogram cells is removed by sorting data into narrow categories. However, because much of the data is scaled to intensity and is converted to magnitude using correlations whose coefficients range between .5 and .67 (Equations 2, 3 and 4), resolution of magnitude ranges finer than these values is prohibited. Therefore, the standard method of sorting the data into 0.5 magnitude cells is appropriate and is used in the following section.

7.0 MAGNITUDE-FREQUENCY MODELS FOR THE WESTERN NEW ENGLAND FOLDBELT

The magnitude-frequency model originally determined in analyses made during mid-1979 (see discussion in Section 1.0) for the Western New England Foldbelt (WNEF), and used in YAEC-1263 is given in Equation 10.

$$\text{Log } N_{\geq} = 3.039 - 1.099\ m_b \qquad (10)$$

This model is compared in this section to others developed for the WNEF using the three catalogs, the various correlations, the arguments about catalog completeness and the statistical procedure used in the previous section for the larger area of the northeast.

7.1 WGC Catalog

7.1.1 Models Based on WGC Correlations

Seismicity of the Western New England Foldbelt, the boundaries of which are shown on Figure 1, is plotted on Figure 15. All instrumentally determined events with

magnitudes greater than or equal to 2.5 m_b are shown as square symbols. Historical events, whose magnitudes are estimated using the WGC correlations (Equations 4 and 5) are plotted as square symbols, rotated 30° counterclockwise.

The interpretation of recurrence rates using the WGC Catalog and correlations is presented on Tables 15 and 16. Figure 16 is a plot of these recurrence data compared to the original magnitude-frequency model (Equation 10) used in YAEC-1263.

The data on Figure 16 are difficult to interpret, because there exists only one earthquake with magnitude larger than 4.0, namely the 4.9 m_b Quebec-Maine (Q-M) border event of June, 1973. The rates of occurrence of this size event and also events in the 4.0 and 4.5 categories are assumed to be reciprocals of the time intervals within which it is assumed that such events would be detected. For this analysis, completeness for magnitude 5.0 m_b is assumed to be in the range of 180-250 years, therefore data points for 4.0 - 5.0 m_b are plotted at .004 and .0071, although these values clearly do not represent well constrained recurrence rates. The trend of the data for repeated events in the magnitude range of 2.0 - 3.5 m_b define b-values of -1.14 to -1.34. One model, fit through data for 2.5 - 3.5 m_b, is shown as a dotted line on Figure 16. Parameters for models fit through several other segments of the data are listed on Table 16. At those steep recurrence model slopes the data points at 5.0 m_b

are considerably above the model suggesting that recurrence intervals for this size event are longer than those assumed as the reciprocal of the complete catalog length.

Alternatively, it can be postulated that the Q-M border earthquake is an outlier in the WNEF recurrence data set, because it is genetically affiliated to a tectonic environment characterized by different rates of seismicity. For example, the Q-M border event is spatially correlated to the Megantic Intrusive of the "White Mountain Plutonic Series." This geologic feature is observed as an elongate grouping of alkaline intrusive plugs and stocks which were emplaced during Permo-Triassic to Middle Cretaceous time in the last major tectonic activity identified in the northeast. Geographically, the region of most intense plutonic activity extends in a narrow zone from northern New Hampshire to south coastal Maine. The northern end of the region intersects the WNEF, and on this basis the Q-M border event is included in the WNEF analyses. It is noted, however, that the Q-M border event is not anomalous with respect to the recurrence of earthquakes in the region bounding the White Mountain Intrusives, since several events of this size and larger are known for the region. Nonetheless, the Q-M border event is included in this analysis of the WNEF and, as is seen on Figure 16, the original model Equation 10 provides a conservative fit to the recurrence

data, because it over-estimates annual rates for most magnitudes, except for 5.0 m_b, which are not well constrained.

7.1.2 Models Based on Alternate Correlations

Equation 10 was determined during the 1979 study using the Nuttli and Herrmann (1978) m_b-I_o correlation (Equation 2) and the EUS m_b - M_L relation (Equation 6). The seismicity of the Western New England Foldbelt, which is plotted on the basis of these correlations, is shown on Figure 17. As in the previous section, events are $\geq$ 2.5 m_b and events with m_b estimated using correlations are plotted as rotated symbols. This analysis is repeated using an updated version of the WGC Catalog, which includes recent instrumental data not available for the 1979 study. Also, the effect of other combinations of empirical correlations on resulting recurrence rates are examined.

The sensitivity analyses performed include the following:

1. WGC Catalog, m_b - I_o by Equation 2; m_b - M_L by Equation 6. This is the methodology used in the 1979 analyses.

2. WGC Catalog, m_b - I_o by Equation 2; m_b - M_L by Equation 5.

3. WGC Catalog, m_b - I_o by Equation 2; No m_b - M_L relation is used, i.e. M_L is assumed equal to m_b.

Results of these three sensitivity analyses are shown on Tables 17, 18 and 19. Cumulative recurrence rates determined for the sensitivity analyses are plotted on Figures 18a, 18b and 18c. The original model for the WNEF (Equation 10) is

superimposed over the data points on these figures. Also, plotted on Figure 18d are rates determined using the preferred procedure of Section 7.1.1 using the WGC correlations.

The following observations are made on the results of these sensitivity analyses.

1. The original model (Equation 10) fits through the same two data points for each of the four cases. figures 18a-d. These include, first, the data point at 2.5 m_b which is determined by the instrumental observation of 8 events $\geq$2.5 m_b in the past 5 1/2 years of dense seismograph coverage. The second is the data point for 5.0 m_b which is determined by one occurrence (June 15, 1973, 4.9 m_b) in an assumed complete catalog interval of 250 years for this category event, 4.8 - 5.2 m_b.
2. Major differences in recurrence rates, amounting to factors of 3 to 5 variations at 3.5 m_b result from choice of m_b - I_o correlations, (i.e. Figure 18d versus Figures 18a, b, and c). On Figure 18d, which is based on Equation 4, the rates at these magnitudes are below the original model. On the other hand, the rates at these magnitudes for Figures 18a, b and c, determined using Equation 2, are above the original model, Equation 10 and significantly above the data on Figure 18d. The conservative assignment of magnitude

by Equation 2 (see Section 4.1) results in the major differences observed in the seismicity plots (Figures 15 and 17) and in the recurrence data (Figures 18a-d).

3. The use of m_b - M_L correlations affects data points at the 3.0 to 4.0 m_b range, but the influence is small compared to that introduced by varying the m_b - I_o correlation. The largest variation in recurrence rates (Figure 18c versus 18b) is approximately a 50% to 60% increase at 4.0 m_b resulting from assuming m_b equals M_L and therefore no corelation is used (Figure 18c). Differences in rates attributed to the two correlations, Equation 5 and 6 (Figure 18a versus 18b) are slight.

7.2 Chiburis Preliminary Catalog - CH77

The earthquake catalog for the WNEF, based on the preliminary Chiburis listing (CH77), and also on the Nuttli and Herrmann (1978) correlation of m_b to I_o is plotted on Figure 19. This map shows all events $\geq$ 2.5 m_b with historical events indicated by rotated symbols.

Interpretation of recurrence rates is given on Tables 20 and 21. Cumulative annual rates are plotted on Figure 20. Also, plotted on the figure as a solid line is Equation 10, the original model for the WNEF. The distribution of data points for the CH77 Catalog is similar to that shown on Figure 18c which is for the WGC Catalog, and the Nuttli and Herrmann

correlation. Therefore, although some differences exist between the catalogs, as can be seen by comparing Figures 17 (WGC) and Figure 19 (CH77), these differences do not significantly impact the resulting recurrence model interpretations.

Also, the positive residuals for data at magnitudes 3.5 and 4.0 m_b are seen on Figure 20 and again this characteristic, also seen on Figures 18a-c, is attributed to the use of Equation 2 which conservatively assigns m_b-magnitude to the lower values of I_o.

Several magnitude-frequency relationships are calculated for different subsets of the recurrence data plotted on Figure 20. The parameters of these models are given on Table 21. The preferred model, fit through data for m_b in the range of 2.5 to 5.0, inclusive, is plotted as a dotted line on Figure 20. This preferred model for the CH77 Catalog is in close agreement with the original model, Equation 10.

7.3 Chiburis Revised Catalog - CH81

The revised Chiburis Catalog, CH81 for the WNEF is plotted on Figure 21. As for the previous catalogs, the map shows events $\geq$ 2.5 m_b. In this case, however, m_b is assumed to be equal to the undifferentiated magnitude, M, employed by Chiburis (1981). Also, events scaled to M, from intensity are shown as rotated symbols.

The interpretation of mean annual recurrence rates for the CH81 Catalog using Equation 3 and no m_b - M_L relationship

is given on Tables 22 and 23. Cumulative rates are plotted on Figure 22, and parameters for several recurrence models are given on Table 23. The preferred magnitude-frequency model, fit through magnitudes 2.5 to 5.0 inclusive, is shown as the dotted line on Figure 22. This model is in close agreement to the original model for the WNEF (Equation 10) plotted as a solid line.

Positive residuals are again noted on Figure 22 for magnitudes 3.5 and 4.0. These again can be primarily attributed to conservative magnitude estimates resulting from the use of Equation 3, and secondarily to the procedure of mixing various magnitude types as is done in the CH81 listing.

8.0 DISCUSSION

Results of the magnitude-frequency analyses given in Sections 6.0 and 7.0 for the northern Appalachian region and for the Western New England Foldbelt, respectively, are discussed in this section. To facilitate the discussion, observed recurrence rates of magnitudes $\geq$ 3.5 m_b and those determined from magnitude-frequency models are compared on Figure 23. For the purpose of this comparison, results for the northern Appalachian region (Equations 7, 8 and 9) are normalized to the area of the Western New England Foldbelt, therefore all rates are given on Figure 23 as cumulative annual number of events $\geq$ 3.5 m_b (or M for the CH81 Catalog) per area of 123,000 km^2.

Observed rates are plotted as bars which define the high and low estimates of activity rates for complete segments of

the catalogs. Rates computed from recurrence models are shown as median values and one standard error bounds. Two sets of results are shown for the Western New England Foldbelt. These include results of regression analyses performed on the range of magnitudes from 2.5 to 5.0 m_b and on the range from 2.5 to 4.5 m_b after the highest magnitude (5.0 m_b) recurrence data are eliminated due to their poor definition, which are based on one historical occurrence of this size event (see Section 7.1.1). Also plotted on Figure 23 is the originally interpreted cumulative annual number of events $\geq$ 3.5 m_b for the Western New England Foldbelt of .156 which was used in YAEC-1263.

Results of this study, summarized and compared on Figure 23, illustrate the following: First, the seismic activity rate is lower, by a factor of 2.5 to 4.0 for the Western New England Foldbelt than for the larger area of the northern Appalachians. Second, recurrence rates for both source zones are higher on the basis of the Chiburis Catalog, especially for the CH77 list versus the WGC Catalog, but these differences result primarily from the m_b - I_o correlation used in the interpretation of the various catalogs (see Sections 6.5.1 and 7.1.2). Essentially, differences in recurrence rates are attributed to the use of median magnitude estimates in the WGC Catalog analyses compared to conservative magnitude estimates used in the Chiburis Catalog analyses. Due to the importance of the m_b - I_o relationship, and because

the correlation is poor as is seen by the scatter of data on Figure 2, uncertainty introduced by using the m_b - I_o correlation should be reflected in estimated recurrence rates. One approach for incorporating this uncertainty is to use a weighted average of results of the WGC and Chiburis Catalog interpretations.

The basis for deriving weights involves the choice of m_b - I_o correlation. For example, at intensity IV, Equation 2 (CH77 analyses) predicts a magnitude of 3.75 m_b, while Equation 4 (WGC analyses) predicts 3.12 m_b, which is a median value for the northeastern events analyzed. The value of 3.75 m_b is near one standard error above the median value because the standard error derived in the determination of Equation 4 is $\sigma m_b = 0.65$. This fact is therefore used to assign the following weights to results of the CH77 and WGC analyses. The CH77 results which are based on a prior assignment of magnitude near the + 1σ level are weighted at .30, while the WGC results are weighted at .70. Application of these weights towards an average of the cumulative rates (Log N_c/yr) greater than or equal to 3.5 m_b gives the following results.

$$\text{Rate/yr} \geq 3.5\ m_b = .1063$$

$$\sigma \text{Log}\ N_c \geq 3.5\ m_b = .356 \text{ (or, factor of 2.27)}$$

In contrast, a simple average of results for the WGC and CH77 Catalogs gives the following recurrence rates.

$$\text{Rate/yr} \geq 3.5\ m_b = .147$$

$$\sigma_{\text{Log } N_c} \geq 3.5\ m_b = .428 \text{ (or, factor of 2.68)}$$

Finally, weighted regression analyses on the CH77 and WGC recurrence data in the magnitude range of 2.5 to 5.0 m_b, using the weights described above, results in a synthesized recurrence model for the Western New England Foldbelt (Equation 11).

$$\text{Log } N_c = 2.775 - 1.08\ (\pm .04)\ m_b \qquad (11)$$

$$\sigma_{\text{Log } N_c} = 0.37$$

This preferred model predicts median annual rates $\geq 3.5\ m_b$ of 0.099 with one standard error equal to a factor of 2.34.

9.0 CONCLUSIONS

The important conclusions made on the basis of results of magnitude-frequency analyses performed in this study and summarized on Figure 23 include the following.

1. The seismic activity rates for the Western New England Foldbelt region of the northeast are lower, by factors of 2.5 to 4.0, than those inferred for the entire northeast region.

2. The choice of relationship used to correlate magnitudes to historical intensity data has a significant effect on interpreted recurrence rates. For example, results for the WGC Catalog are based on median estimates of magnitude versus epicentral intensity, I_o, while results for the CH77 and CH81 Catalogs are determined using conservative estimates of magnitude, especially for low values of I_o in the IV and V MMI range. Differences in interpretation of these lower intensity data are primarily responsible for the variation in recurrence rates seen on Figure 23 (see Section 6.5.1 and Section 7.1.2) between the WGC and CH77-81 analyses for the two source regions.

3. The originally determined recurrence rate of .156/year $\geq$ 3.5 m_b is conservative when median magnitude estimates are used as in the WGC analyses. When conservative magnitude estimates are used, the original rate is near the median of rates determined from recurrence models as is seen in the CH77 and CH81 analyses. Catalog differences are not primarily responsible for the variation observed on Figure 23, because use of different correlations with the WGC Catalog gives results similar to the CH77 and CH81 analyses (see Section 7.1.2).

4. The preferred analysis for estimating recurrence rates is to employ empirical relationships for assigning magnitudes which are specific to the northeast region as in the case of interpretation of the WGC Catalog.

5. The preferred cumulative annual rate of events $\geq 3.5m_b$ in the Western New England Foldbelt is approximately 0.10 with one standard error equal to a factor of 2.3. A comparison of this preferred estimate with that originally determined as .156/yr illustrates that recurrence rates used in YAEC-1263 lie roughly between the median and + 1σ levels determined in this analysis.

10.0 REFERENCES

Bernreuter, D. L., 1981, Review of Report (YAEC-1263), Seismic Response Spectra for the Yankee Nuclear Power Station, Rowe, Massachusetts, Yankee Atomic Company, June, 1981, Draft, submitted to W. T. Russell, Chief SEP Branch of U.S. NRC on November 4, 1981.

Bollinger, G. A., 1969, Seismicity of the Central Appalachian States of Virginia, West Virginia, and Maryland - 1758 through 1968: Bulletin of the Seismological Society of America, v. 59, no. 5, p. 2103-2111.

Bollinger, G. A., and Hopper, M. G., 1971, The Earthquake History of Virginia 1774 to 1900: Department of Geological Science, Virginia Polytechnic Institute and State University, Blacksburg, Virginia, 87 p.

_____, 1972, The Earthquake History of Virginia 1900-1970: Department of Geological Sciences, Virginia Polytechnic Institute and State University, Blacksburg, Virginia 85 p.

Bollinger, G. A., 1973, Seismicity of the Southeastern United States: Bulletin of the Seismological Society of America, v. 63, no. 5, p. 1785-1808.

Brigham, William, T., 1871, Volcanic Manifestations in New England: Being an Enumeration of the Principal Earthquakes from 1683 to 1869: Memoirs of the Boston Society of Natural History, 28 pp.

Brooks, John E., S. J., 1960, A Study in Seismicity and Structural Geology (Part I and II): Bulletin de Géophysique, Observatorie de Géophysique, Collège, Jean-de-Brébeuf, Montreal, Quebec, no. 6 and 7.

Chiburis, E. F., 1977, Preliminary Version of the Earthquake Listing that accompanies the Chiburis, 1981, publication.

Chiburis, E. F., 1981, Seismicity, Recurrence Rates and Regionalization of the Northeastern U.S. and Adjacent Southeastern Canada, NUREG/CR-2309.

Coffman, Jerry L. and von Hake, Carl A., 1973, Earthquake History of the United States, Publication 41-1, Revised Edition (through 1970): National Oceanic and Atmospheric Administration, Environmental Data Service, 208 p.

Docekal, J., 1970, Earthquakes in the Stable Interior, with emphasis on the Midcontinent: Ph.D Thesis, Graduate College, University of Nebraska, 2 Volumes.

Earthquake Data File, 1977, United States Department of Commerce, NOAA, Terrestrial Data Center, Boulder, Colorado, Mangetic Data Tape.

Earth Physics Branch (various authors), 1972-1981, Canadian Earthquakes - 1966-1979: Energy, Mines and Resources, Ottawa, Canada.

Gutenberg, B. and Richter, C. F., 1944, Frequency of Earthquakes in California: Bulletin of the Seismological Society of America, v. 34, p. 185-188.

Heck, N. H. and Eppley, R. A., 1958, Earthquake History of the United States: United States Department of Commerce, Coast and Geodetic Survey, Washington.

Mather, K. F. and Godfrey, H., assisted by K. Hampson, 1927, The Record of earthquakes Felt by Man in New England: Copy of the manuscripts of a paper presented to the Eastern Section of the Seismological Society of America.

Northeast Seismological Association, 1938-1950, Network Bulletins #1-240.

Northeast United States Seismic Network, 1975-1981, Network Bulletins #1-19.

Nuttli, O. W., 1973, The Mississippi Valley earthquakes of 1811 and 1812: Intensities, ground motion and magnitudes: Bulletin of the Seismological Society of America, vol. 63, p. 227-248.

Nuttli, O. W., 1974, Magnitude-recurrence relation for central Mississippi Valley earthquakes: Bulletin of the Seismological Society of America, v. 64, no. 4, p. 1189-1207.

Nuttli, O. W., 1979, State-of-the-art for assessing earthquake hazards in the United States, Report 16 - The relation of sustained maximum ground acceleration and velocity to earthquake intensity and magnitude: United States Army Engineer Waterways Experiment Station Miscellaneous Paper S-73-1, Report 16.

Nuttli, O. W. and Brill, K. G., Jr., 1980, Earthquake source zones in the central United States determined from historical seismicity: prepared for the Nuclear Regulatory Commission (preprint).

Nuttli, O. W. and Herrmann, R. B., 1978, State-of-the-art for assessing earthquake hazards in the United States, Report 12 - Credible earthquakes for the central United States: U.S. Army Engineers Waterways Experiment Station Miscellaneous Paper S-73-1, Report 12.

Richter, C. F., 1935, An Instrumental Earthquake Magnitude Scale: Bulletin of the Seismological Society of America, v. 25, p. 1-32.

Smith, W. E. T., 1962, Earthquakes of Eastern Canada and Adjacent Areas, 1534-1927, Publications of the Dominion Observatory, Ottawa, Canada, v. 26, no. 5.

_____, 1964, Earthquakes of Eastern Canada and Adjacent Areas, 1954-1959, Seismological Series of the Dominion Observatory, Ottawa, Canada.

_____, 1966, Canadian Earthquakes, 1963, Seismological Series of the Dominion Observatory, Ottawa, Canada.

_____, 1967, Earthquakes of Eastern Canada and Adjacent Areas, 1928-1959, Publications of the Dominion Observatory, Ottawa, Canada, v. 32, no. 3.

Stepp, J. C., 1972, Analysis of Completeness of the Earthquake Sample in the Puget Sound Area and its Effect on Statistical Estimates of Earthquake Hazard, Proceedings of International Conference on Microzonation, v. 2, p. 897-910.

Stevens, A. E., W. G. Milne, R. J. Wetmiller, and G. Leblanc, 1973, Canadian Earthquakes - 1967: Seismological Series of Earth Physics Branch, Ottawa, Canada, no. 65.

Street, R. L. and Turcotte, F. T., 1977, A study of Northeastern North American Spectral Moments, Magnitudes, and Intensities: Bulletin of the Seismological Society of America, v. 67, no. 3, p. 599-614.

TERA Corporation, 1979, Seismic Hazard Analysis: Solicitation of Expert Opinion, submitted to D. L. Bernreuter, Lawrence Livermore Laboratory.

TERA Corporation, 1981, Final Report - Seismic Hazard Analysis: Results, Nureg/CR-1582, v. 4, Draft.

United States Earthquakes, United States Coast and Geodetic Survey; 1928-1935, 1936-1940, 1941-1945, annual editions published 1946-1977.

Weston Geophysical Corporation, 1979, "Earthquake Data File for Eastern North America, Private Compilation from various sources, P.O. Box 550, Westboro, Massachusetts 01581.

Yankee Atomic Electric Company, 1981, Seismic Response Spectra for the Yankee Nuclear Power Station, Rowe, Massachusetts, YAEC-1263, Nuclear Services Division, 1671 Worcester Rd., Framingham, Massachusetts 01701, June, 1981.

TABLES

TABLE 1

DISCREPANCIES IN EARTHQUAKE CATALOGS
FOR THE NORTHEAST

YR	MO	DA	HR	LAT. N.	LONG. W.	I_o	m_b	M_L	SOURCE
1568				41.83	71.42	Felt	--	--	WGC
1568				41.50	72.50	VI	--	--	CH81
1568				41.50	72.50	VII	--	--	CH77
	(Not Listed)								WGC
1627				42.60	70.80	VI	--	--	CH81
1627				42.59	70.80	VI	--	--	CH77
1727	11	10	03	42.80	70.60	VII	--	--	WGC
1727	11	10	03	42.80	70.60	VII	--	--	CH81
1727	11	10	03	42.79	70.59	VIII	--	--	CH77
1732	09	16	16	45.50	73.60	VIII	--	--	WGC
1732	09	16	16	45.50	73.60	VIII	--	--	CH81
1732	09	16	16	45.50	73.59	IX	--	7.0	CH77
1766	02	02		42.35	68.00	Felt	--	--	WGC
1766	02	02		42.00	68.00	VI	--	--	CH81
1766	02	02		42.00	68.00	VI	--	--	CH77
1791	05	16	13	41.50	72.50	VI-VII	--	--	WGC
1791	05	16	13	41.50	72.50	VI	--	--	CH81
1791	05	16	13	41.50	72.50	VII	--	--	CH77
1817	10	05	16	42.50	71.20	V-VI	--	--	WGC
1817	10	05	16	42.50	71.20	VI	--	--	CH81
1817	10	05	16	42.50	71.20	VII-VIII	--	--	CH77
1840	11	11		39.80	75.20	V	--	--	WGC
1840	11	11		39.80	75.20	VII	--	--	CH81
1840	11	11		39.80	75.20	VII	--	--	CH77
1855	02	08	11	46.00	64.50	V	--	--	WGC
1855	02	08	11	46.00	64.50	VII	--	--	CH81
1855	02	08	11	46.00	64.50	VII	--	--	CH77
1877	11	04	06	45.20	73.90	VI	--	--	WGC
1877	11	04	06	45.20	73.90	VI	--	--	CH81
1877	11	04	06	45.20	73.90	VII	--	--	CH77

TABLE 1

DISCREPANCIES IN EARTHQUAKE CATALOGS
FOR THE NORTHEAST

YR	MO	DA	HR	LAT. N.	LONG. W.	I_o	m_b	M_L	SOURCE
1904	03	21	06	45.00	67.20	VI	--	--	WGC
1904	03	21	06	45.00	67.20	VI	--	--	CH81
1904	03	21	06	45.00	67.20	VII	--	--	CH77
1914	02	10	18	46.00	75.00	VII	--	5.5	WGC
1914	02	10	18	46.00	75.00	V	--	5.5	CH81
	(Not Listed)								CH77
1918	08	21	05	44.20	70.50	VI	--	--	WGC
1918	08	21	05	44.20	70.50	VI	--	--	CH81
1918	08	21	05	44.20	70.50	VII	--	--	CH77
1940	12	20	07	43.80	71.30	VII	5.4	--	WGC
1940	12	20	07	43.80	71.30	VII	--	5.8	CH81
1940	12	20	07	43.80	71.30	VII	--	5.8	CH77
1940	12	24	13	43.80	71.30	VII	5.4	--	WGC
1940	12	24	13	43.80	71.30	VII	--	5.8	CH81
1940	12	24	13	43.80	71.30	VII	--	5.8	CH77
1954	02	21	20	(non-tectonic event; possible mine collapse)					WGC
1954	02	21	20	41.20	75.90	VII	--	--	CH81
1954	02	21	20	41.20	75.90	VII	--	--	CH77
1963	10	16	15	42.50	70.80	V	3.9	--	WGC
1963	10	16	15	42.50	70.80	VI	--	4.2	CH81
1963	10	16	15	42.50	70.80	VI	--	4.2	CH77
1963	10	30	22	42.70	70.80	IV-V	2.4	--	WGC
1963	10	30	22	42.70	70.80	VI	--	--	CH81
1963	10	30	22	42.70	70.80	VI	--	--	CH77

TABLE 2

EARTHQUAKES USED TO DETERMINE RELATIONSHIP OF m_b-MAGNITUDE TO EPICENTRAL INTENSITY IN THE NORTHEAST

YR	MO	DA	LAT. N.	LONG. W.	I_o	m_b
1924	09	30	47.60	69.70	VII-VIII	5.5
1925	03	01	47.60	70.10	IX	6.6
1929	08	12	42.87	78.35	VIII	5.2
1931	04	20	43.40	73.70	VII	4.7
1935	11	01	46.78	79.07	VII	6.2
1938	08	23	40.10	74.50	V	3.9
1939	10	19	47.80	70.00	VI	5.6
1940	01	28	41.63	70.80	V	2.6
1940	12	20	43.80	71.30	VII	5.4
1943	01	14	45.30	69.60	V	4.4
1944	09	05	44.97	74.90	VIII	5.8
1947	12	28	45.20	69.20	V	4.4
1949	10	05	44.80	70.50	V	4.5
1951	09	03	41.25	74.25	V	3.8
1957	04	26	43.60	69.80	VI	4.8
1963	10	16	42.50	70.80	V	3.9
1963	10	30	42.70	70.80	IV-V	2.4
1964	04	01	43.60	71.50	IV	1.8
1964	06	26	43.30	71.90	V	2.6
1966	01	01	42.80	78.20	VI	4.7
1967	06	13	42.90	78.20	VI	3.9
1967	07	01	44.40	69.90	IV	2.9
1967	07	01	44.38	69.87	V	3.4
1968	10	19	45.30	74.12	V	3.2
1969	08	13	43.30	78.22	IV	2.5
1973	06	15	45.39	71.03	VI	4.9
1975	09	02	48.20	69.74	IV	3.3
1976	04	15	44.24	70.14	II-III	2.4
1976	04	24	41.46	72.49	IV	2.2
1976	05	10	41.54	71.01	V	2.7
1976	07	13	45.18	74.10	III-IV	2.9
1976	10	23	47.82	69.79	V	4.2
1977	08	08	49.77	67.05	IV	3.9
1977	12	20	41.82	70.76	IV	3.1
1977	12	20	41.84	70.70	III	2.4
1977	12	25	43.20	71.64	IV	3.2
1978	01	04	44.07	70.55	III-IV	3.0
1979	01	29	44.83	73.19	II	2.8
1979	04	23	43.04	71.24	III-IV	3.1
1979	12	30	41.16	73.72	III	2.2
1980	04	03	48.69	68.05	IV	4.1

TABLE 3

EARTHQUAKES USED TO DETERMINE RELATIONSHIP OF m_b-MAGNITUDE TO M_L-MAGNITUDE IN THE NORTHEAST

YR	MO	DA	LAT. N.	LONG. W.	I_o	m_b	M_L
1925	03	01	47.60	70.10	IX	6.6	7.0
1929	08	12	42.87	78.35	VIII	5.2	5.8
1931	04	20	43.40	73.70	VII	4.7	5.0
1935	11	01	46.78	79.07	VII	6.2	6.3
1938	08	23	40.10	74.50	V	3.9	4.6
1938	08	23	40.25	74.25	--	4.0	4.8
1938	08	23	40.25	74.25	--	3.7	4.6
1939	10	19	47.80	70.00	VI	5.6	5.8
1940	01	28	41.63	70.80	V	2.6	4.3
1940	12	20	43.80	71.30	VII	5.4	5.8
1940	12	24	43.80	71.30	VII	5.4	5.8
1940	12	25	43.80	71.30	--	3.7	4.0
1940	12	27	43.80	71.30	--	3.8	3.9
1941	01	21	43.80	71.30	--	2.8	3.6
1943	01	14	45.30	69.60	V	4.4	5.4
1944	09	05	44.97	74.90	VIII	5.8	5.9
1947	12	28	45.20	69.20	V	4.4	4.5
1949	10	05	44.80	70.50	V	4.5	4.0
1951	09	03	41.20	74.25	V	3.8	4.4
1952	10	14	48.02	69.78	--	4.9	5.6
1957	04	26	43.60	69.80	VI	4.8	4.7
1963	10	16	42.50	70.80	V	3.9	4.2
1963	10	30	42.70	70.80	IV-V	2.4	5.0
1964	06	26	43.30	71.90	V	2.6	3.6
1967	07	01	44.40	69.90	IV	2.9	3.2
1967	07	01	44.38	69.87	V	3.4	3.8

TABLE 4

RECURRENCE OF EARTHQUAKES IN THE NORTHERN APPALACHIANS
WESTON GEOPHYSICAL CATALOG

Time from Present (Yr.)	m_b - magnitude 2.0	2.5	3.0	3.5	4.0	4.5	5.0	5.5	6.0
300							7	1	2
250						19	7	1	2
180				77	6	17	5	1	1
140	94	228	173	69	5	17	4	1	1
100	86	183	146	53	3	14			
60	86	133	92	38	2	11			
20	78	71	27	16					
10	75	52	19	4					
5.5	71	48	14	3					

Mean Annual Recurrence Rates

300									(.0067)
250						.0760	(.0280)	(.0040)	(.0080)
180				.4278	.0333	.0944	.0278	.0056	.0056
140	.6714	1.6286	1.2357	.4929	(.0357)	(.1214)	(.0357)	(.0071)	.0071
100	.8600	1.8300	1.4600	.5300	.0300	.1400	.0400		
60	1.4333	2.2167	1.5333	.6333	(.0333)	(.1833)			
20	3.9000	3.5500	1.3500	(.8000)					
10	(7.5000)	(5.2000)	(1.9000)	.4000					
5.5	(12.9091)	(8.7273)	(2.5455)	(.5455)					

Parentheses indicate preferred rates, based on time intervals assumed to represent complete segments of the catalog.

TABLE 5

MAGNITUDE-FREQUENCY RELATIONSHIPS FOR
THE NORTHERN APPALACHIANS
WESTON GEOPHYSICAL CATALOG

m_b	Preferred Incremental Rates		Cumulative Rates	
2.0	7.5	12.91	15.3434	25.2598
2.5	5.2	8.73	7.8434	12.3498
3.0	1.9	2.55	2.6434	3.6198
3.5	0.55	0.80	.7434	1.0698
4.0	0.0333	0.0357	.1934	.2698
4.5	0.1214	0.1833	.1601	.2341
5.0	0.0280	0.0357	.0387	.0508
5.5	0.0040	0.0071	.0107	.0151
6.0	0.0067	0.0080	.0067	.0080

Range of Data: $2.0 \leq m_b \leq 6.0$

$\text{Log } N_c = 3.119 - 0.891\ (\pm .026)\ m_b$

S.E. = .146

Range of Data: $2.5 \leq m_b \leq 5.5$

$\text{Log } N_c = 3.267 - 0.930\ (\pm .039)\ m_b$

S.E. = .147

TABLE 6

RECURRENCE OF EARTHQUAKES IN THE NORTHERN APPALACHIANS
PRELIMINARY CHIBURIS CATALOG - CH77

Time from Present (Yr.)	m_b - magnitude 2.0	2.5	3.0	3.5	4.0	4.5	5.0	5.5	6.0
300									1
250						19	10	3	1
180	64	206	201	198	74	18	8	2	1
140	64	200	187	183	66	18	8	1	1
100	64	180	131	143	51	13	8		
60	64	125	94	83	32	12			
18	54	49	37	11	12	3			
8	43	32	16	1	1				
3	37	25	12	-					

Mean Annual Recurrence Rates

300									(.0033)
250						.0760	(.0400)	(.0120)	(.0040)
180	.3556	1.1444	1.1167	1.1000	.4111	.1000	.0444	.0111	.0056
140	.4571	1.4286	1.3357	1.3071	(.4714)	(.1286)	(.0571)	(.0071)	.0071
100	.6400	1.8000	1.3100	(1.4300)	.5100	.1300	.0800		
60	1.0667	2.0833	1.5667	1.3833	(.5333)	(.2000)			
18	3.0000	2.7222	2.0556	(.6111)	.6667	.1667			
8	(5.3750)	(4.0000)	(2.0000)	.1250	.1250				
3	(12.3333)	(8.3333)	(4.0000)	-					

Parentheses indicate preferred rates, based on time intervals assumed to represent complete segments of the catalog.

TABLE 7

MAGNITUDE-FREQUENCY RELATIONSHIPS
FOR THE NORTHERN APPALACHIANS - CH77 CATALOG

m_b	Preferred Incremental Rates		Cumulative Rates	
2.0	5.3750	12.3300	12.6365	26.8964
2.5	4.0000	8.3300	7.2615	14.5664
3.0	2.0000	4.0000	3.2615	6.2364
3.5	0.6111	1.4300	1.2615	2.2364
4.0	0.4714	0.5333	.6504	.8064
4.5	0.1286	0.2000	.1790	.2731
5.0	0.0400	0.0571	.0504	.0731
5.5	0.0071	0.0120	.0104	.0160
6.0	0.0033	0.0040	.0033	.0040

Range of Data: $2.0 \leq m_b \leq 6.0$

Log N_c = 3.399 - .938 ($\pm$ .037) m_b

S.E. = .205

Range of Data: $2.5 \leq m_b \leq 5.5$

Log N_c = 3.521 - .952 ($\pm$ .044) m_b

S.E. = .166

TABLE 8

RECURRENCE OF EARTHQUAKES IN THE NORTHERN APPALACHIANS
REVISED CHIBURIS CATALOG - CH81

Time from Present (Yr.)	M - magnitude 2.0	2.5	3.0	3.5	4.0	4.5	5.0	5.5	6.0
300								1	2
250			180	199	71	21	7	1	2
180			169	186	69	19	5	1	1
140	235	82	157	171	61	18	5	1	1
100	217	82	117	137	47	14	5		
60	166	82	86	78	29	11	4		
20	106	79	37	11	9	2			
10	88	63	23	1	1	1			
5.5	81	54	18	1	1				

Mean Annual Recurrence Rates

300								.0033	(.0067)
250			.7200	.7690	.2840	.0840	(.0280)	(.0040)	(.0080)
180			.9389	1.0333	.3833	.1056	.0278	.0056	.0056
140	1.6786	.5857	1.1214	1.2214	(.4357)	(.1286)	(.0357)	(.0071)	.0071
100	2.1700	.8200	1.1700	(1.3700)	.4700	.1400	.0500		
60	2.7667	1.3667	1.4333	1.3000	(.4833)	(.1833)	.0667		
20	5.3000	3.9500	1.8500	(.5500)	.4500	.1000			
10	(8.8000)	(6.3000)	(2.3000)	.1000	.1000	.1000			
5.5	(13.5000)	(9.0000)	(3.0000)	.1667	.1667				

Parentheses indicate preferred rates, based on time intervals assumed to represent complete segments of the catalog.

TABLE 9

MAGNITUDE-FREQUENCY RELATIONSHIPS
FOR THE NORTHERN APPALACHIANS - CH81 CATALOG

M	Preferred Incremental Rates		Cumulative Rates	
2.0	8.8000	13.5000	18.5530	27.5874
2.5	6.3000	9.0000	9.7530	14.0874
3.0	2.3000	3.0000	3.4530	5.0874
3.5	.5500	1.3700	1.1530	2.0874
4.0	.4357	.4833	.6030	.7174
4.5	.1286	.1833	.1673	.2341
5.0	.0280	.0357	.0387	.0508
5.5	.0040	.0071	.0107	.0151
6.0	.0067	.0080	.0067	.0080

Range of Data: $2.0 \leq m_b \leq 6.0$

$\text{Log } N_c = 3.356 - .923 (\pm .026) M$

S.E. = .141

Range of Data: $2.5 \leq m_b \leq 5.5$

$\text{Log } N_c = 3.604 - .981 (\pm .034) M$

S.E. = .128

TABLE 10

COMPARISON OF PREFERRED MODELS
FOR THE NORTHERN APPALACHIAN FOLDBELT

Catalog	Recurrence Model a	b	σ_b	S.E.[b]	Rate ≥ 3.5 m_b obs.[c]	Model	Rate ≥ 5.5 m_b obs.[c]	Model
WGC	3.267	-.930	.039	.147	.7434 1.0698	1.0280	.0107 .0151	.0142
CH77	3.521	-.952	.044	.166	1.2615 2.2364	1.5453	.0104 .0160	.0193
CH81	3.604	-.981	.034	.128	1.1530 2.0874	1.4808	.0107 .0151	.0162

[a] Area = 3.94×10^5 Km^2

[b] S.E. = Standard Error of Estimate on $Log_{10}N_c$.
Equivalently S.E. .128 = factor of 1.343 per standard error.
.147 = factor of 1.403, .166 = factor of 1.466

[c] Observed rates include high and low estimates from Tables 5, 7 and 9.

TABLE 11

SENSITIVITY TO CHOICE OF CONVERSION RELATIONSHIPS
WESTON GEOPHYSICAL CATALOG

Time from Present (Yr.)		2.0	2.5	3.0	3.5	4.0	4.5	5.0	5.5	6.0
	a							7	1	(2)
300	b							10	2	(1)
	a						19	(7)	(1)	(2)
250	b						25	(10)	(2)	(1)
	a				77	6	17	5	(1)	1
180	b				170	68	24	7	(1)	1
	a	94	228	173	69	(5)	(17)	(4)	1	1
140	b	98	151	202	163	(60)	(23)	(7)	1	1
	a	86	183	146	(53)	3	14			
100	b	98	140	149	(136)	44	18			
	a	86	133	92	38	(2)	(11)			
60	b	97	124	100	81	(29)	(14)			
	a	78	71	27	(16)					
20	b	89	63	39	(11)					
	a	(75)	(52)	(19)	4					
10	b	(79)	(53)	(21)	4					
	a	(71)	(48)	(14)	3					
5.5	b	(73)	(46)	(17)	3					

a - WGC conversion relationships; equations 4 and 5.

b - Nuttli and Herrmann (1978) equation 2; no $m_b - M_L$ correlation.

Parentheses indicate preferred recurrence rates.

TABLE 12

MAGNITUDE-FREQUENCY RELATIONSHIPS FOR
THE NORTHERN APPALACHIANS
WESTON GEOPHYSICAL CATALOG

Sensitivity Analysis - Nuttli and Herrmann (1978)
m_b - I_o Relationship; No M_b - M_L Relationship

m_b	Preferred Incremental Rates		Cumulative Rates	
2.0	.9000	13.2727	16.4918	26.8558
2.5	5.3000	8.3636	8.5918	13.5831
3.0	2.1000	3.0909	3.2918	5.2195
3.5	0.5500	1.3500	1.1918	2.1286
4.0	0.4286	0.4833	0.6418	0.7786
4.5	0.1643	0.2333	0.2132	0.2953
5.0	0.0400	0.0500	0.0489	0.0620
5.5	0.0056	0.0080	0.0089	0.0120
6.0	0.0033	0.0040	0.0033	0.0040

Range of Data: $2.0 \leq m_b \leq 6.0$

Log N_c = 3.460 - .956 ($\pm$ .035) m_b

S.E. = .191

Range of Data: $2.5 \leq m_b \leq 5.5$

Log N_c = 3.584 - .972 ($\pm$ .046) m_b

S.E. = .172

TABLE 13

RECURRENCE OF EARTHQUAKES IN THE NORTHERN APPALACHIANS
WESTON GEOPHYSICAL CATALOG
(Histogram Centers by Equation 4)

Time from Present (yr.)	m_b - magnitude 1.8	2.5	3.1	3.8	4.5	5.1	5.8
300							2
250						9	2
180				81	21	7	1
140	187	256	209	73	20	7	1
100	176	203	182	57	15	6	
60	160	154	127	42	11		
20	105	88	54	18			
10	100	72	31	4			
5.5	93	63	25	3			

Mean Annual Recurrence Rates

300							(.0067)
250						(.0360)	(.0080)
180				.4500	.1167	.0389	.0056
140	1.3357	1.8286	1.4929	(.5214)	(.1429)	(.0500)	.0071
100	1.7600	2.0300	1.8200	.5700	.1500	.0600	
60	2.6667	2.5667	2.1167	(.7000)	(.1833)		
20	5.2500	4.4000	2.7000	.9000			
10	(10.0000)	(7.2000)	(3.1000)	.4000			
5.5	(16.9091)	(11.4545)	(4.5455)	.5455			

Parentheses indicate preferred rates

TABLE 14

MAGNITUDE-FREQUENCY RELATIONSHIPS FOR
THE NORTHERN APPALACHIANS
WESTON GEOPHYSICAL CATALOG
(Histogram Centers by equation 4)

m_b	Preferred Incremental Rates		Cumulative Rates	
1.8	10.0000	16.9091	21.0070	33.8504
2.5	7.2000	11.4545	11.0070	16.9413
3.1	3.1000	4.5455	3.8070	5.4868
3.8	0.5214	0.7000	0.7070	0.9413
4.5	0.1429	0.1833	0.1856	0.2413
5.1	0.0360	0.0500	0.0427	0.0580
5.8	0.0067	0.0080	0.0067	0.0080

Range of Data: $1.8 \leq m_b \leq 5.8$

Log $N_c = 3.272 - .901 (\pm .035) m_b$

S.E. = .175

Range of Data: $2.5 \leq m_b \leq 5.1$

Log $N_c = 3.457 - .927 (\pm .033) m_b$

S.E. = .100

TABLE 15

RECURRENCE OF EARTHQUAKES IN THE WESTERN NEW ENGLAND FOLDBELT
WESTON GEOPHYSICAL CATALOG

Time from Present (Yr.)	m_b - magnitude 2.0	2.5	3.0	3.5	4.0	4.5	5.0
250							1
180	17	38	31	7	-	-	1
140	17	38	30	6	-	-	
100	17	30	23	5			
60	17	22	14	5			
20	13	12	-	1			
10	12	9	-	-			
5.5	12	8	-	-			
Mean Annual Recurrence Rates							
250							(.0040)
180	.0944	.2111	.1722	.0398	-	-	.0056
140	.1214	.2714	(.2143)	(.0429)			(.0071)
100	.1700	.3000	.2300	.0500			
60	.2833	.3667	(.2333)	(.0833)			
20	.6500	.6000	-	.0500			
10	(1.2000)	(.9000)	-	-			
5.5	(2.1818)	(1.4545)	-	-			

Parentheses indicate preferred rates, based on time intervals assumed to represent complete segments of the catalog.

TABLE 16

RECURRENCE OF EARTHQUAKES
IN THE WESTERN NEW ENGLAND FOLDBELT
WESTON GEOPHYSICAL CATALOG

m_b	Preferred Incremental Rates		Cumulative Rates	
2.0	1.2000	2.1818	2.3612	3.9600
2.5	.9000	1.4545	1.1612	1.7782
3.0	.2143	.2333	.2612	.3237
3.5	.0429	.0833	.0469	.0904
4.0	-	-	.0040	.0071
4.5	-	-	.0040	.0071
5.0	.0040	.0071	.0040	.0071

Recurrence Models

Range of Data	a-Value	b-Value	S. E.	Rate ≥ 3.5 m_b
2.0 - 3.5	2.870	-1.142	.1612	.075
2.5 - 3.5	3.510	-1.344	.1252	.064
2.5 - 4.5	3.396	-1.320	.2706	.060
2.5 - 5.0	2.556	-1.054	.3792	.074
2.0 - 5.0	2.590	-1.063	.3494	.074

TABLE 17

RECURRENCE OF EARTHQUAKES IN THE WESTERN NEW ENGLAND FOLDBELT
WESTON GEOPHYSICAL CATALOG

(m_b - I_o, Equation 2; m_b - M_L, Equation 6)

Time from Present (Yr.)	m_b - magnitude 2.0	2.5	3.0	3.5	4.0	4.5	5.0
250							1
180	19	29	31	31	5	-	1
140	19	29	31	30	4	-	1
100	19	29	23	23	3		
60	18	27	15	14	3		
20	17	11	3	1	-		
10	15	9	-	-	-		
5.5	15	8	-	-	-		
Mean Annual Recurrence Rates							
250							(.0040)
180	.1056	.1611	.1722	.1722	.0278	-	.0056
140	.1357	.2071	.2214	(.2143)	(.0286)	-	(.0071)
100	.1900	.2900	.2300	.2300	.0300		
60	.3000	.4500	(.2500)	(.2333)	(.0500)		
20	.8500	.5500	(.1500)	.0500	-		
10	(1.5000)	(.9000)	-	-			
5.5	(2.1818)	(1.4545)	-				

TABLE 18

RECURRENCE OF EARTHQUAKES IN THE WESTERN NEW ENGLAND FOLDBELT
WESTON GEOPHYSICAL CATALOG

(m_b - I_o, Equation 2; m_b - M_L, Equation 5)

Time from Present (Yr.)	m_b - magnitude 2.0	2.5	3.0	3.5	4.0	4.5	5.0
250							1
180	18	28	29	27	5	-	1
140	18	28	29	26	4	-	1
100	18	28	21	19	3		
60	17	26	13	10	3		
20	13	12	-	1	-		
10	12	9	-	-	-		
5.5	12	8	-	-	-		
Mean Annual Recurrence Rates							
250							(.0040)
180	.1000	.1556	.1611	.1500	.0278	-	.0056
140	.1286	.2000	(.2071)	(.1857)	(.0286)	-	(.0071)
100	.1800	.2800	.2100	.1900	.0300		
60	.2833	.4333	(.2167)	(.1667)	(.0500)		
20	.6500	.6000	-	.0500	-		
10	(1.2000)	(.9000)	-				
5.5	(2.1818)	(1.4545)	-				

TABLE 19

RECURRENCE OF EARTHQUAKES IN THE WESTERN NEW ENGLAND FOLDBELT
WESTON GEOPHYSICAL CATALOG

(m_b - I_o, Equation 2; No m_b - M_L used)

Time from Present (Yr.)	m_b - magnitude 2.0	2.5	3.0	3.5	4.0	4.5	5.0
250							1
180	19	28	29	31	7	-	1
140	19	28	29	30	6	-	1
100	19	28	21	23	5		
60	18	26	13	14	5		
20	16	11	3	-	1		
10	14	9	-	-	-		
5.5	12	8	-	-	-		
Mean Annual Recurrence Rates							
250							(.0040)
180	.1056	.1556	.1611	.1722	.0389	-	.0056
140	.1357	.2000	.2071	(.2143)	(.0429)	-	(.0071)
100	.1900	.2800	.2100	.2300	.0500		
60	.3000	.4333	(.2167)	(.2333)	(.0833)		
20	.8000	.5500	(.1500)		.0500		
10	(1.4000)	(.9000)	-				
5.5	(2.1818)	(1.4545)	-				

TABLE 20

RECURRENCE OF EARTHQUAKES
IN THE WESTERN NEW ENGLAND FOLDBELT
CH77 CATALOG

Time from Present (Yr.)	m_b - magnitude 2.0	2.5	3.0	3.5	4.0	4.5	5.0
250							1
180	12	45	25	35	8	-	1
140	12	44	25	34	7		1
100	12	40	13	26	6		
60	12	27	14	17	5		
18	8	13	4	1	1		
8	6	8	1	-			
3	4	7	1	-			
Mean Annual Recurrence Rates							
250							(.0040)
180	.0667	.2500	.1389	.1944	.0444	-	.0056
140	.0857	.3143	.1786	(.2429)	(.0500)		(.0071)
100	.1200	.4000	.1900	.2600	.0600		
60	.2000	.4500	(.2333)	(.2833)	(.0833)		
18	.4444	.7222	.2222	.1556	.0556		
8	(.7500)	(1.0000)	.1250				
3	(1.3333)	(2.3333)	(.3333)				

TABLE 21

MAGNITUDE-FREQUENCY RELATIONSHIP
FOR THE WESTERN NEW ENGLAND FOLDBELT
CH77 CATALOG

m_b	Preferred Incremental Rates		Cumulative Rates	
2.0	.7500	1.3333	2.2802	4.3736
2.5	1.0000	2.3333	1.5302	3.0403
3.0	.2333	.3333	.5302	.7070
3.5	.2429	.2833	.2969	.3737
4.0	.0500	.0833	.0540	.0904
4.5	-	-	.0040	.0071
5.0	.0040	.0071	.0040	.0071

Recurrence Models

Range of Data	a-Value	b-Value	S. E.	Rate $\geq$ 3.5 m_b
2.5 - 3.5	2.315	- .811	.145	.299
2.5 - 4.5	3.553	-1.231	.268	.175
2.5 - 5.0	3.253	-1.1368	.267	.188
2.0 - 5.0	2.825	-1.034	.288	.161

TABLE 22

RECURRENCE OF EARTHQUAKES
IN THE WESTERN NEW ENGLAND FOLDBELT
CH81 CATALOG

Time from Present (Yr.)	m_b - magnitude 2.0	2.5	3.0	3.5	4.0	4.5	5.0
250							1
180	47	17	23	34	8	-	1
140	46	17	23	33	7	-	1
100	44	17	19	25	6		
60	33	17	14	16	5		
20	21	16	5	1	1		
10	17	12	1	-	-		
6	15	10	1	-	-		
Mean Annual Recurrence Rates							
250							(.0040)
180	.2611	.0944	.1278	.1889	.0444	-	.0056
140	.3286	.1214	.1643	(.2357)	(.0500)	-	(.0071)
100	.4400	.1700	.1900	.2500	.0600		
60	.5500	.2833	.2333	(.2667)	(.0833)		
20	1.0500	.8000	(.2500)	.0500	.0500		
10	(1.7000)	(1.2000)	.1000	-			
6	(2.5000)	(1.6667)	(.1667)				

TABLE 23

MAGNITUDE-FREQUENCY RELATIONSHIP
FOR THE WESTERN NEW ENGLAND FOLDBELT
CH81 CATALOG

m_b	Preferred Incremental Rates		Cumulative Rates	
2.0	1.7000	2.5000	3.3564	4.7738
2.5	1.2000	1.6667	1.6564	2.2738
3.0	.1667	.2500	.4564	.6071
3.5	.2357	.2667	.2897	.3571
4.0	.0500	.0833	.0540	.0904
4.5	-	-	.0540	.0071
5.0	.0040	.0071	.0040	.0071

Recurrence Models

Range of Data	a-Value	b-Value	S. E.	Rate ≥ 3.5 m_b
2.5 - 3.5	2.181	- .781	.125	.281
2.5 - 4.5	3.417	-1.200	.267	.165
2.5 - 5.0	3.138	-1.112	.263	.177
2.0 - 5.0	2.859	-1.045	.259	.159

FIGURES

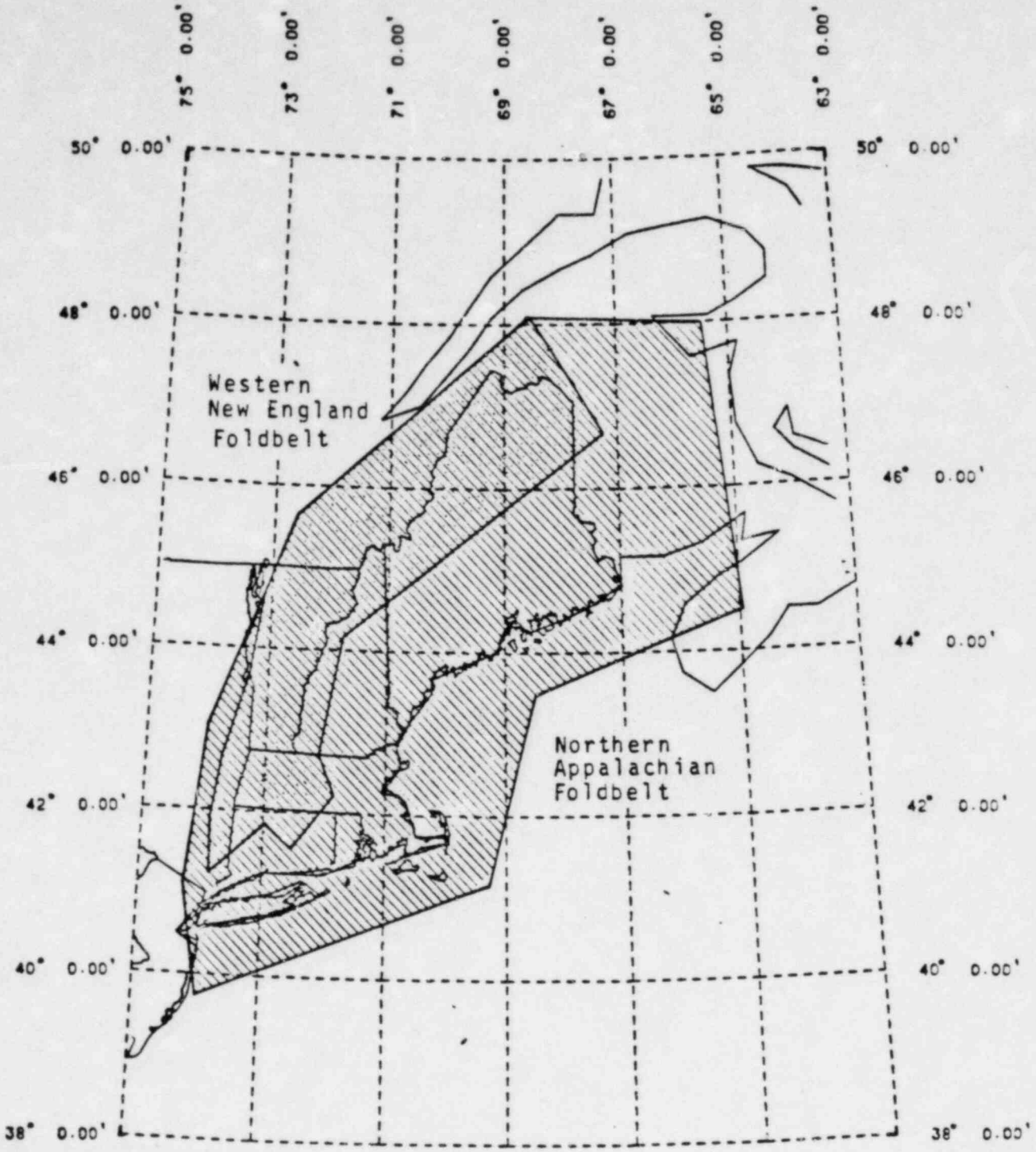

EARTHQUAKE SOURCE ZONES

FIGURE 1

Weston Geophysical

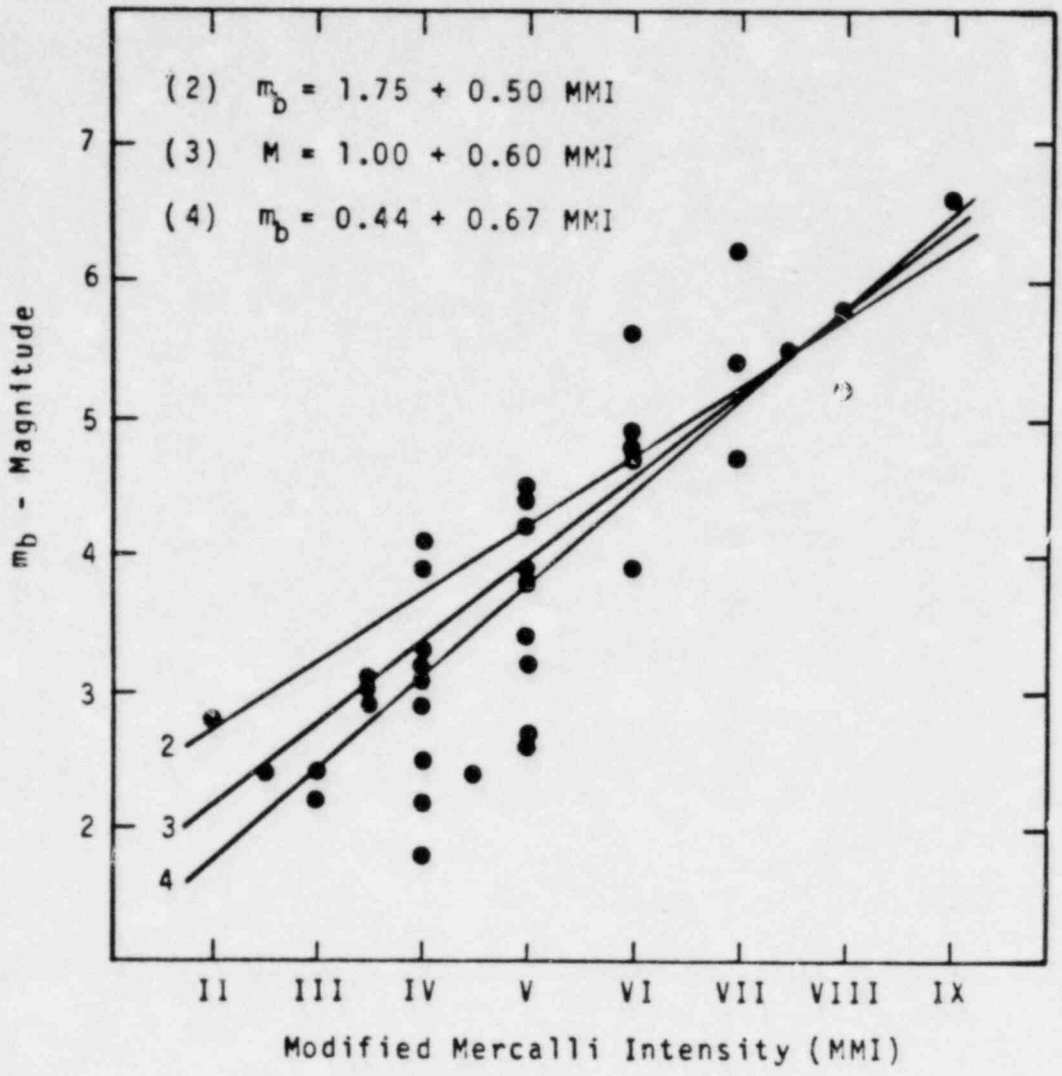

● m_b vs. MMI Data for the NE; WGC Catalog 40°-50° N; 65°-80° W

(2) - Nuttli and Herrmann (1978)

(3) - Chiburis (1981)

(4) - WGC; This Study Least Squares Best Fit for NE Data

FIGURE 2

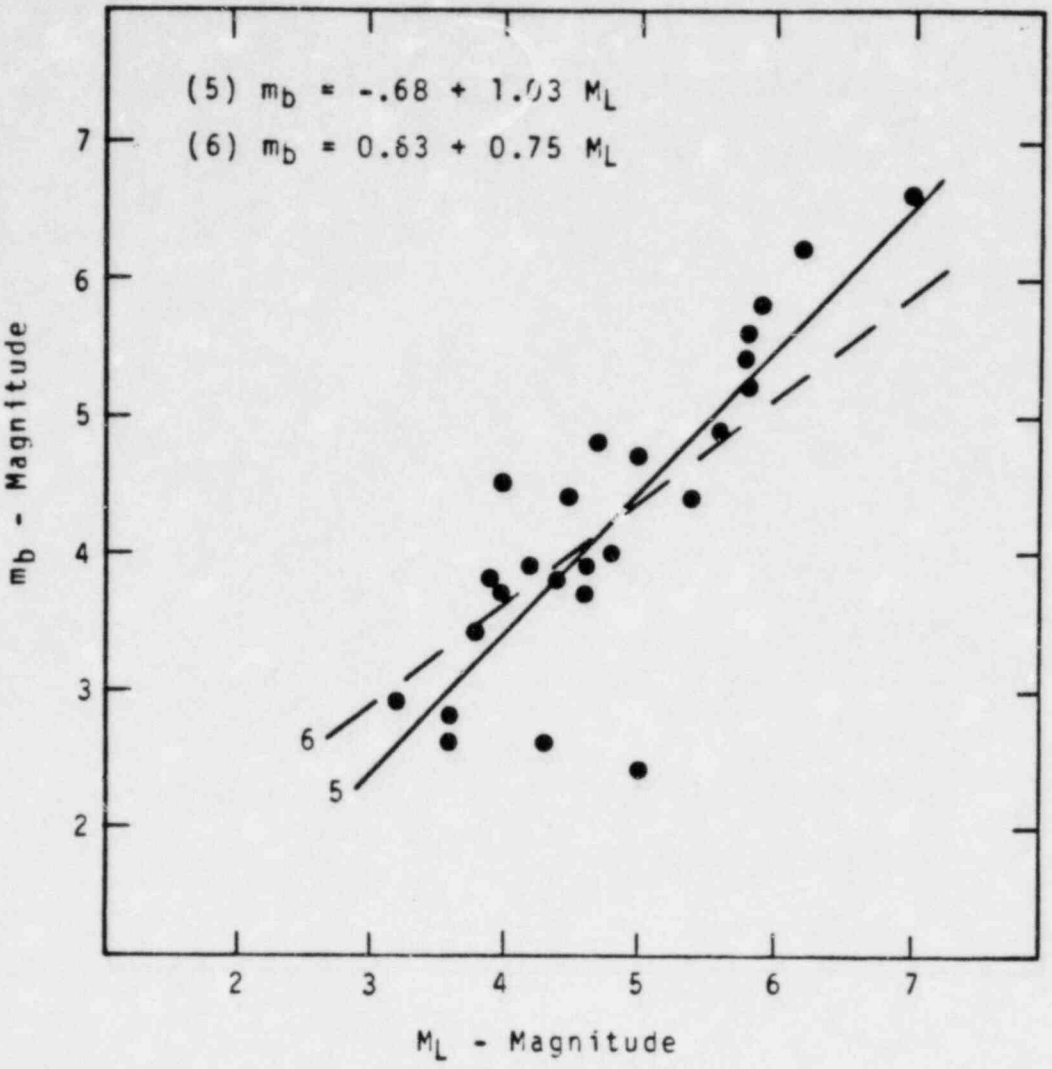

● m_b vs. M_L Data for the NE; WGC Catalog; 40°-50° N; 65°-80° W Prior to 1970

(5) WGC, This Study Least Squares Best Fit for NE Data

(6) WGC, Least Squares Best Fit for Central and Eastern Regions 30°-50° N, 60°-100° W, prior to 1975

FIGURE 3

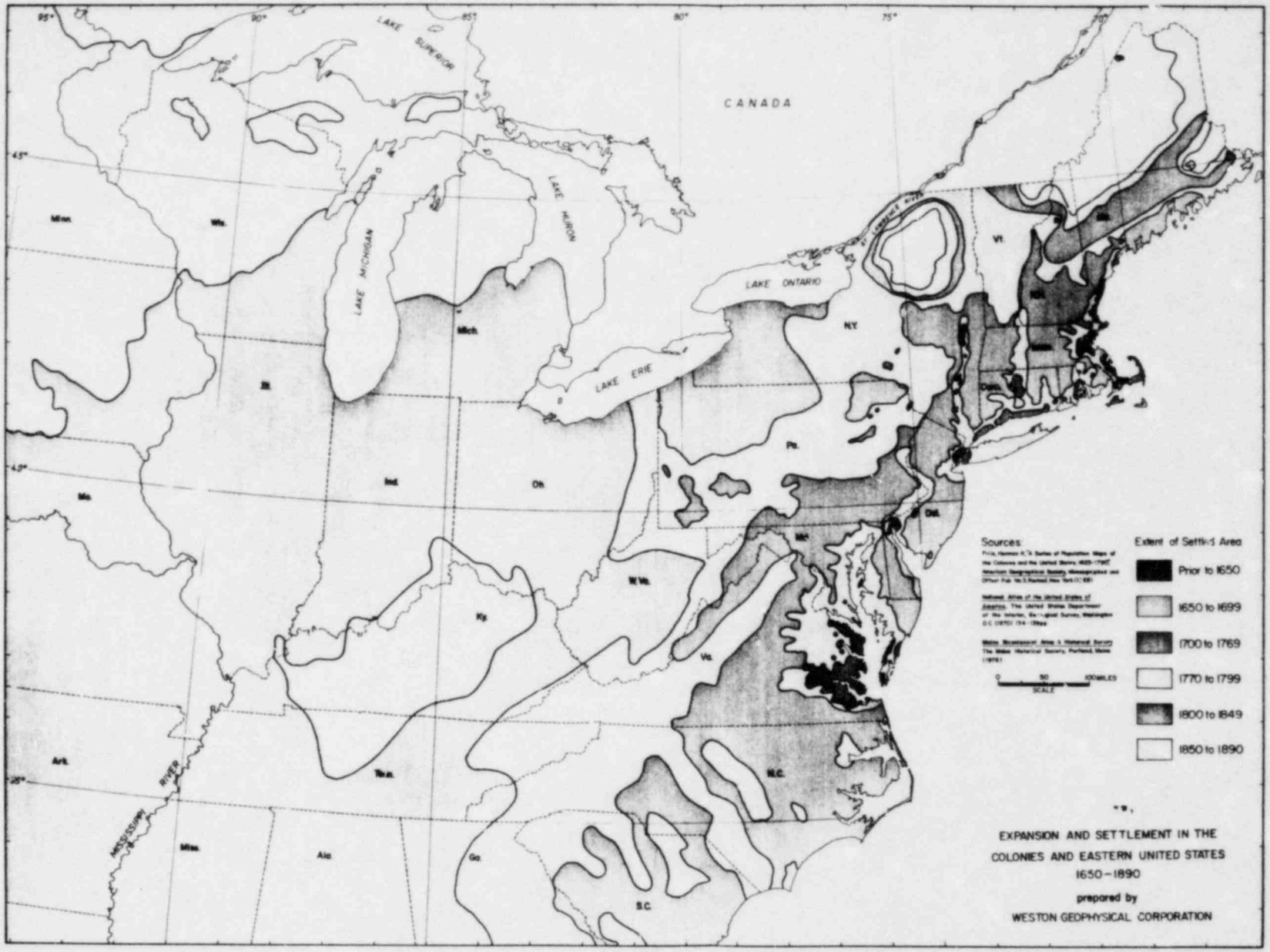
CANADA
LAKE SUPERIOR
LAKE MICHIGAN
LAKE HURON
LAKE ONTARIO
LAKE ERIE
ST. LAWRENCE RIVER
MISSISSIPPI RIVER
Minn.
Wis.
Mich.
Ill.
Ind.
Oh.
Ky.
W.Va.
Va.
N.C.
S.C.
Ga.
Ala.
Miss.
Ark.
Tenn.
N.Y.
Pa.
Me.
N.H.
Vt.
Mass.
R.I.
Conn.
Del.
Md.
Sources:
Extent of Settled Area
Prior to 1650
1650 to 1699
1700 to 1769
1770 to 1799
1800 to 1849
1850 to 1890
0 50 100 MILES
SCALE
EXPANSION AND SETTLEMENT IN THE
COLONIES AND EASTERN UNITED STATES
1650–1890
prepared by
WESTON GEOPHYSICAL CORPORATION

FIGURE 4

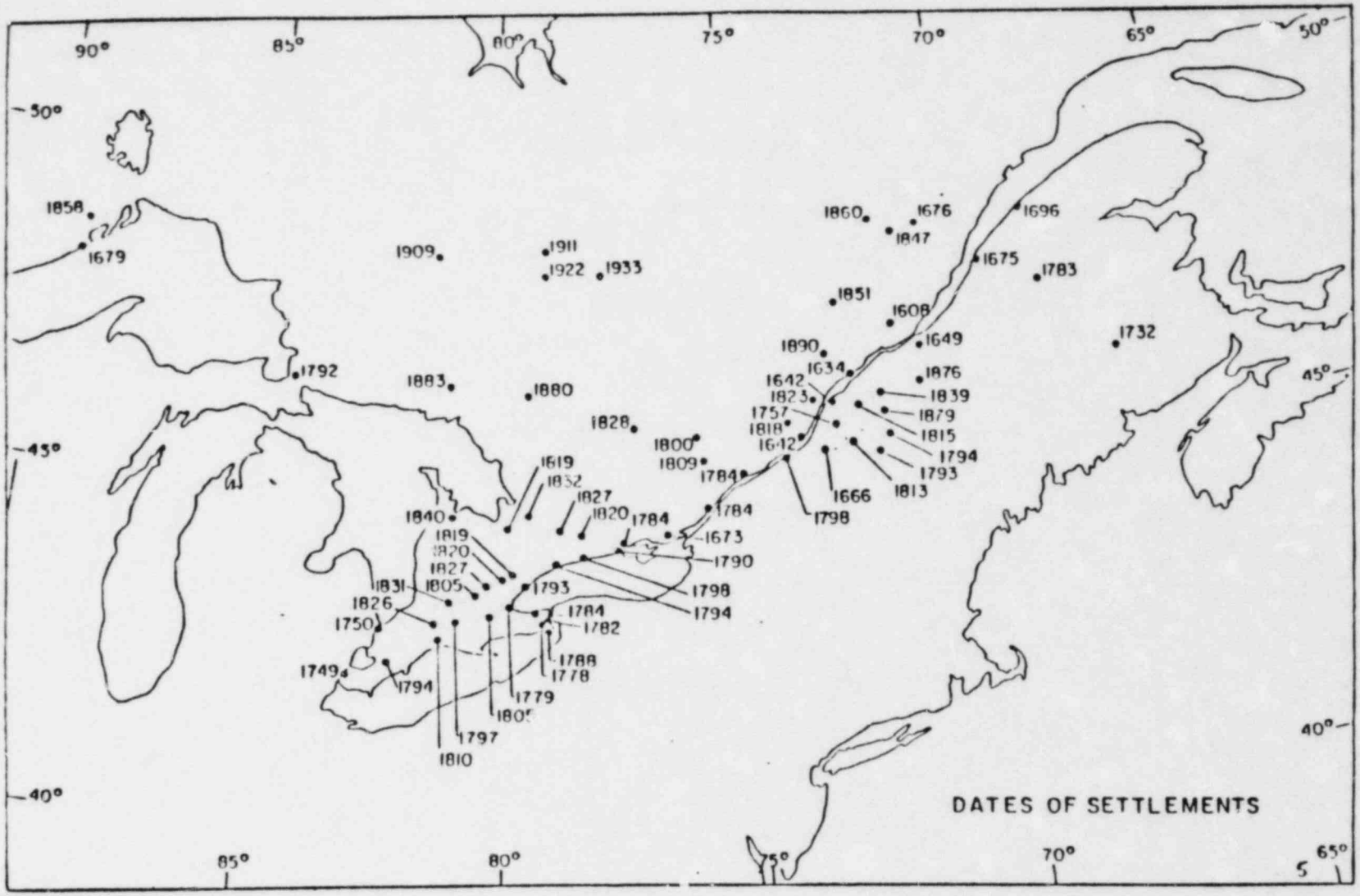

SETTLEMENTS IN CANADA

FIGURE 5

Weston Geophysical

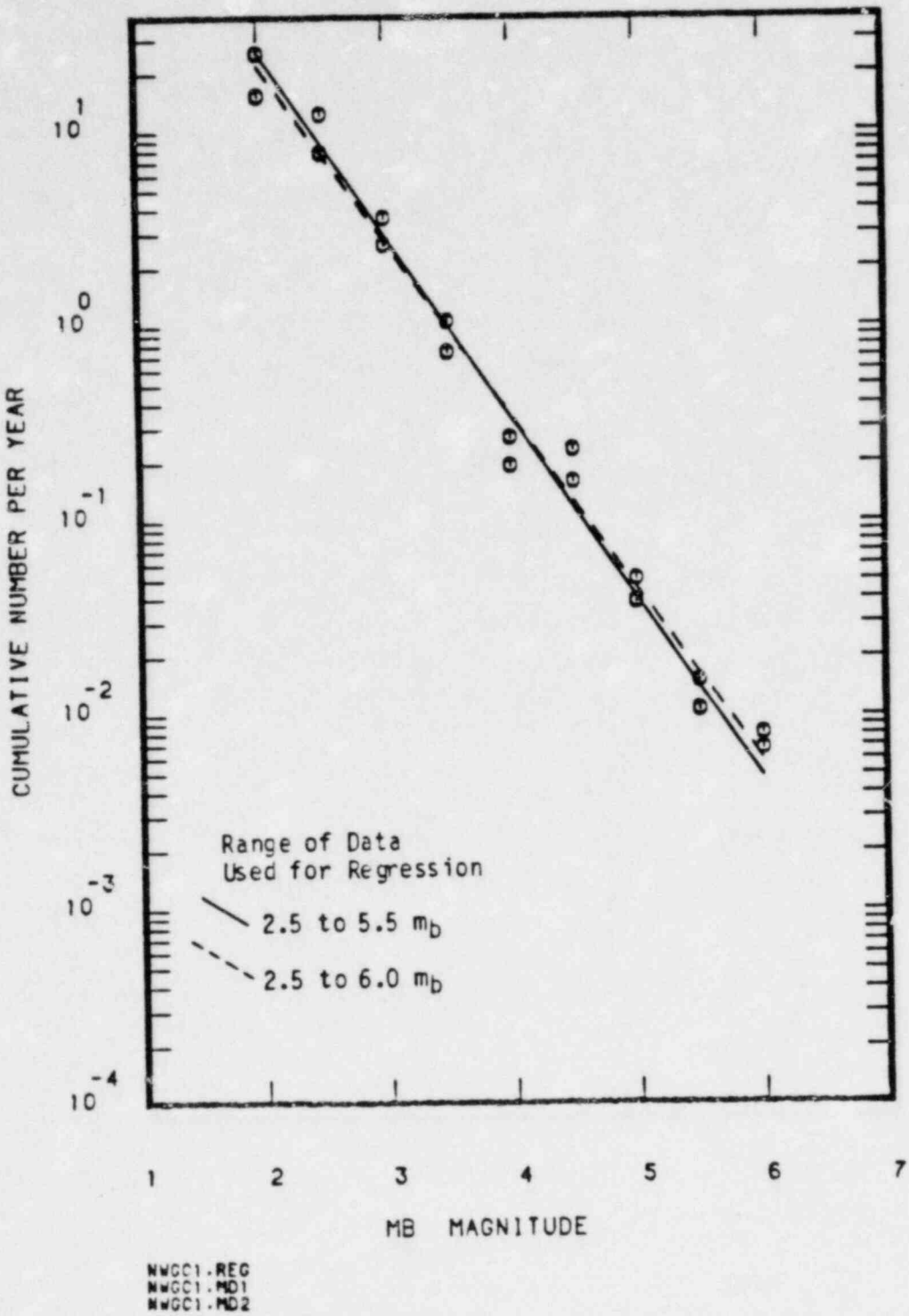

NORTHERN APPALACHIANS
WGC CATALOG

FIGURE 6

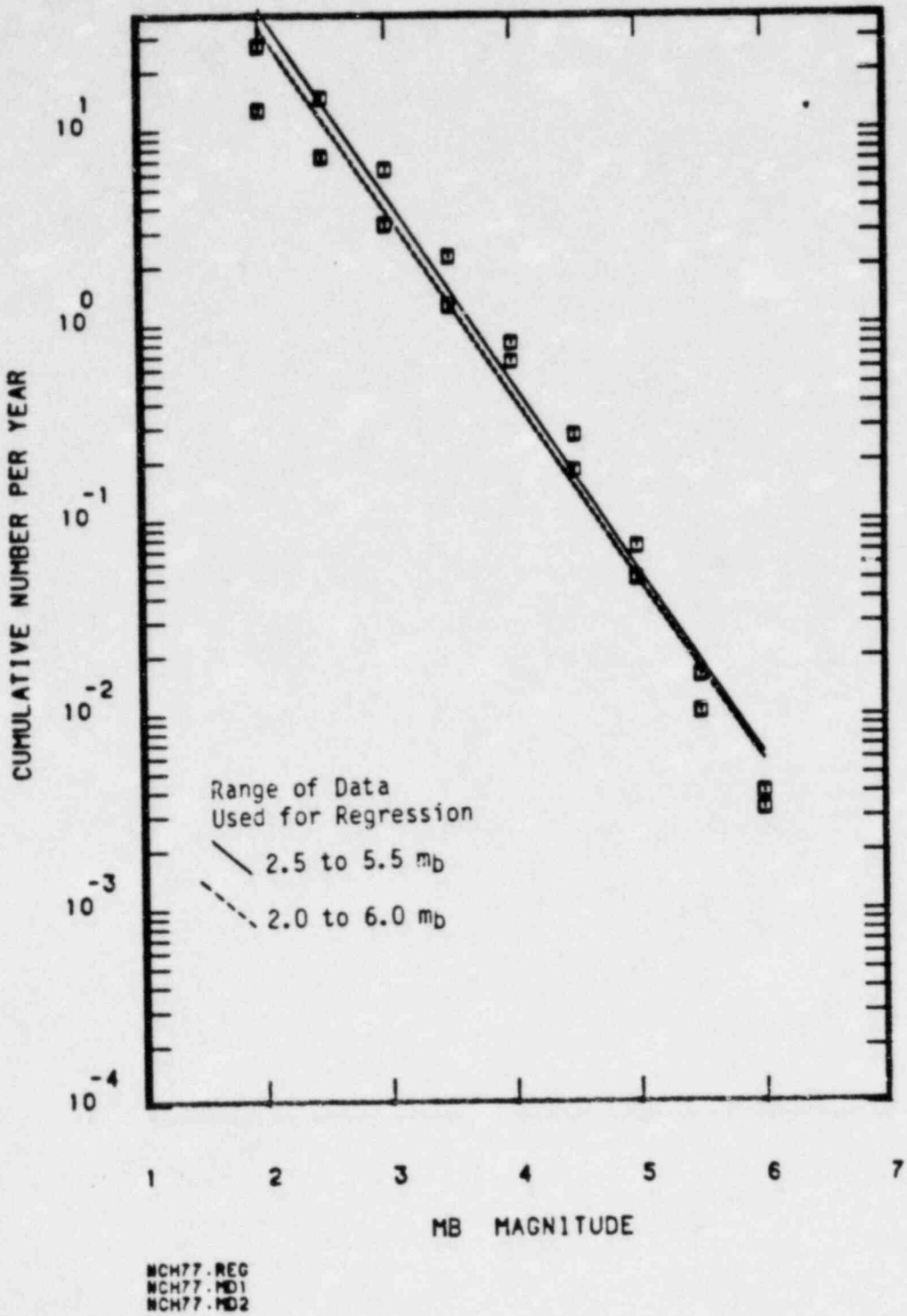

NORTHERN APPALACHIANS
CH77 CATALOG

FIGURE 7

Weston Geophysical

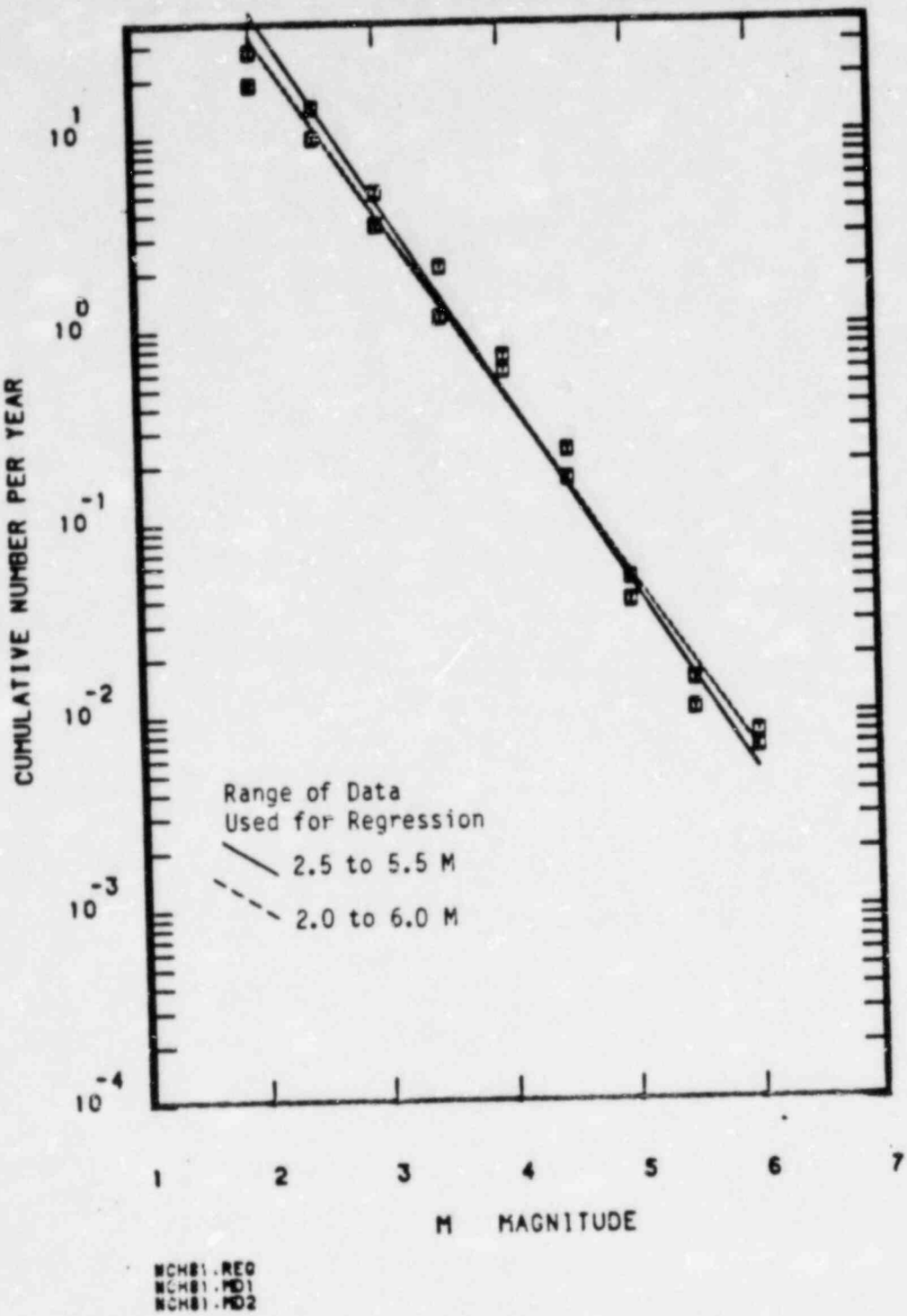

NORTHERN APPALACHIANS
CH81 CATALOG

FIGURE 8

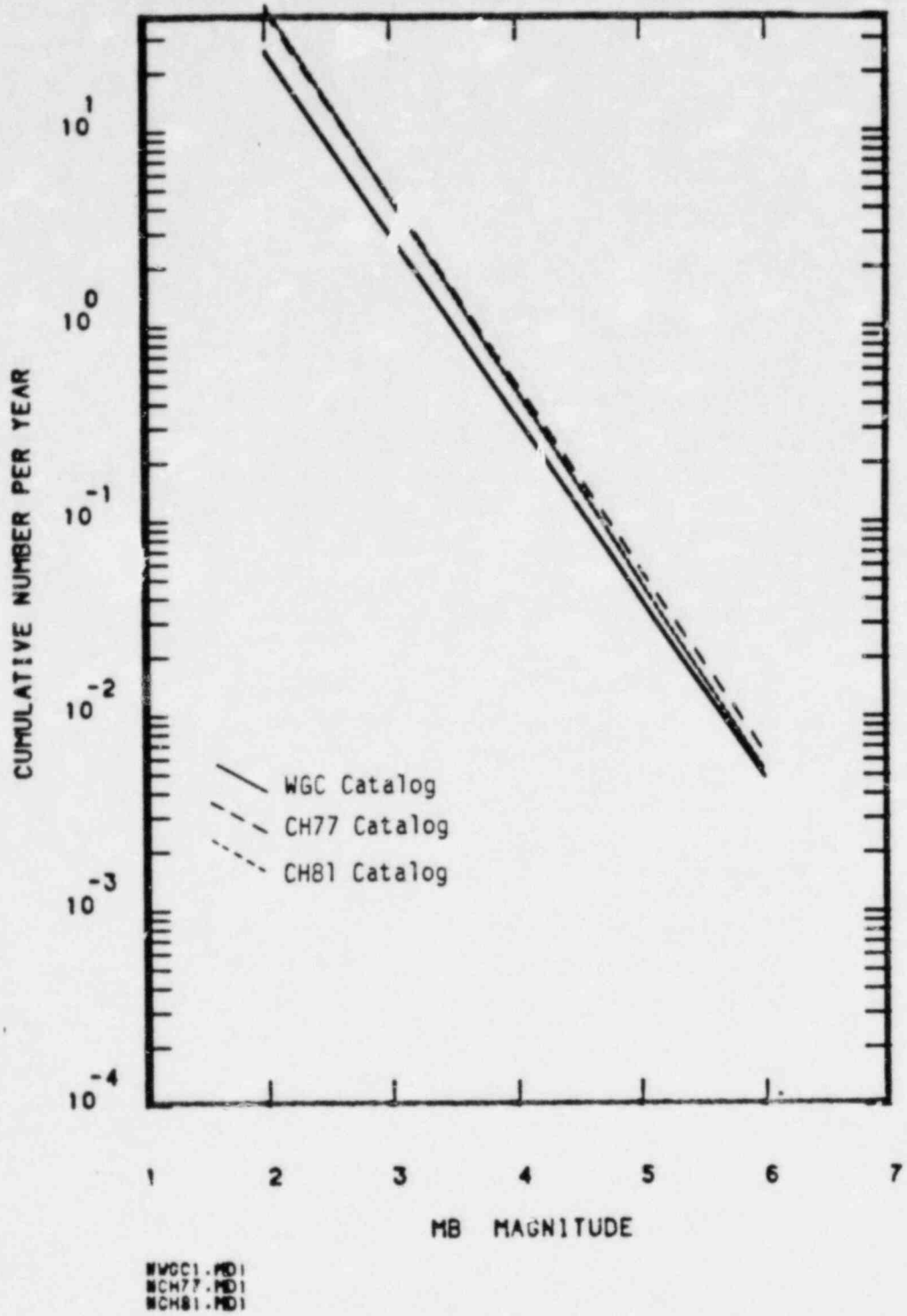

COMPARISON OF MODELS FOR
THE NORTHERN APPALACHIANS

FIGURE 9

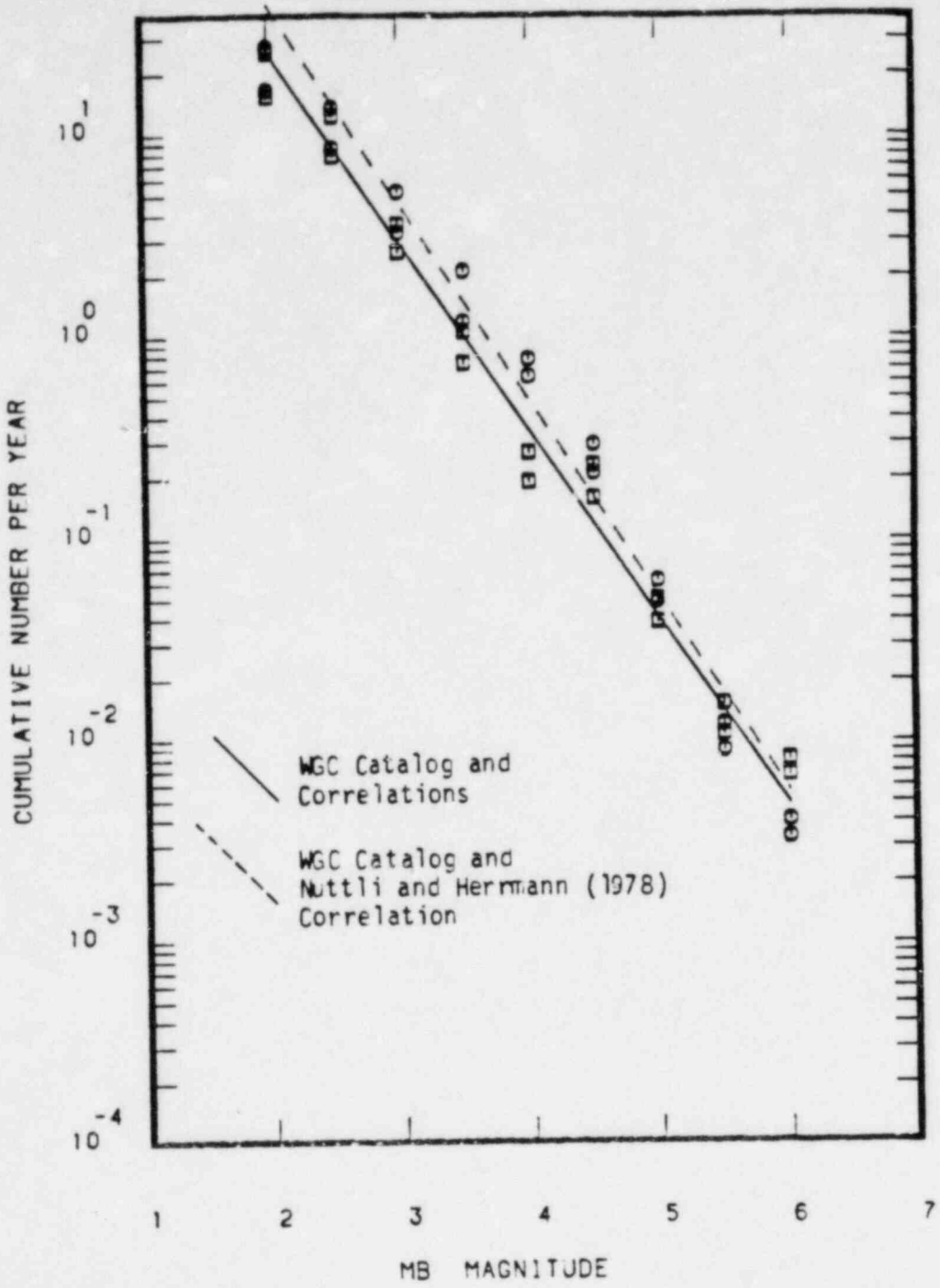

NORTHERN APPALACHIANS:
SENSITIVITY TO MAGNITUDE-
INTENSITY CORRELATIONS

FIGURE 10

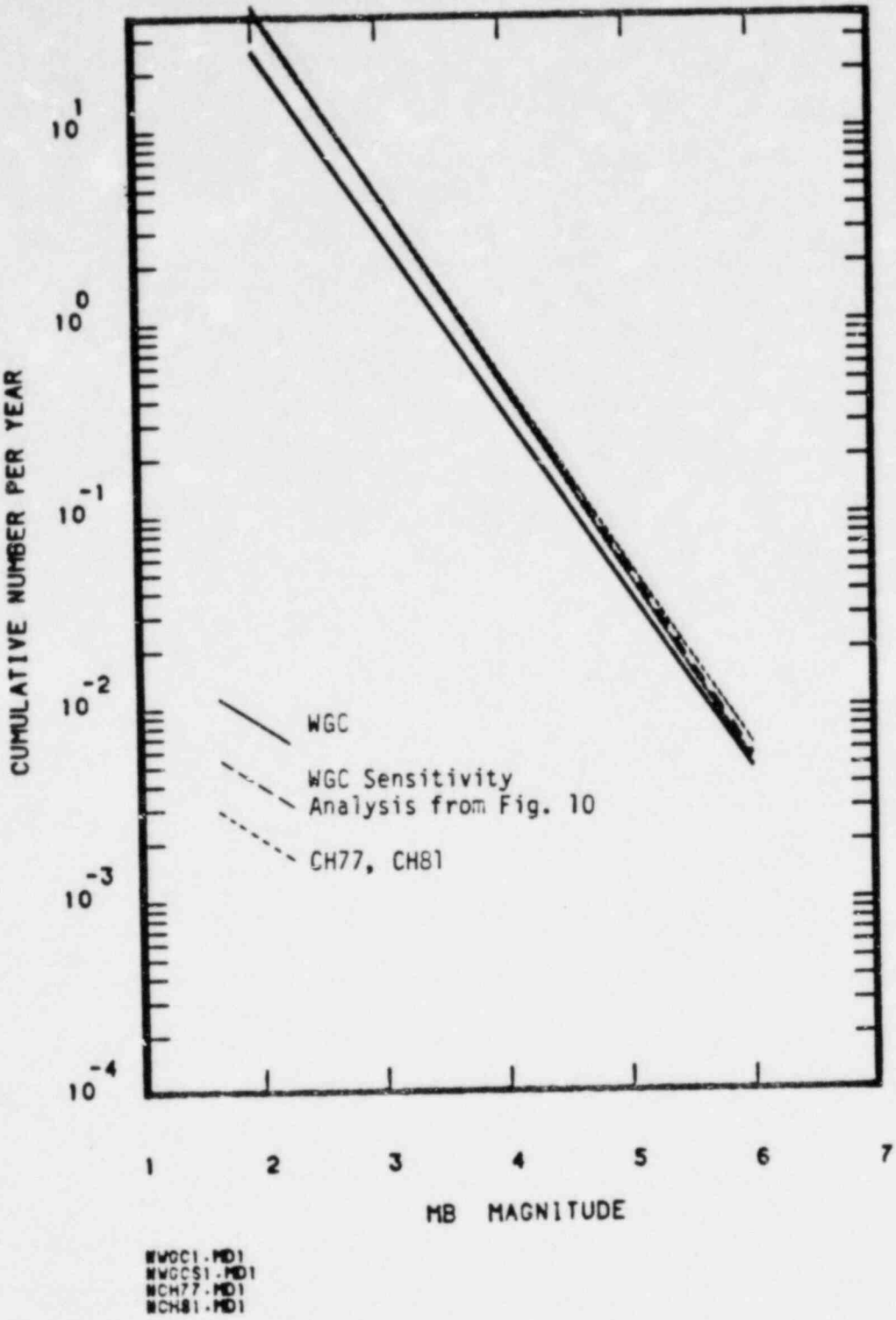

WWGC1.MD1
WWGCS1.MD1
WCH77.MD1
WCH81.MD1

COMPARISON OF WGC AND CH77, CH81 MODELS

FIGURE 11

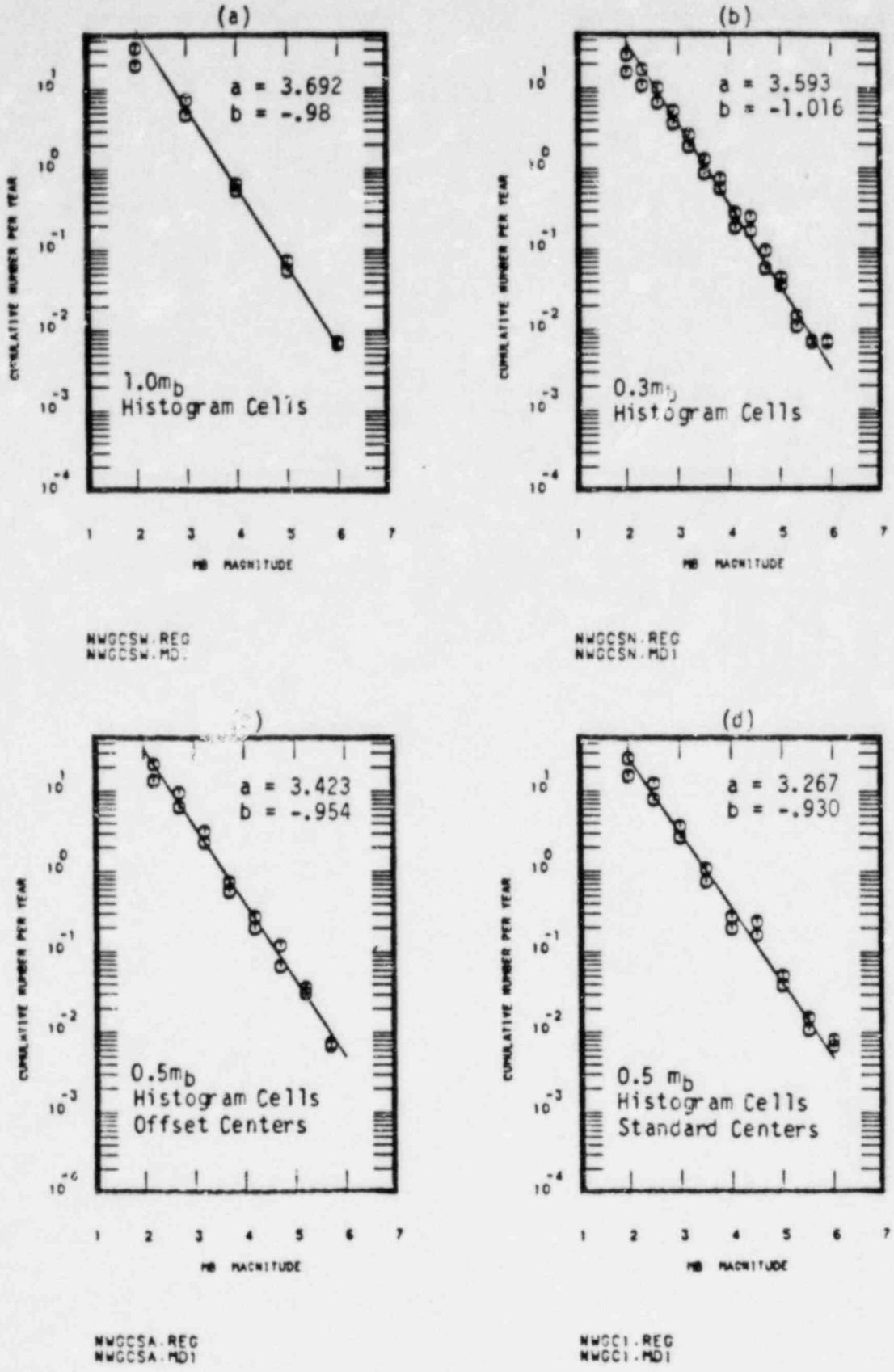

SENSITIVITY ANALYSIS
WGC CATALOG

FIGURE 12

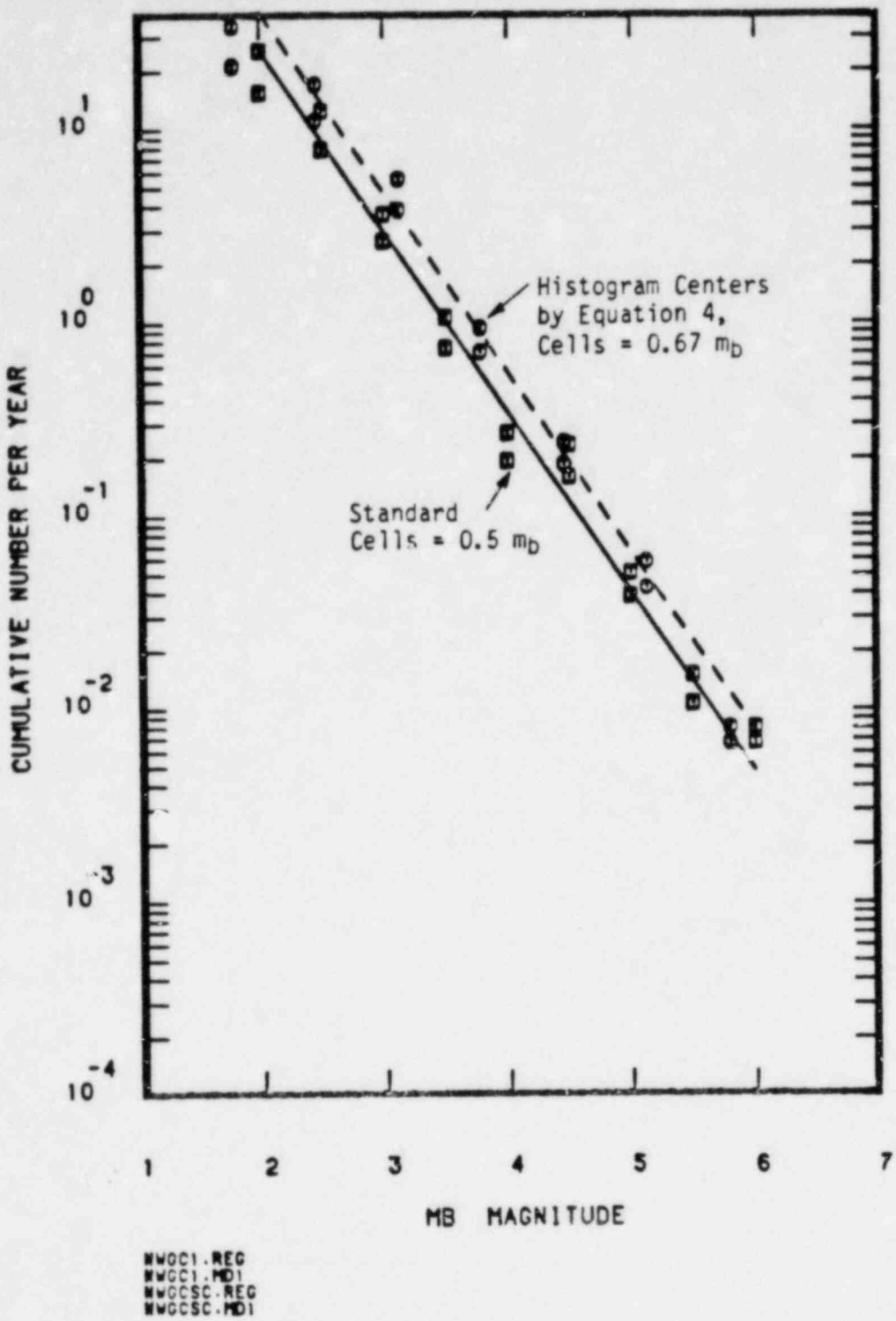

SENSITIVITY TO MAGNITUDE
HISTOGRAM CENTERS

FIGURE 13

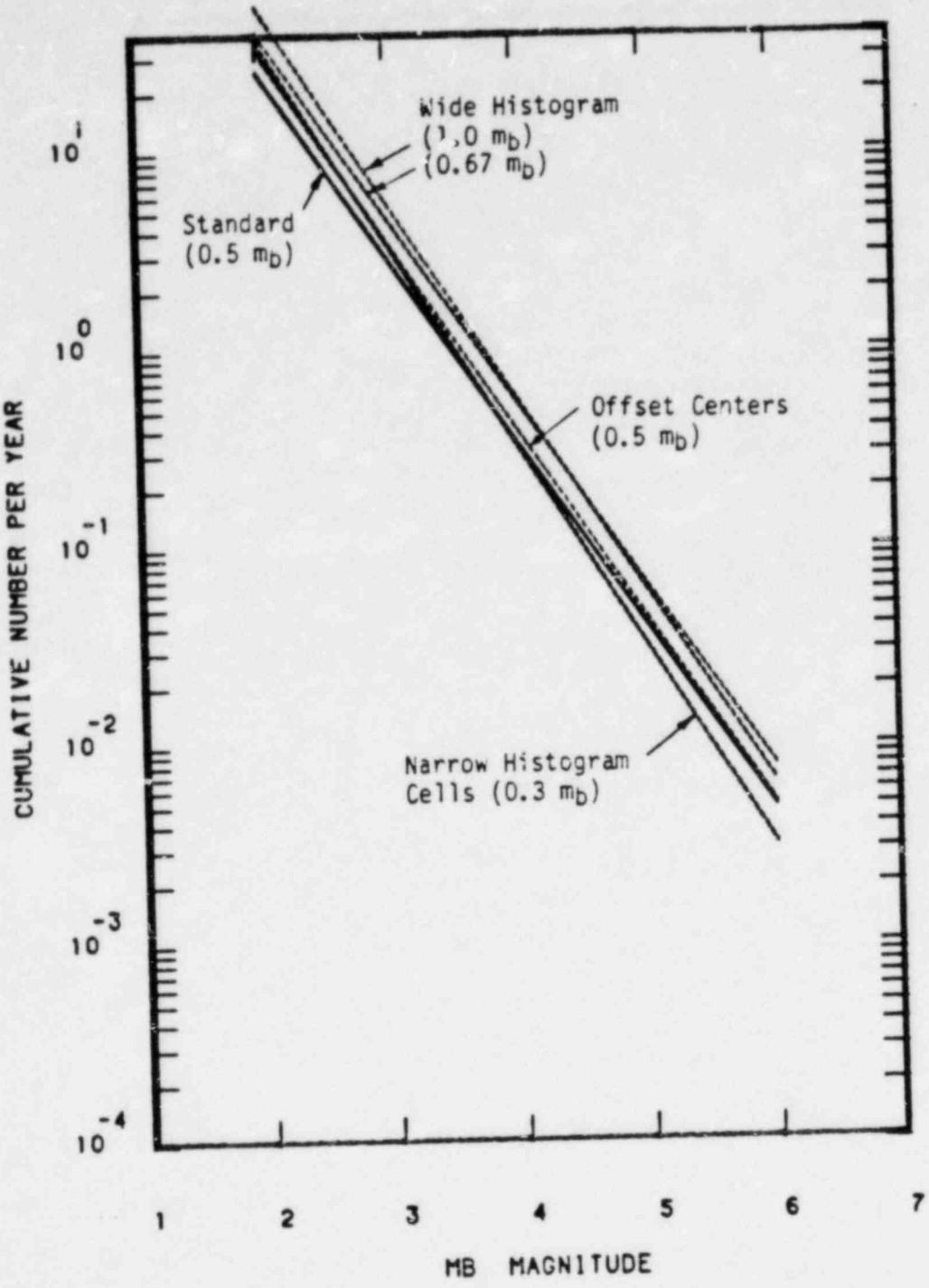

COMPARISON OF SENSITIVITY ANALYSIS RESULTS

FIGURE 14

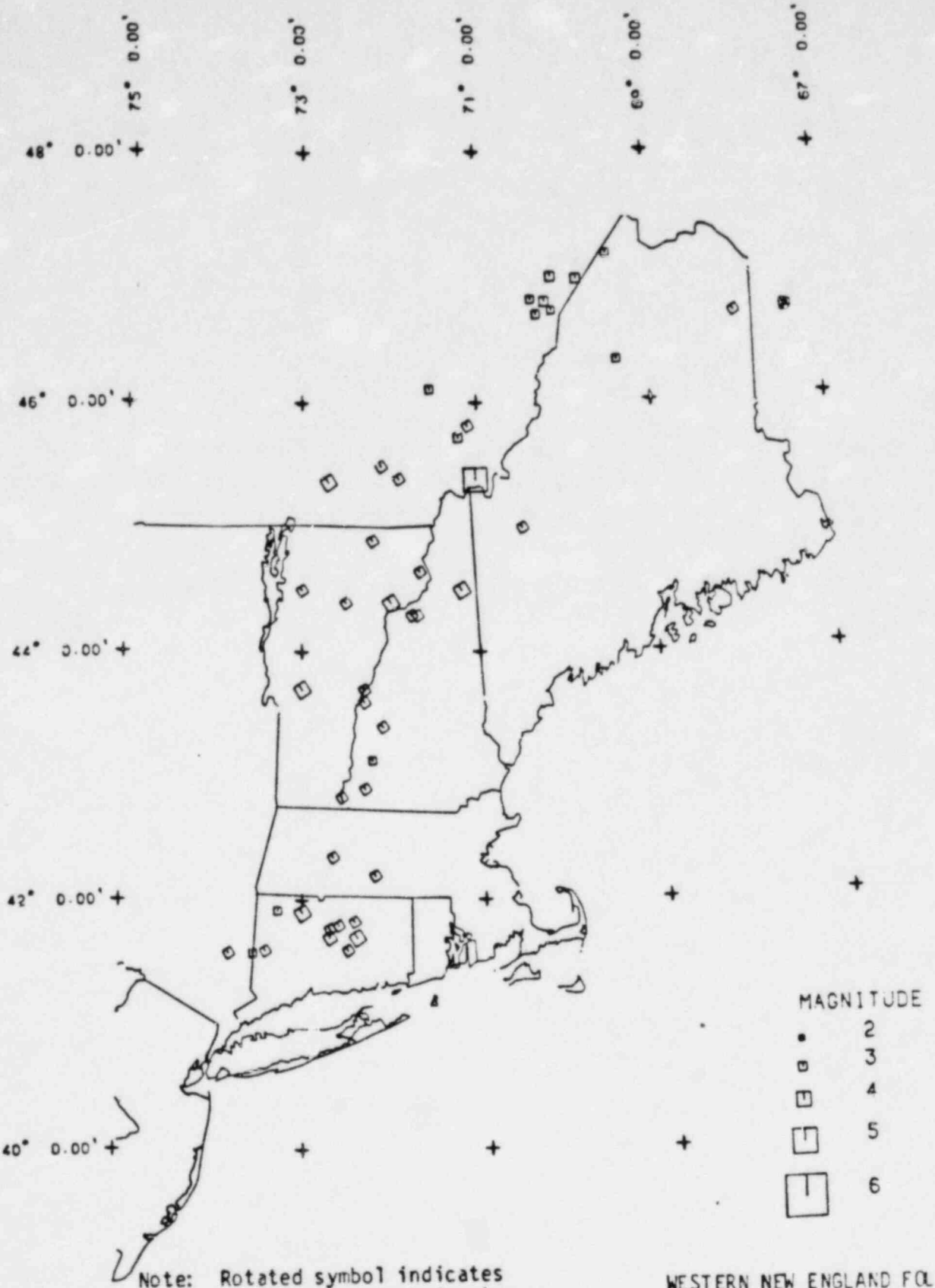

Note: Rotated symbol indicates magnitude estimated using an empirical correlation; otherwise, magnitude is instrumentally determined.

WESTERN NEW ENGLAND FOLDBELT
WESTON GEOPHYSICAL CATALOG
AND m_b CORRELATIONS ($\geq 2.5 m_b$)

FIGURE 15

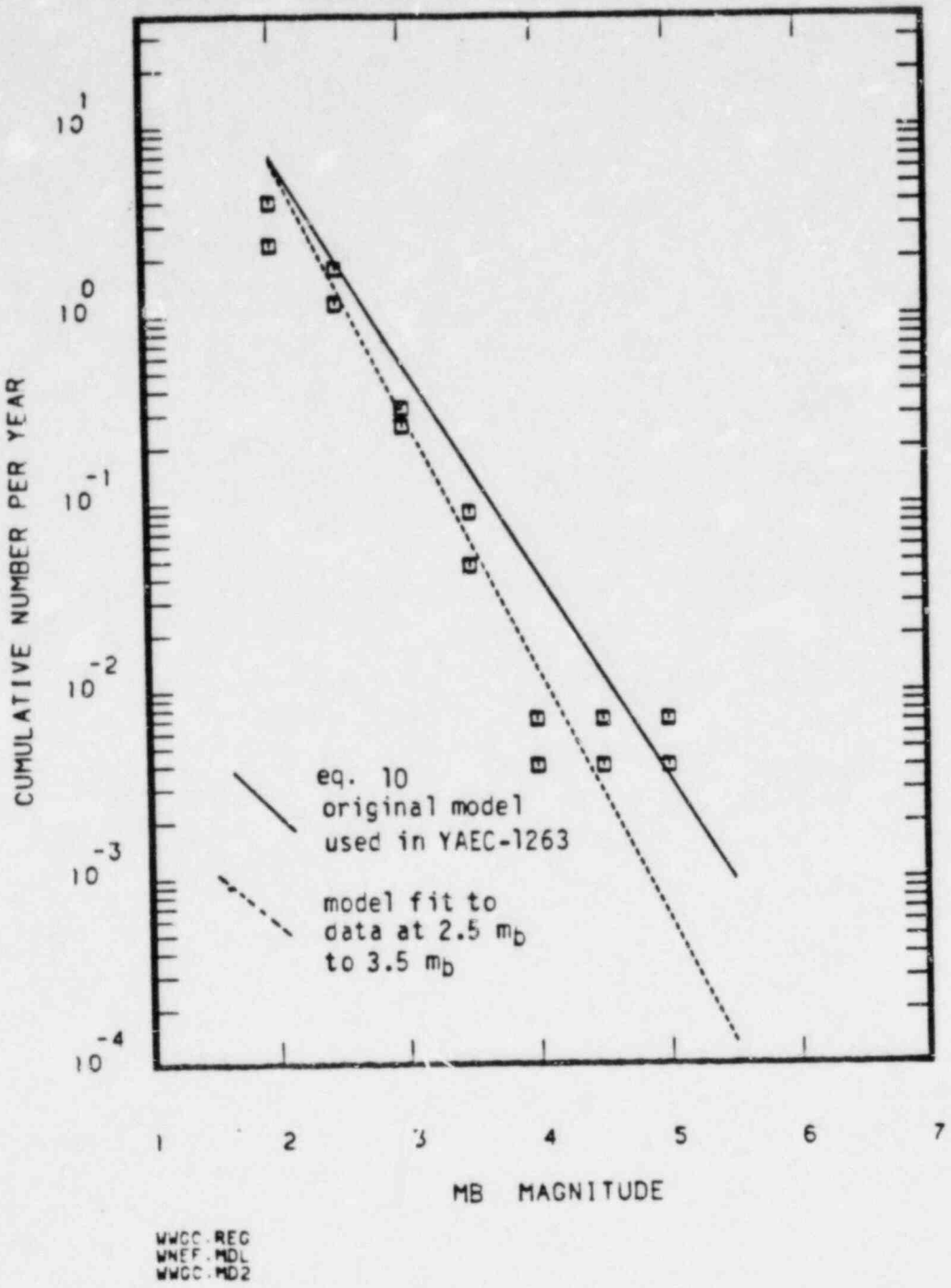

WESTERN NEW ENGLAND FOLDBELT
WGC CATALOG

FIGURE 16

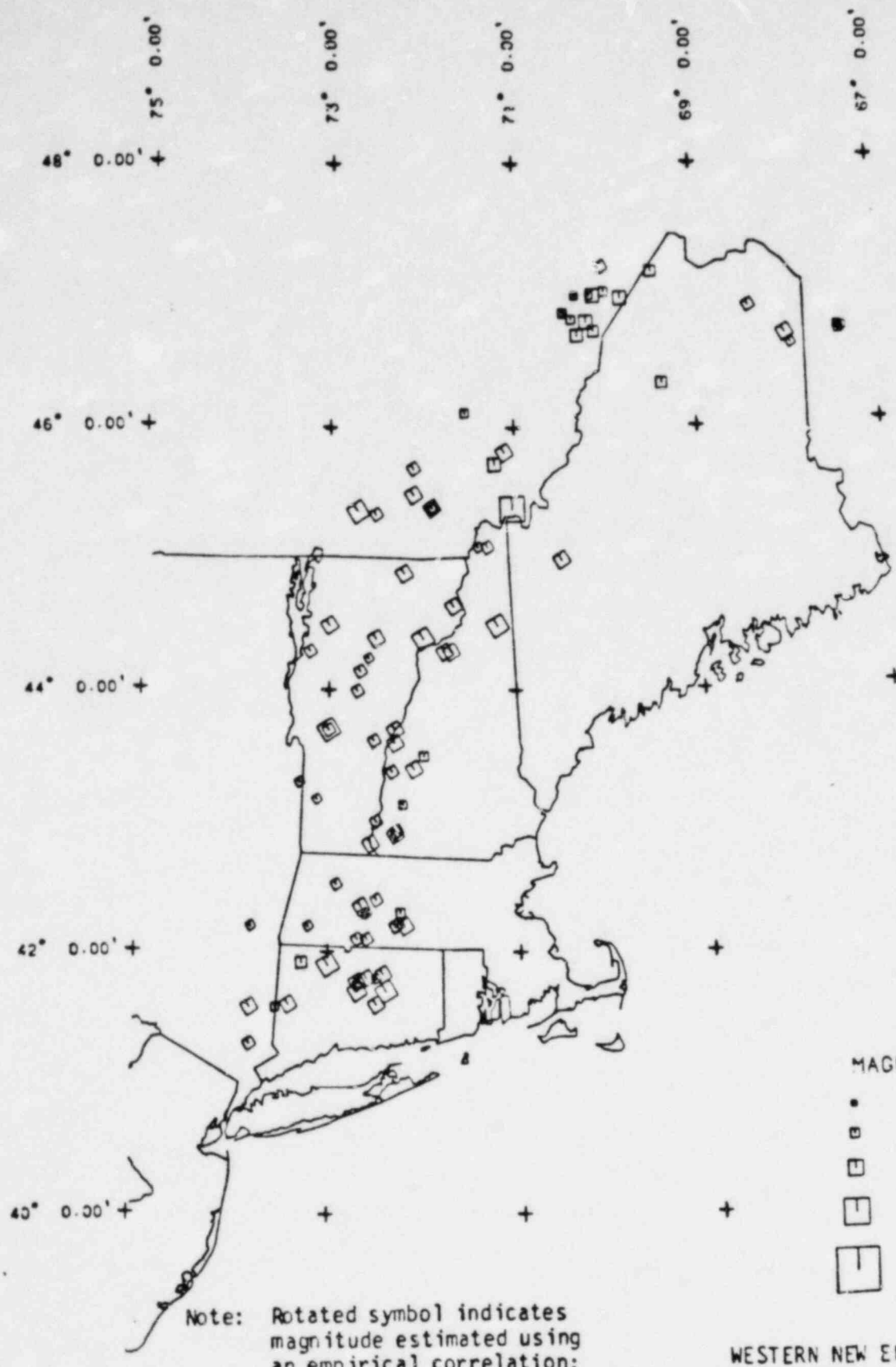

Note: Rotated symbol indicates magnitude estimated using an empirical correlation; otherwise, magnitude is instrumentally determined.

WESTERN NEW ENGLAND FOLDBELT
WGC CATALOG; NUTTLI AND HERRMANN (1978) m_b-I_o CORRELATION ($\geq 2.5 m_b$)

FIGURE 17

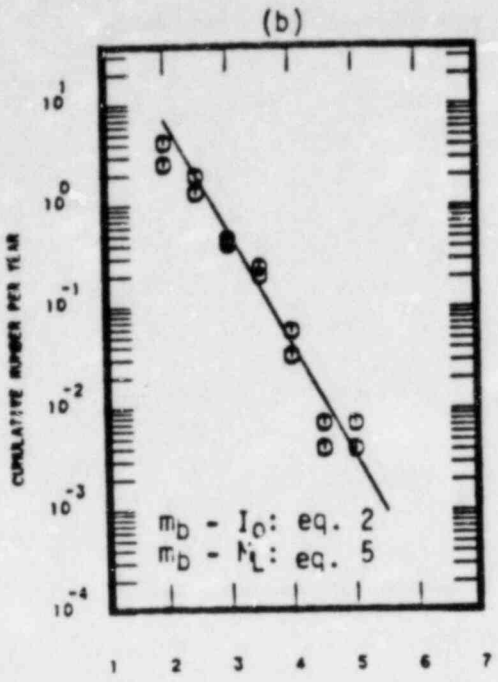

WWGCS2.REG
WNEF.MDL

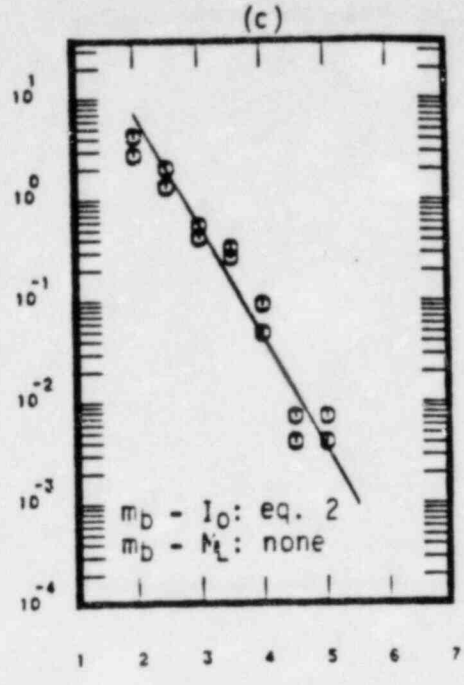

WWGCS3.REG
WNEF.MDL

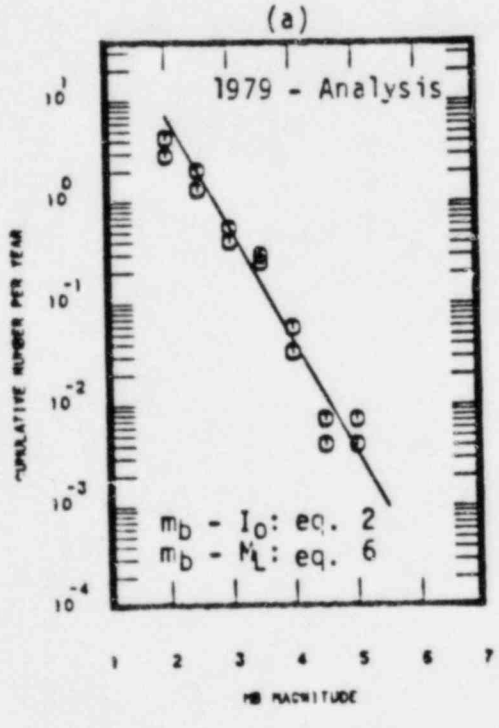

WWGCS1.REG
WNEF.MDL

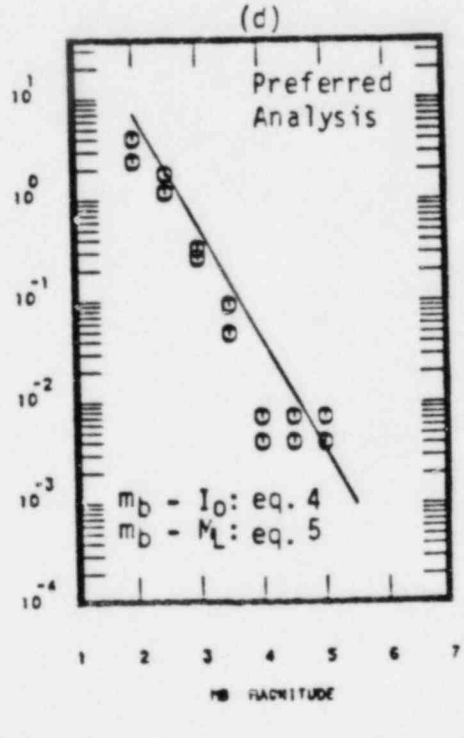

WWGC.REG
WNEF.MDL

WESTERN NEW ENGLAND FOLDBELT
SENSITIVITY ANALYSIS

FIGURE 18

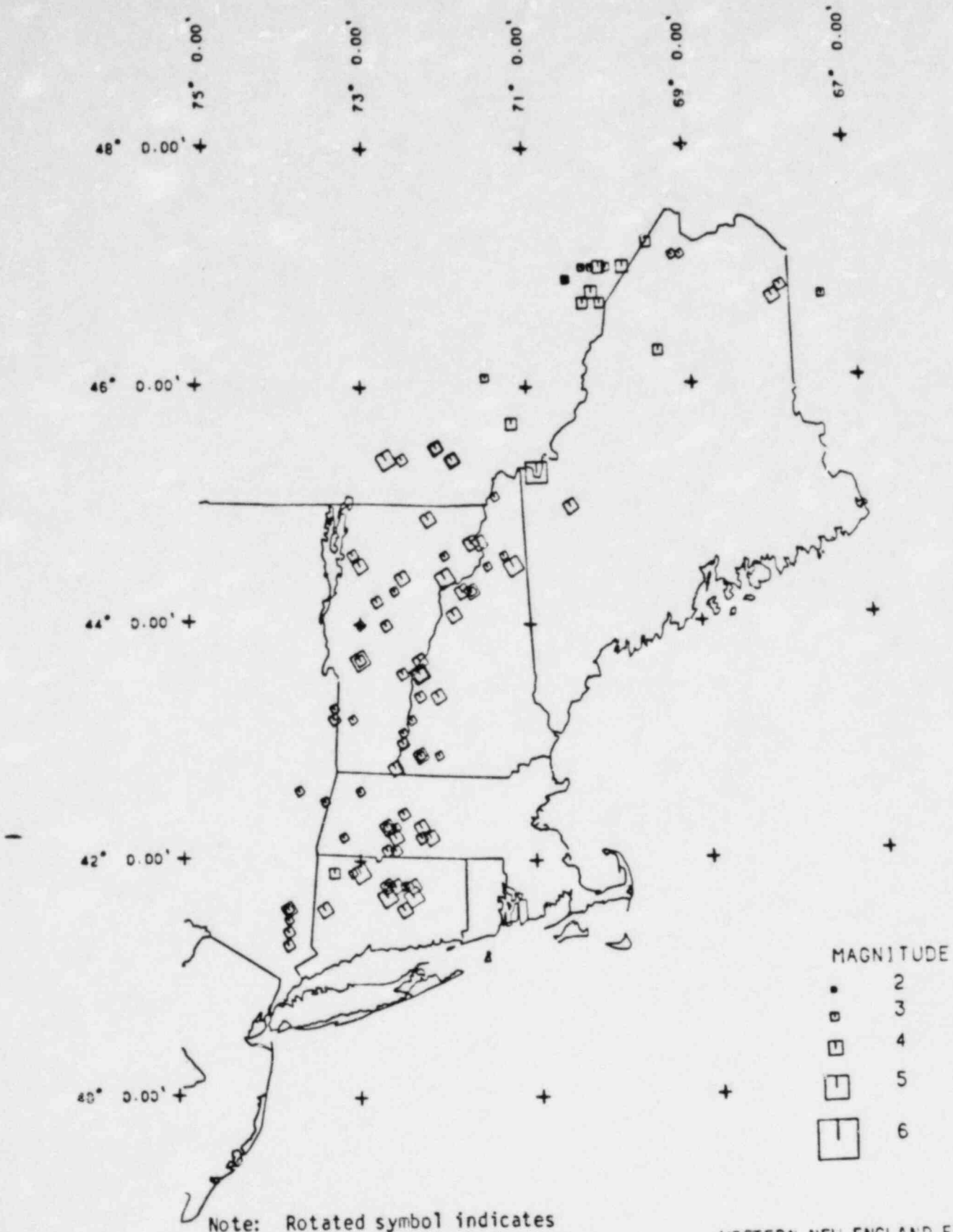

Note: Rotated symbol indicates magnitude estimated using an empirical correlation; otherwise, magnitude is instrumentally determined.

WESTERN NEW ENGLAND FOLDBELT
PRELIMINARY CHIBURIS, CH77
CATALOG ($\geq$ 2.5 m_b)

FIGURE 19

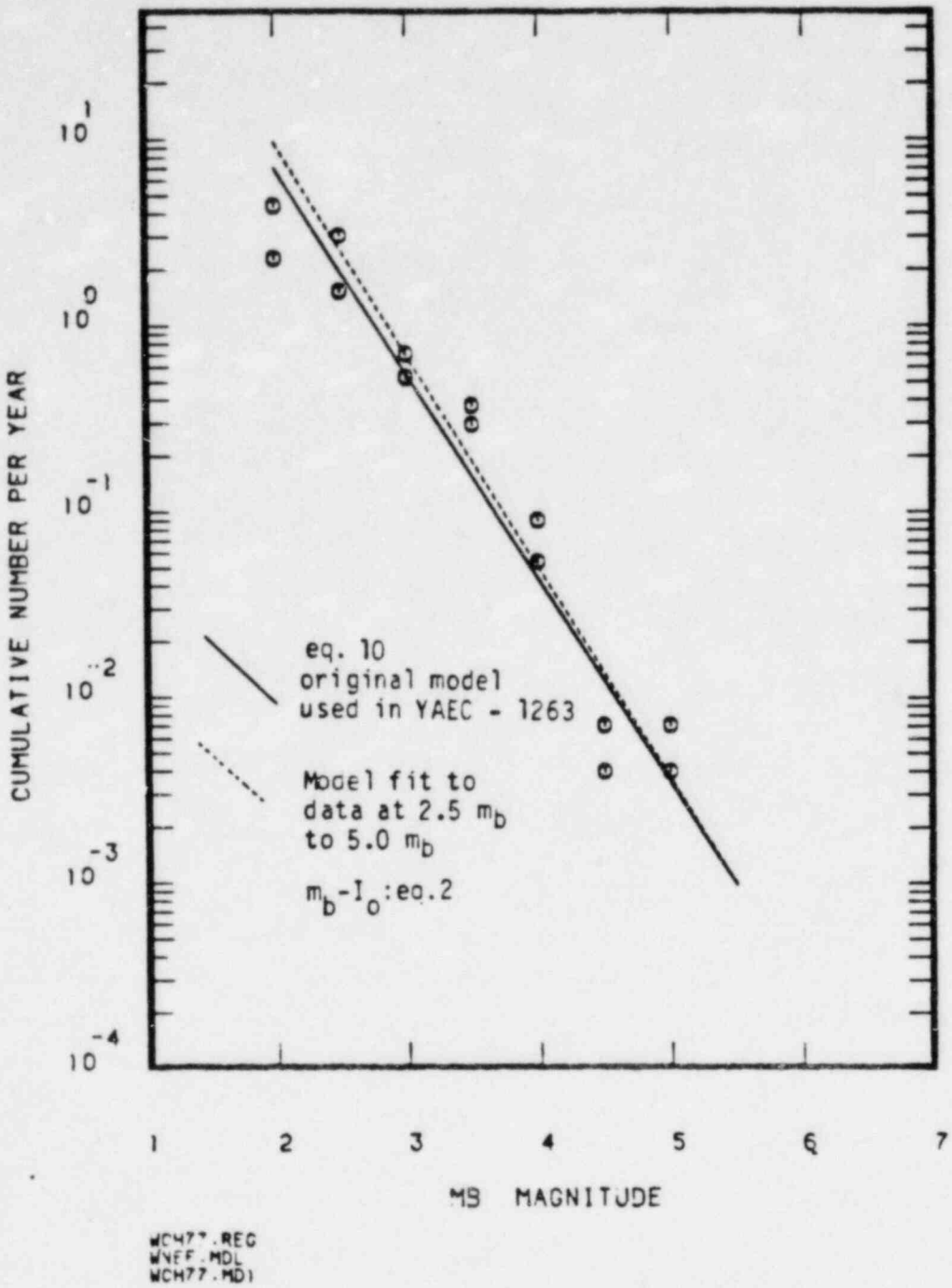

WESTERN NEW ENGLAND FOLDBELT
CH77 CATALOG

FIGURE 20

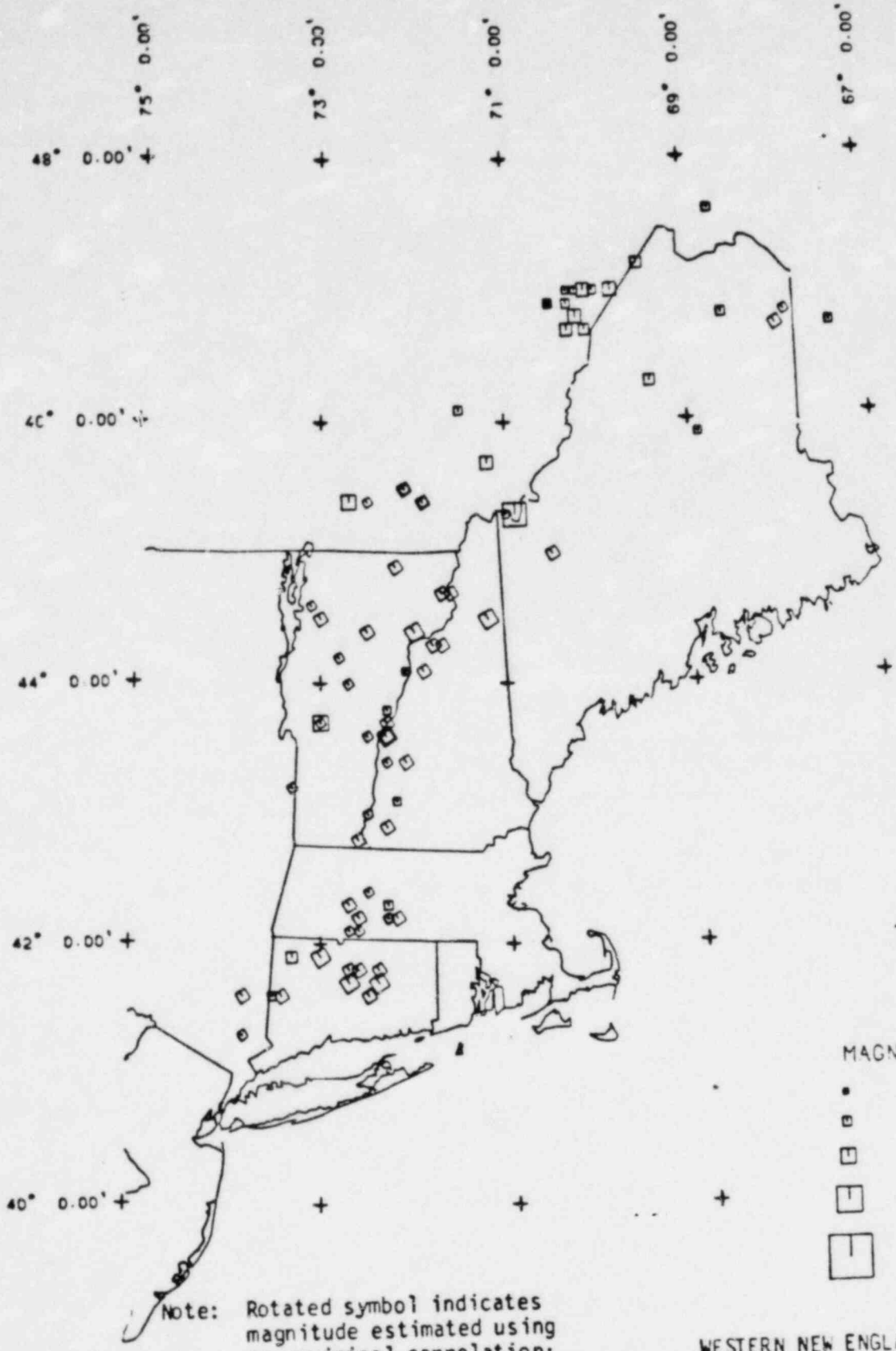

Note: Rotated symbol indicates magnitude estimated using an empirical correlation; otherwise, magnitude is instrumentally determined.

WESTERN NEW ENGLAND FOLDBELT
REVISED CHIBURIS, CHSI
CATALOG (≥2.5M)

FIGURE 21

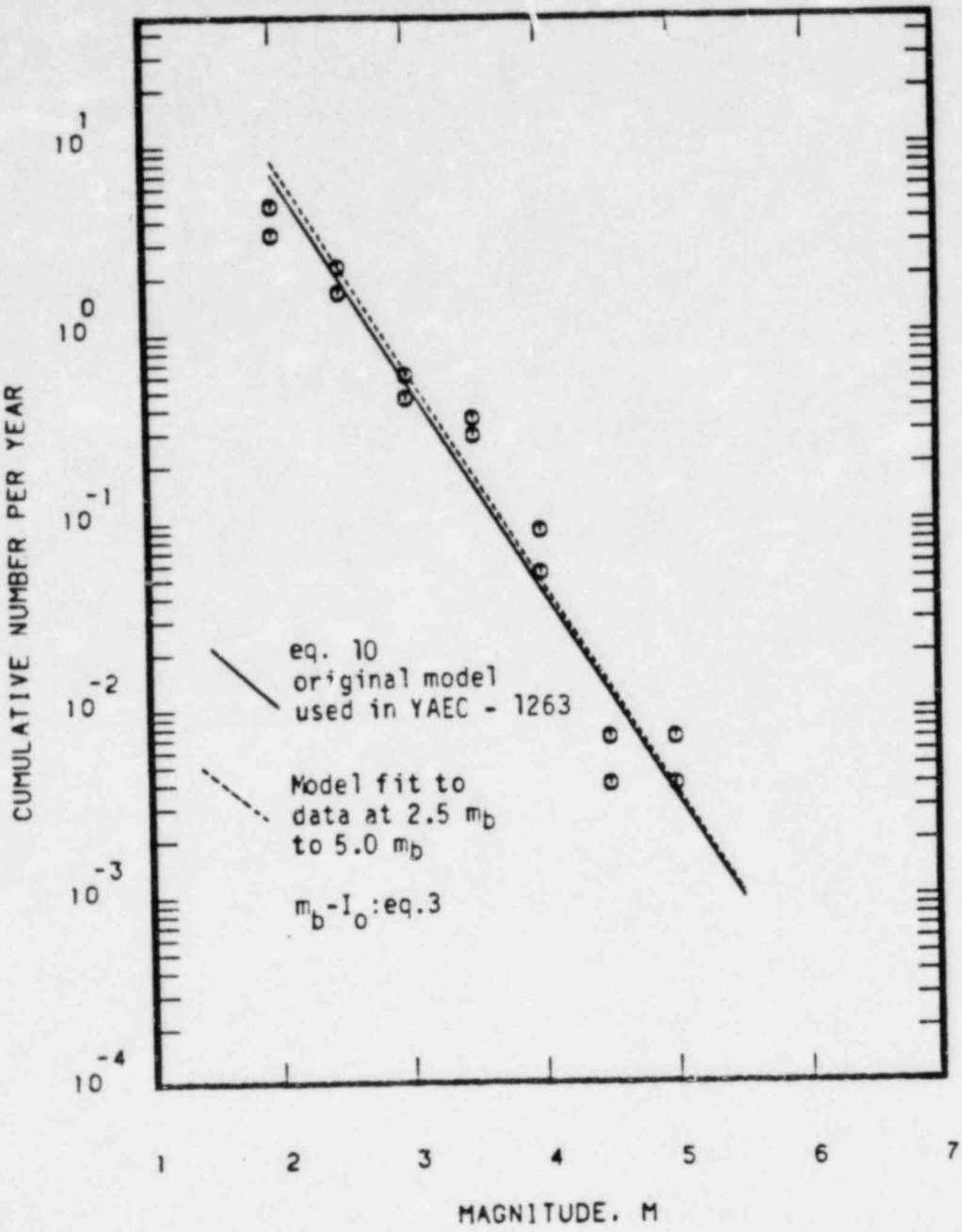

WCH81.REC
WNEF.MDL
WCH81.MD1

WESTERN NEW ENGLAND FOLDBELT
CH81 CATALOG

FIGURE 22

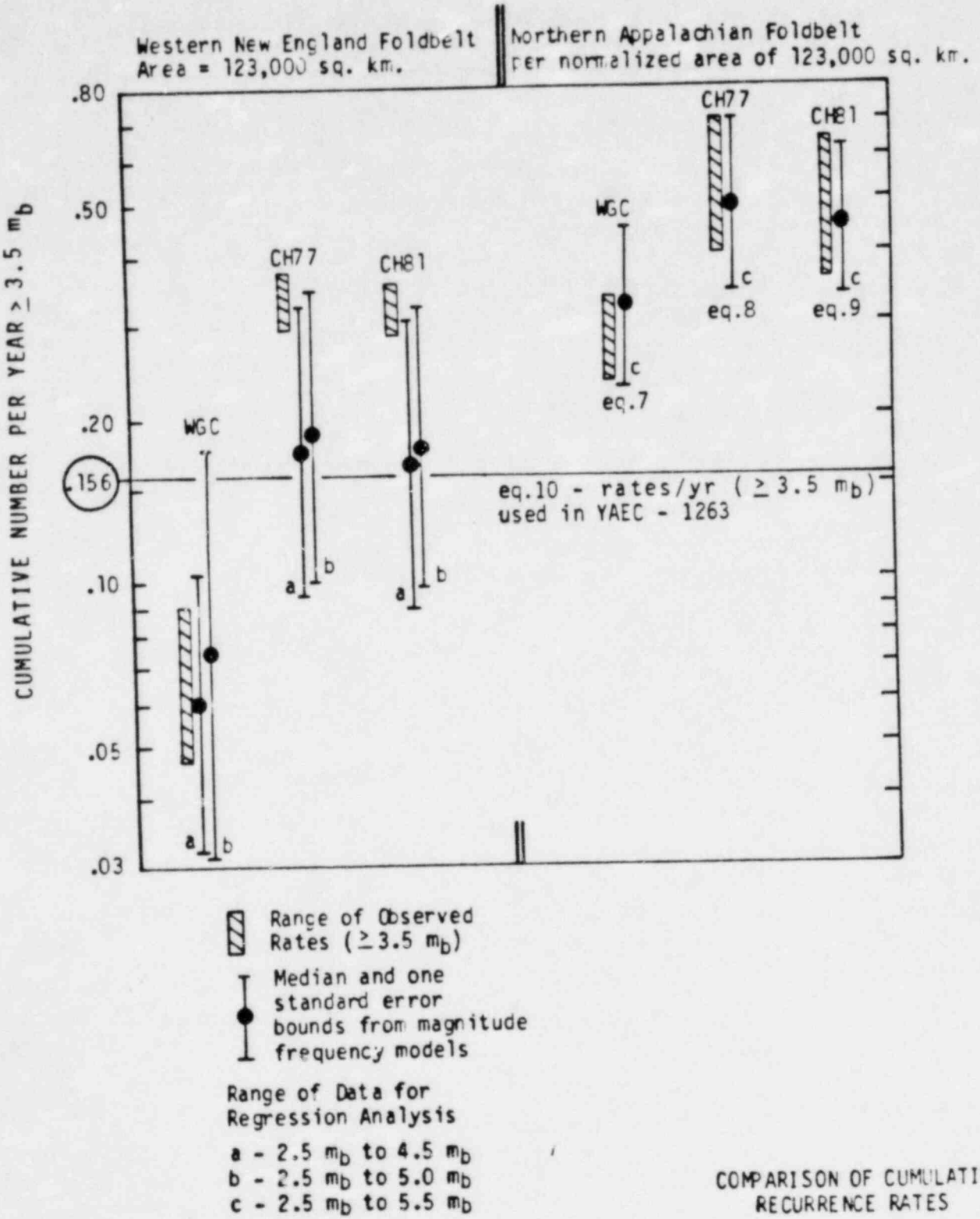

COMPARISON OF CUMULATIVE
RECURRENCE RATES

FIGURE 23

APPENDIX E

ATTENUATION MODELS FOR NEW ENGLAND

Five attenuation models have been used in this analysis with three different distributions of the attenuation error term E. In YAEC-1263 [1], three attenuation models were used. They were:

1. Nuttli Theoretical [2]
2. Weston Geophysical Corporation [3]
3. Bollinger [4]

In this report, modifications have been made to the WGC model, and Nuttli Theoretical has been replaced by the latest Nuttli-Herrmann [5] model. The Gupta-Nuttli [6] model has been added and a Bollinger model using a Nuttli-Herrmann conversion from intensity to magnitude has also been added. The mathematical and graphical forms of these models will be shown on figures referred to below.

Nuttli-Herrmann Model

This attenuation model was recently published [5] and is an extension of the Nuttli Theoretical model. At a recent conference (Earthquakes and Earthquake Engineering: The Eastern United States, September 1981), Nuttli stated publicly that his theoretical model (Figure E1) was about 0.2 m_b units too low. In other words, his curve for 5.0 m_b was really a 5.2 m_b curve. Figure E2 shows the effect of adjusting the Nuttli Theoretical curve by 0.2 m_b units. As can be seen, the results are generally lower by about 20%. The latest Nuttli-Herrmann (Figure E3) model is essentially equivalent to the adjusted Nuttli Theoretical model at distances less than 100 km but attenuates more rapidly at distances greater than 100 km. This can be seen in Figures E1, E2 and E3.

Several observations about this model (and/or its predecessors (e.g., Reference 2)) are in order:

1. The ground motion panel meeting held for NUREG/CR-1582 stated a preference for a theoretical model of this type (while recognizing the difficulties inherent in this approach when instrumental data are limited);

2. D. Bernreuter in his May 23, 1980, letter to L. Reihter prefers the Nuttli Theoretical model;

3. The model is applicable to eastern (as well as central) United States.

Weston Geophysical Corporation Model

A strong reason for including the WGC model is that, unlike all others, it is based on the observed intensity attentuation for four well-documented northeastern United States earthquakes.* Details on these four earthquakes are in YAEC-1263. As observed by D. Bernreuter in July 1981 telephone conversations, the WGC model, as utilized in YAEC-1263, underestimates the dependence of acceleration on magnitude outside the m_b 4 to 5 range. Its results were much too high for smaller magnitudes and too low for larger values. The problem was traced to the data set; the four events encompass a very small magnitude range (m_b = 3.5 to m_b = 5.8) yielding, therefore, a very unreliable estimate of this slope (i.e., a large standard error of estimation). To correct this problem, we introduced a magnitude slope of 1.1 (similar to virtually all other attenuation models). We then adjusted the intercept so that the model would predict the same results as the original WGC model at the magnitude value equal to the mean of the data (i.e., at m_b = 4.875). This change does not effect the distance dependent terms which are specific to the Northeast. Figures E4 and E5 show the effect of this adjustment.

Bollinger Attenuation Models

This model was also chosen because MM site intensity (I_s) is

---

* Furthermore, unlike some others available, it is based on a proper regression analysis of intensity on distance.

correctly regressed as a function of distance, and because it applies to the eastern United States. Two different versions of the Bollinger model are used in this study. The difference between the two models is the procedure used to convert epicentral intensity (I_o) to magnitude. As was pointed out in YAEC-1263, previous conversions from magnitude to epicentral intensity are simply the functional inverses of the intensity to magnitude equation. Furthermore, it was found that even these latter relationships were fit by eye rather than resulting from formal regressions. Sensitivity of the results to both of these methods of converting I_o to m_b is examined by:

1. Using Nuttli-Herrman ($I_o = 2m_b - 3.5$) (Model B1); and

2. Using correct regression of Gutenberg-Richter data converted to ($I_o = 1.37m_b - 0.134$)

Figures E6 and E7 show the effect of these conversions.

Gupta-Nuttli Attenuation Model

This model is included here only because of its common use in NUREG/CR-1582. The Gupta-Nuttli model is a modified version of the published model; the modified version is taken from NUREG/CR-1582. The original model was based upon isoseismals from the November 9, 1968, southern Illinois and December 6, 1811, New Madrid, Missouri earthquakes. The model was calculated from isoseismals not from the individual data points, implying effectively an averaging on R for given I (rather than averaging on I given R), as it is now understood one should do in such an attenuation model. To approximate a correction for this problem, NUREG/CR-1582 authors reduced by 1/2 intensity unit the values predicted by the published model. Figure E8 depicts this model.

Error Term Distribution

Three different values for the attenuation error term distributions have been used in this analysis. They have been chosen based upon current

information in the literature. The error term is assumed to have mean zero and the following truncated or untruncated normal distributions:

1. σ_E = 0.60, untruncated

2. σ_E = 0.70, truncated $\pm 3\sigma_E$

3. σ_E = 0.90, truncated $\pm 2\sigma_E$

The basis for the specific error term models is primarily the numerous comments in NUREG/CR-1582 [6], and also the June 8, 1981 letter [8] from the NRC to Yankee. The values previously used in some YAEC-1263 cases (namely for the WGC and Bollinger models) are believed to reflect not only natural variability about a given model but also the error in the model itself. This latter effect is dealt with in this study directly, namely by using several models with weights. Therefore, the higher values of σ_E are not necessary here.

Other Attenuation Models

Because of its importance in NUREG/CR-1582 results, an additional possible choice for an attenuation model to be used in this study was the "Ossipee" model. The Ossipee model there, as shown in NUREG/CR-1582, is, however, based upon "wrong-way" regression. It predicts a mean distance for a given intensity, rather than a mean intensity at a given distance. The May 23, 1980, letter between D. Bernreuter and L. Reiter describes the problems associated with this model. A copy of this letter is attached, along with documentation of L. White concerning the results if the "New Ossipee" model, based upon correct regression, were to be used.

Weights on Attenuation Models

Lacking any set of experts' opinions in assigning weights to the attenuation models, we followed a process of incremental modification to be explained below. In doing so, however, we tried to insure that the models and

the final weights maintained some "representativeness" over the class of all possible attenuation models; more precisely, we did not want to lose either a spectrum of distance (R)-dependence levels, or a spectrum of magnitude (M)-dependence levels, or a range of general (high/low) acceleration predictions. Comparing the formulas and figures (E1 through E8), it is clear that the Gupta-Nuttli (GN) model provides a substantially different R-dependence, the Bollinger models (B1 and B2) a spread in the M-dependence, and either WGC vs. Bollinger or Nuttli-Herrmann (NH) vs. Bollinger provide a general higher vs. lower spread.

We start with a "neutral" set of weights: 1 in 4 (0.25) to each fundamentally different model, the 0.25 being split equally between the two versions of Bollinger. Then we modify the weights incrementally to reflect the following factors:

a. Independent Basis

The Nuttli-Herrmann model is an independent ("theoretical") approach viz-a-viz the other (intensity-based) models. Therefore, we should add weight to NH at the roughly equivalent expense of the others. We add 0.05 to NH and subtract 0.015 from WGC and GN, and 0.01 from each of the B's.

b. Author Preference

Nuttli (in a public statement at the meeting cited above) stated his preference for NH over his prior theoretical model, i.e., a common author is "renouncing" one in favor of the other. This also implies his preference for this model above his other models. To reflect this, we subtract 0.05 from GN and add it to NH.

c. Local Data Base

The WGC model has a local northeast data base, in contrast to GN or B. NH has been adjusted to the northeast, but only "theoretically" through the modified Q values they recommended. Therefore, we add

to WGC a weight of 0.05 at the expense of only GN and B (i.e., subtract 0.025 from GN and 0.0125 from B1 and B2).

d. Proper Regression

Among the intensity-based models, WGC and B were based on proper regressions upon R; GN was only modified for this effect in an ad hoc way. Therefore, we subtract 0.05 from GN and distribute to WGC and B (0.03 and 0.02; the latter split equally between B1 and B2).

e. Sample Size

Among the intensity-based models, B is based on only a single event. We subtract 0.05 from B (equally again) and add 0.03 to WGC and 0.02 to GN (WGC was based on 4, GN on two events).

f. Intensity vs. Magnitude

A minor adjustment is made within the two B models to reflect the writers' preference in the two treatments of magnitude vs. intensity discussed above (and in YAEC-1263). We take 0.0125 from B1 and place it on B2.

The net results are weights of 0.35 on WGC and NH, a weight of 0.13 on GN, and weights of 0.06 and 0.11 on B1 and B2 respectively (a total of 0.17 on B). The scheme for weighting is not unique, but the general results seem consistent with generally perceived preferences: about one-third each on the theoretical model (NH), the local, high-quality intensity model (WGC), and "others". The "others" recall help given representativeness.

In addition, we tried three other weighting schemes:

1. Starting without GN and proceeding as above. This produces weights of 0.38, 0.41 and 0.21 on NH, WGC and B (combined), respectively.

2. Putting either much more weight or much less weight on the theoretical approach (specifically modifying the 0.05 of weight distributed in item a above to 0.15 or to 0.0, respectively). Roughly, the results keep the WGC weight at about one-third in both cases and change the NH weight to 0.45 or 0.3, respectively; the remaining weight being distributed about equally between B and GN.

Seeing the relatively small changes and preferring the first scheme, we accepted for presentation here the original set above:

NH = 0.35
WGC = 0.35
B1/B2 = 0.06/0.11
GN = 0.13

Sensitivity runs were made, however, using for each model the lowest and highest weight it received in all four assignment procedures and the individual weights were renormalized to sum to one. The effects on final results are not significant: the 10^{-3} acceleration for the median hazard curve varied by only a few percent. This conclusion is consistent with the relatively small sensitivity of hazard results to attenuation models (see Figures F6 to F10 in Appendix F).

With respect to weights on the $_E$ values, we reviewed the opinions of the attenuation panel [6] and others, reconsidered as described above the Cornell, Banon, Shakal Reference [7] that led to the 0.9 value, and assigned a relatively low value, 0.1, to the $_E = 0.9$ (truncated at $\pm 2\ _E$) hypothesis. For spectral velocities, the somewhat higher value 0.7 (truncated at $\pm 3\ _E$) seems preferable to 0.6 (untruncated). Therefore, we assign them weights 0.6 and 0.3 respectively. Sensitivity results (Figures F11 to F13) show that the weight choice here is not critical.

Appendix E References

[1] YAEC-1263, 1981, Seismic Response Spectra for the Yankee Nuclear Power Station", Rowe, Massachusetts.

[2] O. W. Nuttli, 1979, "State-of-the-Art for Assessing Earthquake Hazards in the United States", Report 16, United States Army Engineers, Waterways Experiment Station, November 1979.

[3] G. Klimkiewicz, 1981, Personal Communication, Weston Geophysical Corporation.

[4] G. A. Bollinger, 1976, "Reinterpretation of the Intensity Data for the 1886 Charleston, South Carolina, Earthquake", USGS Professional Paper 1028-B.

[5] O. W. Nuttli and R. B. Herrmann, 1981, "Consequences of Earthquakes in the Mississippi Valley", ASCE Preprint 81-519.

[6] NUREG/CR-1582, 1981, "Seismic Hazard Analysis: Application of Methodology, Results and Sensitivity Studies".

[7] C. A. Cornell, H. Banon and A. F. Shakal, 1979, "Seismic Motion and Response Prediction Alternative", Earthquake Engineering and Structural Dynamics, Vol. 7, pp. 295-315.

[8] Letter from NRC to Yankee, 1981, "Site-Specific Ground Response Spectra for SEP Plants Located in Eastern United States".

Nuttli Theoretical November 1979
Miscellaenous Papers S-73-1
Waterways Experiment Station
Sustained acceleration converted
to peak (conversion factor = (1.37x0.9)

$\ell_n A_p = 1.433+1.15m_b-0.833\ell_n R-0.$ [illegible] $e^{-0.45m_b R}$

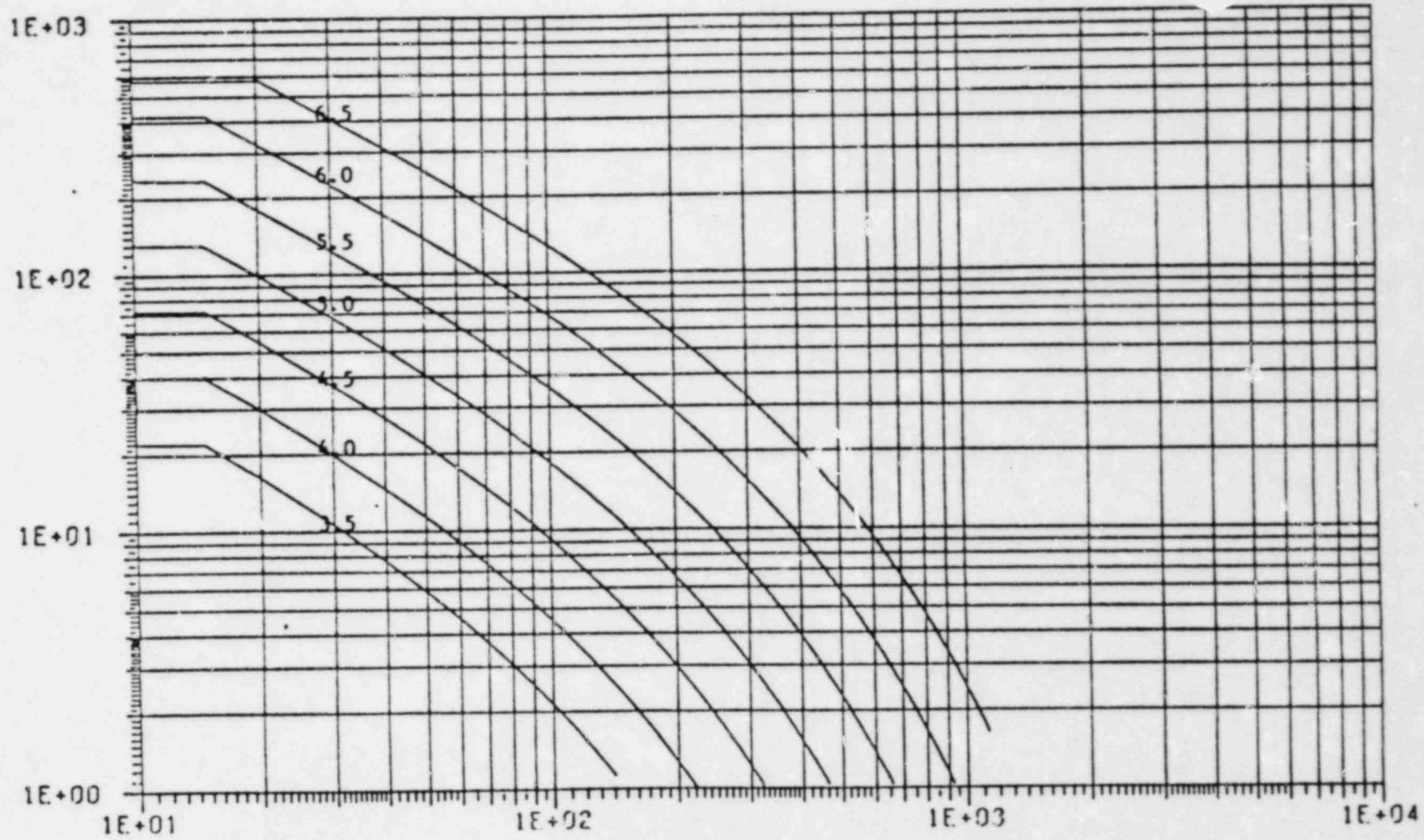

Figure E1.

Nuttli Theoretical 1981 Earthquake Conference
(Knoxville, Tennessee)
Nuttli stated that all curves from Nuttli-
Theoretical 1979 be adjusted down by $.2m_b$.

$$\ell_n A_p = 1.036+1.15m_b-.833\ell_n R-0.047e^{-0.45m_b}R$$

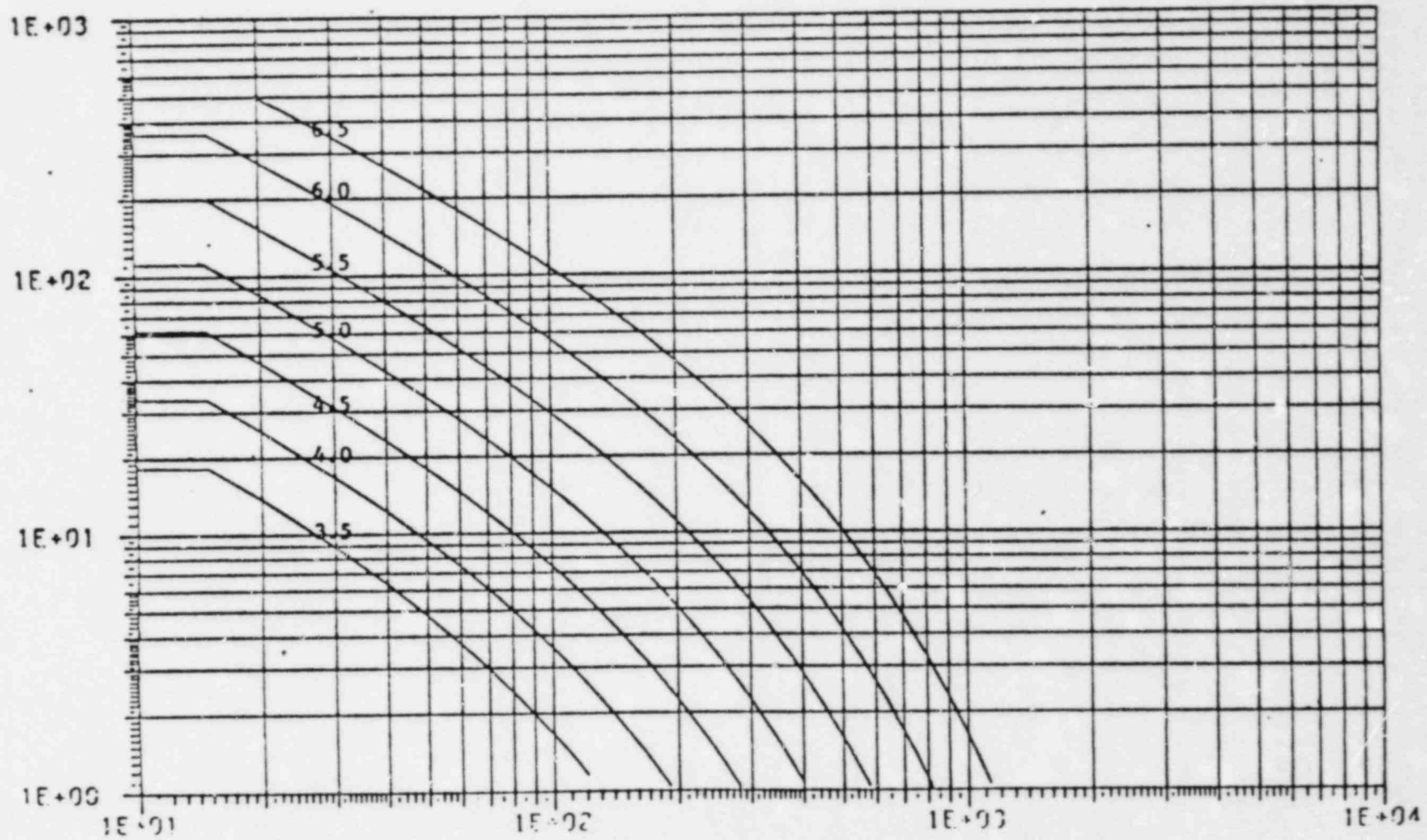

Figure E2.

Herrmann 1981
Earthquake Conference (Knoxville, Tenn.)
(Nuttli endorsed this model over his)

$$\ln A_\mu = 1.265+1.15m_b-0.0044R-0.833\ln R$$

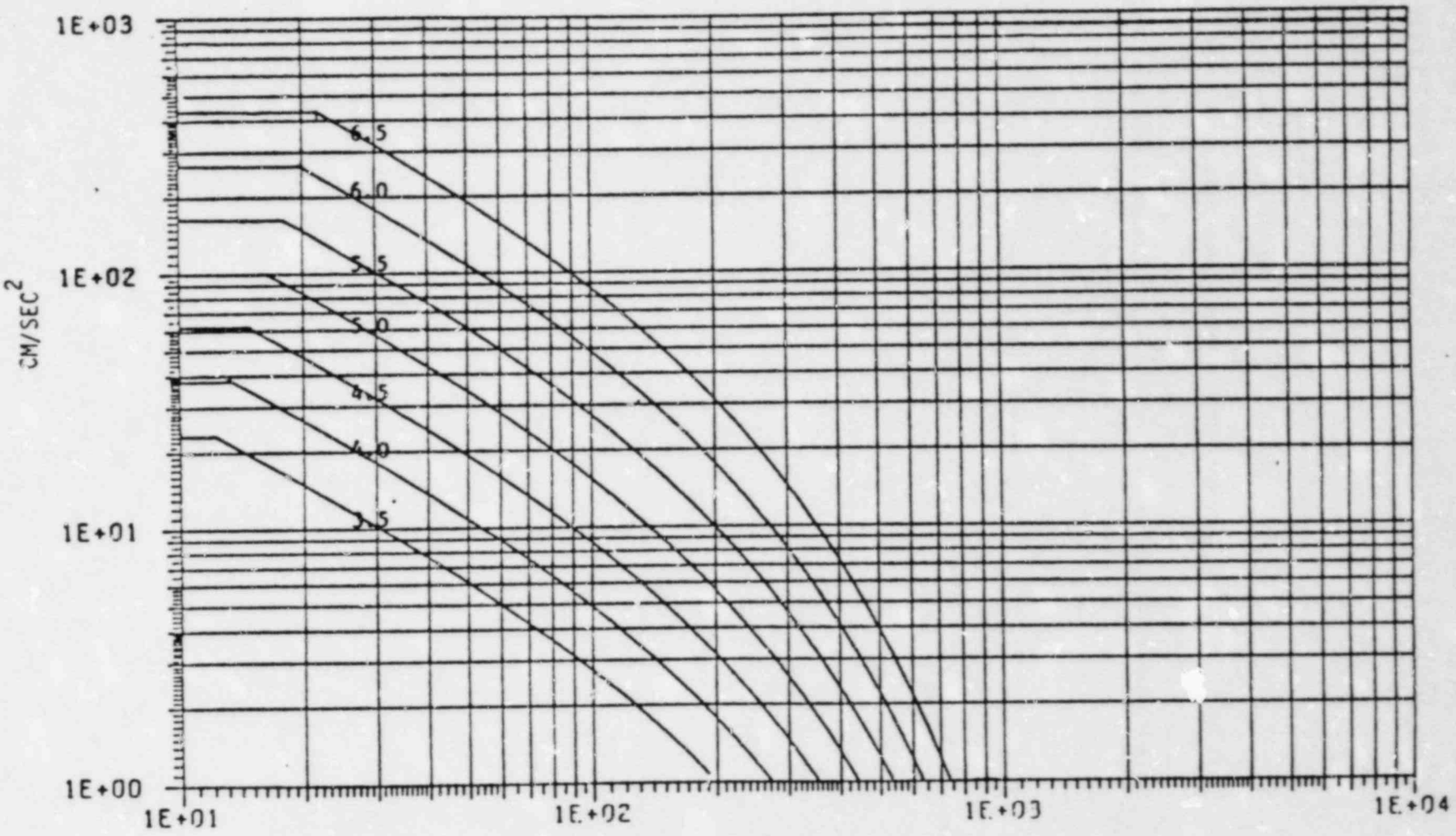

Figure E3.

Weston Geophysical Model (Early)
Based upon 4 Northeast earthquakes
Predicts median I at a given R
McGuire conversion $\ell_n A_p = 1.45-0.359\ell_n R+0.68I_s$

$\ell_n A_p = 3.428+0.70m_b-0.0017R-0.876\ell_n R$

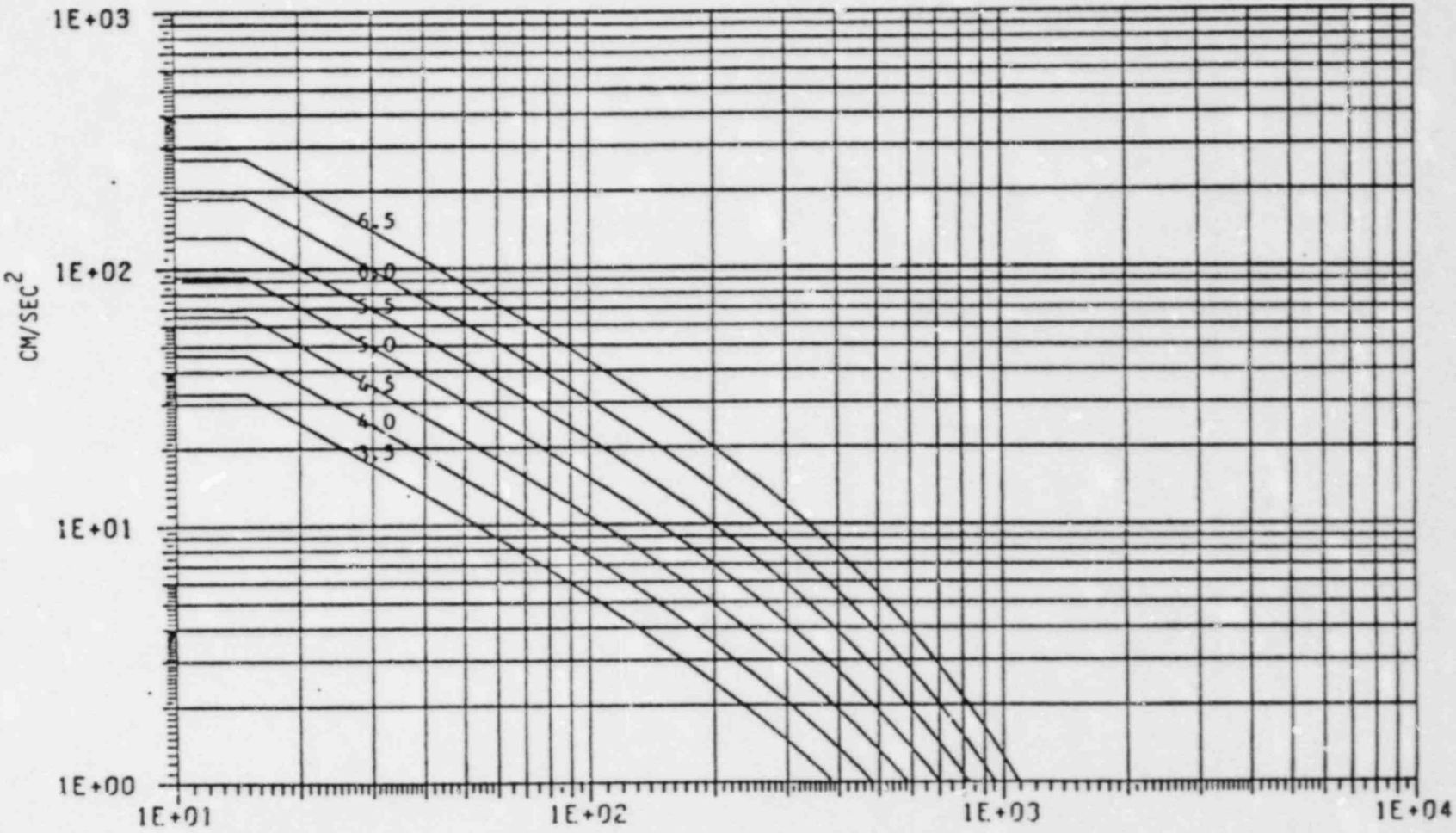

Figure E4.

Weston Geophysical Corporation
Scaled to 1.1 M_b
McGuire Conversion
$\ell n A_p = 1.45-0.359\ell nR+.68I_s$
$\ell n A_p = 1.47+1.1M_b-0.876\ell nR-0.0017R$

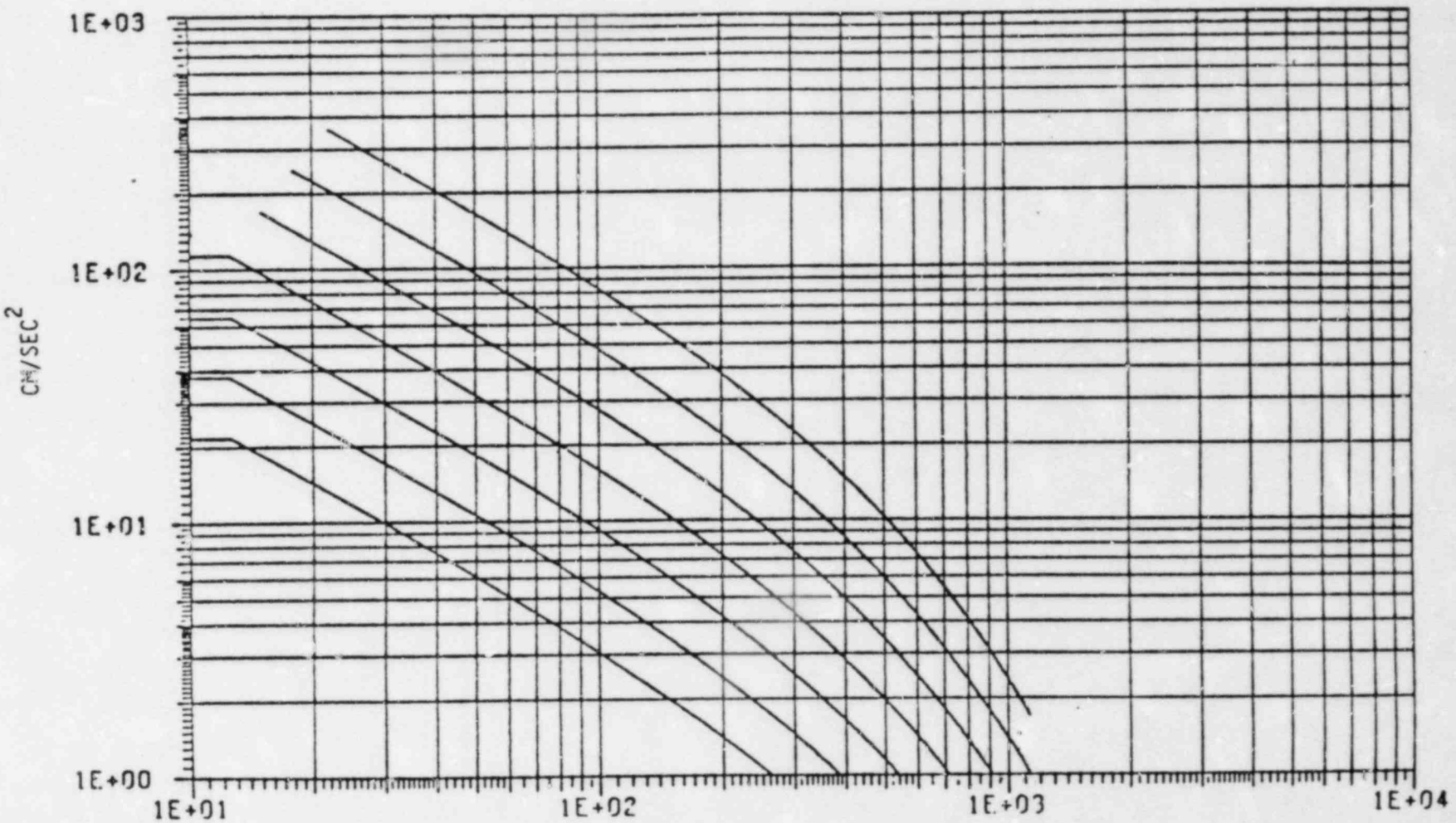

Figure E5.

Bollinger (Charlestown earthquake)
$I_o \rightarrow m_b$ conversion ($I_o = 1.37m_b - 0.134$)

$I_s \rightarrow \ell_n A_p$ (McGuire) $\ell_n A_p = 1.45 - 0.359\ell_n R + 0.68 I_s$

$\ell_n A_p = 3.325 + 0.93m_b - .00035R - 1.209\ell_n R$

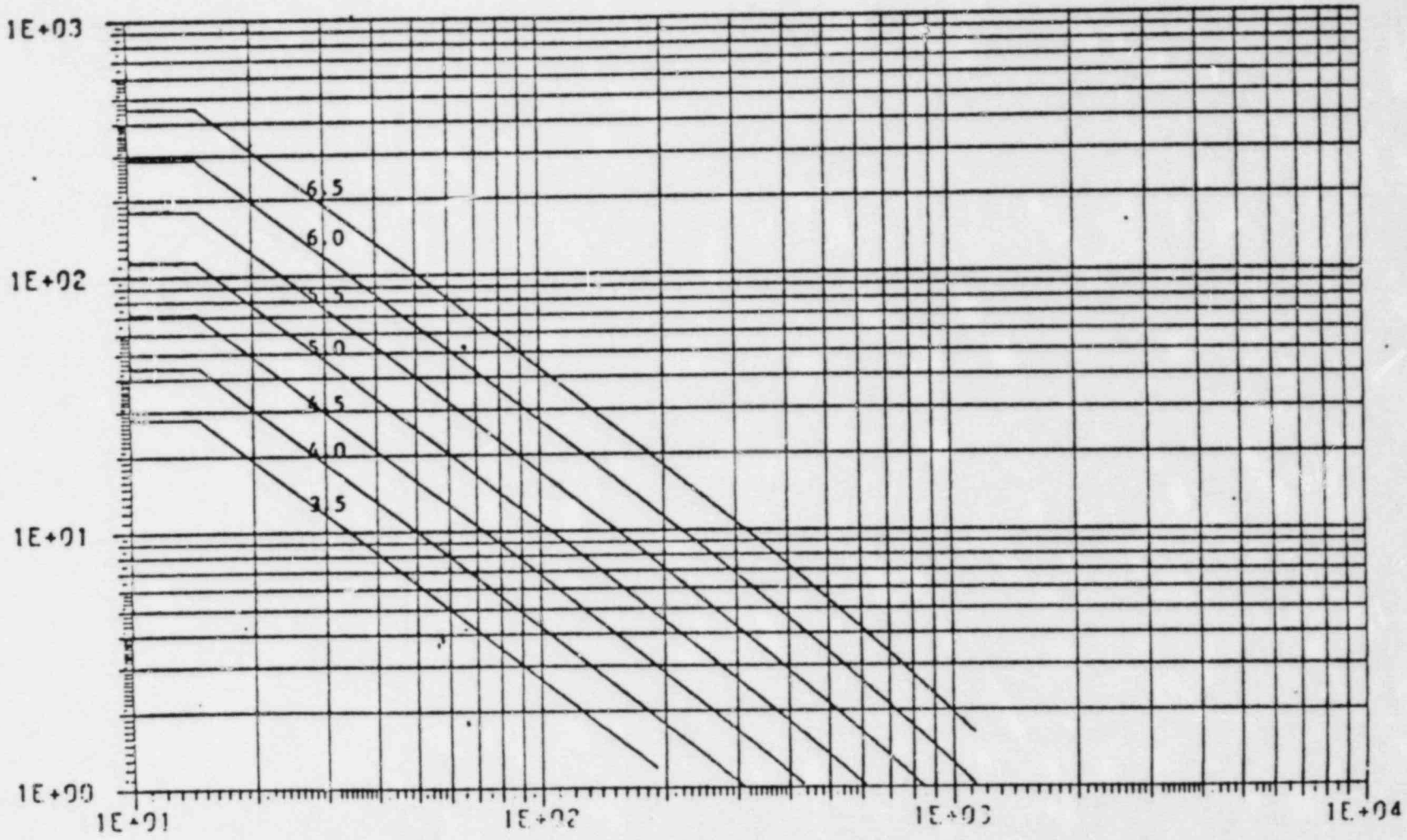

Figure E6.

Bollinger (Charlestown earthquake)

$I_0 \rightarrow m_b$ conversion ($I_0 = 2m_b - 3.5$)

$I_s \rightarrow \ell n A_p$ (McGuire) $\ell n A_p = 1.45 - 0.359 \ell n R + .68 I_s$

$\ell n A_p = 1.029 + 1.36 m_b - 0.0035R - 1.209 \ell n R$

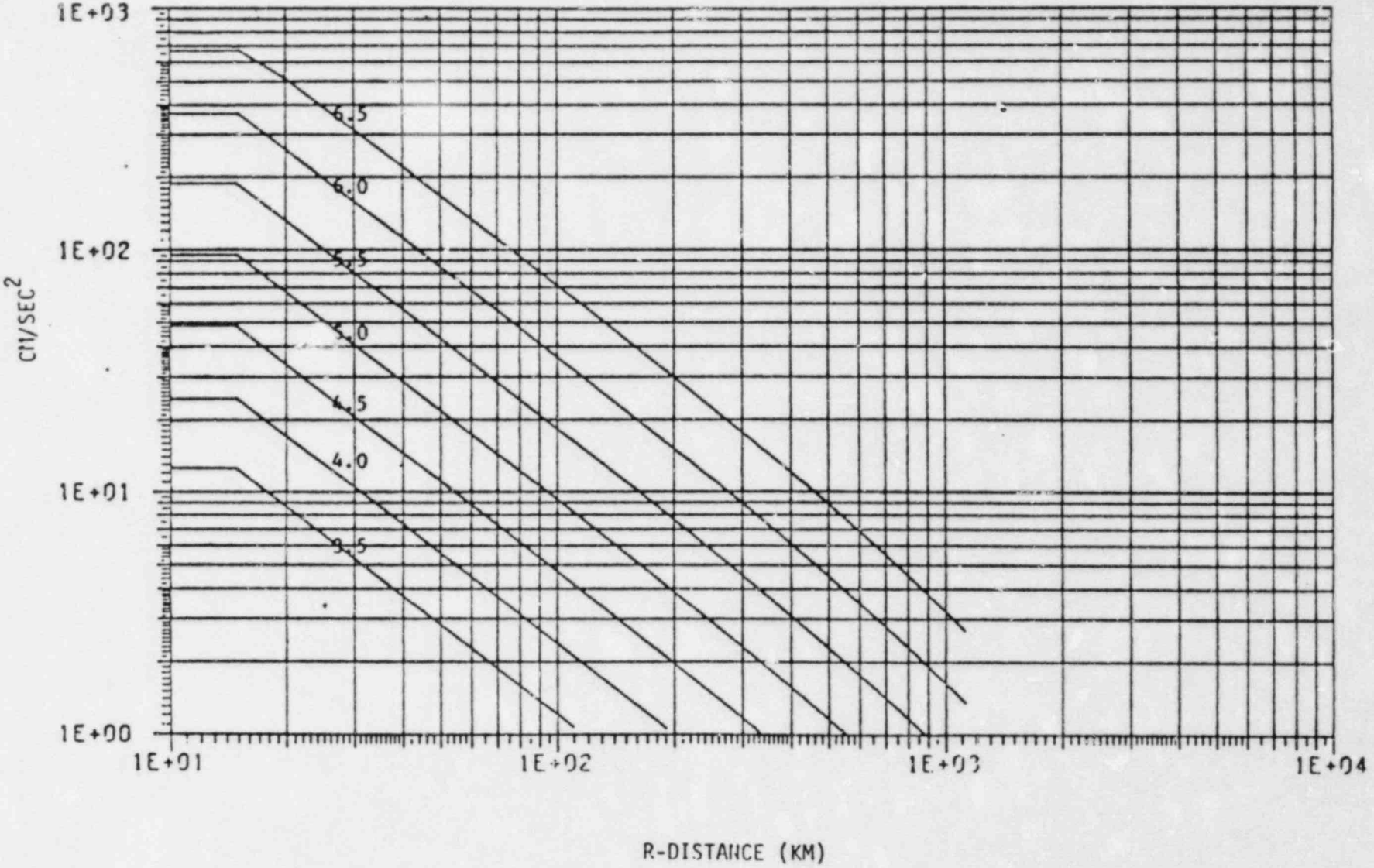

Figure E7.

Gupta-Nuttli (Vol. 4, NUREG/CR-1582)
Based on Isoseismals from
1968 Southern Illinois earthquake
and 1812 New Madrid earthquakes
Equation based on isoseismals is
reduced by 1/2 Intensity unit.

$\ell_n A_p = 0.74+1.12m_b-0.0007R-.733\ell_n R$

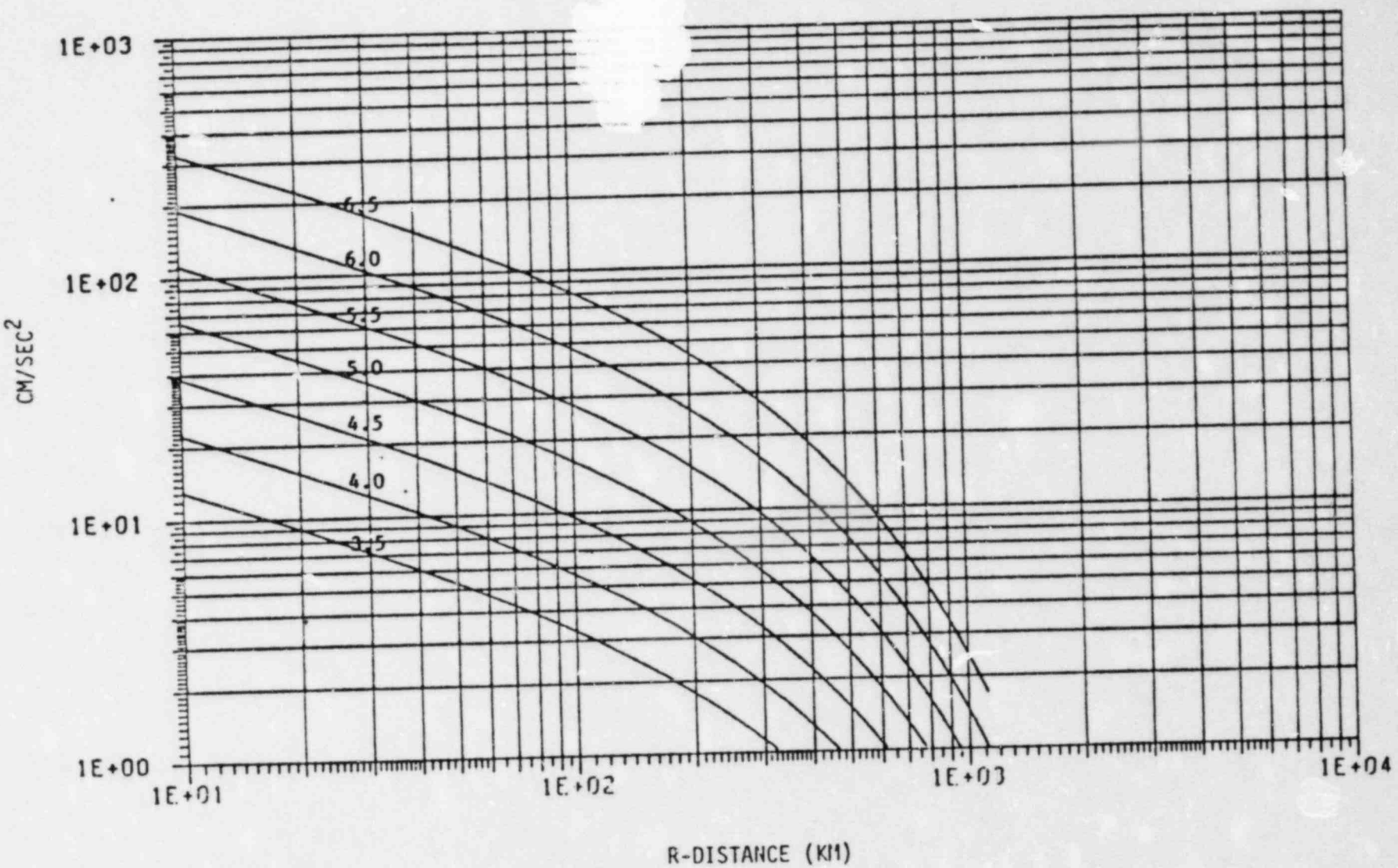

Figure E8.

APPENDIX F

SENSITIVITY OF HAZARD TO INPUT PARAMETERS

The two values of acceleration that are exceeded with annual probability 10^{-3} and 10^{-4} (referred to as A_{10}-3 and A_{10}-4, respectively) have been used in Section 2 to provide an approximation of any estimated hazard function at the site. With such a representation, an entire hazard curve can be reduced to a single "acceleration point" in the (A_{10}-4, A_{10}-3) plane, facilitating comparison with other estimates when there are many such curves. The cloud of 450 acceleration points that correspond to all but one of the input alternatives used for the zonation method is shown in Figure 10. Only one set of "a" values is used in this plot, namely the most highly weighted set. This appendix collects 18 similar plots, each obtained by fixing one parameter (zonation, median attenuation, attenuation dispersion σ_E and truncation, "b" values, m_1 values) while leaving all the other parameters free. Therefore, each plot contains a subset of the points in Figure 10. There are:

- 5 plots for zonation (Figures F1 to F5)
- 5 plots for the median attenuation (Figures F6 to F10)
- 3 plots for σ_E and truncation (Figures F11 to F13)
- 2 plots for b (Figures F14 and F15)
- 3 plots for m_1 (Figures F16 to F18)

Comparing, for example, the three plots F16 to F18, one sees that increasing m_1 values generally shift the cloud of 150 points to the upper right, implying a general increase in both A_{10}-3 and A_{10}-4, in turn implying an upward shift of any given hazard curve. Alternative values of "a" are not shown because the sensitivity of hazard estimates to uniform changes in "a" is so simple: at these small probability levels, the hazard H is simply proportional to "a".

ZONATION 1 (BOSTON-OTTAWA/PIEDMONT)

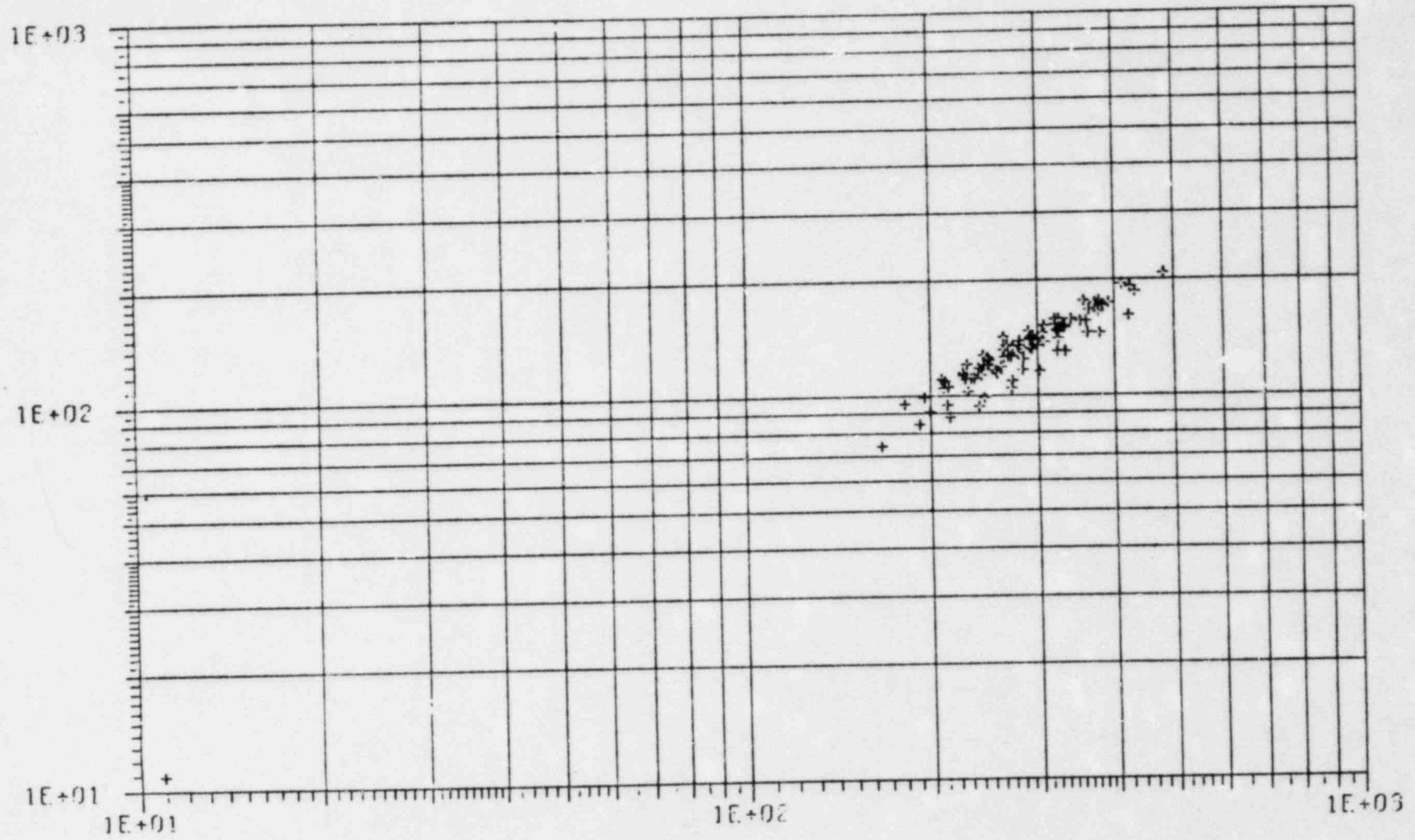

Figure F1.

GROUPING PLOT

ZONATION 2 (WESTON GEOPHYSICAL CORPORATION (WGC))

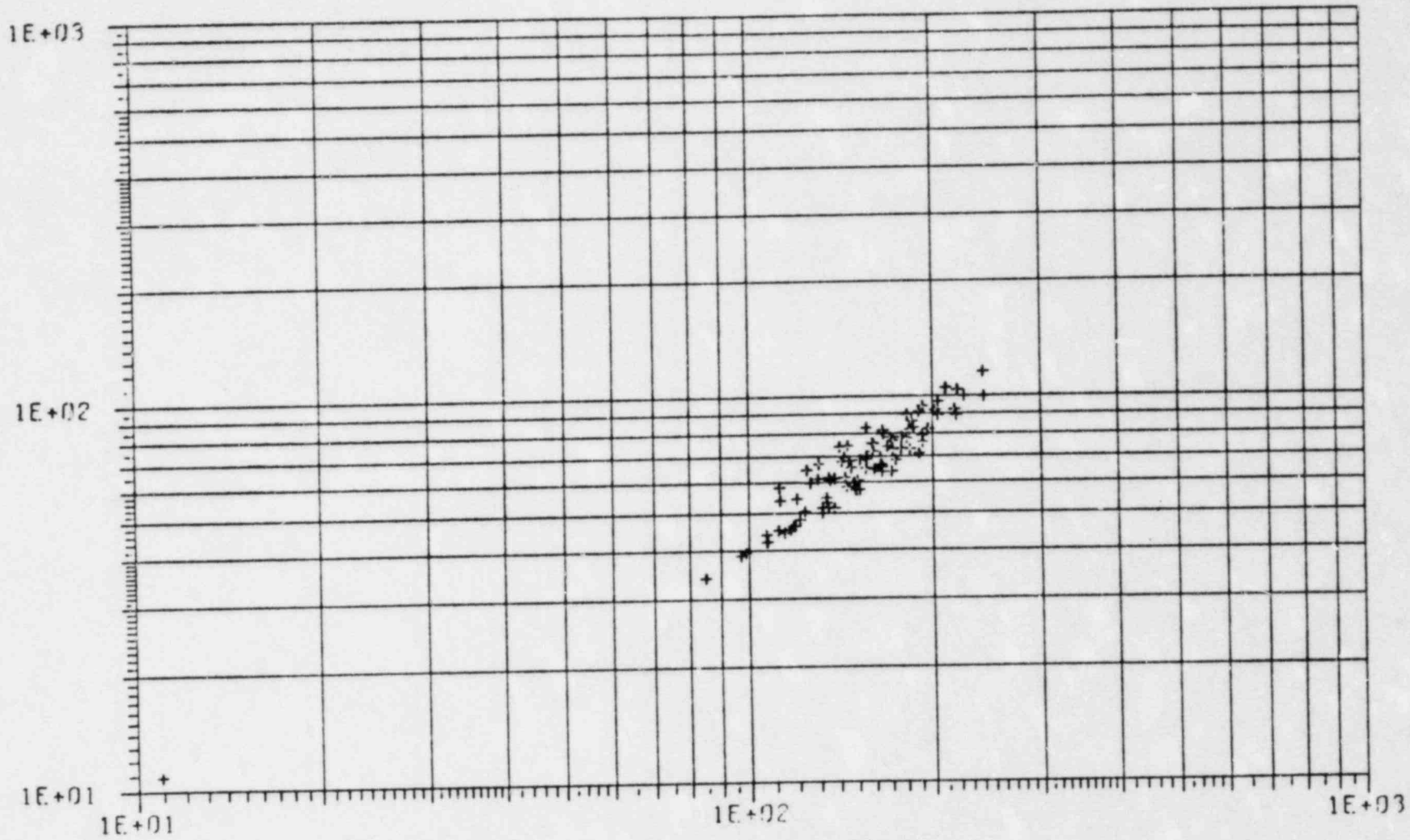

Figure F2.

GROUPING PLOT

ZONATION 3 (WGC SOUTH/BOSTON-OTTAWA NORTH)

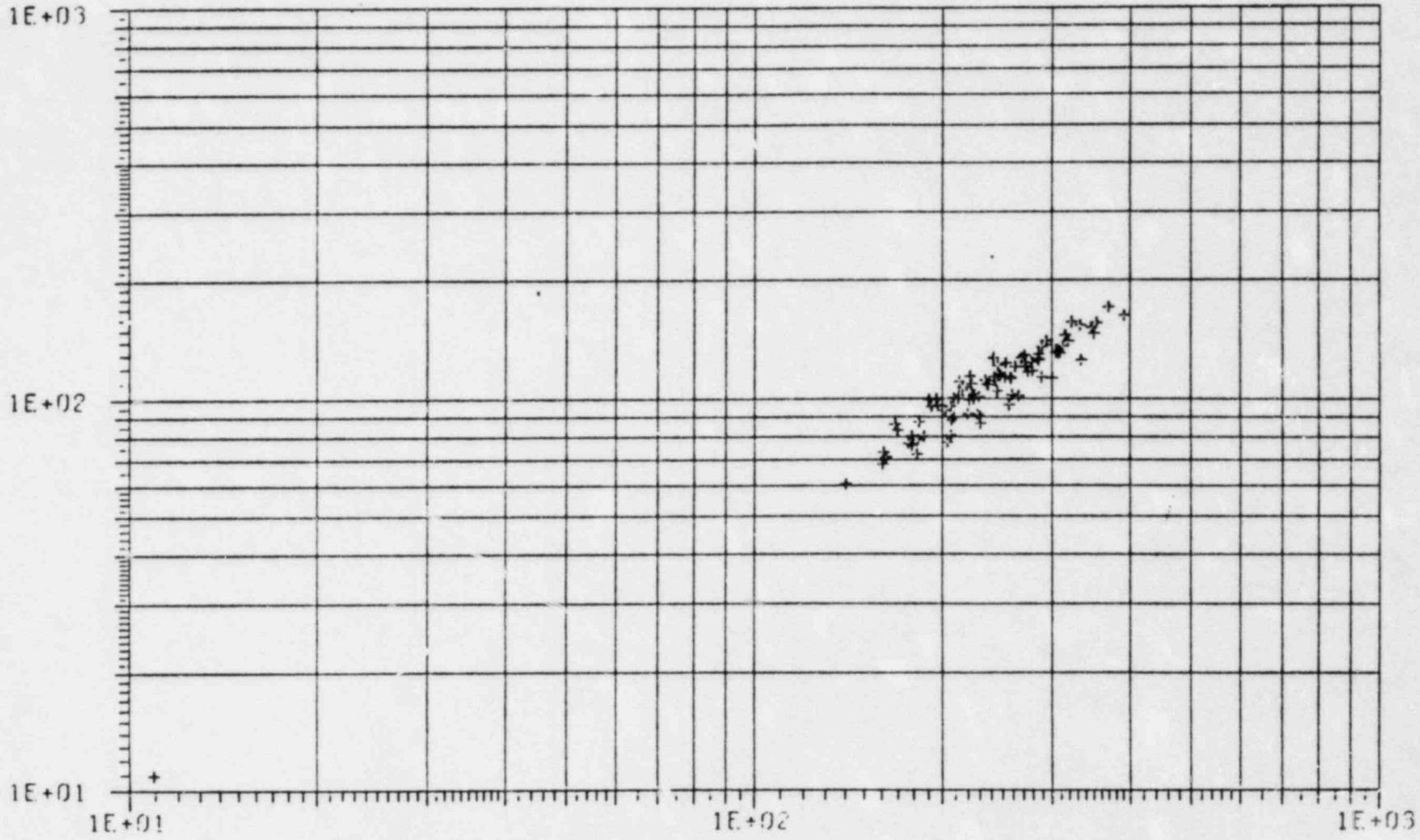

Figure F3.

GROUPING PLOT

ZONATION 4 (WGC NORTH/PIEDMONT SOUTH)

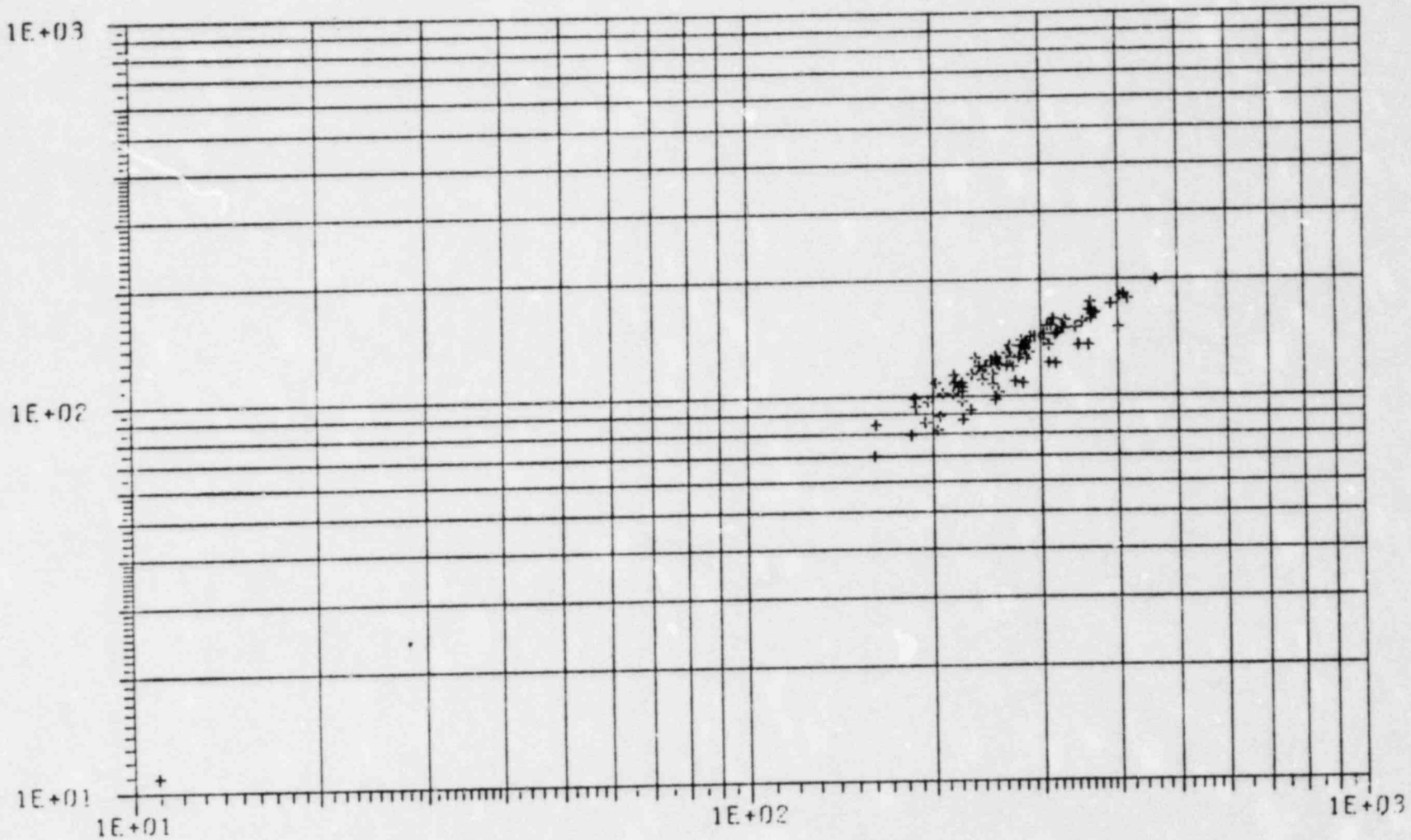

Figure F4.

A(C.0011

ZONATION 5 (PIEDMONT CARVED)

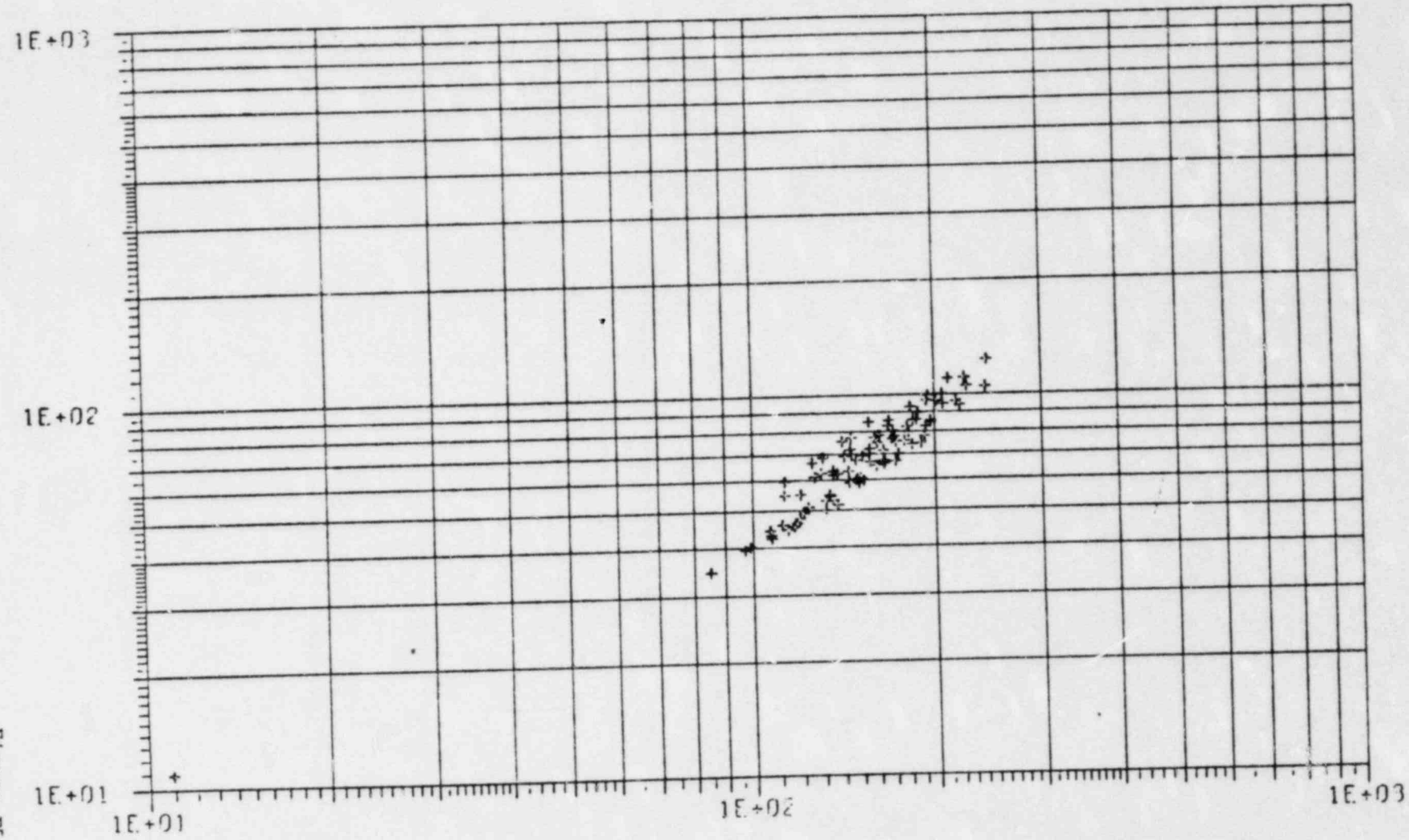

Figure F5.

ATTENUATION 1 (HERRMANN 1981)

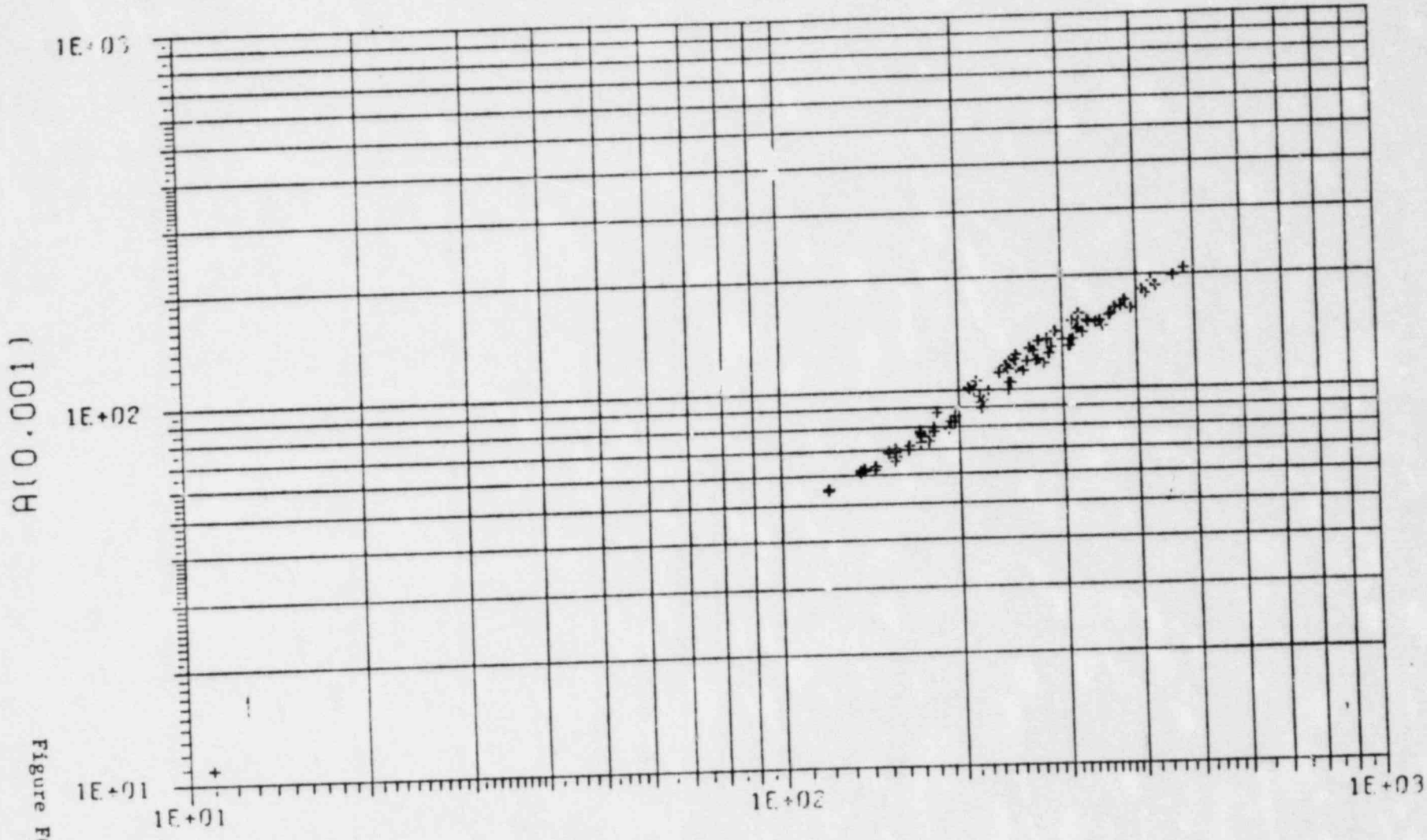

Figure F6.

GROUPING PLOT

ATTENUATION 2 (BOLLINGER $I_o=2m_b-3.5$)

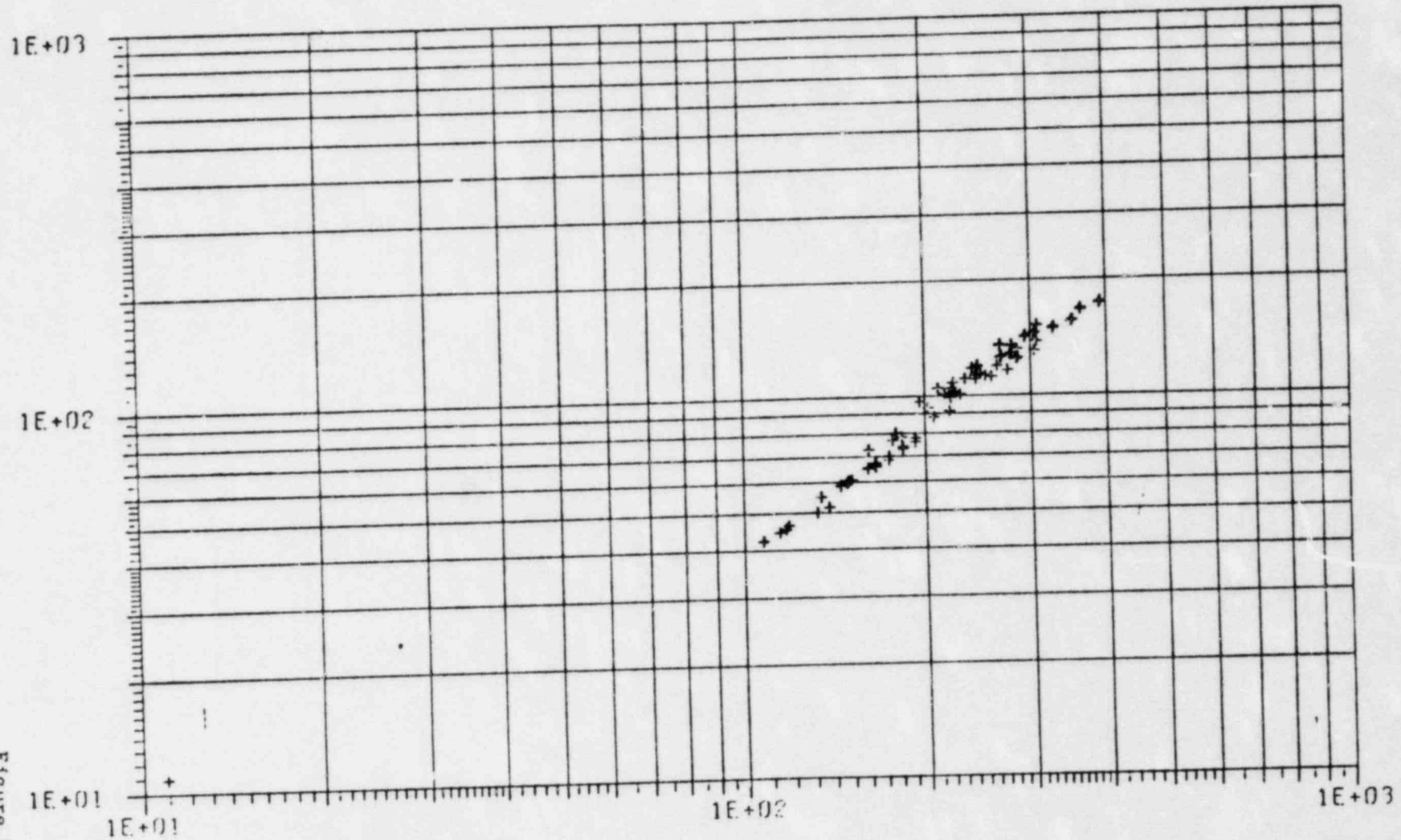

Figure F7.

GROUPING PLOT

ATTENUATION 3 (BOLLINGER $I_o=1.3m_b-.134$)

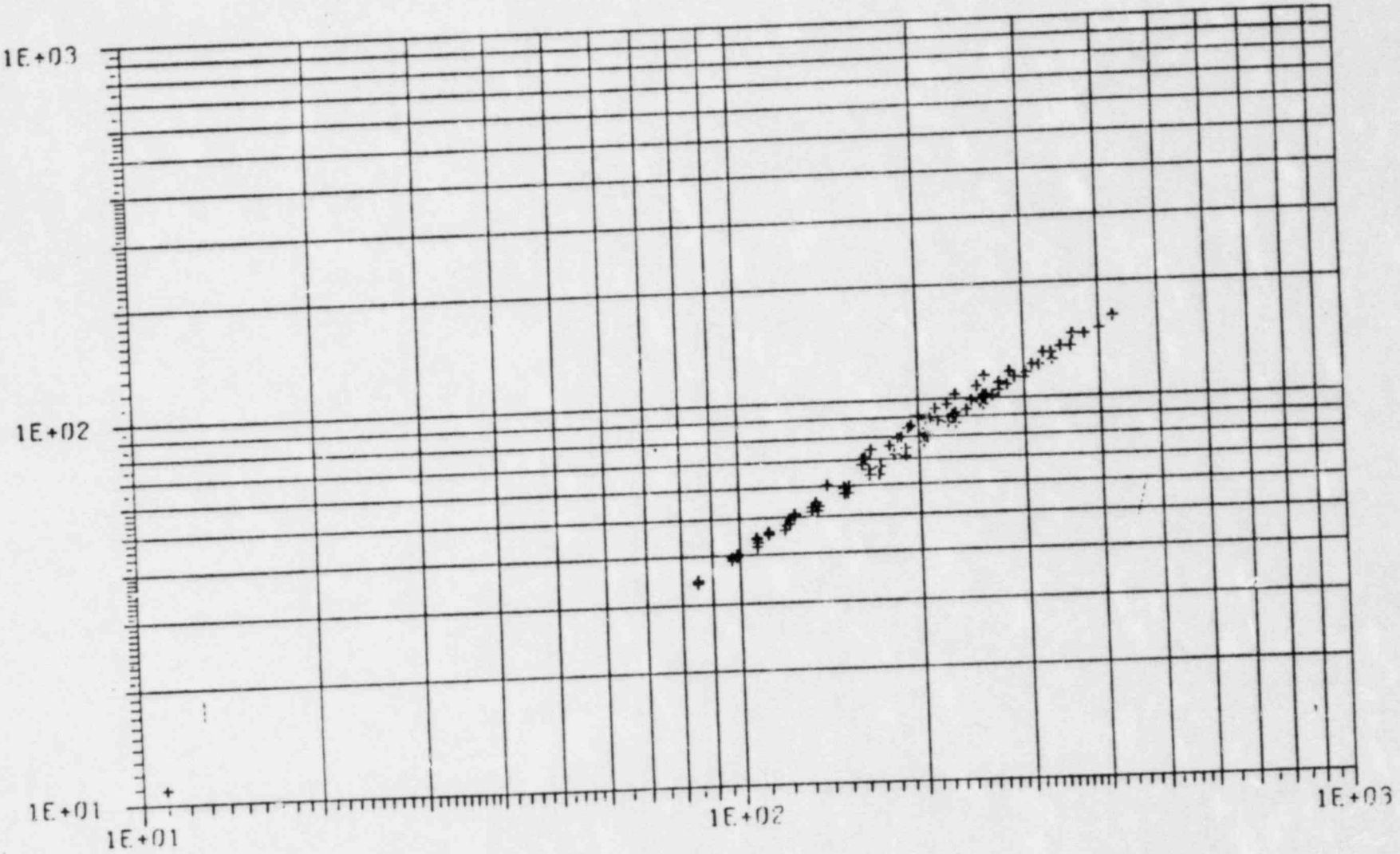

Figure 8.

A(0.001)

SCATTER PLOT

ATTENUATION 4 (WGC SCALED TO 1.1 m_b)

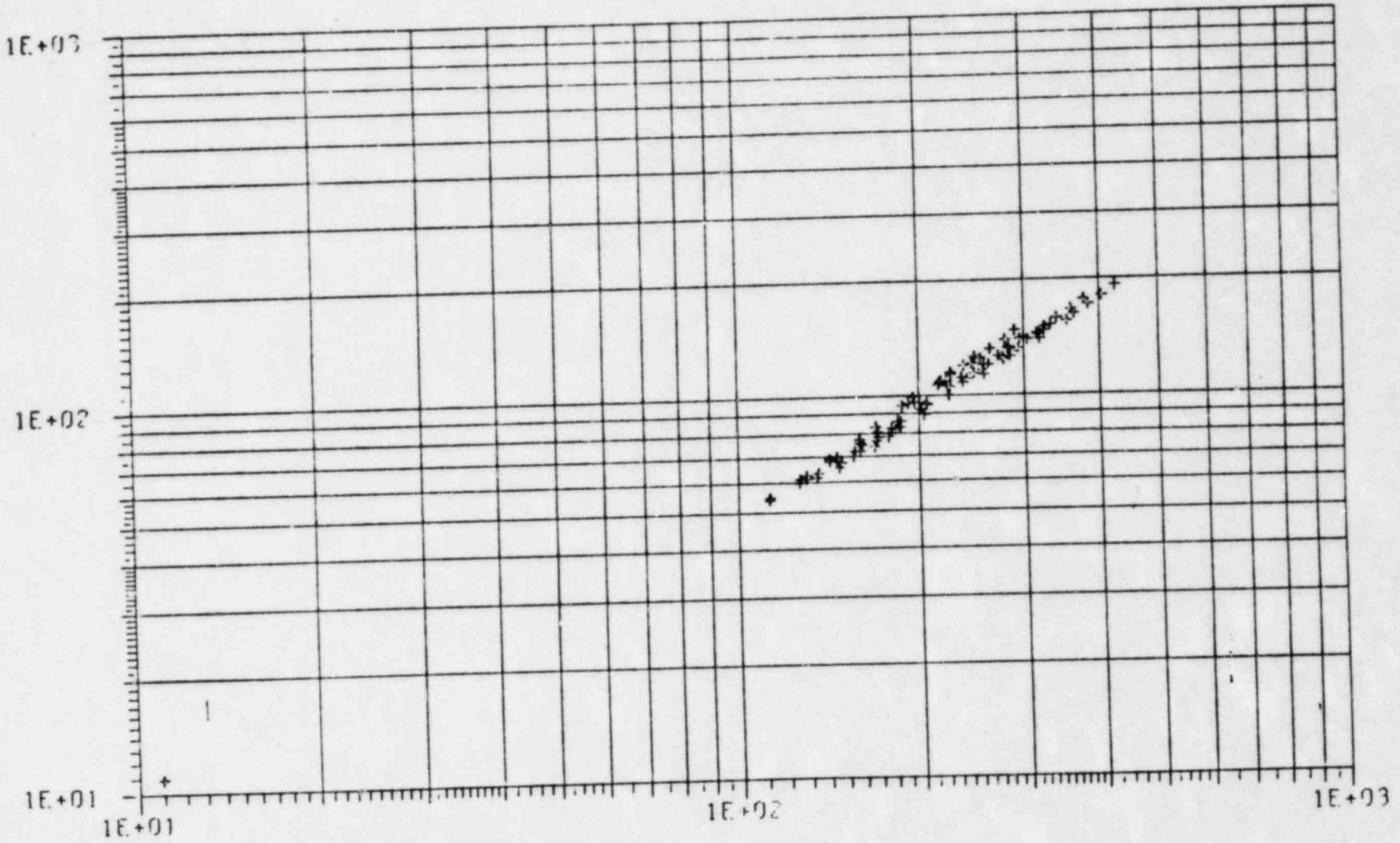

Figure F9.

GROUPING PLOT

ATTENUATION 5 (GUPTA/NUTTLI)

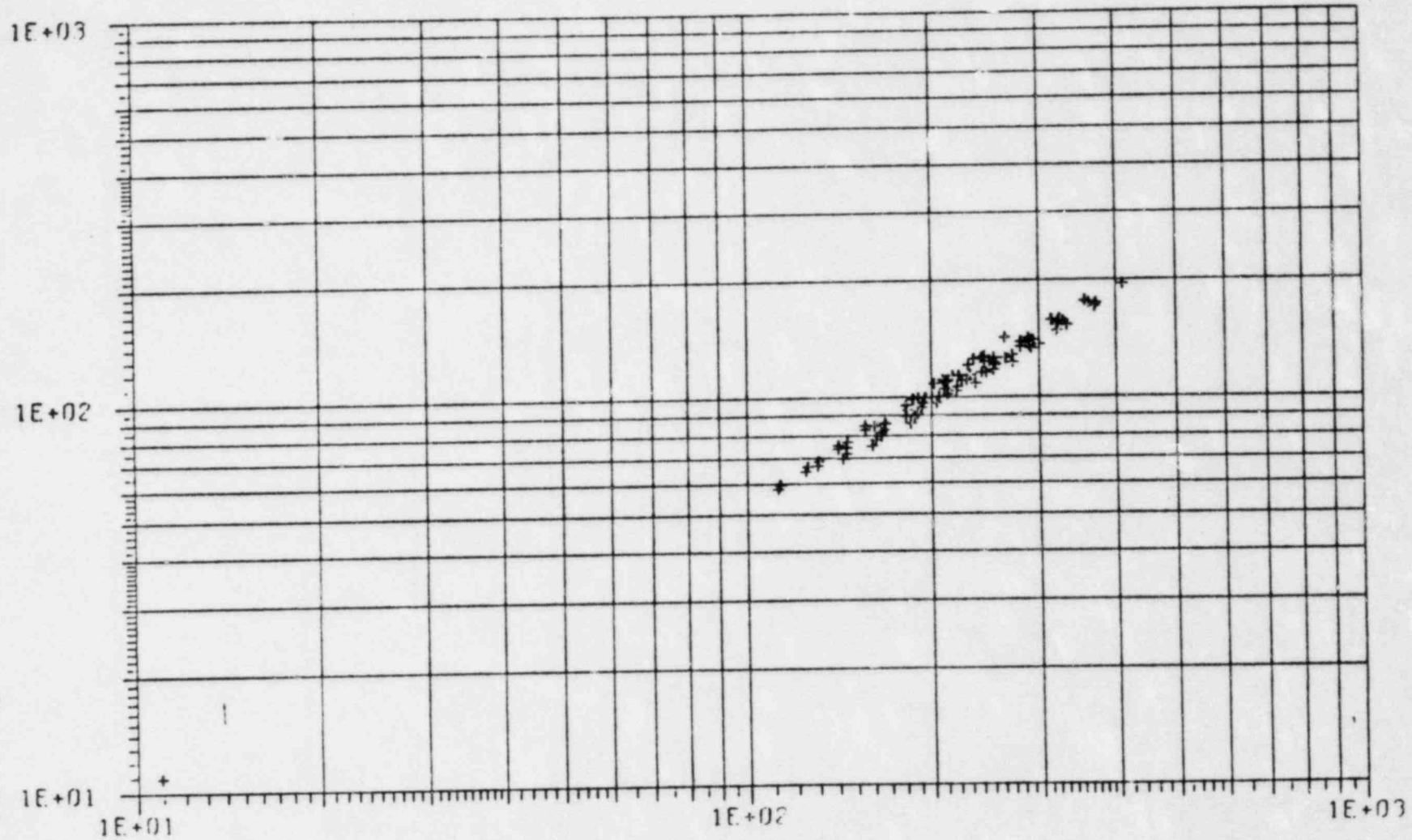

Figure F10.

GROUPING PLOT

SIGMA = 0.60 UNTRUNCATED

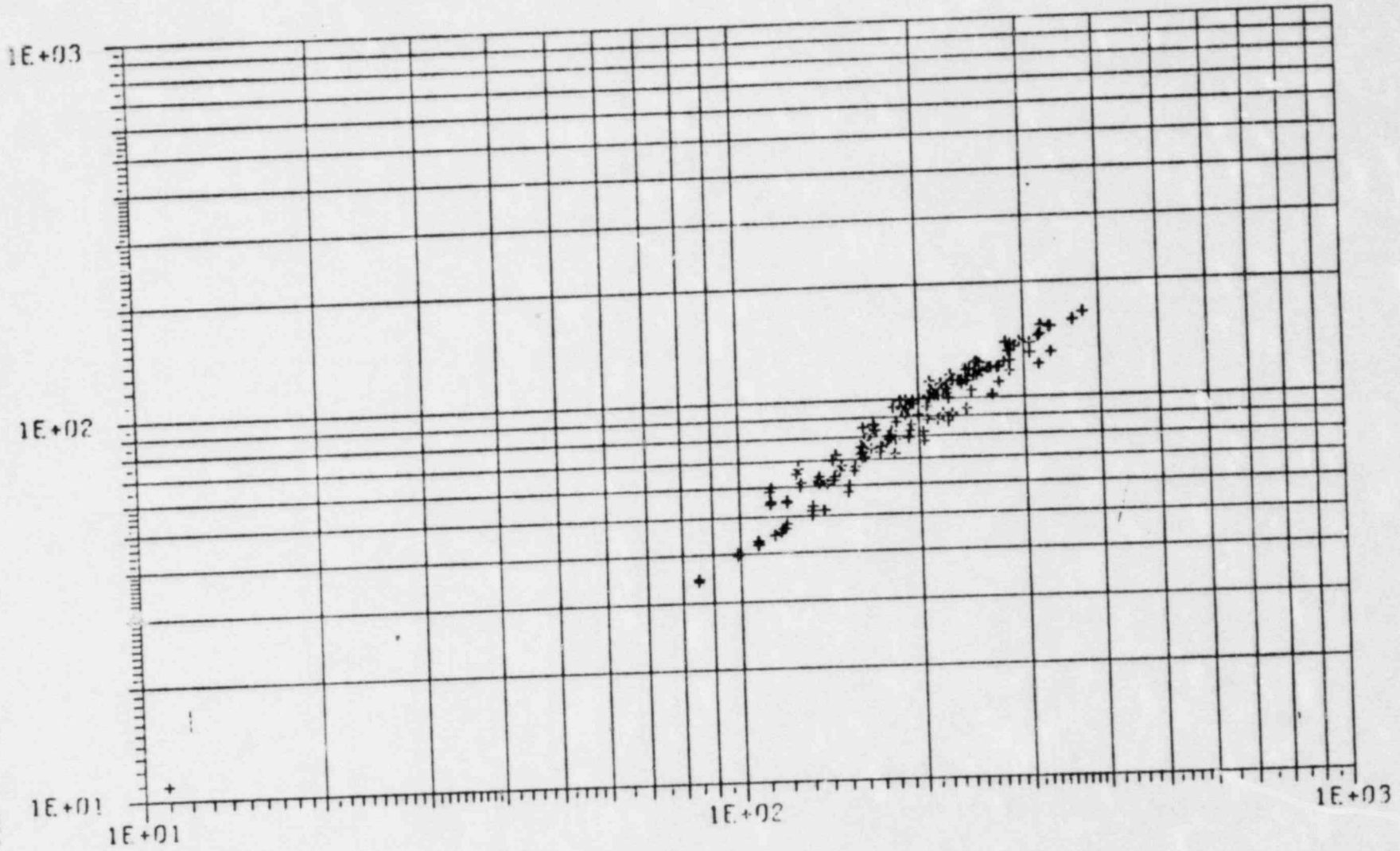

Figure F11.

GROUPING PLOT

SIGMA = 0.70 TRUNCATED AT 3 SIGMA

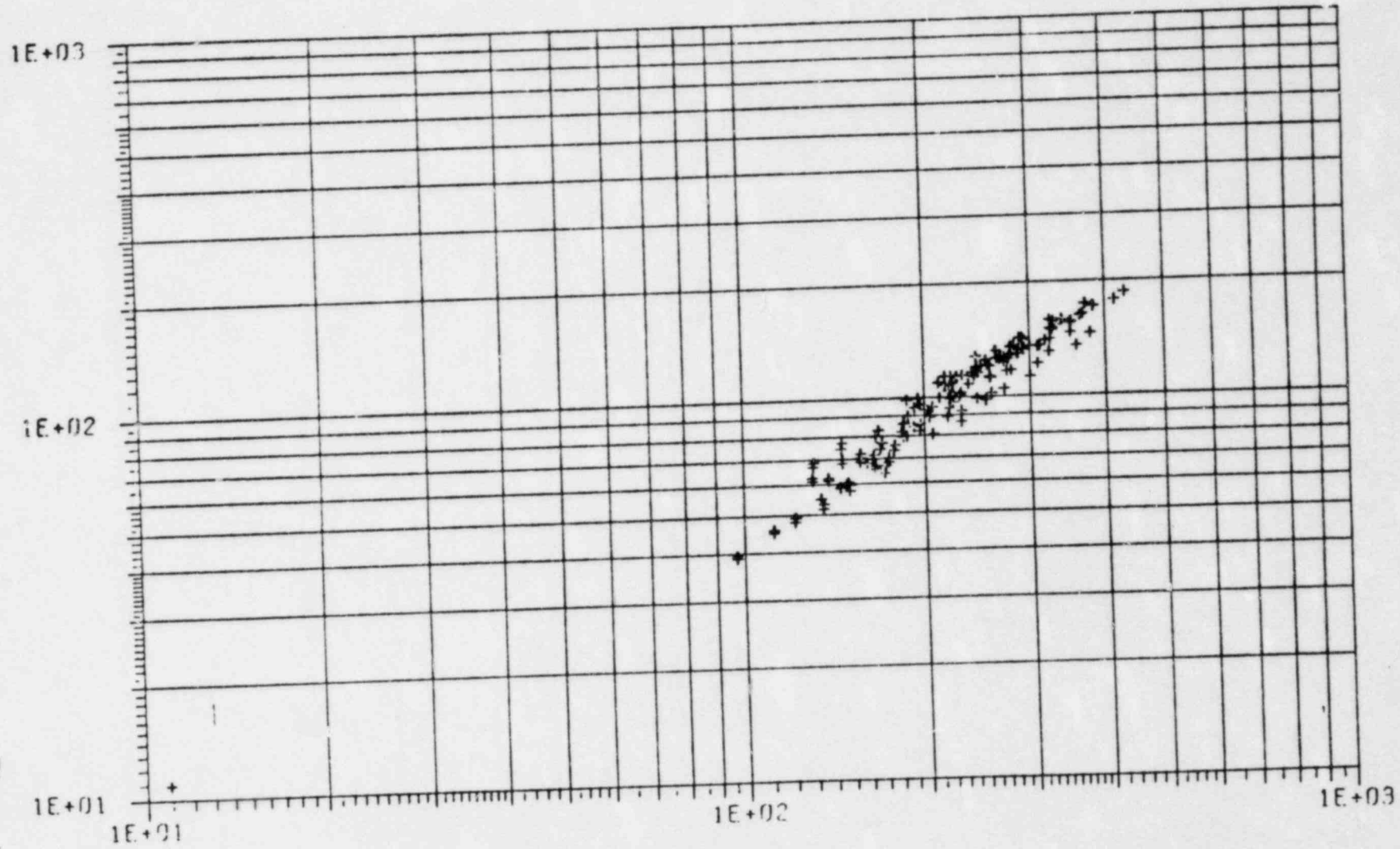

Figure F12.

GROUPING PLOT

SIGMA = 0.90 TRUNCATED AT 2 σ

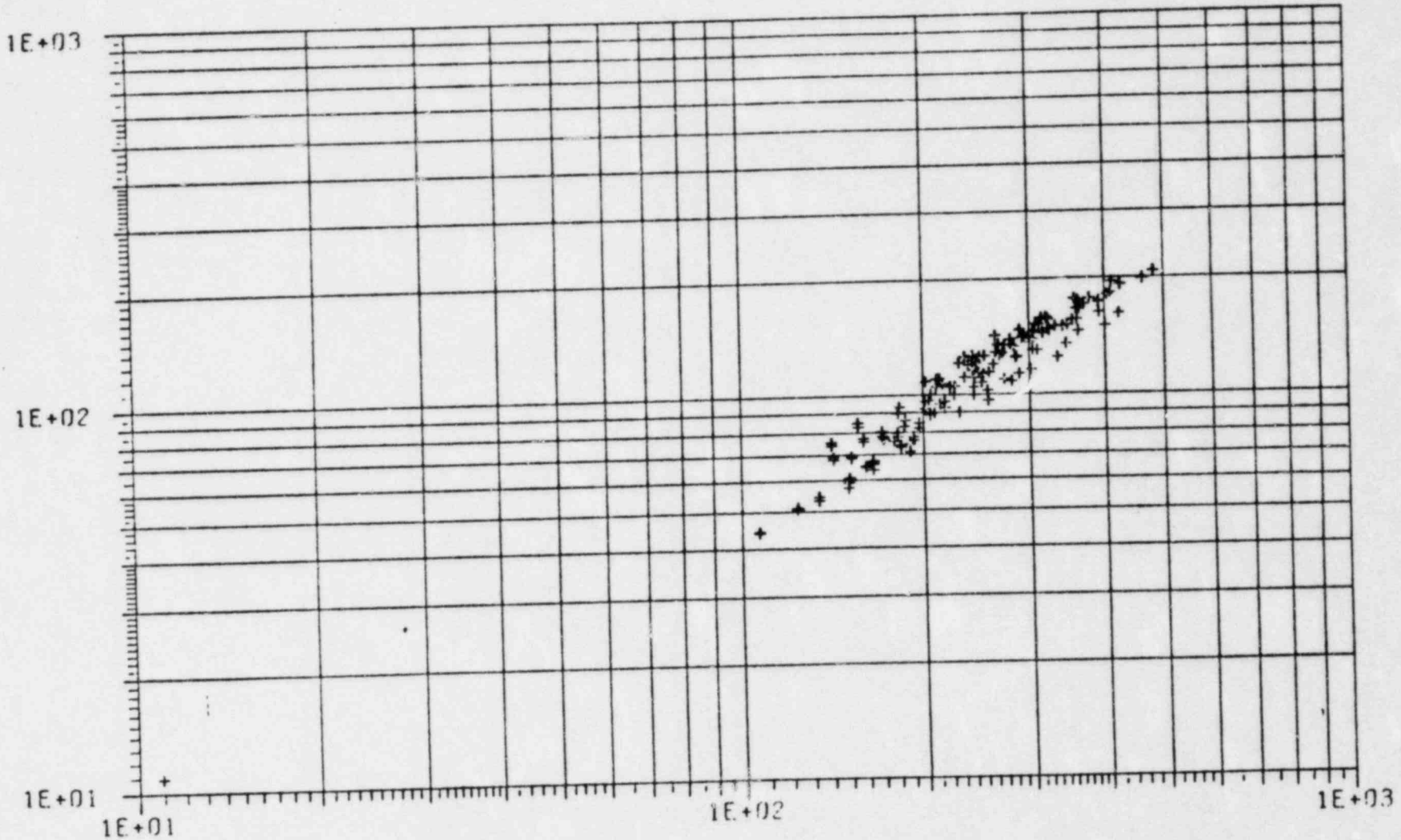

Figure F13.

GROUPING PLOT

WESTON B VALUES

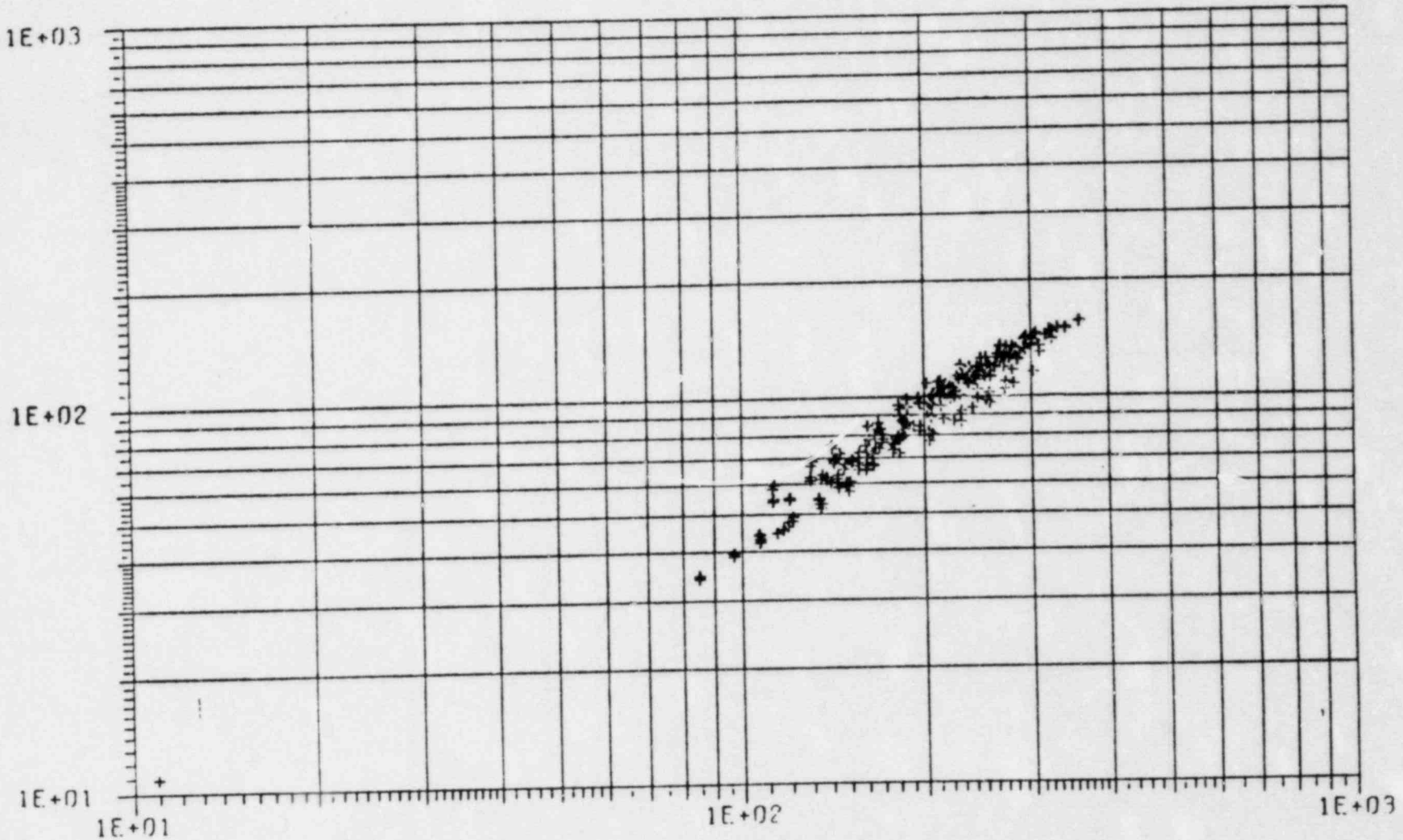

Figure F14.

GROUPING PLOT

B = 0.9 FOR ALL SOURCES

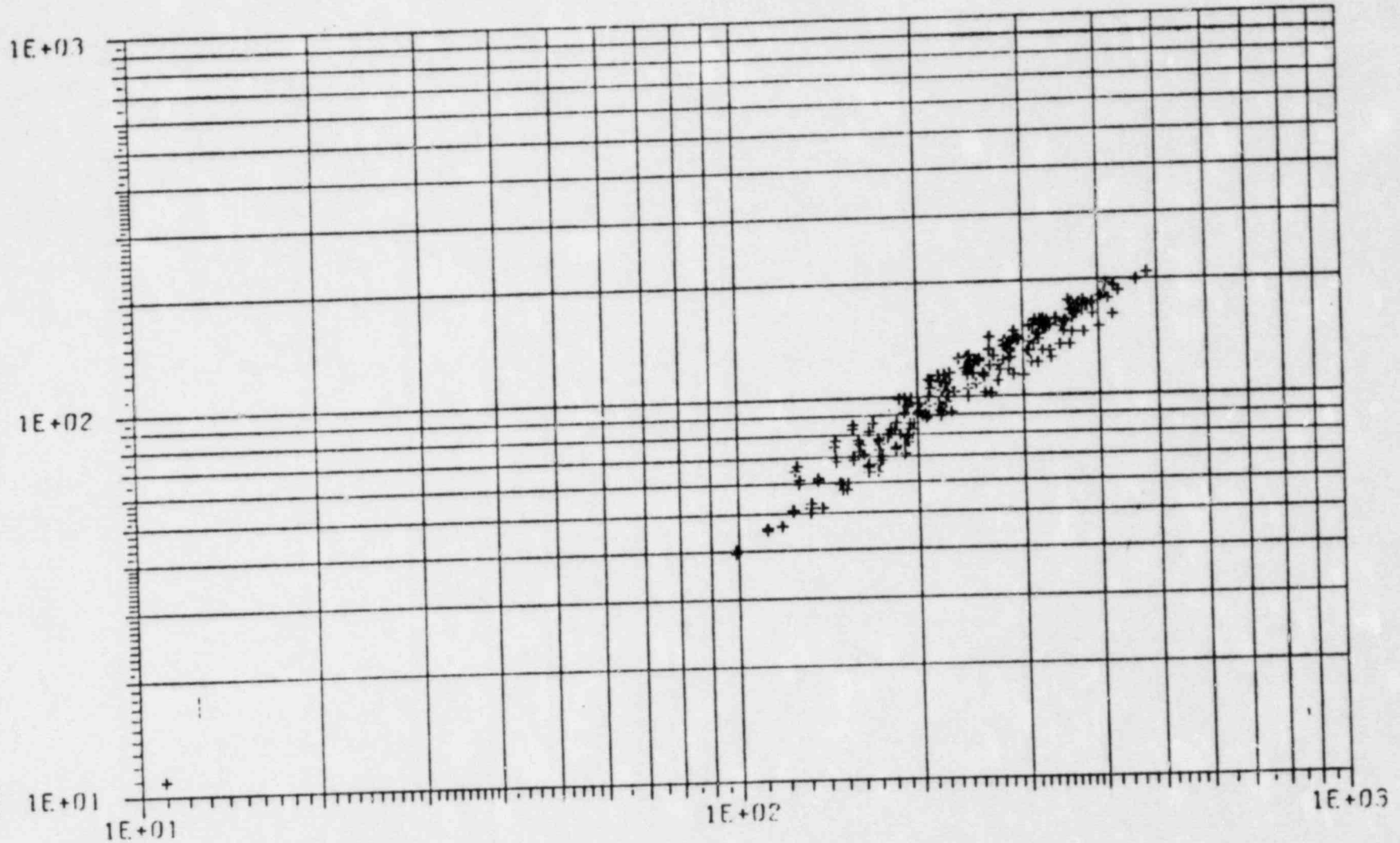

Figure F15.

GROUPING PLOT

M1 = WESTON VALUES

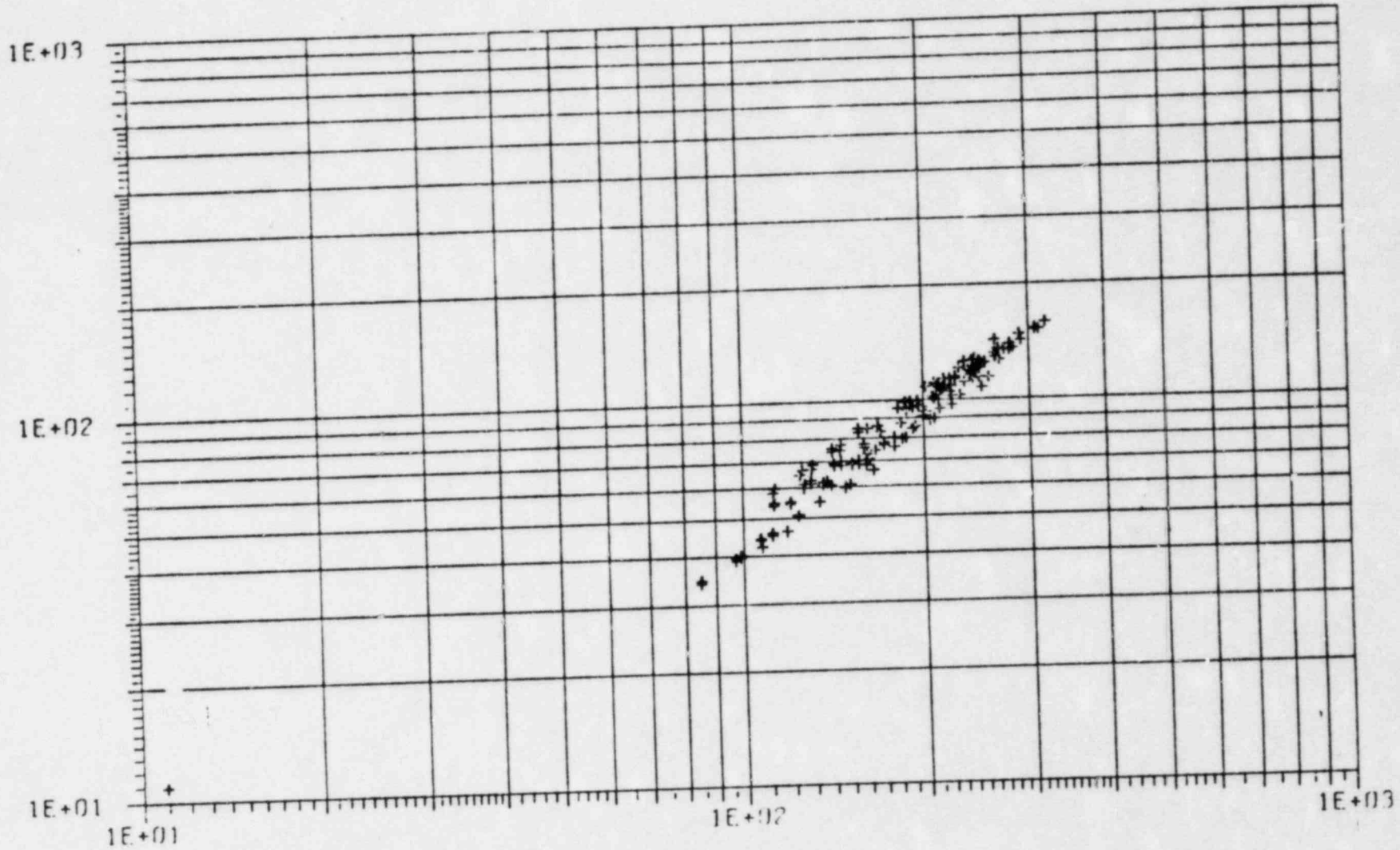

Figure F16.

GROUPING PLOT

M1 = WESTON + 0.50

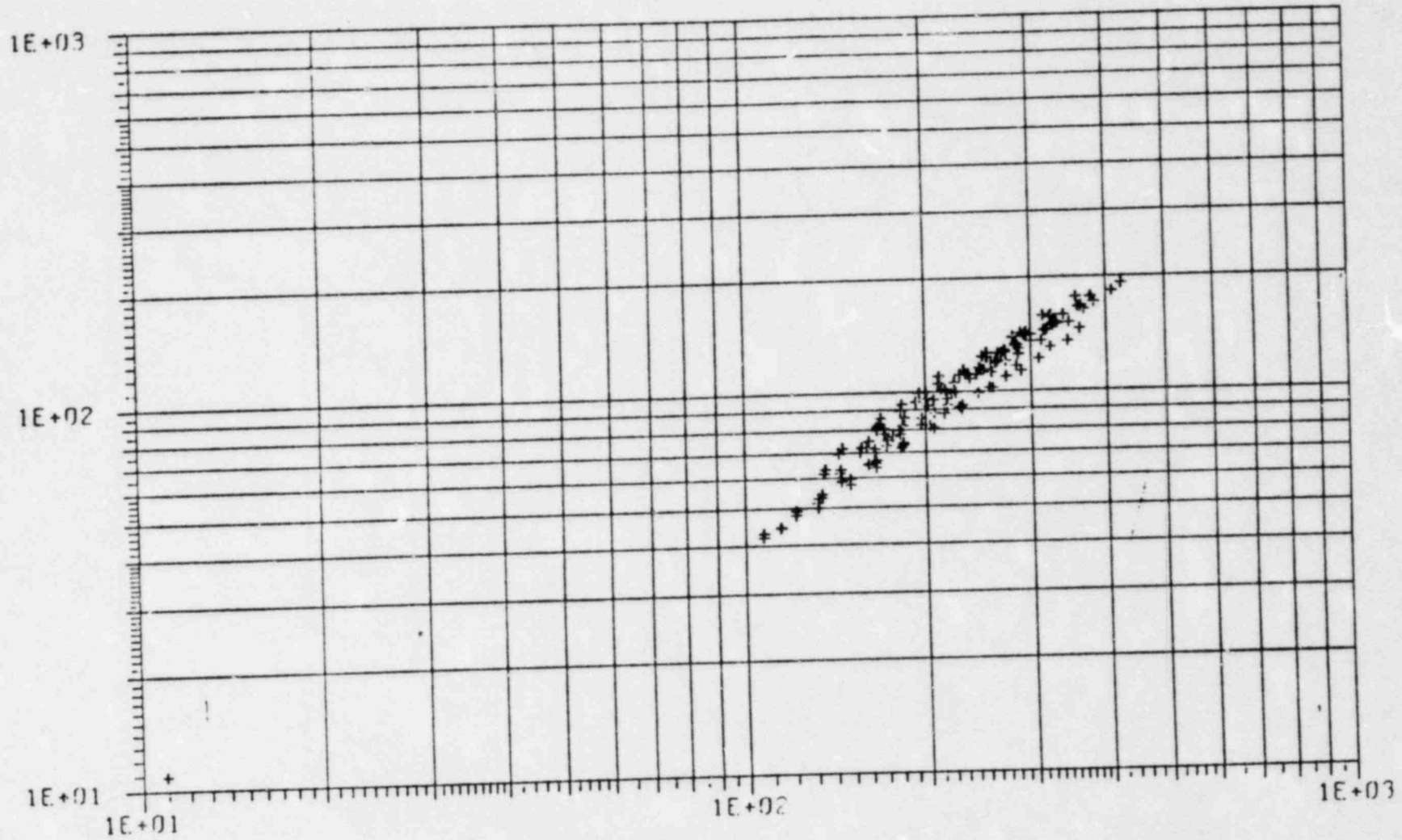

Figure F17.

GROUPING PLOT
M1 = WESTON + 0.75
1E+03
1E+02
1E+01
A(C.C01)
1E+01
1E+02
1E+03
A(C.0001)

Figure F18.

APPENDIX G

HISTORIC METHODS OF SEISMIC HAZARD ANALYSIS

1.0 INTRODUCTION

In the eastern United States, the mechanism of intraplate earthquake generation and the geographical locations of the earthquake sources are not well established. This lack of knowledge makes the use of so-called zonation methods somewhat less appealing because such methods usually require a precise description of the earthquake sources and their seismic activity. So-called historical procedures represent an attractive alternative in that they replace the description of regional seismicity by the catalog of historical events. Properly implemented, one would expect general agreement between the results of the two methods, especially at higher hazard, lower acceleration levels where the historical data alone are relatively complete.

Two procedures of the latter type are used in this study to produce estimates of seismic hazard at Yankee: one corresponds to the method used in NUREG/CR-1582, whereas the other is an extension of the model proposed by Davenport and Milne [1].

Let A denote peak site acceleration (or any other intensity measure at the site) and let H(a) be the hazard function in terms of A (i.e., probability that $A \geq a$ at least once in one year). For the case of earthquakes with independent magnitudes and with Poisson occurrences in time and space, H(a) can be expressed as:

$$H(a) = 1 - e^{-\lambda_A(a)} \qquad (G1)$$

in which $\lambda_A(a)$ is the exceedance rate function (the expected number of events in one year that produce peak acceleration at the site in excess of a). The problem of seismic hazard analysis is that of calculating the function H(a) or, equivalently the function $\lambda_A(a)$.

The first (nonparametric) historic procedure makes no a priori assumptions about the shape of the exceedance rate function λ_A, whereas the second (parametric) procedure assumes that the upper tail of λ_A (more

precisely, the upper tail of a function closely related to λ_A) is proportional to the tail of a Weibull distribution, with uncertain shape and scale parameters. A third uncertain parameter of the parametric procedure is the occurrence rate of earthquakes with site acceleration higher than a minimum value of practical concern. Both methods include attenuation uncertainty from epicentral intensity at a given distance. Both methods also allow for incompleteness of the catalogs. There is a fundamental difference, however, in the results the two methods produce: the nonparametric procedure yields a single hazard curve, $\hat{H}(a)$, which may be viewed as a "point estimate" of the true function H(a), whereas the parametric method produces a family of hazard functions, $H_q(a)$, one function for each non-exceedance probability q. That is, functions which provide:

$$P[H(a) \leq H_q(a)] = q \tag{G2}$$

Functions $H_q(a)$ of this type are sometimes referred to as uniform-probability hazard functions.

Nonparametric Method

Suppose that the attenuation model has the form:

$$\ln A = g(I_o, R) + E$$

$$= \ln \hat{A} + E \tag{G3}$$

in which g is a suitable function of epicentral intensity I_o and epicentral distance R, and E is a zero-mean random term, with untruncated or symmetrically truncated Gaussian distribution. It follows that the quantity

$$\hat{A} = \exp\left[g(I_o, R)\right] \tag{G4}$$

is the median value of acceleration at the site for an earthquake with given characteristics I_o and R.

From a catalog of earthquake events of the type $(T, I_o, R)_i$ with T_i the time of occurrence of the ith earthquake, a nonparametric estimate of $\lambda_A(a)$ can be obtained.

Consider now a catalog for the past N years. It contains, in effect, for each earthquake, i, the date T_i, the epicentral distance R_i, and the epicentral intensity I_{o_i}. Now, if the catalog were complete and the attenuation law had no error, E, one could simply calculate the site acceleration A_i for each event as $\exp [g (I_{o_i}, R_i)]$ and then estimate $\lambda_A(a)$ by the total number of events with A_i greater than "a", divided by N. To correct for attenuation uncertainty, however, we must recognize that any event will have caused acceleration greater than "a" only with a certain probability, which is:

$$P [A_i > a] = 1 - F_E (\ln a - \ln \hat{A}_i) \tag{G5}$$

in which $F_E (\cdot)$ is the cumulative distribution function of E. Also, to allow for the fact that only a given fraction of all events of intensity I_{o_i} are contained in the catalog, we must multiply each event by a factor (≥ 1), called a "completeness factor" Q_i, which is equal to the reciprocal of the probability that any event of intensity I_o in the region in the last N years has been recorded. Putting these pieces together, we obtain as a (nonparametric) estimate of $\lambda_A(a)$:

$$\hat{\lambda}_A(a) = \frac{1}{N} \sum_i Q_i [1 - F_E(\ln a - \ln \hat{A}_i)] \tag{G6}$$

in which

N = total number of years spanned by the catalog,

$A_i = g(I_{o_i}, R_i)$,

$Q_i = 1/P_{c_{I_o}}(I_{o_i})$ = completeness factors (see Table G1),

$P_{c_{I_o}}(I_o)$ = probability that an earthquake of epicentral intensity I_{o_i} that took place within the geographical region of interest, sometime during the last N years, was recorded. For the estimation of this probability, see Section 3,

F_E = cumulative distribution function (CDF) of E. In particular, if E has normal distribution with truncation at $\pm B$ standard deviations from its zero mean, then:

$$F_E = \begin{cases} 0, & \text{IF } \frac{E}{\sigma_E} \leq -\beta \\ \frac{\Phi(E|\sigma_E) - \Phi(-\beta)}{1 - 2\Phi(-\beta)} & \text{IF } -\beta < \frac{E}{\sigma_E} < \beta \\ 1, & \text{IF } \frac{E}{\sigma_E} \end{cases} \qquad \text{(G7)}$$

with Φ = standard normal CDF.

The estimator $\lambda_A(a)$ in (G6) corresponds to the expected number of events per year in the last N years that have produced ground acceleration values at the site in excess of a. The associated estimate of H(a) is, from (G1),

$$H(a) = 1 - e^{-\lambda_A(a)} \qquad \text{(G8)}$$

The monotonicity of the hazard function allows one to equivalently work in terms of the inverse hazard function A(h). The function gives the peak ground acceleration that is exceeded at the site with probability h in any given year (see Figure G-1).

Parametric Method Objective and Notation

The objective of the parametric method is to calculate the posterior (Bayesian) distribution of the hazard H(a) for any given a, i.e., to calculate the exceedance probability

$$G_{H(a)}(h) = P[H(a) \mid h] \tag{G9}$$

for any given a and h (Figure G-2).

Let $\lambda_{\hat{A}}(a)$ be the exceedance rate function for the median attenuated site acceleration $\hat{A} = \exp\left(g(I_o, R)\right)$, i.e.,

$$\lambda_{\hat{A}}(a) = \text{mean rate of events for which } A > a. \tag{G10}$$

and denoted by:

$\overline{\lambda}_{\hat{A}}(a) = \lambda_{\hat{A}}(a) / \lambda_{\hat{A}}(\bar{A})$ the exceedance rate function normalized so that $\overline{\lambda}_{\hat{A}}(\bar{A}) = 1$ for some given acceleration $\bar{A}$.

For $a \geq \bar{A}$, the function $\overline{\lambda}_{\hat{A}}(a)$ equals the complementary CDF of $(\hat{A} \mid \hat{A} \geq \bar{A})$ (see Figure G-3).

The present method calculates the probability of Equation (G9) under the parametric assumption that for $a \geq \bar{A}$, the exceedance rate function $\lambda_{\hat{A}}(a)$ has a specific shape, namely proportional to the upper tail of a complementary Weibull CDF. Precisely, it is assumed $\lambda_{\hat{A}}(a)$ is given by the function:

$$\lambda_{\hat{A}}(a) = e^{-(a^c - \bar{A}^c)/(A_o^c - \bar{A}^c)} \tag{G11}$$

This is a function in terms of two parameters, the scale parameter A_o (with $A_o > \bar{A}$) and the shape parameter c (with $c > o$). This estimation method treats the three parameters, $\overline{\lambda}_{\bar{A}}$, A_o, and c, as uncertain parameters and applies to them standard Bayesian statistical theory. This particular problem has not been previously treated in the literature, however; therefore some detail must be given here. We assume a noninformative prior distribution is assumed of the type:

$$f'_{\overline{\lambda}_{\hat{A}}, A_o, c}(\lambda, a, c) \propto \frac{1}{\lambda} \frac{1}{a - \bar{A}}, \text{ for } \begin{array}{l} \lambda > 0 \\ a > A \\ 0 < c < 2 \end{array} \tag{G12}$$

$$= 0, \quad \text{otherwise}$$

The range of c, from 0 to 2, includes the log-exponential ($c \to 0$) and the exponential distribution ($c = 1$), as well as distributions that decay faster than the negative exponential ($c > 1$) (see Figure G-3).

Other notation to be used in the sequel is:

$\lambda^*_A(a) = \lambda_A(a)/\bar{\lambda}_A$ = normalized exceedance rate of peak ground acceleration A (notice that $\lambda^*_A(\bar{A})$ is not necessarily 1).

$P_{c_{I_o}}(I)$ = probability that the catalog contains any event of epicentral intensity I_o that occurred during the time interval spanned by the catalog.

$P_{c_A}(a)$ = probability that the catalog contains any historical event with median peak site acceleration A = a that occurred during the time interval spanned by the catalog.

$Q_{I_o}(I) = 1/P_{c_{I_o}}(I)$, catalog completeness factor.

$Q_A(a) = 1/P_{c_A}(a)$, catalog completeness factor.

$\hat{A}'$ = median peak site acceleration due to a generic recorded event (same as A but includes catalog incompleteness).

$\lambda_{\hat{A}'}(a)$ = exceedance rate function of $\hat{A}'$.

$\lambda_{\bar{A}'} = \lambda_{\hat{A}'}(\bar{A})$ = rate at which $\hat{A}' > \bar{A}$.

$\underline{\theta} = (A_o, c)$ = vector of parameters of the exceedance rate function in Equation (G11).

Calculation of $G_{H(a)}(h)$ in Equation (G9)

For the case of Poisson earthquake events, one can express the probability of Equation (G9) as:

$$G_{H(a)}(h) = P[\lambda_A(a) > -\ln(1-h)]$$

$$= P[\lambda_{\hat{A}}(a) \cdot \lambda_A(a) > -\ln(1-h)] \qquad \text{(G13)}$$

$$= P[\bar{\lambda}_{\hat{A}} > -\frac{\ln(1-h)}{\lambda^*_A(a)}]$$

Both sides of the last inequality are uncertain quantities: the normalized rate $\lambda^*_A(a)$, which can be expressed in terms of the function $\lambda^*_A(a)$ in Equation (G11), and of the probability distribution of the attenuation error term E (see later), is uncertain because the vector of parameters $\underline{\theta} = (Ao, c)$ is not exactly known. The other uncertain quantity is $\bar{\lambda}_{\hat{A}}$, which is also not exactly known for a given $\underline{\theta}$.

From the relationship

$$\bar{\lambda}_{\hat{A}'} = \bar{\lambda}_{\hat{A}} \int_{\bar{A}}^{\infty} P_{C_{\hat{A}}}(a) f_{\hat{A}|\hat{A}\geq\bar{A}}(a)\, da \qquad \text{(G14)}$$

it follows that

$$\bar{\lambda}_{\hat{A}} = \bar{\lambda}_{\hat{A}'} \left[\int_{\bar{A}}^{\infty} P_{C_A} f_{\hat{A}|\hat{A}\geq\bar{A}}(a)\, da \right]^{-1} \qquad \text{(G15)}$$

Although the rate $\bar{\lambda}_{\hat{A}'}$ is uncertain, it does not depend on $\underline{\theta}$ (see later). On the contrary, the rate $\bar{\lambda}_{\hat{A}}$ depends on $\underline{\theta}$ because $f_{\hat{A}|\hat{A}>\bar{A}}$ does, from Equation (G11).

$$f_{\hat{A}|\hat{A}\geq A,\theta}(a) = \frac{-d\lambda^*_{\hat{A}}(a)}{da} \qquad \text{(G16)}$$

$$= \frac{c}{A_O^c - \bar{A}^c}\, a^{c-1}\, e^{-(a^c-\bar{A}^c)/(A_O^c-\bar{A}^c)}$$

for $a \geq \bar{A}$.

With the notation:

$$\bar{\lambda}_{\hat{A}} = \lambda_{\hat{A}'} \left[\int_{\bar{A}}^{\infty} P_{C_{\hat{A}}}(a)\, f_{\hat{A}|\hat{A} \geq \bar{A}}(a)\, da \right]^{-1} \tag{G17}$$

Equations (G15) and (G13) can be written as:

$$\lambda_{\hat{A}|\underline{\theta}} = \bar{\lambda}_{\hat{A}'} \frac{1}{E\left[P_{C_{\hat{A}}} | \theta\right]} \tag{G18}$$

and

$$G_{H(a)}(h) = \underset{\underline{\theta}}{E} \left\{ P\left[\bar{\lambda}_{\hat{A}|\underline{\theta}} > -\frac{\ln(1-h)}{\lambda^{*}_{A|\underline{\theta}}(a)} \right] \right\} \tag{G19}$$

Substitution for $_{A}\underline{0}$ from Equation (G18) transforms Equation (G19) into:

$$G_{H(a)}(h) = \underset{\underline{\theta}}{E} \left\{ P\left[\bar{\lambda}_{\hat{A}'} > -\ln(1-h) \frac{E\left[P_{C_{\hat{A}}} | \underline{\theta}\right]}{\lambda^{*}_{A|\theta}(a)} \right] \right\} \tag{G20}$$

The only uncertain quantity inside the brackets is now $\lambda_{\hat{A}}'$.

In order to calculate $G_{H(a)}(h)$ from Equation (G20), one needs to know:

1. The posterior distribution of $\underline{\theta}$ = (Ao, c).

2. The posterior distribution of $\lambda_{\hat{A}}'$. (Notice that a posterior $\underline{\theta}$ and $\lambda_{\hat{A}}'$ are independent.)

3. The function (P_{C_A} (a) and the quantity $E[P_{C_A} | \underline{\theta}]$ in Equation (G17) for each given $\underline{\theta}$.

4. The normalized exceedance rate $\lambda^{*}_{A|\underline{\theta}}(a) = \lambda_{A|\underline{\theta}}(a)/\bar{\lambda}_{\hat{A}|\underline{\theta}}$ for each $\underline{\theta}$ and for the values of a of interest.

The remainder of the appendix is devoted to calculation of these four quantities.

1. The Posterior Distribution of $\underline{\theta} = (A_o, c)$

Suppose that there are exactly M recorded historical events with associated median peak site acceleration A in excess of A and denoted by $A_{(i)}$ (i = 1, ..., M) such median values in decreasing order. Then the likelihood of $\underline{\theta}$ from only $A_{(1)}, \ldots, A_M$ is:

$$\ell\left(\underline{\theta}\,\middle|\,\begin{matrix}\text{historical}\\ \text{catalog}\end{matrix}\right) \propto \prod_{i=1}^{M} f_{\hat{A}|\hat{A}\geq\bar{A},\underline{\theta}}(\hat{A}_i) \tag{G21}$$

$$= \prod_{i=1}^{M} \frac{P_{C_{\hat{A}}}(\hat{A}_{(i)})\, f_{\hat{A}|\hat{A}\geq\bar{A},\underline{\theta}}(A_{(i)}))}{\int_{\bar{A}}^{\infty} P_{C_{\hat{A}}}(\xi) f_{\hat{A}|\hat{A}\geq\bar{A},\underline{\theta}}(\xi)\,d\xi}$$

i.e.,

$$\ell\left(\underline{\theta}\,\middle|\,\begin{matrix}\text{historical}\\ \text{catalog}\end{matrix}\right) \propto \frac{1}{\left(E[P_{C_{\hat{A}}}|\underline{\theta}]\right)^{M}} \prod_{i=1}^{M} f_{\hat{A}|\hat{A}\geq\hat{A},\underline{\theta}}(\hat{A}_{(i)}) \tag{G22}$$

with $f_{\hat{A}|\hat{A}\geq A,\underline{\theta}}$ in Equation (G16). The posterior density of $\underline{\theta}$ is given by:

$$f''(A_o,c) \propto \frac{1}{A_o - \bar{A}}\, \ell\left(\underline{\theta}\,\middle|\,\begin{matrix}\text{historical}\\ \text{catalog}\end{matrix}\right), \quad \begin{matrix}\text{for } A_o > \bar{A}\\ 0 \ll\ll 2\end{matrix} \tag{G23}$$

$$= 0 \qquad \text{otherwise.}$$

2. Posterior Distribution of $\bar{\lambda}_{\hat{A}'}$

With N the number of years spanned by the catalog, M the number of recorded events with median site acceleration larger than A, and for a noninformative prior density of the type:

$$f'_{\bar{\lambda}}(\lambda) \propto \frac{1}{\lambda} \quad , \quad \lambda \geq 0 \tag{G24}$$

the posterior distribution of $\bar{\lambda}_{\hat{A}'}$ is Gamma, with density

$$f''_{\bar{\lambda}_{\hat{A}'}}(\lambda) \propto \lambda^{M-1} e^{-\lambda N} \quad , \lambda \geq 0 \tag{G25}$$

3. Estimation of the Probability Function $P_{c_{\hat{A}}}(a)$

One first estimates the completeness-probability function $P_{c_{I_o}}(I)$, i.e., the completeness of the catalog in terms of epicentral intensity. If $N_c(I)$ is the number of years during which the catalog is complete with respect to events with epicentral intensity I, then one can estimate $P_{c_{I_o}}(I)$ as:

$$P_{c_{I_o}}(I) = \frac{M(I)}{N} \frac{N_c(I)}{M_c(I)} \tag{G26}$$

in which

M(I) = total number of recorded earthquakes with $I_o = I$,

$M_c(I)$ = number of such earthquakes during the last $N_c(I)$ years.

For the eastern United States catalogs used in this study (see Appendix C), N equals 446 (years). Values of $N_c(I)$ from NUREG/CR-1582 are given in Col. 2 of Table G1.

The last two columns of the table give the value of the completeness factors $Q_{I_o}(I) = 1/P_{c_{I_o}}(I)$ from Equation (G26). For intensities IX, X and XI, data has been pooled together in order to add statistical stability to the estimates. (The completeness factors in Table G1 have been used also in the nonparametric method, as factors Q_i in Equation (G6).)

		$Q_{I_o} = 1/P_{c_{I_o}}$	
I	N_c (Years)	NUREG/CR-1582	CHIBURIS (1981) (completed)
4	70	4.0	3.7
5	100	3.7	3.5
6	100	3.7	3.5
7	150	2.6	2.7
8	200	1.6	1.7
9	200	1.4	1.6
10	200	1.4	1.6
11	200	1.4	1.6

TABLE G1

Completeness Function $Q_{I_o}(I) = 1/P_{c_{I_o}}(I)$

for the NUREG and Chiburis 1981 (Completed) Catalog Results, Refer to 446 Years of Data

For each recorded historical event i, one then calculates the median site attenuation value A_i and the completeness probability $P_{c_i} = P_{c_{I_o}}(I_{o_i})$. At this point, one can estimate P_{c_A} over a range of values of A as the average value of P_{c_i} in that range. Alternatively, one can estimate $Q_{\hat{A}}$ as the average of $1/P_{c_i}$ in the same range of $\hat{A}$ and then take $P_{c_{\hat{A}}}$ as $P_{c_{\hat{A}}} = 1/Q_{\hat{A}}$. Estimates of $Q_{\hat{A}}$ of the latter type were calculated for four different attenuation functions. The analytical fits in the form of exponential functions are:

$$P_{c_A}(a) = \begin{cases} [1.4 + 2.4e^{-(a-5)/11}]^{-1}, & \text{for the NUREG catalog} \\ [1.6 + 2.1e^{-(a-5)/9}]^{-1}, & \text{for the Chiburis (1981) and Weston catalogs} \end{cases} \quad \text{(G27)}$$

Different analytical functions should in principle be used for different attenuation models, but in this case, such a distribution does not seem warranted.

4. Calculation of the Normalized Exceedance Rate $\lambda_{A|\underline{\theta}}(a)$

This function is obtained by considering the exceedance rate $\lambda_{A|\underline{\theta}}(a)$ in Equation (G11) with the probability density function of $E' = e^{E}$, as follows:

$$\lambda^{*}_{A|\underline{\theta}}(a) = \int_0^{\infty} \lambda^{A}_{\hat{A}|\underline{\theta}}\left(\frac{a}{E'}\right) f_{E'}(E')\,dE' \quad \text{(G28)}$$

with $f_{E'}$ in the form of a (truncated) lognormal density function. Alternatively, one can work with lnA and calculate $\lambda_{\ln A\,\underline{\theta}}(\ln a)$ as:

$$\lambda^{*}_{\ln A|\underline{\theta}}(\ln a) = \int_{-\infty}^{\infty} \lambda^{*}_{\ln \hat{A}|\underline{\theta}}(\ln a - E) f_E(E)\,dE \quad \text{(G29)}$$

with f_E a (truncated) normal density function.

In summary, when using the parametric historic procedure, one uses Equation (G20) to calculate the exceedance probability $G_{H(a)}(h)$ in Figure G2 for any given a and h. The posterior distributions of the Weibull parameter $\underline{\theta} = (A_o, c)$ and of the exceedance rate λ_A' do not depend on a or h and are found from Equations (G23) and (G25). For each given $\underline{\theta}$, one finds $E[P_{c_A} \underline{\theta}]$ from Equation (G17) in which $\lambda_{\hat{A}|\hat{A}_-}$ A, $\underline{\theta}$ is the function in Equation (G16) and $P_{c_A}(a)$ is given by Equation (G27). Finally, for each given a and $\underline{\theta}$, the exceedance rate $\lambda_{A|\underline{\theta}}(a)$ is calculated using either Equation (G28) or Equation (G29).

These steps require a significant amount of (rather straightforward) numerical integration* but the benefits are obvious: the product is an historic-based hazard estimate with a quantitative measure of the uncertainty in the estimate.

---

* The authors will gladly make the programs available; they anticipate publishing these new methods shortly.

APPENDIX H

SEISMIC PROBABILISTIC RISK ASSESSMENT RESULTS

One of the main objectives of this study is to develop input for the plant's Seismic Probabilistic Risk Assessment (SPRA). This requires a "full Bayesian" seismic hazard analysis. Such an analysis includes a complete quantitative statement about the uncertainty in the annual frequency of exceeding ground acceleration level, A, as a function of A.

The first step in the SPRA is to estimate the frequency of exceedance of earthquake induced ground motion at the site. This methodology is well known and is described in the main body of this report. The second step is to quantify uncertainty. The method we have chosen in this anaysis is by enumeration (i.e., examine all possible combinations of parameters). This required an explicit consideration of a set of contending hypotheses about each critical input parameter or assumption in the seismic hazard analysis (e.g., zonation, a, b, m, attenuation, error term, catalog). Weights on the hypotheses produce weights (probabilities) on the results which are pooled statistically for presentation. Figure H1 is an example of the quantitative uncertainty in the results.

A better representation of these results, for input to the SPRA, is shown in Figure H2. The family of curves in Figure H2 is a discretization of the seismic hazard curves from the zonation methodology. This is accomplished by partitioning the "cloud plot" of 10^{-3}, 10^{-4} results into ten subsets as shown in Figure H3. The curves in each subset are then analyzed to define an average frequency of exceedance curve. Weights associated with each curve in the subset are added to determine the probability to be assigned that curve. This procedure is followed for all subsets resulting in Figure H2. This kind of result is necessary to make feasible subsequent input into PRA studies which require a small set of curves.

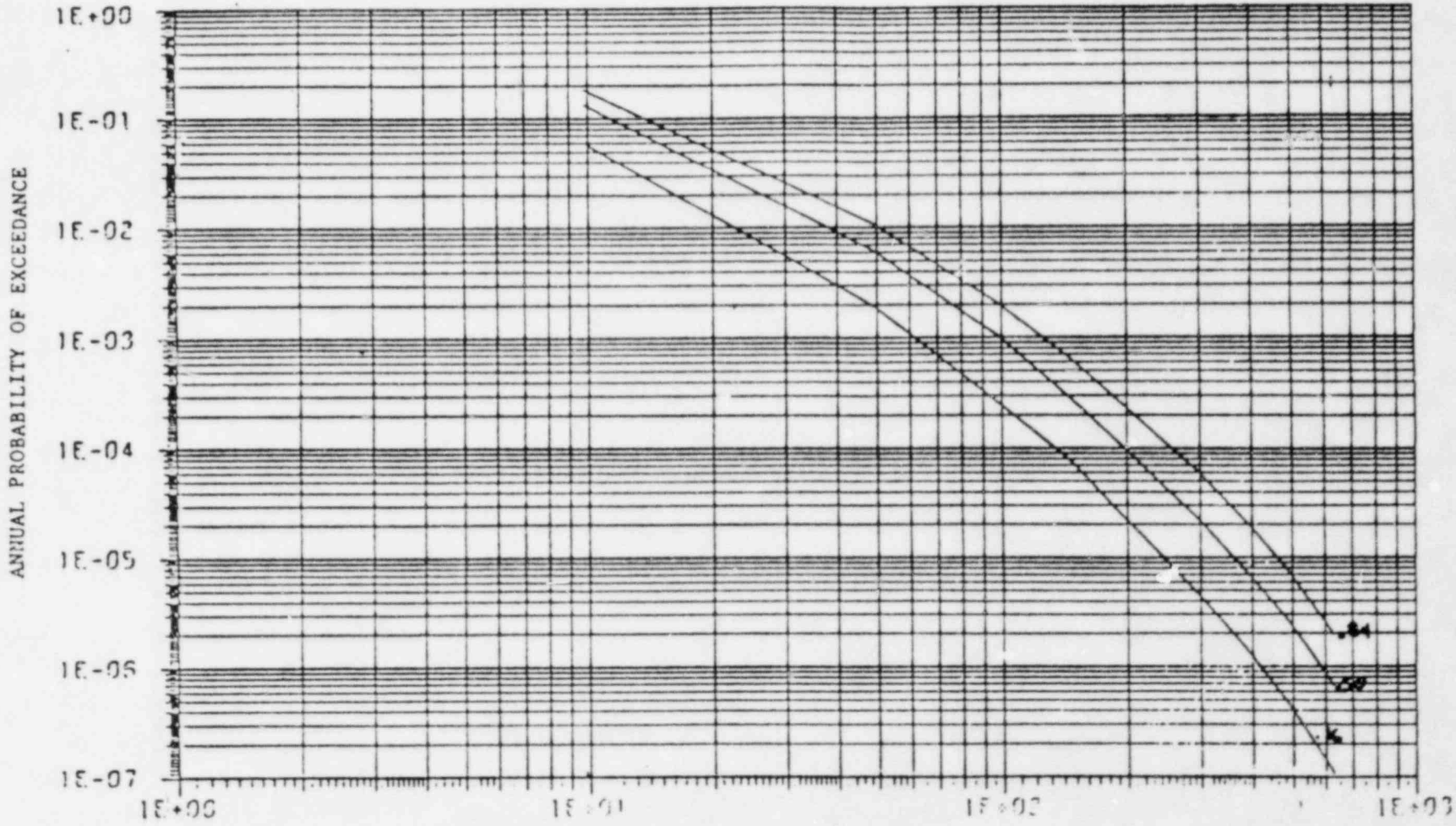
1E+00
1E-01
1E-02
1E-03
1E-04
1E-05
1E-06
1E-07
ANNUAL PROBABILITY OF EXCEEDANCE
1E+00
1E+01
1E+02
1E+03
PEAK GROUND ACCELERATION (CM/SEC^2)

Figure H1.

GROUPED HAZARD FUNCTION

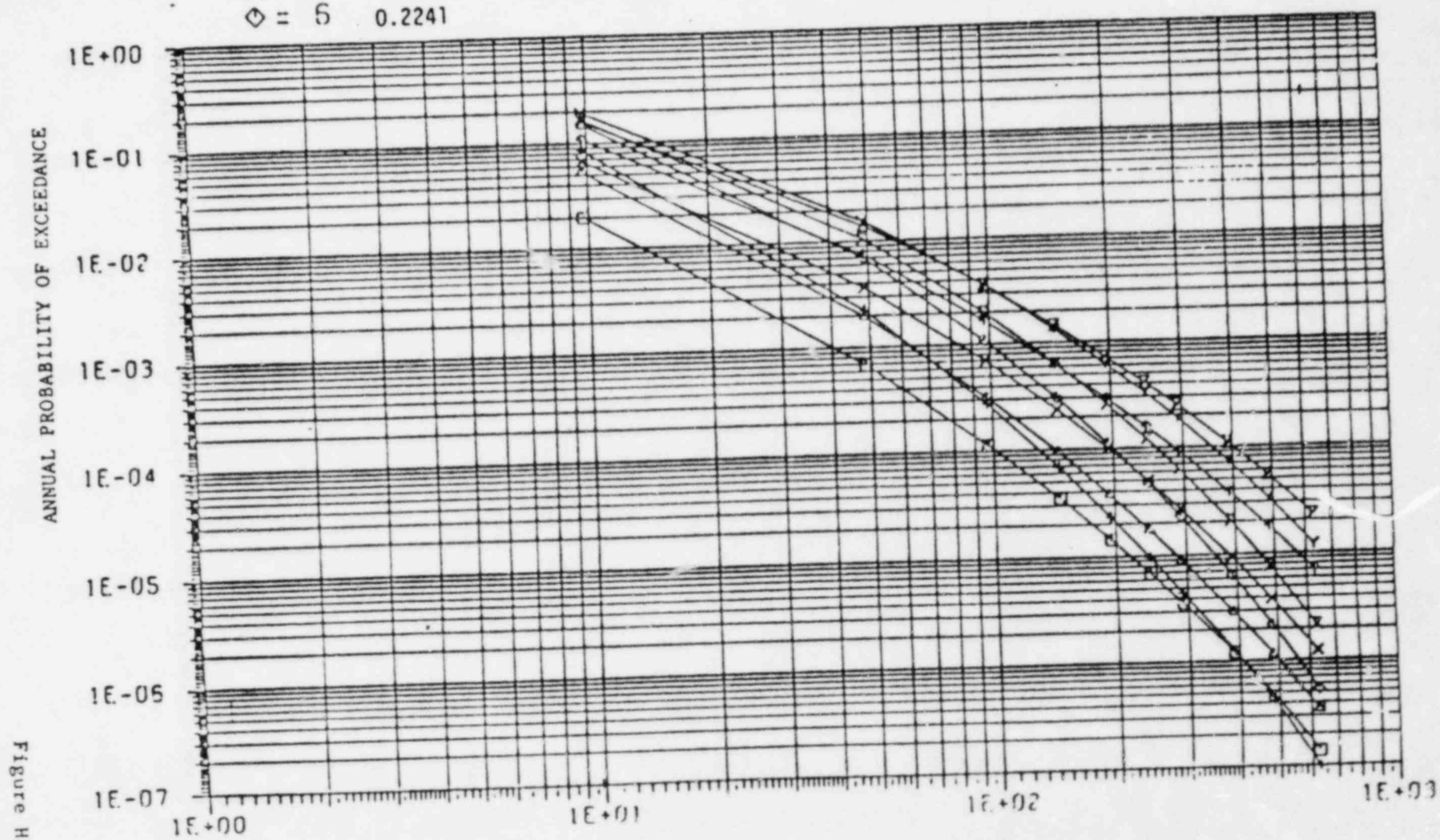

Figure H2.

Figure H3.

APPENDIX I

RESULTS OF VELOCITY HAZARD ANALYSIS

The main body, appendices, and methodology of this report is primarily concerned with the estimation of peak ground acceleration. Because certain structures at the Yankee plant may be more sensitive to velocity than acceleration, it was decided to apply the methodology developed for estimation of acceleration to velocity, but in a less exhaustive manner. Less exhaustive in that only two source area zonations are used and no attempt is made to merge historic results with the zonation results. But, a check is made of the zonation results by comparing them with the results of a simplified historic analysis.

Description of Alternative Hypotheses

1. Zonation

As has been stated, only two source area zonations are used in this analysis. But, the two used represent the most and least detailed description of seismic source areas of those presented in the main body of this report, and therefore can be considered, in our opinion, as "best" and "worst" case zonations. These source areas are:

a. Weston Geophysical Corporation (WGC), and

b. Boston-Ottawa/Piedmont

Appendix B contains maps of these zonations and a detailed review of the relevant literature. Weights previously assigned have been normalized to reflect two source areas resulting in weights of:

$P_1 = 0.60$, $P_2 = 0.40$

2. Seismicity Parameters, a, b and m_1

Uncertainty on the upper-bound magnitude m_1 and on the Gutenberg-Richter slope parameter "b" has been included. Uncertainty on "a", the activity rate, is not included because it has been shown to contribute minimally to the hazard. Treatment of "b" and m_1 is to assume perfect spatial dependence (e.g., that is if m_1 is high for one source, then m_1 is necessarily high for all other sources). The following cases were examined:

For m_1,

a. Historical maximum in each source plus 0.5 (basically the WGC estimates), (Probability $P_1 = 0.8$).

b. Historical maximum in each source plus 1.0 ($P_2 = 0.15$).

c. Historical maximum in each source plus 1.25 ($P_3 = 0.05$). If this value exceeds $m_b = 7.30$, the value is taken equal to $m_b = 7.30$.

For b,

a. As calculated by WGC for each source ($P_1 = 2/3$).

b. $b = 0.9$ for all sources ($P_2 = 1/3$).

As can be seen for each parameter, we have added what we believe to be conservative alternatives to the WGC estimates. In particular, the hypothesis that $b = 0.9$ for all sources without modification of the activity rates produces significantly larger hazard values at the site.

3. Attenuation Models

The methodology used to estimate velocity is exactly the same as that used to estimate acceleration, but modifications of the attenuation laws are necessary. The Bollinger 1, Bollinger 2, and Weston Geophysical Corporation

(WGC) model is converted to the prediction of velocity by using the McGuire [1] conversion:

$$\ln V_p = -3.61 - 0.064 \ln R + 0.923 I_s$$

where

V_p is peak ground velocity
R is distance in kilometers
I_s is site intensity

The peak ground velocity is converted to spectral velocity by using the median amplification factor of 1.65 from NUREG/CR-0098.

$$\ln S_v = \ln 1.65 + \ln V_p$$

where

S_v = spectral velocity
V_p = peak ground velocity
1.65 = median amplification factor

The Nuttli-Herrmann [2] and Gupta-Nuttli [3] attenuation models are given in terms of velocity and therefore, only the conversion to spectral velocity is required.

The attenuation models in terms of spectral velocity used in this analysis are as follows:

a. $S_v = -7.79 + 2.30 m_b - 0.00025 - 0.833 \ln R$ [Nuttli-Herrmann]

b. $S_v = -2.24 + 1.28 m_b - 0.0006 - 0.645 \ln R$ [Gupta-Nuttli]

c. $S_v = -4.01 + 1.67 m_b - 0.0023 - 0.765 \ln R$ [Weston Geophysical Corporation]

d. $S_v = -3.69 + 1.84\ m_b - 0.0005 - 1.218\ \ln R$ [Bollinger 1]

e. $S_v = -0.58 + 1.26\ m_b - 0.0005 - 1.218\ \ln R$ [Bollinger 2]

The following weights have been assigned to each of the above models:

$P_1 = 0.35,\ P_2 = 0.13,\ P_3 = 0.35,\ P_4 = 0.06,\ P_5 = 0.11$

Dispersion about each median attenuation model has been included through a random error term. This term is assumed to have mean zero and the following truncated or untracted normal distribution:

a. $\sigma_E = 0.6$, no truncation ($P_1 = 0.3$)

b. $\sigma_E = 0.7$, truncation at $\pm 3\sigma_E$ ($P_2 = 0.6$)

c. $\sigma_E = 0.9$, truncation at $\pm 2\sigma_E$ ($P_3 = 0.1$)

The indicated probability assignments are discussed in Appendix E.

Analysis of the Results

The 180 hazard curves produced by the McGuire program under the conditions of input previously specified have been statistically analyzed in the same manner as was discussed in the main body of this text for acceleration. Figure I1 is a plot of the 0.16, 0.50 and 0.84 fractiles of the 180 cases. As can be seen, the 10^{-3} median spectral velocity is about 4 inches/second with the 0.16 and 0.84 fractile being 2.8 and 6.3 inches/second, respectively. The 10^{-4} median spectral velocity is about 10 iches/second with the 0.16 and 0.84 fractile being 6.3 and 15.0 inches/second, respectively.

As a check, the 10^{-3} and 10^{-4} spectral velocities have been computed using the historical method. This analysis used only the WGC catalog and the attenuation models with their associated weights as stated in the main body of this report. Dispersion about each median attenuation model is

included through a random error and is equal to 0.70 in all cases. The resulting weighted average 10^{-3} and 10^{-4} spectral velocities are 3 and 6 inches/second, respectively.

Appendix I References

[1] R. K. McGuire, 1977, "The Use of Intensity Data in Seismic Hazard Analysis Proceedings", 6th World Conference on Earthquake Engineering, New Dehli, India, Vol. 2, pp. 353-358.

[2] O. W. Nuttli and R. B. Herrmann, 1981, "Consequences of Earthquakes in the Mississippi Valley", ASCE Preprint 81-519.

[3] NUREG/CR-1582, 1981, "Seismic Hazard Analysis: Review Panel, Ground Motion Panel and Feedback Results".

□ = 0.16
○ = 0.50
△ = 0.84

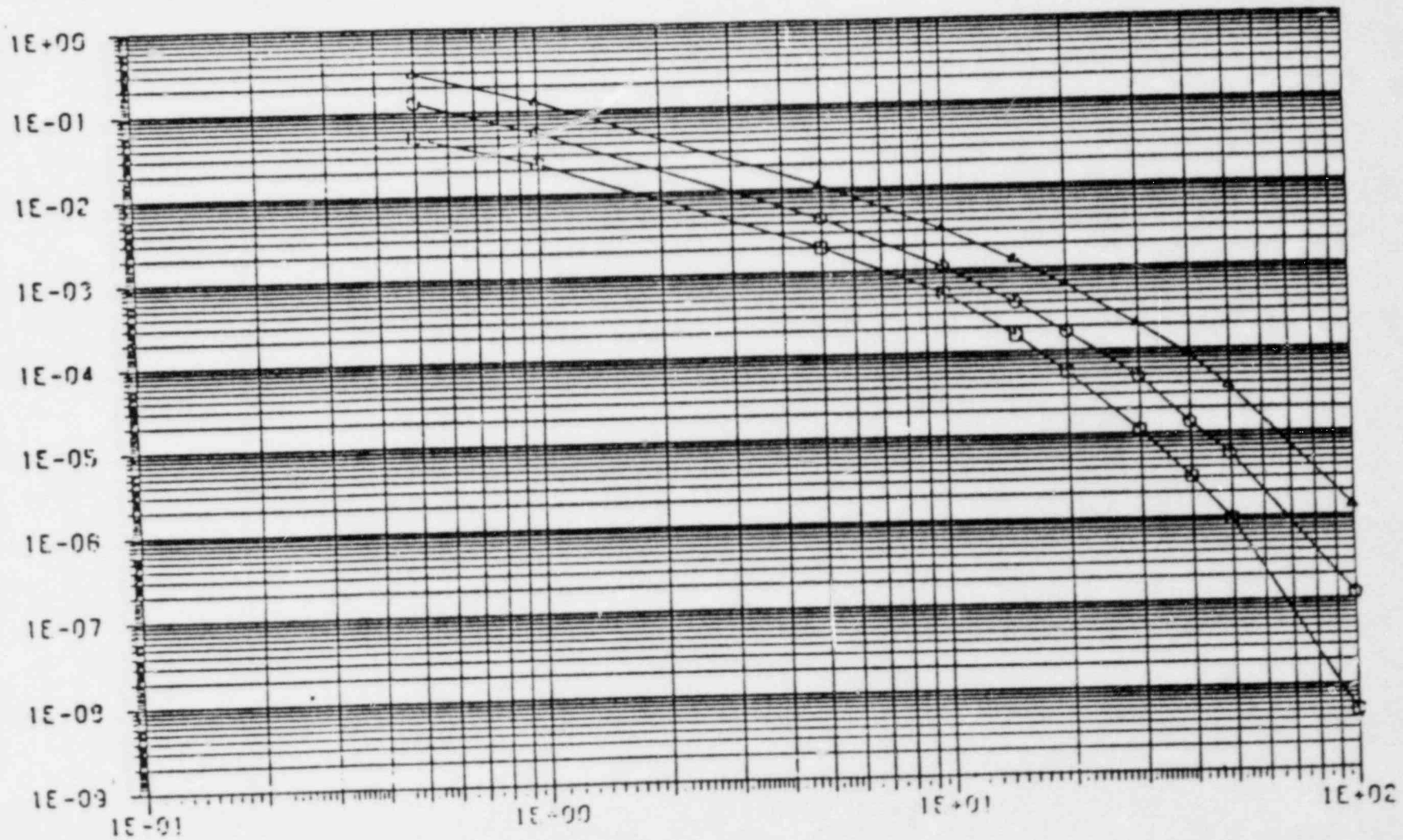

Figure 11.

APPENDIX J

COMMENTS CONCERNING RECENT EARTHQUAKES IN NEW BRUNSWICK AND NEW HAMPSHIRE

This appendix discusses the potential effect of the recent earthquakes that occurred in New Brunswick and New Hampshire on this study and YAEC-1263. The location and quantification of these events were supplied by Weston Observatory [1] and are as follows:

1. On January 9, 1982, a magnitude 5.7 earthquake occurred at 47.00 N and 66.50 W in the province of New Brunswick, Canada. The Modified Mercalli intensity of this event is estimated at about $I_o = 6$. The distance of this event to Rowe, Massachusetts, is approximately 600 kilometers.

2. On January 18, 1982, a magnitude 4.7 earthquake occurred at 43.60 N and 71.62 W in Franklin, New Hampshire. The Modified Mercalli intensity of this event is expected to be set at $I_o = 5$ or $I_o = 6$. The distance of this event to Rowe, Massachusetts, is approximately 120 kilometers.

A minimal amount of damage has been associated with both of these events, which is reflected in the lower than expected intensity evaluations. Damage that has been reported is typically that of cracks in basement floors, foundations and ceilings. It is difficult to determine to what degree these cracks are due to the earthquake. Evidence of major structural damage to well-engineered modern structures has not been found.

Specific to this current study and YAEC-1263, these events could impact in the following areas:

1. Strong motion data may allow the opportunity to determine how well the attenuation models fit the data; and

2. Determine what the effect on the results would be if the New Brunswick event is assumed to occur in the Yankee site source area.

Presently, the U.S. Geological Survey (Menlo Park, California) has possession of the strong motion recordings from the New Brunswick events, and the U.S. Army Engineer's Waterways Experiment Station, Vicksburg, Mississippi, has possession of the Franklin, New Hampshire, event. Until these records are processed and released, it is not possible to test the fit of the attenuation models.

To determine the effect of allowing the New Brunswick event to occur in the site source area, a sensitivity analysis was performed. Only the Weston Geophysical Corporation (WGC) zonation and seismicity parameter (a's and b's) are used in this analysis. The Nuttli-Herrmann attenuation model (see Appendix E) with three levels of uncertainty (see Chapter 2) was also used. With a site source upperbound set at magnitude 6.5, it was found that the hazard was increased by about 10-20 percent. This represents acceleration from 0.07-0.08g at the 10^{-3} frequency of exceedance.

This specific consideration of these recent events in New Brunswick and New Hampshire indicate that they have little influence upon the results and conclusions in both YAEC-1263 and this current study.

Appendix J References

[1] V. Vudler, 1982, Personal Communication, Weston Observatory, Boston College, Weston, MA.

APPENDIX K

INTEGRATION OF THE RESULTS OF SOIL AMPLIFICATION AND PROBABILISTIC SEISMIC ANALYSIS YANKEE NUCLEAR POWER PLANT, ROWE, MASSACHUSETTS

Introduction

This appendix presents and summarizes results of soil amplification studies for the Yankee Nuclear Power Plant at Rowe, Massachusetts. One-dimensional and two-dimensional mathematical modeling of the Yankee substrata as well as investigation of spectra recorded at geologically and geophysically similar sites was accomplished. These analyses formed the basis for inclusion of potential soil amplification effects into the determination of the probabilistic seismic spectra for the Yankee site. This appendix demonstrates that the Yankee Composite Spectrum (1) is a conservative estimate of the 10^{-3} spectrum when soil amplification is incorporated in the analysis.

Original Amplification Studies

Studies were undertaken in 1980 to determine the potential for local site amplification effects on earthquake motion. Local site features which could potentially cause amplification were identified as the sloping bedrock surface and the dense glacial till soil column underlying the Yankee site. The original amplification studies (1) accounted for these site features and included:

1. A one-dimensional model of the soil column beneath the Yankee site, and

2. Development of an undampened two-dimensional model of a bedrock valley filled with alluvium.

These different models predict similar amplification values at the fundamental mode (natural frequency) of the glacial till overburden. The two-dimensional study, which accounts for sloping bedrock and basin configuration at the Yankee site, predicts amplification similar to that

obtainable by the conventional one-dimensional soil amplification analysis. The results of this study indicated that no anomalous amplification effects attributable to the sloping bedrock and two-dimensional basin configuration were present at the Yankee site. In this sense, it was concluded that the Yankee site is typical of soil sites in terms of local dynamic amplification potential.

Final Amplification Study

Subsequent analyses were undertaken to further study the potential amplification of earthquake motion at the Yankee site (2). These comprehensive studies (2) expand upon the previously reported work (1) by including new supporting analyses. The conclusion of all these studies is that Yankee is a typical soil site and that the expected amplification at any given frequency is minor.

This conclusion is supported by analysis using three different methodologies:

1. Two-dimensional amplification analysis (now including material damping) in which a two-dimensional profile representative of the local geology at the Yankee site is subjected to wave excitations at various incidence angles;

2. Amplification analysis in which the model is a single layer above elastic halfspace excited by waves at different incidence angles; and

3. Conventional one-dimensional amplification analysis under vertically propagating shear wave excitation, including the study of observed amplification in recorded accelerograms at sites predicted by such analyses to be similar to the Yankee site.

In method 3, multi-layer and two-layer models were compared, the influence of soil property nonlinearity was assessed, and sources of variability in local amplification factors were evaluated. The amplification factors predicted at Yankee were also compared to those obtained for a number

of strong-motion accelerograph stations selected by Weston Geophysical Corporation as similar geologically and geophysically to the Yankee site. Records from two of these sites were processed to estimate empirically the true amplification.

The two-dimensional amplification studies indicated that local soil amplification effects at the Yankee site are conservatively predicted by modeling the soil overburden as a horizontal layer overlying bedrock. Also, from the comparison of amplification effects for different angles of wave incidence, it was concluded that the assumption (common in one-dimensional amplification analysis) that shear waves are vertically incident leads to conservative estimates of local soil amplification factors.

Various one-dimensional (hence, upper bound) amplification analyses were carried out to test the sensitivity of predicted amplification factors to (a) the analytical model used (multi-layer versus two-layer); (b) parameters such as soil layer thickness and shear wave velocity, impedance contrast, and damping; and (c) whether or not soil nonlinearity is accounted for. Based on these studies, a most likely value and a range are determined for the dominant frequency, f_p, and the predicted peak Fourier soil amplification factor A_p at that frequency. At the Yankee site, the best-estimate of the dominant frequency is between 3.4 and 4.4 Hz, but f_p may range between about 1 Hz and 9 Hz depending on values of input parameters. The corresponding peak Fourier soil amplification factor predicted by deterministic one-dimensional analysis (assuming 5% damping) ranges between 1.25 and 4.5, with the most probable theoretical peak values being in the range from 2.8 to 3.8.

The dominant frequency and peak amplification factor predicted at the Yankee site compare favorably with the corresponding parameters predicted theoretically for a number of selected accelerograph stations. This suggests that the Yankee site is not unusual as regards local soil effects on earthquake ground motion. Examination of the 5% damped response spectra recorded at two of the sites, where multiple records are available, shows the absence of strong and/or systematic amplification attributable to the influence of local soil.

All sources of uncertainty and bias in local soil effects can be expressed in terms of a random spectral soil amplification factor which multiplies the response spectra over a range of frequencies (hence, 1 to 9 Hz). In the case of the Yankee site, it is appropriate to use a median spectral soil amplification factor less than the peak amplification factor predicted by linear one-dimensional analysis because of (a) the two-dimensional valley geometry; (b) the likelihood of nonvertical wave incidence; (c) soil nonlinearity causing increased damping; (d) uncertainty about effective soil layer thickness, and hence f_p; and (e) the fact that response spectra are amplified less than Fourier amplitude spectra. When all these factors are accounted for, relatively little systematic local soil amplification is expected at the Yankee site at any given natural frequency. The spectral soil amplification factor is estimated to be 1.18 or less by theoretical analysis at the Yankee site; this value agrees with a mean factor of 1.155 obtained by an approximate empirical analysis of the response spectra of a set of motions recorded at accelerograph stations whose local site conditions resemble those at the Yankee site. The dispersion in the response spectra soil amplification factor is estimated to be 20%.

Probabilistic Accounting of Soil Amplification

The Composite Spectrum (Figure 1) developed in YAEC-1263 (1), is the result of a comprehensive probabilistic analysis to conservatively estimate the 10^{-3} probabilistic spectrum. This analysis was based upon methodology that is well documented in the literature (3,4,5). Probabilities were calculated based upon site-specific source areas and seismicity parameters, and attenuation models that are appropriate for the Northeast. The resultant Composite Spectrum bounded all Reference 10^{-3} probabilistic spectra (1). The results of YAEC-1263 are supported by this report. The Composite Spectrum envelopes spectra derived from various attenuation models that represent soil sites and, hence, implicitly incorporate typical soil amplification effects. Now, using the results of the more explicit site-specific analysis of the amplification effect at Yankee given here, we confirm that the effect of site amplification was adequately accounted for by the attenuation models and dispersion in YAEC-1263 (1). The basis for this confirmation is given next.

Implicitly or explicitly, spectral ordinate prediction includes both an attenuation model component and a component associated with local amplification effects. Both components contain statistical dispersion. It is commonly accepted that the data used to estimate the dispersion in typical attenuation models are "contaminated" (increased) by a broad selection of earthquake source types, of propagation paths, and of soil amplification effects. It has been shown (6), that if one explicitly accounts for amplification effects (i.e., holds the soil conditions constant), the dispersion of the data is significantly reduced. After removal of the site amplification effect, numbers of 0.4 and less have been suggested (e.g., 6) for σ, the standard deviation of the natural log of the ground motion. As an initial hypothesis, a σ value of no more than 0.5 to 0.6 (say, 0.55) is reasonable for a typical attenuation model without the soil amplification uncertainty component.

The conclusions of the amplification study (2) summarized above are that the median* response spectra soil amplification at any frequency in the amplified frequency range at Yankee (about 1 to 9 Hz) is 1.18, with a standard deviation of approximately 20%. By taking the square root of the sum of the squares, the net spectral ordinate uncertainty is estimated. The net value is:

$$\sigma_{net} = \sqrt{(0.55)^2 + (0.20)^2} = 0.58$$

To understand the effect of introducing amplification explicitly into the seismic hazard analysis, we consider the following case study. It is based on the preferred input parameters (1), but the results for other hypothesis combinations would be qualitatively and quantitatively similar.

The input parameters for the unmodified case (i.e., the original analysis without explicit soil amplification treatment) are those as defined in YAEC-1263. They are the Weston Geophysical Corporation estimates of source area geometry, seismicity, and upper bound magnitudes. In this report, the

* For near-symmetrical unimodal distributions with low dispersion, the mean, mode, and median are approximately equal.

1981 Nuttli - Herrmann (7) attenuation model is now used to predict the attenuation of acceleration with distance; this is the most recently reported of the sequence of "theoretical" models developed by Nuttli and Herrmann and is used in this case study because its authors favor it over the predecessor formulas (Appendix E). In particular, it replaces the so-called "Nuttli Theoretical" model (8) used in YAEC-1263. The newer model predicts comparable peak accelerations and lower peak velocities. A typical net standard deviation of 0.7 is assumed.

For the modified case, that with explicit accounting of soil amplification, we use the same input assumptions as above, with two modifications: First, as discussed, the standard deviation of 0.7 is decreased to 0.58. Second, to reflect the predicted soil amplification, we increase the spectral ordinates, between the frequencies of 1 and 9 Hz, by a median soil spectral amplification factor of 1.18.

The results of these two analyses are shown in Figure K1. There are four curves shown on this figure. They are:

1. Modified case:

   a. The 10^{-3} spectrum explicitly accounting for amplification (σ = 0.58, median soil spectral amplification factor of 1.18 between 1 and 9 Hz).

   b. The same case but with a median soil amplification factor of 1.0 for all frequencies.

2. Unmodified case: The 10^{-3} spectrum implicitly accounting for amplification (σ = 0.7).

3. The Yankee Composite Spectrum anchored at 0.1g.

Note that the effects of simultaneously reducing the dispersion and increasing the median spectrum tend to compensate one another in the amplified frequency range. Elsewhere the uniform hazard spectrum is lower (see

Figure K1) because the σ is reduced. Also, even in the amplified region, the Yankee Composite Spectrum is substantially higher (by about 35%) than the explicitly soil amplified 10^{-3} spectrum.

Conclusion

As discussed in Reference (1), the Yankee Composite Spectrum is a conservative estimate of the 10^{-3} spectrum. This is also supported by this report. As shown in the attached Figure K1, the Composite Spectrum adequately incorporates the effect of local soil amplification.

Appendix K References

[1] Yankee Atomic Electric Company, 1981. Seismic Response Spectra for the Yankee Nuclear Power Station, Rowe, Massachusetts. YAEC-1263.

[2] Weston Geophysical Corporation, E. VanMarcke, E. Kausel, M. Bouchon, 1982. Local Soil Amplification Effects at the Yankee Nuclear Plant Site, Rowe, Massachusetts.

[3] Cornell, C. A., 1968. Seismic Risk Analysis, BSSA, Volume 58, No. 5, Pages 1583-1606.

[4] Cornell, C. A. and H. Merz, 1975. Seismic Risk Analysis of Boston, Journal Structural Division, ASCE Volume 101, Pages 2027-2043.

[5] McGuire, R. K., 1976. Fortran Computer Program for Seismic Risk Analysis, USGS Open File Report 76-67.

[6] Campbell, K. W., 1982. A Comparative Analysis of the Ground Motion Models of TERA Corporation and the USGS, TERA Corporation Technical Report B-81-187, Submitted to Southern California Edison, February 19, 1982.

[7] Nuttli, O. W., R. B. Herrmann, 1981. Consequence of Earthquakes in the Mississippi Valley, ASCE, Pre-print 81-519.

[8] Nuttli, O. W., 1979. State-of-the-Art for Assessing Earthquake Hazards in the United States, Report 16, U. S. Army Engineer Waterways Experiment Station.

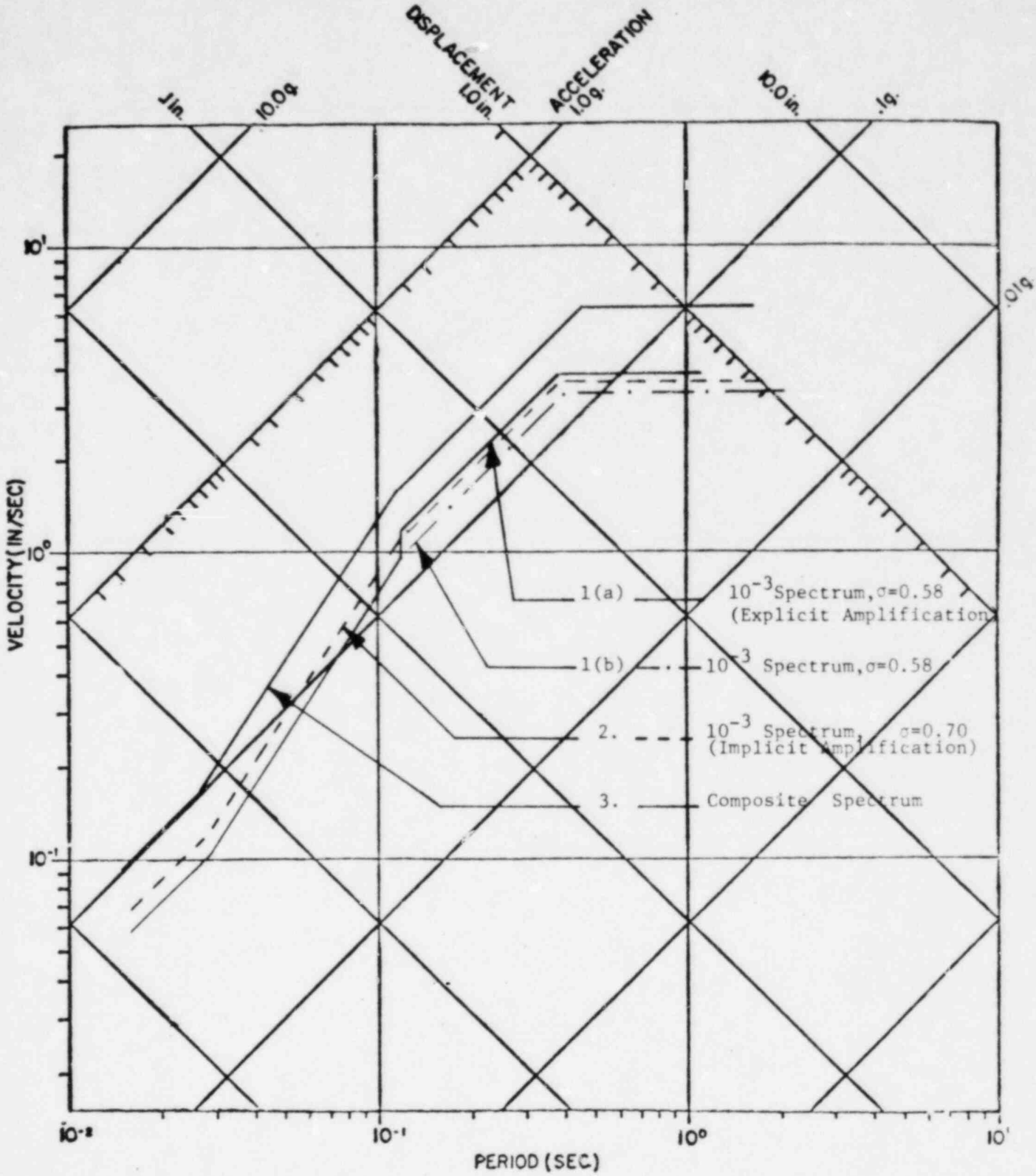

Comparison of Spectra Resulting from Implicit and Explicit Accounting of Soil Amplification Effects with the Composite Spectrum

Figure K1